Comparative Evaluation of Well-Defined IgG1 Fc Glycoforms as a Model System for Biosimilar Comparability Analysis

By

Solomon Z. Okbazghi

Submitted to the graduate degree program in Pharmaceutical Chemistry and the Graduate Faculty of the University of Kansas in partial fulfillment of the requirements for the degree of Doctor of Philosophy.

Committee members:

_____
Chairperson Thomas Tolbert Ph.D.

_____
David Volkin Ph.D.

_____
Teruna Siahaan Ph.D.

_____
Michael Wang Ph.D.

_____
Christian J Ray Ph.D.

Date Defended: June 2 , 2017

The Dissertation Committee for Solomon Z. Okbazghi
certifies that this is the approved version of the following dissertation:

Comparative Evaluation of Well-Defined IgG1 Fc Glycoforms as a Model System for Biosimilar Comparability Analysis

_____
Chairperson Thomas Tolbert Ph.D.

Date Approved: June 2, 2017

Abstract

The patents of several best-selling biologic therapeutic products are expiring soon. Consequently, the interest of developing biosimilar products is growing. A biosimilar product is developed if there are no clinically meaningful differences in terms of safety, efficacy, and purity after evaluating side-by-side with the originator. Biosimilar products are anticipated to be accessible to healthcare providers and patients at a lower cost compared to the originators. Unlike small-molecule generic drug products, which are structurally replicable and well-defined, that guarantee the safety and efficacy, biologic products are structurally complex, larger in size and often contain mixtures of various posttranslational modifications. Consequently, demonstrating the similarity of a biosimilar molecule with the reference product requires extensive characterization to ensure safety and efficay.

One of the challenges in developing a biosimilar product is the lack of knowledge about the reference product's manufacturing process, which is not accessible to the public because it is a proprietary knowledge. Therefore, the biosimilar sponsor needs to develop a process by extensive characterization of a biosimilar candidate side-by-side with a reference product. This is an iterative process aimed at developing a biosimilar molecule similar to the reference product. The first step in biosimilarity assessment is to establish structural similarity by extensive characterization using several analytical techniques. Therefore, analytical tools play a vital role in demonstrating structural similarity as well as process development of a biosimilar candidate. In addition, the level of similarity established by the analytical tools guides the type of non-clinical and clinical data packages required for regulatory approval. If a high degree of similarity is demonstrated using analytical techniques, then phase II clinical trials are not required for

registration of a biosimilar candidate. Consequently, this will lower the cost of developing a biosimilar product. Hence, developing sensitive and robust analytical techniques is vital in a biosimilar development process.

In this dissertation, four homogeneous glycoforms of IgG1 Fc (HM-Fc, GlcNAc-Fc, Man5-Fc, and N297Q-Fc) were produced using recombinant protein expression combined with *in-vitro* enzymatic reactions to be utilized as a model for biosimilar comparability analysis. These glycoforms were characterized by mass spectrometry, SEC, SDS-PAGE, and cIEF. The main focus of the project was to produce homogeneous glycoforms of IgG1 Fc and to utilize them to develop new biolayer interferometry (BLItz) assay methods. Two biolayer interferometry methods with different immobilization techniques were developed to measure the binding affinity of IgG1 Fc glycoforms to FcγRIIIa and FcγRIIb. In addition, these four glycoforms were mixed in pre-defined composition to examine the characteristics of mixtures of glycoforms and to study important biological and physicochemical features of protein drugs in a biosimilar analysis. For the mixture samples, differences in binding were observed when the two immobilization formats were employed. Furthermore, these glycoforms were incubated at low and elevated temperatures for an elongated time, and a trend of decreasing binding affinity was observed with the increasing incubation period.

Acknowledgement

The accomplishments described in this dissertation would not have been possible without the tremendous contributions from many talented people and to all of them, I owe my sincerest gratitude. First, I would like to express my deep appreciation and gratitude to my advisor, Dr. Thomas Tolbert for all of his support, leadership, patience, motivation, and mentorship throughout my research. A lot of resources and efforts were invested in this dissertation, and all of this was made possible through his support. Dr. Tolbert has been very instrumental in my growth as an independent thinker and researcher. I have learned a lot from his extensive knowledge, and I admire his enthusiasm for science, and willingness to share his knowledge. His contributions made my research and life as a graduate student less daunting. I appreciate all of his efforts and contributions.

The work described in this dissertation was done in collaboration with Dr. Volkin, and I want to express my deepest gratitude for all of his input. I will forever be thankful to Dr. David Volkin for his guidance, inspiration, and continuous support throughout my research. With his help, I was able to accomplish a lot, and I am very much appreciative of that. Dr. Volkin has been a great resource for me. I admire his vision, knowledge, and organizational skills.

I would like to thank Dr. Teruna Siahaan, Dr. Michael Wang, and Dr. Christian J. Ray for agreeing to serve on my dissertation defense committee. I appreciate your commitment, helpful suggestions, and corrections. Thank you very much for finding time to evaluate my thesis research. I would like to specifically thank Dr. Siahaan for the advice and mentorship in my biotech training. This was truly a great learning experience for me. I would like to thank all the faculty in the Department of Pharmaceutical Chemistry for the excellent coursework, discussions,

and lectures that helped me advance my scientific knowledge. I would also like to extend my gratitude to all the students and members of the department. My interactions with various individuals in the department helped me develop and master my research skills, and this laid the foundation for all the good research, presentations, and scientific writings that I was able to accomplish. I would like to thank Dr. Russell Middaugh, Dr. Christian Schöneich, and Dr. Sangeeta Joshi for their support and all the contributions. I will forever be grateful.

Finally, I would like to thank my family for their love, unwavering support, and inspiration throughout my life. Thank you very much for giving me the strength, faith, and confidence to pursue my dreams. I owe them a lot for all the things that I have achieved.

Dedicated to:

My

Mother

(Tsehaytu Isaack)

Father

(Zeray Okbazghi)

Table of Contents

Chapter 1

Introduction

1.1 Impact of Glycosylation on Antibody Structure and Activity

Immunoglobulin G (IgG) contains two heavy chains and light chains that form the fragment crystallizable (Fc) and fragment antigen binding (Fab) regions. The Fc is a homodimer containing, a conserved glycosylation site within the C_H2 at Asparagine-297 (Figure 1). This glycosylation site is known to play a critical role in the structural integrity, functional activity, and stability of therapeutic monoclonal antibodies (mAbs).[1] For example, a significant number of publications reported that non-fucosylated mAbs bind to FcγRIIIa about 50- to 100-fold more tightly than their fucosylated counterparts. This increase in binding affinity correlated with a higher antibody-dependent cytotoxicity (ADCC) response.[2-9] Similarly, the presence of sialic acid in the Fc glycans (e.g., G2F+ NANA in Figure 1) was proposed to be necessary for the anti-inflammatory activity of Intravenous Immunoglobulin (IVIG). Interestingly, it has been shown that the removal of sialic acid abrogates the anti-inflammatory effect and turns the activity to pro-inflammatory.[10-12] Additionally, glycans influence the pharmacokinetics of therapeutic mAbs. One such example is the systemic clearance of antibodies containing 100% of high-mannose which is found to be faster than antibodies that contain complex glycans. This faster clearance is presumably due to mannose binding receptors in the liver.[13-14] As shown in Figure 1 Man8 and G2F+NANA are examples of high-mannose and complex glycans, respectively. In addition, differentially sialylated glycoprotein therapeutics may also display decreased pharmacokinetic and pharmacodynamic (PK/PD) properties due to carbohydrate binding to asialoglycoprotein receptor expressed in the liver. This desialylated glycoprotein is selectively taken and rapidly degraded in the liver.[15-16] Immunogenicity is another important clinical factor that can be affected by glycans. For instance, it has been reported that murine cells can potentially produce non-

human immunogenic glycoforms, such as a terminal N-glycosyl-sialic acid (NeuSGc) and gal-1,3 gal linkage.[17] As a result, close monitoring of the glycan profile is required during the production and development of therapeutics mAbs.

1.2 Glycosylation Heterogeneity and its Effect on Product Development

Glycosylation is heterogeneous by nature that includes the differential addition of fucose, alternative mannose branching linkages, presence or absence of galactose, and terminal sialylation as shown in Figure 1. Furthermore, there could be site-occupancy heterogeneity in which one of the heavy chains is non-glycosylated, resulting in asymmetric glycosylation.[17] This heterogeneity in glycosylation pattern could be due to several factors such as culture media composition, growth condition, cultivation procedure, and type of cell line used.[18-22] One typical example is a significant difference in sialylation observed when the same mAb was produced in myeloma cell line (NSO) vs. Chinese hamster ovary (CHO).[23] In another study, it has been reported that a significant variability was observed in galactosylation among therapeutic mAbs produced by different manufacturers. Therapeutic mAbs expressed in CHO cells showed a higher level of G0 glycans when compared with mAbs expressed in mouse myeloma cell lines.[24] The variability in glycosylation profile indicates that the production of therapeutic antibodies with a homogeneous glycosylation profile for a particular functional activity remains a significant challenge.[1] In contrast to the primary amino acid sequence of proteins which is a template-driven process, glycosylation of recombinant proteins is not a guided synthesis. As a result, glycosylation is subject to a high degree of heterogeneity.[25-26] X-ray crystallographic studies have shown that the pair of carbohydrate chains are buried inside the hydrophobic core of the two C_H2 domains.[27] The Man α-1,6 arm makes contact with an inner surface of the C_H2 domain, whereas the Man α-

1,3 arm protrudes into the space between the C_H2 domains (Figure 2). This structural environment creates steric hindrance that restricts access to the glycan processing enzymes, such as glycosyltransferases and glycosyl hydrolases in the endoplasmic reticulum and Golgi complex.[26-28]

1.3 Recombinant Protein Expression in Yeast

Mammalian cell cultures have been commonly used for the production of monoclonal antibodies. However, compared to mammalian cells, glycoengineered *P. pastoris* provides many advantages, such as easy genetic manipulation, reduced cultivation time, high-yield, low-cost fermentation, and no risk of human pathogenic viral contamination.[29-30] The Pichia expression system has more considerable flexibility in producing glycoengineered IgGs compared to mammalian expression system.[31] As a result, a particular focus was given to the production of mammalian complex-type structures in *P.pastoris* by engineering the N-glycosylation pathway. Recently, an advance has been made in improving glycosylation site occupancy at Asn297 to greater than 99%, which is comparable to the site occupancy expected from mammalian cell line expression.[32] It has been reported that Pichia produces stable IgGs with comparable aggregation, charge variant, and oxidation profile compared to the same IgGs produced from mammalian cell line.[31] Thus, glycoengineered Pichia offers a promising platform for the production of IgGs.

1.4 Demonstrating Biosimilarity of Protein Therapeutics

Several top-selling commercialized biologics are coming off patent; as a result, biosimilars are expected to be accessible to patients and healthcare providers at a lower cost in the near future. Biosimilars are biological products that are approved because they are “highly similar” to an already-approved biological product, known as the reference product (originator). Food and

Drug Administration (FDA) defines biosimilarity to mean "That the biological product is highly similar to the reference product notwithstanding minor differences in clinically inactive components" and that "there are no clinically meaningful differences between the biological product and the reference product in terms of the safety, purity, and potency of the product".[33] Biosimilars should demonstrate no clinically meaningful differences in terms of safety and effectiveness when they are compared with the reference product. Likewise, biosimilars should have the same mechanism of action and use for the same indication as for the reference product.[34]

The processes of developing a biosimilar heavily depend on the depth of knowledge collected from the reference product, which will aid in getting faster regulatory approval (Figures 3 and 4).[34] The first step in biosimilarity assessment is an extensive characterization of the reference product to identify critical quality attributes (Figure 3). After studying the reference product, in the early phase of the development processes, analytical techniques are employed to establish structural and functional similarity.[34-35] Technically, a biosimilar candidate is compared head-to-head with the reference product at each stage of the development processes to ensure safety and efficacy.[34]

The type of additional test required for regulatory approval is determined on a case-by-case basis and by the level of similarity demonstrated during the analytical assessment. In other words, the degree of similarity demonstrated by the analytical methods ultimately guides the type of next steps required for approval.[34] For instance, if "highly similar" is confirmed by the analytical data then, a reduced clinical test may be required which ultimately resulting in time and cost savings.[34, 36-37] In addition, the discovery phase as well dose-finding studies (phase II) are

not required in the development process because biosimilar development uses the same dosing as the reference product and this may contribute to the reduction of time and cost of development (Figure 4). Filgrastim-sndz, a biosimilar to Neupogen, was the first biosimilar product approved by the Food and Drug Administration (FDA) in 2015.[38] One additional example was Inflectra (infliximab-dyyb), a biosimilar to Remicade which was approved in 2016.[39]

1.4.1 Biological Evaluation in Biosimilarity Study

Protein molecules are complex in structure and possess a dynamic three-dimensional structure. The folded conformation of a protein can be altered by process and storage conditions, such as pH, temperature, and pressure. Functional activity is dependent on the conformation of the protein, which is a higher-order structure. Therefore, testing the primary structure without the tertiary structure does not necessarily guarantee the biological activity.[23] In a biosimilar assessment, extensive functional characterization of both the proposed product and the originator is required to establish similarity. Therapeutic mAbs mediate their effector function by the Fc region (Figure 1). Thus, biological characterizations for examination of the Fc effector function are used in similarity exercise. Such tests are necessary even if the mechanism of action is not related to the Fc because a change in glycosylation profile can have a negative impact on the safety of therapeutic mAbs. As a result, the Fc region is important for the safety, structure, and function of the mAbs.[40] Moreover, monitoring glycosylation of mAbs during a biosimilar development process is essential because differential glycosylation can alter the functional activity (ADCC and CDC),[19, 41] immunogenicity,[21, 37, 42-45] pharmacokinetics,[15-16, 46-48] and the stability of therapeutic mAbs.[49]

Biological tests (e.g., potency assay) are routinely used in quality control setting to monitor the potency of a product during manufacturing. These assay methods should be sensitive enough to detect structural changes with a potential impact on the safety as well as efficacy of the product. Although such techniques can provide relevant information, the correlation between potency assay and the mechanism of action of the treatment cannot be established with a high degree of certainty. Nevertheless, biological assays can be used to establish functional equivalence in a biosimilar comparability assessment. In addition, functional assays can be employed together with biophysical assays to confirm higher-order structural similarity.[40] overall, a biological assay provides critical information about the characteristics of a biosimilar candidate related to its function and thereby demonstrates the similarity with the originator. Furthermore, a biological assay complements the physicochemical analysis by demonstrating potential effects of structural difference between a reference product and the biosimilar candidate.[34, 50]

1.4.1.1 Fc Receptor Binding Assays

Monoclonal antibodies are composed of two Fab regions and one Fc region. These regions regulate the functional activity and may need to be tested for their capacity to interact with their specific targets.[51] For instance, the Fc region specific targets include but are not limited to FcγRIIIa, FcγRIIb, FcγRIIa, and FcγRI. Several mAbs exert their activity by binding their Fc region with Fc receptors. Therefore, Fc receptor binding is part of the functional characterization in the comparative assessment during a biosimilar product development. This binding interaction is substantially affected by the N-linked glycans in the Fc region of the mAbs. As a result, characterization of glycosylation is one of the main characteristics of mAbs that received

significant attention by the regularity agencies.[42] Determining the binding activity of monoclonal antibody drugs is performed using a series of *in-vitro* binding assays, such as bioLayer Interferometry (BLI), surface plasmon resonance (SPR), and enzyme-linked immunosorbent assays (ELISA).[52]

For instance, the binding interactions of Remicade (originator) and Remsima (a biosimilar product) with FcγRIIIa were compared using a biolayer interferometry technique. The result showed that Remicade binds with a two-fold higher affinity when compared with Remsima. This higher binding affinity was attributed to the substantial proportion of non-fucosylation level in Remicade when compared to Remsima. This difference in fucosylation level was due to the differences in cell line (subtle genetic variants) used for production.[39] In general, binding assays can provide information to predict how a biosimilar may behave *in-vivo*, although not as much regarding safety. Thus, such tests together with other analytical data may provide evidence of clinical testing.[34, 50] If a higher level of similarity was established using physicochemical and *in-vitro* bioassay studies, there would be fewer chances that a new safety issue would rise at a later stage.[35]

1.5 Binding Interaction Models and Equations

1.5.1 1:1 Binding Model

The ideal model of interaction, in which one ligand molecule binds with one analyte molecule assumes all interaction sites on the ligand are equivalent and independent of one another. Additionally, the 1:1 binding model assumes the interaction between ligand and analyte follows the pseudo-first-order kinetics. The association and dissociation phases display a time-resolved signal that is described by a single exponential function. Furthermore, analyte molecules bind and dissociate at the same rate to every ligand binding site. The association curve follows a hyperbolic binding profile, with the exponential increase in signal followed by a leveling off to plateau as the binding reaches equilibrium.[53,54] The dissociation curve follows single exponential decay with signal eventually returning to baseline.

Kinetic analysis of 1:1 binding model is based on the concept that the interaction between a monovalent analyte, A, and immobilized component, B, on the sensor surface is described by the reaction scheme as follows.[53]

$$\mathrm{A} + \mathrm{B} \rightleftharpoons \mathrm{AB}$$

The interaction between the two components is assumed to be reversible complex.[54]

The rate of formation of the product AB at a time t can be written as follows:

$$\frac{d[AB]}{dt} = k_{on}[A][B] - k_{off}[AB] \cdots\cdots\cdots\cdots\cdots\cdots\cdots\cdots\cdots\cdots (1)$$

Where k_{on} and k_{off} are the respective association and dissociation rate constants.[55] The term k_{off} measures the stability of the complex, or the fraction of complexes that decay per second, and is expressed in units of sec^{-1}. The association rate constant, k_{on}, represents the number of AB complexes formed per second in a 1 molar solution of A and B. The k_{on} is

expressed in $M^{-1}sec^{-1}$. K_D is the affinity constant, or equilibrium dissociation constant, which measures how tightly the ligand binds to its analyte. It represents the ratio of the on-rate to the off-rate and can be calculated using k_{on} and k_{off}. K_D is expressed in molar units (M).

After some time, t, the concentration of unbound immobilized ligand is expressed as:

$$[B] = [AB]_{max} - [AB]$$

$[AB]_{max}$ is the maximum complex formed when all ligand binding sites are occupied, which is theoretical binding capacity. Substituting into equation 1 gives.[54]

$$\frac{d[AB]}{dt} = k_{on}[A]([AB]_{max} - [AB]) - k_{off}[AB] \dots\dots\dots\dots\dots\dots\dots\dots\dots\dots (2)$$

This equation describes the interaction between the analyte in solution, and the free binding sites on the surface, minus the simultaneously occurring dissociation of the complex formed.[56] The signal observed R is proportional to the formation of AB complex at the surface of the biosensor, and the maximum signal R_{max} is proportional to the maximum complex formation $[AB]_{max}$. R_{max} is the maximum response that would be obtained if all ligand binding sites were saturated.[56] Therefore, equation two can be written as shown below.[56]

$$\frac{d[R]}{dt} = k_{on}C(R_{max} - R) - k_{off}R \dots\dots\dots\dots\dots\dots (3)$$

Where dR/dt is the rate of formation of the complexes on the surface of the biosensor, (i.e., the derivative of the observed response curve), C is the concentration of the analyte in solution; R_{max} is the maximum capacity of the immobilized ligand surface expressed in resonance units, and R_{max} -R represents the number of unoccupied surface binding sites at the time t.[54] The above equation was rearranged and integrated to give the final equation as shown below.

$$R = \frac{k_{on}CR_{max}}{k_{on}C + k_{off}}\left(1 - e^{-(k_{on}C + k_{off})(t - t_0)}\right) \dots\dots\dots\dots\dots\dots (4)$$

The above equation describes 1:1 binding where a single analyte molecule interacts with one ligand molecule. The assumption in the above equation is that all binding sites are equivalent and independent of one another. In addition, it is assumed that all binding events are governed by the same free energy of binding. This is a reasonable assumption if all immobilized antigens are equally accessible, and only monovalent complexes are involved. This assumption many not be valid when bivalent binding occurs, since bridging complexes of different geometries will be obtained, leading to a range of on rates and off-rates.[56] One additional assumption is that the analyte concentration maintains its initial value, C due to the presence of the excess analyte in the cuvette. Hence the interaction is pseudo first order.[53]

The dissociation phase is described by the equation as follows:

$$R = R_d e^{-(t-t_c)k_{off}} + R_\infty \ldots\ldots\ldots\ldots\ldots\ldots\ldots\ldots\ldots\ldots\ldots\ldots (5)$$

Where R_d is *the* initial response before the dissociation starts R_∞ is the response at the end of the dissociation phase. To account for the fact that even after complete dissociation of the complex, AB, from the surface of the sensor chip the instrument response is not zero.[54]

The final equation that combines the association and dissociation phases is given below

$$R = \frac{k_{on}CR_{max}}{k_{on}C + k_{off}}\left(1 - e^{-(k_{on}C + k_{off})(t-t_0)}\right) + R_0 e^{-(t-t_c)k_{off}} + R_\infty \ldots\ldots\ldots\ldots\ldots\ldots\ldots\ldots\ldots (6)$$

$$R_{eq} = \frac{k_{on}CR_{max}}{k_{on}C + k_{off}}$$

R_{eq} is the equilibrium response for a given concentration.

The final equation can be further modified to as shown below.

$$R = R_{eq}\left(1 - e^{-(k_{on}C + k_{off})(t-t_0)}\right) + R_0 e^{-(t-t_c)k_{off}} + R_\infty \ldots\ldots\ldots\ldots\ldots\ldots\ldots\ldots (7)$$

1.5.2 Heterogeneous Ligand Binding Model

The 2:1 heterogeneous ligand model assumes one analyte binding at two independent ligand sites. Each ligand site binds the analyte independently and with a different rate constant. Mathematically, the equation used to fit a 2:1 binding interaction is a combination of two 1:1 curve fits. Two sets of rate constants are given, one for each interaction: where A represents the analyte and B represents the immobilized ligand.

The binding interaction is the sum of two independent reactions.

$$\mathrm{A} + \mathrm{B1} \rightleftharpoons \mathrm{AB1}, \quad \mathrm{A} + \mathrm{B2} \rightleftharpoons \mathrm{AB2}$$

Let $[AB_1] = R_1$is the complex formed between the analyte and ligand one and $[AB_1]_{max}$ is the maximum available sites for binding site B_1 or maximum binding capacity of ligand one and $[AB_2] = R_2$ is the complex formed between the analyte and ligand one and $[AB_2]_{max}$ is the maximum available sites for binding site B_2, maximum binding capacity of ligand two, A= is the analyte concentration expressed as C.

$$[B_1] = [AB_1]_{max} - [AB_1] = R_{max1} - R_1, \qquad [B_2] = [AB_2]_{max} - [AB_2] = R_{max2} - R_2$$

$$\frac{d[AB_1]}{dt} = k_{on1}[A][B_1] - k_{off1}[AB_1] \qquad \frac{d[AB_2]}{dt} = k_{on2}[A][B_2] - k_{off2}[AB_2]$$

After integration, the response for the association phase is expressed by the equation

$$R = \frac{k_{on1}CR_{max1}}{k_{on1}C + k_{off1}}\left(1 - e^{-(k_{on1}C + k_{off1})(t-t_0)}\right) + \frac{k_{on2}CR_{max2}}{k_{on2}C + k_{off2}}\left(1 - e^{-(k_{on2}C + k_{off2})(t-t_0)}\right) \ldots\ldots\ldots\ldots\ldots\ldots (8)$$

The dissociation phase is given as a biphasic model as shown below let R_{d1} is the initial response before dissociation phase 1 and R_{d2} is the initial response before dissociation phase 2.

Where k_{on1} and k_{off1} are the rate constants describing one interaction with a maximal response of R_{max1} , and k_{on2} and k_{off2} are the rate constants describing the second interaction with a maximum response of R_{max2}.[54]

$$y = R_{d1}\, e^{-(t-t_c)k_{off1}} + R_{d2}\, e^{-(t-t_c)k_{off2}} + R_{\infty} \ldots\ldots\ldots\ldots (9)$$

The final equation for the heterogeneous binding model is shown below.

$$R = \frac{k_{on1}CR_{max1}}{k_{on1}C + k_{off1}}\left(1 - e^{-(k_{on1}C + k_{off1})(t-t_0)}\right) + \frac{k_{on2}CR_{max2}}{k_{on2}C + k_{off2}}\left(1 - e^{-(k_{on2}C + k_{off2})(t-t_0)}\right) + R_{d1}\, e^{-(t-t_c)k_{off1}} + R_{d2}\, e^{-(t-t_c)k_{off2}} + R_{\infty}$$

Equation (10)

The above equation can be rewritten in more simplified form as follows:

$$R = R_{eq1}\left(1 - e^{-(k_{on1}C + k_{off1})(t-t_0)}\right) + R_{eq2}\left(1 - e^{-(k_{on2}C + k_{off2})(t-t_0)}\right) + R_{d1}\, e^{-(t-t_c)k_{off1}} + R_{d2}\, e^{-(t-t_c)k_{off2}} + R_{\infty} \ldots\ldots\ldots\ldots (11)$$

1.5.3 Heterogeneous Analyte Competing for a Single Ligand Binding Site Model

Two analytes in solution are competing for a sing ligand immobilized onto the biosensor surface.[57] The concentration and molecular weight of the two components should be known before analysis. A_1 and A_2 are two analytes competing for a single binding site B and the equation can be described as follows:

$A_1 + B \rightleftharpoons A_1B$ $\quad A_1B = R_1$ $\quad A_2 + B \rightleftharpoons A_2B$ $\quad A_2B = R_2$ $\quad$ Let A=C

$[B_1] = [A_1B]_{max} - [A_1B] = R_{max1} - R_1$ $\quad [B_2] = [A_2B]_{max} - [A_2B] = R_{max2} - R_2$

R_1 and R_2 correspond to the concentration of the molecular complexes formed. C_1 and C_2 are the concentrations of the analytes A_1 and A_2.[58]

$$\frac{dR_1}{dt} = k_{on1}C_1(R_{max} - R_1 - R_2P) - k_{off1}R_1 \qquad \frac{dR_2}{dt} = k_{on2}C_2(R_{max}\frac{1}{p} - R_1\frac{1}{p} - R_2) - k_{off2}R_2$$

R_{max} corresponds to the total concentration of the immobilized partner. For competing reactions, p is a normalizing factor. This parameter is introduced since specific responses are different for analytes of different molecular weight.[58] After integration, the above differential equations is described as follows:

$$R = \frac{k_{on1}C_1R_{max}}{2k_{on1}C_1 + k_{off1}}\left(1 - e^{-(2k_{on1}C_1 + k_{off1})(t-t_0)}\right) + \frac{k_{on2}C_2\frac{1}{p}(R_{max})}{2k_{on2}C_2 + k_{off2}}\left(1 - e^{-(2k_{on2}C_2 + k_{off2})(t-t_0)}\right) \ldots\ldots\ldots (12)$$

The dissociation phase is given as a biphasic model as shown below let R_{d1} is the initial response before dissociation phase 1 and R_{d2} is the initial response before dissociation phase 2.

$$y = R_{d1}\, e^{-(t-t_c)k_{off1}} + R_{d2}\, e^{-(t-t_c)k_{off2}} + R_{\infty}$$

Moreover, the final that includes the association and dissociation phases is as described below.

$$R = \frac{k_{on1}C_1R_{max}}{2k_{on1}C_1 + k_{off1}}\left(1 - e^{-\left(2k_{on1}C_1 + k_{off1}\right)(t-t_0)}\right) + \frac{k_{on2}C_2\frac{1}{p}(R_{max})}{2k_{on2}C_2 + k_{off2}}\left(1 - e^{-\left(2k_{on2}C_2 + k_{off2}\right)(t-t_0)}\right) + R_{d1}\, e^{-(t-t_c)k_{off1}} + R_{d2}\, e^{-(t-t_c)k_{off2}} + R_{\infty} \ldots\ldots\ldots (13)$$

1.6 Challenges in Developing a Biosimilar Product

Small molecules are defined by their chemical structure, while protein molecules are not completely defined by their amino acid sequences and are mixtures of different variants due to posttranslational modifications. The challenge of developing biosimilar products is that they are not generic products, and for biologics, the operative paradigm is that the bioprocesses define the product.[52] Moreover, even minor changes in the manufacturing protocol can lead to a significant change in post-translational modifications (PTMs) and product variations.[52, 59] Since the manufacturing process of the originator is undisclosed, a biosimilar product has to be produced with a different process. It is well known that minor changes in the manufacturing process can have a significant effect on the products quality.[34, 50] For instance, glycosylation is relevant for the biological activity; however, a change in glycosylation profile can have a negative impact on the safety and efficacy of a mAb therapeutic.[60] Thus, the biosimilar sponsor is required to demonstrate specific quality attributes of the originator and biosimilar using appropriate techniques.[20] Similarly, chemical modifications, such as deamidation, isomerization, and oxidized forms, can affect the structure. Likewise, non-native structures, such as aggregates generated during production, can have a detrimental effect on the product's quality.[37] Because of these challenges, development timeline for a biosimilar product is longer and expensive compared to small-molecule generic drugs.[61]

1.7 Demonstrating Comparability of Protein Therapeutics

The implementation of changes in process or changes related to the product (e.g., formulation), during development as well as after commercialization, needs an assessment of their effect on the safety and efficacy of the product. This exercise to demonstrate the similarity

between the post-change and pre-change is known as a comparability study.[23] Manufacturers of biological products (e.g., mAbs) often make changes to the manufacturing process of products during development phase as well as after commercialization. Any change made that can potentially affect the product quality, such as manufacturing protocol, formulation condition, and cell-line clone, requires a comparability study. The main reasons behind such changes include the following: improving the bioprocess protocol, scale up, improving product stability, and complying with new regulatory requirements. When changes are made to the bioprocess protocol, the manufacturer examines the critical quality attributes of the product to show that modifications did not occur that would negatively affect the safety and efficacy of the biological product.[62] For example, oligosaccharide moieties in monoclonal antibodies (mAbs) were known to be affected by the bioprocess parameters, duration of expression, and cell-line type. In addition, the protein can undergo physicochemical changes during production, which may lead to more structural heterogeneity. Certainly, the effect of the posttranslational modifications on the safety and efficacy of a post-change product needs to be examined.[23]

Physicochemical characterizations using a vast array of analytical techniques are examined in all comparability studies. In a similar fashion, the extensive biological characterization in combination with pharmacokinetic and pharmacodynamic data can be used to demonstrate functional equivalence. If the results of these characterizations suggest “highly similar,” then other clinical studies are not necessary. However, if the comparison of the pre-change and post-change product is found to be either inconclusive or showed differences, then clinical studies are required for regulatory approval.[23, 62]

1.8 Differences Between Comparability and Biosimilarity Assessments

A comparability study is aimed at demonstrating that the post-change has no negative effect on the safety, efficacy, and quality of the biological product. The primary goal of biosimilarity assessment is to demonstrate the similarity of a biosimilar candidate with the reference product in terms of physicochemical and biological quality attributes as well as safety and efficacy. Therefore, a biosimilar assessment is more deferent than a comparability assessment, which requires extensive characterization of a biologic product. Moreover, development of a biosimilar product by demonstrating similarity with the originator is a more challenging task than comparability assessment of the pre-change and post-change of an originator product.[63-64]

A comparability assessment involves extensive characterization of several lots of the originator's pre- and post-process changes. This characterization data can provide enough evidence to confirm that the safety and efficacy of the post-change remained within the pre-change range. This comparability claim can be supported by the pre-change clinical data, manufacturing history, analytical methods, and a post-approval history. It is worth noting that these historical data are not accessible to a biosimilar sponsor. Therefore, the manufacturing processes of a biosimilar candidate have to be developed by reverse engineering. Manufacturing process development is one of the challenging tasks in biosimilar product development as described below.[63-64]

1.8.1 Manufacturing Processes

Manufacturing biologic products is a complex process because of their large size and structural complexity, coupled with variability in expression system and cell lines.[65-66] Biosimilar

sponsors have to develop a new cell line, cell culture condition, analytical methods, purification, and formulation of the biosimilar candidate with a limited knowledge of a reference product. Developing a new cell line for a biosimilar candidate can potentially lead to differences in glycosylation, aggregation, oxidation, and 3-D structures. This is in contrast to comparability assessment, which is a minor change in manufacturing processes and the post-change is with the available historical data of the pre-change. However, even a minor change in processes change can have a detrimental effect on the product safety and efficacy. For instance, the immunogenicity of epoteins has been attributed to an aggregation that arises after processes change.[67-68] Manufacturing processes are continuously changed during product development as well as after commercialization. Some of the reasons for manufacturing changes are to improve operation, yield, and safety profile, as well as to change raw materials. The manufacturing processes could be minor or major, which depends on the type of change introduced. An example of major manufacturing change would be an alteration of the cell line, culture media composition, and purification processes. All of these changes can potentially affect the safety and efficacy of the biologic product.[63-64]

In a comparability assessment, expression parameters, such as pH, temperature, and shear forces, can have a significant effect on the product safety and efficacy. As a result, heterogeneity between the different batches needs to be assessed on a routine basis. Most of the heterogeneity of the biologic product is attributed to glycosylation and to some extent, additional post-translational modifications, such as oxidation, deamidation, fragmentation, and aggregation. For instance, monoclonal antibodies are glycosylated and controlling glycosylation within a defined range to confirm safety and efficacy is required.[69-70] Moreover, during product

development, the condition of expression can affect the glycosylation profile of a biological product. For instance, a biologic product with α-gal glycans can potentially induce immunogenicity.[63-64]

As described above, the process development, controls, and methods not accessible to a biosimilar sponsor. Thus, biosimilar manufacturing faces a "knowledge gap" and should develop a new cell line, manufacturing protocol, and purification processes aimed at producing a product highly similar to the originator.[71] Furthermore, to address the knowledge gap, the biosimilar sponsor uses an approach of "reverse-engineering" of the manufacturing processes with the main focus being on the critical quality attribute of the biosimilar product. In other words, process development of a biosimilar candidate is an iterative process, in which the manufacturing processes are adjusted until the critical quality attributes of the biosimilar are highly similar to the originator. Therefore, the objective is to reverse-engineer the biosimilar candidate aimed at producing highly similar to the reference product. Again, all the development process is performed with limited knowledge of the reference product manufacturing processes.[63-64]

1.8.2 Regulatory Approval Requirments

In a comparability assessment, a minor change in manufacturing processes can be approved without clinical trials. However, high-risk manufacturing changes require clinical trials to demonstrate the pre-change is similar to the post-change. Unlike comparability, biosimilar development is more than high-risk manufacturing changes because of the knowledge gap as well as the lack of accessible historical data of the reference product. Therefore, as outlined in ICHQSE "more data and information will be needed to establish biosimilarity than would be

needed to establish that a manufacturer's post-manufacturing change product is comparable to the pre-manufacturing change product".[63-64]

Biosimilar sponsors must establish analytical and pre-clinical biosimilarity assessments as well as clinical data for regulatory approval. This is in contrast to comparability that requires a limited data package for regulatory approval. However, if substantial process changes have been implemented during comparability assessment, then clinical and non-clinical tests may be required. For instance, the production scale-up of Lumizyme® within the same manufacturing facility showed significant differences in glycosylation and PK profiles between the pre-change and post-change. Thus, additional clinical data were required for regulatory approval of Lumizyme®. Similarly, after scaling up the fermentation, analytical and PK data failed to demonstrate comparability of alglucosidase Alfa. Therefore, the level of data required for approval in comparability exercise depends on the type of change introduced and its impact on the critical quality attributes. Nevertheless, the approval processes for a biosimilar is different from the processes needed for approval of a comparability process. Moreover, there are clear differences between the data package and approval processes required for a biosimilar product and assessment of comparability (manufacturing changes).[63-64]

In the biosimilarity assessment, the totality of the data is considered for regulatory approval, such as structural and functional characterization, immunogenicity, pharmacodynamic, and comparative clinical study. The first biosimilar to be approved by this regulatory pathway was Zarxio™, which was a recombinant granulocytes colony-stimulator factor. For regulatory approval after the process change (i.e., in comparability assessment), the historical data generated pre-change can be used to compare with the post-change to predict no adverse effect

on the safety and efficacy of the product is anticipated. However, if the analytical test cannot demonstrate comparability, then a non-clinical test of the post-change product should be conducted to ensure safety and efficacy. This is in contrast to the biosimilarity assessment's comprehensive side-by-side testing showing similarity to the reference product is performed. Demonstrating a high degree of similarity is the basis for reduced clinical trials. Unlike comparability, side-by-side non-clinical and clinical safety data as well as immunogenicity assessment are required to support a claim of biosimilarity. In addition, pharmacokinetics and pharmacodynamics profiles as well as efficacy trials are also necessary to gain regulatory approval.[63]

1.9 Stability of Protein Therapeutics

1.9.1 Physical Stability of Proteins

The number of mAbs approved for treatment of various diseases has increased significantly over the last decade, and this trend continues today.[72] There are many advantages of antibodies compared to other proteins, such as specificity, fewer side effects, and less immunogenicity. Also, antibodies can be conjugated with other small-molecule drugs for efficient delivery to their target site. Immunoglobulin G structure comprises the Fab and the Fc. The Fab region contains heavy and light chains. The Fc and the Fab are connected at the hinge region (via disulfide bonds) and form the Y-shaped structure.[73-74] The Fc portion of IgG contains two identical heavy chains, and each comprises C_H2 and C_H3 domain. The C_H2 domains are connected by a disulfide bond, whereas a detailed study indicates that the two C_H3 domains are stabilized by non-covalent interaction (Figures 1 and 2).[75]

Antibodies are heterogeneous in their structure because of the variation in glycosylation pattern and physicochemical changes during production. The chemical modification includes the following: C-terminal variability, oxidation, deamidation, and fragmentation.[76] For instance, in one study that used capillary isoelectric focusing (cIEF), five charge isoforms were isolated indicating the level of heterogeneity generated.[77] Similarly, physical degradation of antibodies was observed in liquid, frozen, and lyophilized states. In most cases, various degradation pathways can occur simultaneously, depending on the type of stress applied and the solution condition.[78] This creates an immense challenge in developing therapeutic protein products.[72]

Antibodies can denature upon exposure to high temperature, shear, and extreme pH, which ultimately leads to loss of potency. For instance, a recombinant scFv antibody fragment functional activity was decreased after a shear, likely due to denaturation.[72, 79-80] Several reports indicate that thermal treatment produces noncovalent linked aggregated, dimers, and monomers.[72 81]Antibody aggregation is usually observed after physical instability and, to some extent, chemical instability. Protein aggregation is known to increase as concentration increases and creates significant challenges in high concentration formulation development.[82] However, one advantage of high-protein concentration formulation is its stability during freeze-thaw. Protein at a high concentration is more resistant to freeze-thaw-induced aggregations, as the interface-induced protein denatures can quickly reach a saturation point.[72] Besides heating, low-temperature storage can induce aggregation. For instance, it has been reported that Igm cryoglobulin precipitated at storage temperature below 10°C.

Other studies indicate that the aggregation of IgG1 at a low temperature and surprisingly the processes are reversible upon increasing the storage temperature.[83] One plausible theory as

to how low temperature causes aggregation and precipitations is that a decrease in temperature reduces the hydrophobic interaction, and consequently, leads to exposure of hydrophobic surfaces. This exposure leads to an increase in protein-protein interaction and results in aggregation.[72]

Glycosylation can affect the physical stability and solubility of antibodies, as shown in many studies.[84] For example, the physical stability of IgG1 Fc glycoforms with a different site occupancy (expressed in *P.pastoris*) was studied in detail. The diglycosylated showed the highest physical stability. The non-glycosylated IgG1 Fc (N297Q-Fc) showed the lowest stability indicating the effect of glycosylation on the stability. The mono-glycosylated IgG1 Fc (glycosylated in one site) showed the least physical stabilities. Furthermore, non-native structure from circular dichroism (CD) and intrinsic fluorescence was observed, which was reversible upon the removal of the glycan (i.e., treatment with PNGase F). Functional activity studies showed that the mono-glycosylated Fc binds two-fold less than the diglycosylated in agreement with other reports.[49] These studies indicated the role of glycosylation on the higher-order structure of IgG, which impacts the stability and functional activity.

In a similar study, the solubility and physical stabilities of four glycoforms (HM-Fc, Man5-Fc. GlcNAc-Fc, and N297Q-Fc) were studied in detail. The results indicated that the diglycosylated HM-Fc ($Man_8GlcNAc_2$) and Man5-Fc ($Man_5GlcNAc_2$) have higher solubility and physical stabilities. Comparatively, the GlcNAc-Fc has lower physical stability and solubility. The solubility and physical stability of N297Q-Fc significantly decreased compared to the other glycoforms, indicating the effect of the glycans. Other studies suggested that removal of glycan exposes the hydrophobic pocket, which ultimately leads to structural alteration and aggregation.[85]

1.9.2 Chemical Degradation of Proteins

Chemical degradation of proteins is one of the common degradation pathways that occurs at all stages of product development. The most common types of chemical degradation include the following: oxidation, fragmentation, glycation, and deamidation.[86] The chemical degradation that alters the higher-order structure of an IgG can lead to aggregation and immunogenicity. Furthermore, alteration in higher-order structure may lead to physical degradation, which consequently, can alter the biological activity of therapeutic antibodies. Therefore, chemical stability is one of the critical quality attributes that needs to be monitored during protein therapeutic development.[86] For instance, oxidation of Trp in antibodies was shown to cause loss of functional activity as well as change in color of a high concentration formulation.[87] Also, the rate of Trp oxidation was pH-dependent processes and at basic conditions, can result in the formation of aggregates.[87] In one study, mAbs MED-493 has reported a loss of binding and biological activity due to Trp oxidation.[88] In another study, antibodies were exposed to 254 nm, and resulted in increased percentage of aggregation over the time of exposure.[89] Other studies showed that photoionization of Trp could reduce disulfide bonds by electron transfer, which led to both chemical and physical degradation of the protein.[90-93]

Oxidation of therapeutic mAbs can occur at any stage of production, purification, storage, and transportation.[94-97] Oxidation hot spots in the Fc region of IgG are Met^{252} and Met^{428}, which are known to affect the conformational stability of the C_H2 domain. The impact of oxidation on the C_H2 domain stability of antibodies has been observed in several studies.[96, 98-99] Unlike other chemical modifications, Met oxidation increased for samples stored at a low temperature (refrigerator) compared to samples stored at high temperature (room). This increase in oxidation

at low temperature was because of the concentration of oxygen at low-temperature increases (solubility of oxygen increases at a low temperature). There are many potential sources of free radicals, such as excipient and container.[100-101]

Besides Met and Trp, there are other sites prone to oxidation, such as His, Cys, and Tyr amino acids. Oxidation of these reactive sites can occur by reaction with a number of reactive oxygen species (ROS).[102-105] The residue that is solvent exposed and accessible to ROS exhibits a high oxidation rate.[97-98, 106-107] Oxidation of protein can be categorized as metal-catalyzed oxidation (site-specific) and photo-oxidation reaction (non-site-specific). For instance, light can lead to oxidation of Met and Trp sites in protein.[86] Another possible oxidation is metal-catalyzed oxidation (MCO), which occurs when redox-active metals, such as iron and copper, bind with the antibody. Metals are known to bind to histidine and cysteine, and these sites are sensitive to oxidation due to the proximity of the ROS generated.[108]

Deamidation is another chemical modification that requires monitoring during therapeutic product developments. Asparagine sites followed by serine, asparagine, and aspartic acid residues appear to exhibit higher deamidation rate.[86] Therefore, sequence plays a critical role in the rate of deamidation.[108-109] In addition to sequence, high order structure can play a significant role in the rate of deamidation.[86, 110-112] Additionally, deamidation of mAbs can be affected by temperature, buffer, and pH condition.[86] For instance, in one study after an extended storage of antibody, chemical degradations, such as deamidation (Asn and Gln), fragment, and oxidation, were observed.[76, 113-114]

The correlation between deamidation rate and glycosylation was not studied extensively. A recent report examined the effect of glycan nature on the chemical stability of well-defined

IgG1 Fc glycoforms. After incubation at 40°C for three months, the results indicated that the deamidation of Asn315 and transformation of Trp into glycine-hydroperoxide were glycan-dependent. The non-glycosylated N297Q-Fc showed higher deamidation followed by GlcNAc-Fc. The Man5-Fc and HM-Fc showed similar deamidation profiles. Furthermore, the data showed different glycoforms lead to different impurity profiles. Therefore, these results are significant in biosimilar development, in which impurity profile difference can have a significant effect on the chemical degradation. The chemical degradation studies of the four well-defined IgG1 Fc glycoforms showed a significant difference in their degradation profile, influenced by the type of glycan at Asn297.[115] Glycation is another modification that can occur when antibodies are incubated in a solution containing a reducing sugar.[86] Some results indicate glycation affects the function,[116] while other results suggest no effect on the binding affinity.[117] Glycation can affect the stability and, consequently, may lead to loss of potency. Glycation can occur in the presence of reducing sugars commonly used as excipients, such as glucose, lactose, and fructose.[86] The common sites of glycation are lysine and arginine, which ultimately results in loss of charge and increase in hydrophobicity.[118] Similarly, formulation of diketopiperazine (DKP) was observed during extended storage.[86] Although forced degradation is essential for formulation screening, the degradation profile may not be the same when compared with the long-term storage.[96] Hence, care must be exercised with analysis degradation profiles generated from forced degradations.

1.9.2.1 Chemical Modification of Proteins During Storage

Chemical degradation is one of the most common degradations of proteins, which include cross-linking, deamidation, isomerization, oxidation, disulfide bond exchange, and

fragmentation.[86] Disulfide bond exchange is typical chemical degradation and may lead to protein aggregation.[119] The disulfide bond exchange is initiated by thiolate ions generated at higher pH; hence, increasing pH leads to more degradation.[120] In a study of lyophilized IgG1 Fc, Storage (1 year at 30°C), it has been demonstrated that the disulfide exchange caused the formation of dimers and trimers. Similarly, other studies indicate non-reduced dimers of IgG1 Fc after storage at elevated temperature and basic pH for several weeks.[94, 121-122] Storage at a high-temperature > 4°C can easily generate a range of dimer products as indicated in several reports.[78, 123]

Besides disulfide bond, isomerization is a common degradation pathway in therapeutic mAbs. For example, a recombinant monoclonal antibody HER2 (Herceptin) showed isomerization and decrease in potency.[124] Similarly, anti-IgE antibody (E25) isomerization reduced the binding activity to 15%.[125] Oxidation is another degradation route for antibodies stored at a low temperature. For example, oxidation was shown in IgG2a during solution stored at 5°C. Similarly, oxidation was observed in rhu mAb anti CD20 after incubation at 4°C for about two months.[126] Light exposure can increase oxidation as indicated in HER2 at 30°C and 40°C. Other degradation pathways during storage are the formation of basic and acidic species. Deamidation is the most common pathway that leads to acid species, and such degradation was observed after incubation at 25°C for twelve weeks.[127] On the other hand, basic species in antibodies were observed after removal of sialic acid as well as after pyroglutamate and succinimide formation. Such a basic species was observed after incubation of a human monoclonal antibody at 37°C for two weeks.[72] Fragmentation is another major degradation pathway of antibodies that can occur after acidic or

basic treatment,[122] thermal stress, freeze-thaw,[78] and storage.[121] There are fragmentation prone sequences in IgG1 Fc, such as Asp-Gly and Asp-pro.[128]

1.9.3 Accelerated and Long-Term Stability Study of Proteins

Stability testing is required to establish shelf-life of therapeutic products. It is well known that environmental factors, such as pH, temperature, ionic strength, and the presence of stabilizers, can impact the conformational stability of the product. Therefore, the stability of the biosimilar in the formulation should be studied.[52] Accelerated stability studies are performed based on the underlying assumption that the degradation profile follows Arrhenius behavior. This is true in small molecules where studies conducted at a higher temperature can predict stability during longer and lower temperatures.[129] A non-Arrhenius behavior was introduced to account for protein aggregation, in which the rate depends on equilibrium (for the formation of aggregation-prone state) and the rate of irreversible aggregation.[130] However, using Arrhenius equation to fit protein stability data can be very difficult,[131] because there are potentially multiple degradation pathways involved.[52]

Forced degradation study include a set of analytical tests applied to examine physicochemical mechanisms of degradation. On the other hand, accelerated stability study measures the rate of a given degradation process over time at a different temperature in specific formulation conditions. Examining the effect of storage time, excipients on the accelerated and long-term stabilities of biologic drug products is an important part of formulation development as well as comparability evaluation. Biological drug products may encounter many environmental stresses during expression, purification, processing, storage, and shipment. Therefore, forced degradation and accelerated stability studies are required to study the degradation profile of a

biologic drug by applying various stress conditions, such as elevated temperature, freeze-thaw, agitation, oxidation environment, light, and the presence of different interfaces as well as pH changes. The design and outcome of successfully forced degradation and accelerated stability studies depends on the analytical techniques employed to identify and characterize the degradants generated.

Temperature-induced unfolding is widely used to predict long-term protein stability at low temperature (storage). For instance, a good correlation between the measured T_m value and aggregation propensity during storage at 40^{o}C has been obtained for mAbs.[132] This study suggests that the closer the T_m value is to the thermal stress, the higher the probability the protein starts to unfold. Consequently, there is a loss of its native structures to form aggregates. However, this mechanism of thermal induced aggregation at an elevated temperature may not help to predict long-term stability at a lower temperature. Moreover, most proteins are conformationally stable at low storage temperature (2 and 8 ^{o}C). The mechanism of aggregation at low temperature is driven by native self-association (colloidal stability) rather than on non-native protein-protein interaction (conformational stability). Although some progress has been achieved, the prediction of a long-term stability (stored at low temperature) still lacks robust and reliable techniques.[133]

1.10 Chapter Overview

1.10.1 Production, Characterization, and Biological Evaluation of Well-Defined IgG1 Fc Glycoforms as a Model System for Biosimilarity Analysis (Chapter 2)

Four different well-defined IgG1 Fc glycoforms are proposed as a model system to examine important biological and physicochemical features for protein drug biosimilar analysis. The IgG1 Fc glycoforms were produced by yeast expression combined with *in-vitro* enzymatic synthesis as a series of sequentially truncated, high-mannose IgG1 Fc glycoforms with an anticipated range of biological activity and structural stability. Initial characterization with mass spectrometry, SDS-PAGE, SEC, and cIEF confirmed the glycoproteins are overall highly similar with the only major difference being glycosylation state. Binding to the activating Fc receptor FcγRIIIa was used to evaluate the potential biological activity of the IgG1 Fc glycoproteins. Two complementary methods utilizing biolayer interferometry (BLI), one with protein G immobilized IgG1 Fc and the other with streptavidin immobilized FcγRIIIa, were developed to assess FcγRIIIa affinity in kinetic binding studies. The HM-Fc and Man5-Fc were highly similar to one another with high affinity for FcγRIIIa, while GlcNAc-Fc had a weak affinity, and the non-glycosylated N297Q-Fc had no measurable affinity for FcγRIIIa.

1.10.2 Comparative Evaluation of Well-Defined Mixtures of IgG1 Fc Glycoforms as a Model for Biosimilar Comparability Analysis (Chapter 3)

Four well-defined IgG1 Fc glycoforms (HM-Fc, Man5-Fc, GlcNAc-Fc, and N297Q-Fc) were prepared and blended to produce well-defined mixtures with evident and subtle differences in physical and functional properties. The mixtures were prepared by mixing HM-Fc with the three glycoforms in pre-defined proportion to make two sets of mixtures (90%HM:10%X, 50%HM:50%X, in which X was N297Q-Fc, Man5-Fc, and GlcNAc-Fc). In addition, a more complex system was prepared by blending the four glycoforms (25% each) to model heterogeneous systems typically encountered in monoclonal antibodies. Seven mixtures of glycoforms were prepared and utilized a model system for biosimilar comparability assessment. Also, the four glycoforms were used as a control in each characterization technique. The focus of this study is to evaluate the functional and physical characteristics of the mixtures as a model system for biosimilar comparability analysis. Two complimentary BioLayer Interferometry (BLI) methods, Fc-immobilized (receptor in solution), and receptor-immobilized (Fc in solution), were employed to examine the functional activity of the mixture of glycoforms. Although both immobilization techniques showed similar K_D (equilibrium dissociation constant) values for the control glycoforms as expected, differences in K_D values were observed for the mixture of glycoforms. These differences in K_D values depended on the type of immobilization technique used, the percentage of composition of the mixtures, and the type of mixtures. Therefore, the result demonstrated that the binding interactions were influenced not only by the type of mixtures, but also by the immobilization technique employed. Response measurements were performed using the Fc-immobilization technique; a trend was observed, which depended on the type and composition of the mixtures. Mixtures containing Man5-Fc and HM-Fc showed higher responses,

followed by a mixture of GlcNAc-Fc and HM-Fc. Meanwhile, combinations of N297Q-Fc and HM-Fc showed the lowest responses.

1.10.3 Characterization of IgG1 Fc Glycoforms After Prolonged Storage at Low and Elevated Temperatures: A Model System for Biosimilar Comparability Analysis (Chapter 4)

Stabilities of therapeutic monoclonal antibodies are routinely tested under accelerated conditions, such as exposure to chemicals and incubation at a high temperature. IgG1 Fc glycoforms were characterized after incubation at -80˚C, 4˚C, and 40˚C for time points at two, four, and twelve weeks. The data indicated that samples stored at 40˚C showed significantly lower binding affinities to FcγRIIIa, while the samples stored at 4˚C and -80˚C showed a moderate change in binding affinities when tested using the Fc-immobilized format. Additionally, a reduction in binding response was observed when the Fc-immobilized technique was used. In addition, the samples stored at 40˚C showed significant chemical modifications, presumably oxidation, whereas a modest change in chemical modification was observed for samples stored at low temperatures (4˚C and -80˚C) at all the time points examined. Furthermore, HM-Fc, Man5-Fc, and GlcNAc-Fc showed significantly lower binding affinities when the measurements were performed using the receptor-immobilized format compared to the measurement conducted using the Fc-immobilized. These data illustrated differences between the two immobilization techniques in detecting a reduction in binding affinities for the samples incubated at low and elevated temperatures.

1.10.4 Summary, Conclusions, and Future Work (Chapter 5)

This chapter summarizes the concepts developed from chapters two to four with the focus being the utility of homogenous well-defined IgG1 Fc glycoforms as a model for biosimilar comparability analysis. The application of the concepts and methods developed in biosimilar and comparability assessments as well as in new-product development was discussed. Finally, areas of future work were addressed.

1.11 Figures

Figure 1. Schematic representation of IgG1 containing two Fab regions and a homodimer Fc region. The domains are marked with variable (V) or constant (C) with a subscription for light (L) and heavy chain (H). The heavy chain is numbered 1, 2, and 3, starting from the N-terminus. The glycosylation site for IgG1 is located at Asn297 (EU numbering). The two heavy chains are connected by the disulfide bonds in the hinge region (marked red).

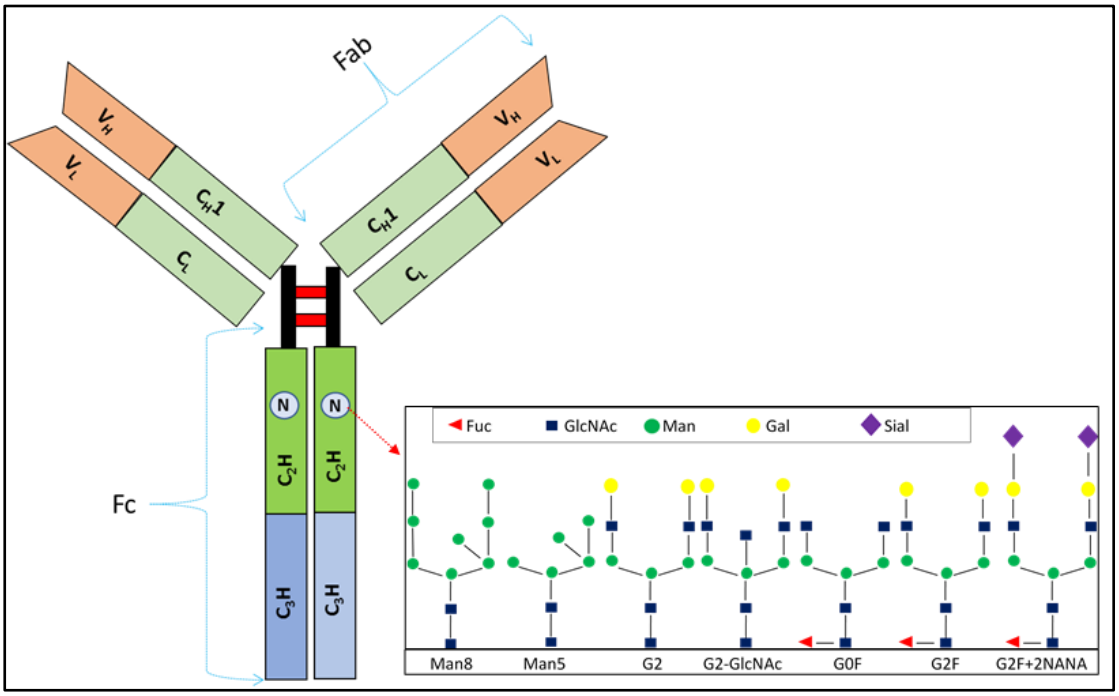

Figure 2. Crystal structure of IgG1 Fc which contains glycosylation at Asn297 (PDB ID: 1H3Y). The Fc glycans are located between the two C_H2 domains.[134]

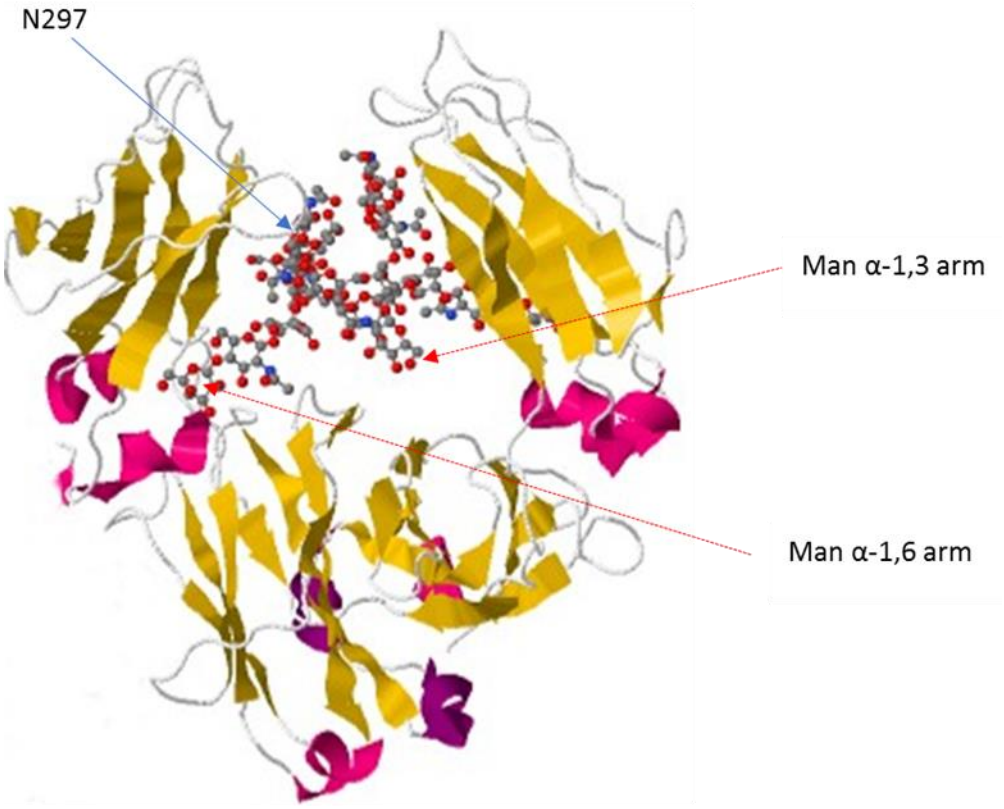

Figure 3. The amount of data required for a biosimilar product compared to a new product. Extensive physicochemical and functional characterizations (analytics) are required in a biosimilar development program, while more clinical phase studies are required in a new biologic product development.

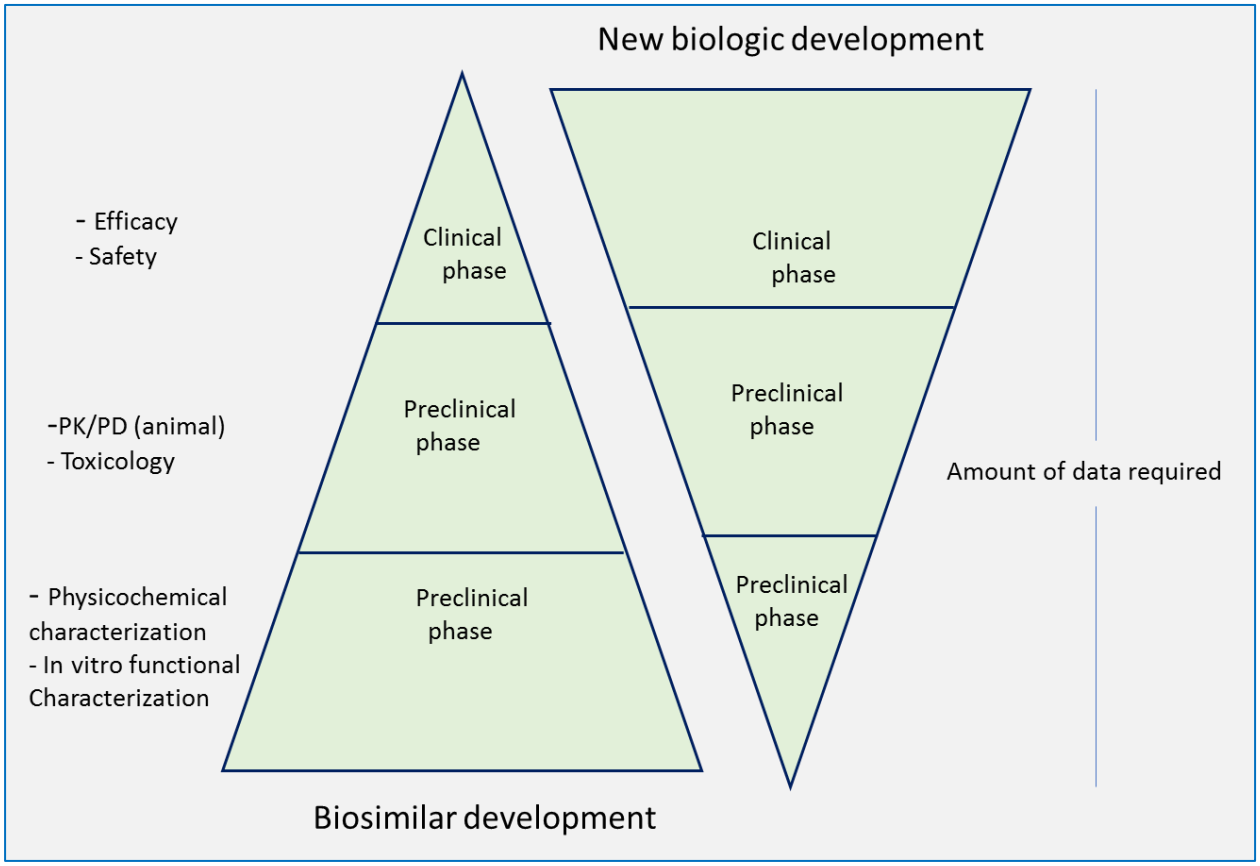

Figure 4. Steps required for developing a biosimilar, small-molecule generic, and new biologic products. In a biosimilar product, the discovery phase and phase II (i.e., dose finding), are not part of the development program.

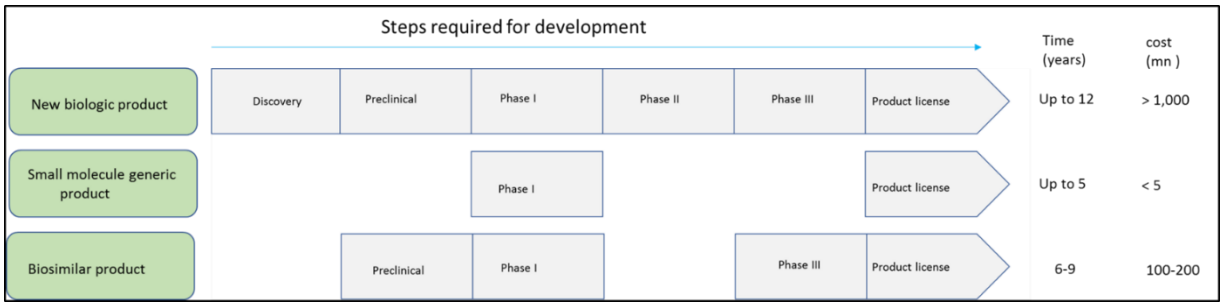

1.12 References

1. Zheng, K.; Bantog, C.; Bayer, R., The impact of glycosylation on monoclonal antibody conformation and stability. *mAbs* **2011,** *3* (6), 568-576.

2. Shinkawa, T.; Nakamura, K.; Yamane, N.; Shoji-Hosaka, E.; Kanda, Y.; Sakurada, M.; Uchida, K.; Anazawa, H.; Satoh, M.; Yamasaki, M.; Hanai, N.; Shitara, K., The Absence of Fucose but Not the Presence of Galactose or Bisecting N-Acetylglucosamine of Human IgG1 Complex-type Oligosaccharides Shows the Critical Role of Enhancing Antibody-dependent Cellular Cytotoxicity. *Journal of Biological Chemistry* **2003,** *278* (5), 3466-3473.

3. Raju, T. S., Terminal sugars of Fc glycans influence antibody effector functions of IgGs. *Current Opinion in Immunology* **2008,** *20* (4), 471-478.

4. Okazaki, A.; Shoji-Hosaka, E.; Nakamura, K.; Wakitani, M.; Uchida, K.; Kakita, S.; Tsumoto, K.; Kumagai, I.; Shitara, K., Fucose Depletion from Human IgG1 Oligosaccharide Enhances Binding Enthalpy and Association Rate Between IgG1 and FcγRIIIa. *Journal of Molecular Biology* **2004,** *336* (5), 1239-1249.

5. Yamane-Ohnuki, N.; Kinoshita, S.; Inoue-Urakubo, M.; Kusunoki, M.; Iida, S.; Nakano, R.; Wakitani, M.; Niwa, R.; Sakurada, M.; Uchida, K.; Shitara, K.; Satoh, M., Establishment of FUT8 knockout Chinese hamster ovary cells: An ideal host cell line for producing completely defucosylated antibodies with enhanced antibody-dependent cellular cytotoxicity. *Biotechnology and Bioengineering* **2004,** *87* (5), 614-622.

6. Mori, K.; Kuni-Kamochi, R.; Yamane-Ohnuki, N.; Wakitani, M.; Yamano, K.; Imai, H.; Kanda, Y.; Niwa, R.; Iida, S.; Uchida, K.; Shitara, K.; Satoh, M., Engineering Chinese hamster ovary cells to maximize effector function of produced antibodies using FUT8 siRNA. *Biotechnology and Bioengineering* **2004,** *88* (7), 901-908.

7. Schuster, M.; Umana, P.; Ferrara, C.; Brünker, P.; Gerdes, C.; Waxenecker, G.; Wiederkum, S.; Schwager, C.; Loibner, H.; Himmler, G.; Mudde, G. C., Improved Effector Functions of a Therapeutic Monoclonal Lewis Y-Specific Antibody by Glycoform Engineering. *Cancer Research* **2005,** *65* (17), 7934-7941.

8. Niwa, R.; Natsume, A.; Uehara, A.; Wakitani, M.; Iida, S.; Uchida, K.; Satoh, M.; Shitara, K., IgG subclass-independent improvement of antibody-dependent cellular cytotoxicity by fucose removal from Asn297-linked oligosaccharides. *Journal of Immunological Methods* **2005,** *306* (1–2), 151-160.

9. Shields, R. L.; Lai, J.; Keck, R.; O'Connell, L. Y.; Hong, K.; Meng, Y. G.; Weikert, S. H. A.; Presta, L. G., Lack of Fucose on Human IgG1 N-Linked Oligosaccharide Improves Binding to

Human FcγRIII and Antibody-dependent Cellular Toxicity. *Journal of Biological Chemistry* **2002,** *277* (30), 26733-26740.

10. Kaneko, Y.; Nimmerjahn, F.; Ravetch, J. V., Anti-Inflammatory Activity of Immunoglobulin G Resulting from Fc Sialylation. *Science* **2006,** *313* (5787), 670-673.

11. Anthony, R. M.; Nimmerjahn, F.; Ashline, D. J.; Reinhold, V. N.; Paulson, J. C.; Ravetch, J. V., Recapitulation of IVIG Anti-Inflammatory Activity with a Recombinant IgG Fc. *Science* **2008,** *320* (5874), 373-376.

12. Anthony, R. M.; Kobayashi, T.; Wermeling, F.; Ravetch, J. V., Intravenous gammaglobulin suppresses inflammation through a novel TH2 pathway. *Nature* **2011,** *475* (7354), 110-113.

13. Maiorella, B. L.; Ferris, R.; Thomson, J.; White, C.; Brannon, M.; Hora, M.; Henriksson, T.; Triglia, R.; Kunitani, M.; Kresin, L.; Dollinger, G.; Jones, R.; Senyk, G.; Young, J.; Moyer, B.; McEntire, J.; Dougherty, J.; Monica, T.; Goochee, C., Evaluation of Product Equivalence During Process Optimization for Manufacture of a Human IgM Monoclonal Antibody. *Biologicals* **1993,** *21* (3), 197-205.

14. Kálmán-Szekeres, Z.; Olajos, M.; Ganzler, K., Analytical aspects of biosimilarity issues of protein drugs. *Journal of Pharmaceutical and Biomedical Analysis* **2012,** *69* (0), 185-195.

15. Schmelzer, A. E.; Miller, W. M., Hyperosmotic Stress and Elevated pCO2 Alter Monoclonal Antibody Charge Distribution and Monosaccharide Content. *Biotechnology Progress* **2002,** *18* (2), 346-353.

16. Stockert, R. J., The asialoglycoprotein receptor: relationships between structure, function, and expression. *Physiological Reviews* **1995,** *75* (3), 591-609.

17. Lubiniecki, A.; Volkin, D. B.; Federici, M.; Bond, M. D.; Nedved, M. L.; Hendricks, L.; Mehndiratta, P.; Bruner, M.; Burman, S.; DalMonte, P.; Kline, J.; Ni, A.; Panek, M. E.; Pikounis, B.; Powers, G.; Vafa, O.; Siegel, R., Comparability assessments of process and product changes made during development of two different monoclonal antibodies. *Biologicals* **2011,** *39* (1), 9-22.

18. Chirino, A. J.; Mire-Sluis, A., Characterizing biological products and assessing comparability following manufacturing changes. *Nat Biotech* **2004,** *22* (11), 1383-1391.

19. Putnam, W. S.; Prabhu, S.; Zheng, Y.; Subramanyam, M.; Wang, Y.-M. C., Pharmacokinetic, pharmacodynamic and immunogenicity comparability assessment strategies for monoclonal antibodies. *Trends in Biotechnology* **2010,** *28* (10), 509-516.

20. Berkowitz, S. A.; Engen, J. R.; Mazzeo, J. R.; Jones, G. B., Analytical tools for characterizing biopharmaceuticals and the implications for biosimilars. *Nat Rev Drug Discov* **2012,** *11* (7), 527-540.

21. Kilgore, B. R.; Kilgore, B. R., Comparability and Monitoring Immunogenic N-linked Oligosaccharides from Recombinant Monoclonal Antibodies from Two Different Cell Lines using HPLC with Fluorescence Detection and Mass Spectrometry. 2008; Vol. 446, pp 333-346.

22. Gawlitzek, M.; Valley, U.; Nimtz, M.; Wagner, R.; Conradt, H. S., Characterization of changes in the glycosylation pattern of recombinant proteins from BHK-21 cells due to different culture conditions. *Journal of Biotechnology* **1995,** *42* (2), 117-131.

23. Federici, M.; Lubiniecki, A.; Manikwar, P.; Volkin, D. B., Analytical lessons learned from selected therapeutic protein drug comparability studies. *Biologicals* **2013,** *41* (3), 131-147.

24. Raju, T. S.; Jordan, R. E., Galactosylation variations in marketed therapeutic antibodies. *mAbs* **2012,** *4* (3), 385-391.

25. Wacker, C.; Berger, C. N.; Girard, P.; Meier, R., Glycosylation profiles of therapeutic antibody pharmaceuticals. *European Journal of Pharmaceutics and Biopharmaceutics* **2011,** *79* (3), 503-507.

26. Hanson, Q. M.; Barb, A. W., A Perspective on the Structure and Receptor Binding Properties of Immunoglobulin G Fc. *Biochemistry* **2015,** *54* (19), 2931-2942.

27. Sondermann, P.; Oosthuizen, V., X-ray crystallographic studies of IgG-Fcγ receptor interactions. *Biochemical Society Transactions* **2002,** *30* (4), 481-486.

28. Liu, L., Antibody Glycosylation and Its Impact on the Pharmacokinetics and Pharmacodynamics of Monoclonal Antibodies and Fc-Fusion Proteins. *Journal of Pharmaceutical Sciences* **2015**, n/a-n/a.

29. Zhang, N.; Liu, L.; Dumitru, C. D.; Cummings, N. R. H.; Cukan, M.; Jiang, Y.; Li, Y.; Li, F.; Mitchell, T.; Mallem, M. R.; Ou, Y.; Patel, R. N.; Vo, K.; Wang, H.; Burnina, I.; Choi, B.-K.; Huber, H.; Stadheim, T. A.; Zha, D., Glycoengineered Pichia produced anti-HER2 is comparable to trastuzumab in preclinical study. *mAbs* **2011,** *3* (3), 289-298.

30. Potgieter, T. I.; Cukan, M.; Drummond, J. E.; Houston-Cummings, N. R.; Jiang, Y.; Li, F.; Lynaugh, H.; Mallem, M.; McKelvey, T. W.; Mitchell, T.; Nylen, A.; Rittenhour, A.; Stadheim, T. A.; Zha, D.; d'Anjou, M., Production of monoclonal antibodies by glycoengineered Pichia pastoris. *Journal of Biotechnology* **2009,** *139* (4), 318-325.

31. Ha, S.; Wang, Y.; Rustandi, R. R., Biochemical and biophysical characterization of humanized IgG1 produced in Pichia pastoris. *mAbs* **2011,** *3* (5), 453-460.

32. Choi, B.-K.; Warburton, S.; Lin, H.; Patel, R.; Boldogh, I.; Meehl, M.; d'Anjou, M.; Pon, L.; Stadheim, T.; Sethuraman, N., Improvement of N-glycan site occupancy of therapeutic glycoproteins produced in Pichia pastoris. *Appl Microbiol Biotechnol* **2012,** *95* (3), 671-682.

33. FDA, Scientific Considerations in Demonstrating Biosimilarity to a Reference Product. https://www.fda.gov/downloads/drugs/guidances/ucm291128.pdf **2015**.

34. Al-Sabbagh, A.; Olech, E.; McClellan, J. E.; Kirchhoff, C. F., Development of biosimilars. *Seminars in Arthritis and Rheumatism* **2016,** *45* (5, Supplement), S11-S18.

35. Beck, A.; Debaene, F.; Diemer, H.; Wagner-Rousset, E.; Colas, O.; Dorsselaer, A. V.; Cianférani, S., Cutting-edge mass spectrometry characterization of originator, biosimilar and biobetter antibodies. *Journal of Mass Spectrometry* **2015,** *50* (2), 285-297.

36. Schneider, C. K.; Vleminckx, C.; Gravanis, I.; Ehmann, F.; Trouvin, J.-H.; Weise, M.; Thirstrup, S., Setting the stage for biosimilar monoclonal antibodies. *Nat Biotech* **2012,** *30* (12), 1179-1185.

37. Xie, H.; Chakraborty, A.; Ahn, J.; Yu, Y. Q.; Dakshinamoorthy, D. P.; Gilar, M.; Chen, W.; Skilton, S. J.; Mazzeo, J. R., Rapid comparison of a candidate biosimilar to an innovator monoclonal antibody with advanced liquid chromatography and mass spectrometry technologies. *mAbs* **2010,** *2* (4), 379-394.

38. Raedler, L. A., Zarxio (Filgrastim-sndz): First Biosimilar Approved in the United States. *American Health & Drug Benefits* **2016,** *9* (Spec Feature), 150-154.

39. Pisupati, K.; Tian, Y.; Okbazghi, S.; Benet, A.; Ackermann, R.; Ford, M.; Saveliev, S. V.; Hosfield, C. M.; Urh, M.; Carlson, E.; Becker, C.; Tolbert, T. J.; Schwendeman, S. P.; Ruotolo, B. T.; Schwendeman, A., A Multidimensional Analytical Comparison of Remicade and the Biosimilar Remsima. *Analytical Chemistry* **2017**.

40. Jiang, X.-R.; Song, A.; Bergelson, S.; Arroll, T.; Parekh, B.; May, K.; Chung, S.; Strouse, R.; Mire-Sluis, A.; Schenerman, M., Advances in the assessment and control of the effector functions of therapeutic antibodies. *Nat Rev Drug Discov* **2011,** *10* (2), 101-111.

41. Jones, A. J. S.; Papac, D. I.; Chin, E. H.; Keck, R.; Baughman, S. A.; Lin, Y. S.; Kneer, J.; Battersby, J. E., Selective clearance of glycoforms of a complex glycoprotein pharmaceutical caused by terminal N-acetylglucosamine is similar in humans and cynomolgus monkeys. *Glycobiology* **2007,** *17* (5), 529-540.

42. Jefferis, R., Glycosylation of Recombinant IgG Antibodies and Its Relevance for Therapeutic Applications. In *Cell Engineering*, Al-Rubeai, M., Ed. Springer Netherlands: 2002; Vol. 3, pp 93-107.

43. Chung, C. H., Cetuximab-Induced Anaphylaxis and IgE Specific for Galactose-α-1,3-Galactose. *The New England journal of medicine* **2008,** *358* (11), 1109-1117.

44. Hokke, C. H.; Bergwerff, A. A.; van Dedem, G. W. K.; van Oostrum, J.; Kamerling, J. P.; Vliegenthart, J. F. G., Sialylated carbohydrate chains of recombinant human glycoproteins expressed in Chinese hamster ovary cells contain traces of N-glycolylneuraminic acid. *FEBS Letters* **1990,** *275* (1–2), 9-14.

45. Borys, M. C.; Dalal, N. G.; Abu-Absi, N. R.; Khattak, S. F.; Jing, Y.; Xing, Z.; Li, Z. J., Effects of culture conditions on N-glycolylneuraminic acid (Neu5Gc) content of a recombinant fusion protein produced in CHO cells. *Biotechnology and Bioengineering* **2010,** *105* (6), 1048-1057.

46. Wright, A.; Sato, Y.; Okada, T.; Chang, K. H.; Endo, T.; Morrison, S. L., In vivo trafficking and catabolism of IgG1 antibodies with Fc associated carbohydrates of differing structure. *Glycobiology* **2000,** *10* (12), 1347-1355.

47. Wright, A.; Morrison, S. L., Effect of glycosylation on antibody function: implications for genetic engineering. *Trends in Biotechnology* **1997,** *15* (1), 26-32.

48. Kálmán-Szekeres, Z.; Olajos, M.; Ganzler, K., Analytical aspects of biosimilarity issues of protein drugs. *Journal of Pharmaceutical and Biomedical Analysis* **2012,** *69*, 185-195.

49. Alsenaidy, M. A.; Okbazghi, S. Z.; Kim, J. H.; Joshi, S. B.; Middaugh, C. R.; Tolbert, T. J.; Volkin, D. B., Physical Stability Comparisons of IgG1-Fc Variants: Effects of N-Glycosylation Site Occupancy and Asp/Gln Residues at Site Asn 297. *Journal of Pharmaceutical Sciences* **2014,** *103* (6), 1613-1627.

50. Tsuruta, L. R.; Lopes dos Santos, M.; Moro, A. M., Biosimilars advancements: Moving on to the future. *Biotechnology Progress* **2015,** *31* (5), 1139-1149.

51. Alsenaidy, M.; Jain, N. K.; Kim, J.; Middaugh, C.; Volkin, D., Protein comparability assessments and potential applicability of high throughput biophysical methods and data visualization tools to compare physical stability profiles. *Frontiers in Pharmacology* **2014,** *5* (39).

52. Falconer, R. J.; Jackson-Matthews, D.; Mahler, S. M., Analytical strategies for assessing comparability of biosimilars. *Journal of Chemical Technology & Biotechnology* **2011,** *86* (7), 915-922.

53. O'Shannessy, D. J.; Winzor, D. J., Interpretation of Deviations from Pseudo-First-Order Kinetic Behavior in the Characterization of Ligand Binding by Biosensor Technology. *Analytical Biochemistry* **1996,** *236* (2), 275-283.

54. Oshannessy, D. J.; Brighamburke, M.; Soneson, K. K.; Hensley, P.; Brooks, I., Determination of Rate and Equilibrium Binding Constants for Macromolecular Interactions Using Surface Plasmon Resonance: Use of Nonlinear Least Squares Analysis Methods. *Analytical Biochemistry* **1993,** *212* (2), 457-468.

55. Roden, L. D.; Myszka, D. G., Global Analysis of a Macromolecular Interaction Measured on BIAcore. *Biochemical and Biophysical Research Communications* **1996,** *225* (3), 1073-1077.

56. Nieba, L.; Krebber, A.; Plückthun, A., Competition BIAcore for Measuring True Affinities: Large Differences from Values Determined from Binding Kinetics. *Analytical Biochemistry* **1996,** *234* (2), 155-165.

57. Fischer, N. J. d. M. a. M. J. E., Kinetic and Thermodynamic Analysis of Ligand–Receptor Interactions: SPR Applications in Drug Development. **10 Mar 2008**.

58. Karlsson, R.; Fält, A., Experimental design for kinetic analysis of protein-protein interactions with surface plasmon resonance biosensors. *Journal of Immunological Methods* **1997,** *200* (1), 121-133.

59. Wang, Y.-M. C.; Chow, A. T., Development of Biosimilars—Pharmacokinetic and Pharmacodynamic Considerations. *Journal of Biopharmaceutical Statistics* **2009,** *20* (1), 46-61.

60. Jefferis, R., Recombinant antibody therapeutics: the impact of glycosylation on mechanisms of action. *Trends in Pharmacological Sciences* **2009,** *30* (7), 356-362.

61. Blackstone, E. A.; Joseph, P. F., The Economics of Biosimilars. *American Health & Drug Benefits* **2013,** *6* (8), 469-478.

62. ICH Q5E: Comparability of Biotechnological/Biological Products Subject to Changes in Their Manufacturing Process www.fda.gov/ohrms/dockets/98fr/2004d-0118-gdl0001.pdf.

63. Azevedo, V.; Hassett, B.; Fonseca, J. E.; Atsumi, T.; Coindreau, J.; Jacobs, I.; Mahgoub, E.; O'Brien, J.; Singh, E.; Vicik, S.; Fitzpatrick, B., Differentiating biosimilarity and comparability in biotherapeutics. *Clinical Rheumatology* **2016,** *35* (12), 2877-2886.

64. Declerck, P.; Farouk-Rezk, M.; Rudd, P. M., Biosimilarity Versus Manufacturing Change: Two Distinct Concepts. *Pharm Res* **2016,** *33* (2), 261-268.

65. Morrow, T.; Felcone, L. H., Defining the difference: What Makes Biologics Unique. *Biotechnology Healthcare* **2004,** *1* (4), 24-29.

66. Kuhlmann, M.; Covic, A., The protein science of biosimilars. *Nephrology Dialysis Transplantation* **2006,** *21* (suppl 5), v4-v8.

67. Carpenter, J. F.; Randolph, T. W.; Jiskoot, W.; Crommelin, D. J. A.; Russell Middaugh, C.; Winter, G.; Fan, Y.-X.; Kirshner, S.; Verthelyi, D.; Kozlowski, S.; Clouse, K. A.; Swann, P. G.; Rosenberg, A.; Cherney, B., Overlooking Subvisible Particles in Therapeutic Protein Products: Gaps That May Compromise Product Quality. *Journal of Pharmaceutical Sciences* **2009,** *98* (4), 1201-1205.

68. JS, P., A critical review of methods for size characterization of non-particulate protein aggregates. *Curr Pharm Biotechnol* **2009** *10* (4), 359-72.

69. Sarpatwari, A.; Avorn, J.; Kesselheim, A. S., Progress and Hurdles for Follow-on Biologics. *New England Journal of Medicine* **2015,** *372* (25), 2380-2382.

70. Nowicki, M., Basic Facts about Biosimilars. *Kidney and Blood Pressure Research* **2007,** *30* (5), 267-272.

71. Lee, J. F.; Litten, J. B.; Grampp, G., Comparability and biosimilarity: considerations for the healthcare provider. *Current Medical Research and Opinion* **2012,** *28* (6), 1053-1058.

72. Wang, W.; Singh, S.; Zeng, D. L.; King, K.; Nema, S., Antibody structure, instability, and formulation. *Journal of Pharmaceutical Sciences* **2007,** *96* (1), 1-26.

73. Furtado, P. B.; Whitty, P. W.; Robertson, A.; Eaton, J. T.; Almogren, A.; Kerr, M. A.; Woof, J. M.; Perkins, S. J., Solution Structure Determination of Monomeric Human IgA2 by X-ray and Neutron Scattering, Analytical Ultracentrifugation and Constrained Modelling: A Comparison with Monomeric Human IgA1. *Journal of Molecular Biology* **2004,** *338* (5), 921-941.

74. Wörn, A.; Plückthun, A., Mutual Stabilization of VL and VH in Single-Chain Antibody Fragments, Investigated with Mutants Engineered for Stability. *Biochemistry* **1998,** *37* (38), 13120-13127.

75. Dall'Acqua, W.; Simon, A. L.; Mulkerrin, M. G.; Carter, P., Contribution of Domain Interface Residues to the Stability of Antibody CH3 Domain Homodimers. *Biochemistry* **1998,** *37* (26), 9266-9273.

76. Harris, R. J.; Shire, S. J.; Winter, C., Commercial manufacturing scale formulation and analytical characterization of therapeutic recombinant antibodies. *Drug Development Research* **2004,** *61* (3), 137-154.

77. Hunt, G.; Moorhouse, K. G.; Chen, A. B., Capillary isoelectric focusing and sodium dodecyl sulfate-capillary gel electrophoresis of recombinant humanized monoclonal antibody HER2. *Journal of Chromatography A* **1996,** *744* (1), 295-301.

78. P.K. Tsai, M. W. B., J.I. Irwin, C.C. Ip, C.N. Oliver, R.W. Nelson,; D.B. Volkin, C. R. M., Chemical and physical stability of chimeric L6, a mouse-human monoclonal antibody. *Pharm. Res* **1993,** (10), 1580.

79. Chen, B.; Bautista, R.; Yu, K.; Zapata, G. A.; Mulkerrin, M. G.; Chamow, S. M., Influence of Histidine on the Stability and Physical Properties of a Fully Human Antibody in Aqueous and Solid Forms. *Pharm Res* **2003,** *20* (12), 1952-1960.

80. Welfle, K.; Misselwitz, R.; Hausdorf, G.; Höhne, W.; Welfle, H., Conformation, pH-induced conformational changes, and thermal unfolding of anti-p24 (HIV-1) monoclonal antibody CB4-1 and its Fab and Fc fragments. *Biochimica et Biophysica Acta (BBA) - Protein Structure and Molecular Enzymology* **1999,** *1431* (1), 120-131.

81. Alexander, A. J.; Hughes, D. E., Monitoring of IgG Antibody Thermal Stability by Micellar Electrokinetic Capillary Chromatography and Matrix-Assisted Laser Desorption/Ionization Mass Spectrometry. *Analytical Chemistry* **1995,** *67* (20), 3626-3632.

82. Shire, S. J.; Shahrokh, Z.; Liu, J., Challenges in the development of high protein concentration formulations. *Journal of Pharmaceutical Sciences 93* (6), 1390-1402.

83. Ramsland, P. A.; Farrugia, W., Crystal structures of human antibodies: a detailed and unfinished tapestry of immunoglobulin gene products. *Journal of Molecular Recognition* **2002,** *15* (5), 248-259.

84. Le Gall, F.; Reusch, U.; Little, M.; Kipriyanov, S. M., Effect of linker sequences between the antibody variable domains on the formation, stability and biological activity of a bispecific tandem diabody. *Protein Engineering, Design and Selection* **2004,** *17* (4), 357-366.

85. More, A. S.; Toprani, V. M.; Okbazghi, S. Z.; Kim, J. H.; Joshi, S. B.; Middaugh, C. R.; Tolbert, T. J.; Volkin, D. B., Correlating the impact of well-defined oligosaccharide structures on physical stability profiles of IgG1-Fc glycoforms. *Journal of Pharmaceutical Sciences*.

86. Manning, M. C.; Chou, D. K.; Murphy, B. M.; Payne, R. W.; Katayama, D. S., Stability of Protein Pharmaceuticals: An Update. *Pharm Res* **2010,** *27* (4), 544-575.

87. Qi, P.; Volkin, D. B.; Zhao, H.; Nedved, M. L.; Hughes, R.; Bass, R.; Yi, S. C.; Panek, M. E.; Wang, D.; DalMonte, P.; Bond, M. D., Characterization of the photodegradation of a human IgG1 monoclonal antibody formulated as a high-concentration liquid dosage form. *Journal of Pharmaceutical Sciences* **2009,** *98* (9), 3117-3130.

88. Wei, Z.; Feng, J.; Lin, H.-Y.; Mullapudi, S.; Bishop, E.; Tous, G. I.; Casas-Finet, J.; Hakki, F.; Strouse, R.; Schenerman, M. A., Identification of a Single Tryptophan Residue as Critical for

Binding Activity in a Humanized Monoclonal Antibody against Respiratory Syncytial Virus. *Analytical Chemistry* **2007,** *79* (7), 2797-2805.

89. Lorenz, C. M.; Wolk, B. M.; Quan, C. P.; Alcala, E. W.; Eng, M.; McDonald, D. J.; Matthews, T. C., The effect of low intensity ultraviolet-C light on monoclonal antibodies. *Biotechnology Progress* **2009,** *25* (2), 476-482.

90. Roy, S.; Mason, B. D.; Schöneich, C. S.; Carpenter, J. F.; Boone, T. C.; Kerwin, B. A., Light-induced aggregation of type I soluble tumor necrosis factor receptor. *Journal of Pharmaceutical Sciences* **2009,** *98* (9), 3182-3199.

91. Vanhooren, A.; Devreese, B.; Vanhee, K.; Van Beeumen, J.; Hanssens, I., Photoexcitation of Tryptophan Groups Induces Reduction of Two Disulfide Bonds in Goat α-Lactalbumin. *Biochemistry* **2002,** *41* (36), 11035-11043.

92. Mozziconacci, O.; Sharov, V.; Williams, T. D.; Kerwin, B. A.; Schöneich, C., Peptide Cysteine Thiyl Radicals Abstract Hydrogen Atoms from Surrounding Amino Acids: The Photolysis of a Cystine Containing Model Peptide. *The Journal of Physical Chemistry B* **2008,** *112* (30), 9250-9257.

93. Miller, B. L.; Hageman, M. J.; Thamann, T. J.; Barròn, L. B.; Schöneich, C., Solid-state photodegradation of bovine somatotropin (bovine growth hormone): Evidence for tryptophan-

mediated photooxidation of disulfide bonds. *Journal of Pharmaceutical Sciences* **2003,** *92* (8), 1698-1709.

94. Kroon, D. J.; Baldwin-Ferro, A.; Lalan, P., Identification of Sites of Degradation in a Therapeutic Monoclonal Antibody by Peptide Mapping. *Pharm Res* **1992,** *9* (11), 1386-1393.

95. Kerwin, B. A.; Remmele, R. L., Protect from light: Photodegradation and protein biologics. *Journal of Pharmaceutical Sciences* **2007,** *96* (6), 1468-1479.

96. Chumsae, C.; Gaza-Bulseco, G.; Sun, J.; Liu, H., Comparison of methionine oxidation in thermal stability and chemically stressed samples of a fully human monoclonal antibody. *Journal of Chromatography B* **2007,** *850* (1–2), 285-294.

97. Bertolotti-Ciarlet, A.; Wang, W.; Lownes, R.; Pristatsky, P.; Fang, Y.; McKelvey, T.; Li, Y.; Li, Y.; Drummond, J.; Prueksaritanont, T.; Vlasak, J., Impact of methionine oxidation on the binding of human IgG1 to FcRn and Fcγ receptors. *Molecular Immunology* **2009,** *46* (8–9), 1878-1882.

98. Pan, H.; Chen, K.; Chu, L.; Kinderman, F.; Apostol, I.; Huang, G., Methionine oxidation in human IgG2 Fc decreases binding affinities to protein A and FcRn. *Protein Science* **2009,** *18* (2), 424-433.

99. Liu, D.; Ren, D.; Huang, H.; Dankberg, J.; Rosenfeld, R.; Cocco, M. J.; Li, L.; Brems, D. N.; Remmele, R. L., Structure and Stability Changes of Human IgG1 Fc as a Consequence of Methionine Oxidation. *Biochemistry* **2008,** *47* (18), 5088-5100.

100. Nguyen, T. H., Oxidation Degradation of Protein Pharmaceuticals. In *Formulation and Delivery of Proteins and Peptides*, American Chemical Society: 1994; Vol. 567, pp 59-71.

101. Yokota, H.; Saito, H.; Masuoka, K.; Kaniwa, H.; Shibanuma, T., Reversed phase HPLC of Met58 oxidized rhIL-11: oxidation enhanced by plastic tubes. *Journal of Pharmaceutical and Biomedical Analysis* **2000,** *24* (2), 317-324.

102. ER, S., Oxidation of Free Amino Acids and Amino Acid Residues in Proteins by Radiolysis and by Metal-Catalyzed Reactions. *Annual Review of Biochemistry* **1993,** *62* (1), 797-821.

103. Hovorka, S. W.; Schöneich, C., Oxidative degradation of pharmaceuticals: Theory, mechanisms and inhibition. *Journal of Pharmaceutical Sciences* **2001,** *90* (3), 253-269.

104. Hawkins, C. L.; Davies, M. J., Generation and propagation of radical reactions on proteins. *Biochimica et Biophysica Acta (BBA) - Bioenergetics* **2001,** *1504* (2–3), 196-219.

105. Davies, M. J., The oxidative environment and protein damage. *Biochimica et Biophysica Acta (BBA) - Proteins and Proteomics* **2005,** *1703* (2), 93-109.

106. Griffiths, S. W.; Cooney, C. L., Relationship between Protein Structure and Methionine Oxidation in Recombinant Human α1-Antitrypsin. *Biochemistry* **2002,** *41* (20), 6245-6252.

107. Lu, H. S.; Fausset, P. R.; Narhi, L. O.; Horan, T.; Shinagawa, K.; Shimamoto, G.; Boone, T. C., Chemical Modification and Site-Directed Mutagenesis of Methionine Residues in Recombinant Human Granulocyte Colony-Stimulating Factor: Effect on Stability and Biological Activity. *Archives of Biochemistry and Biophysics* **1999,** *362* (1), 1-11.

108. Hovorka, S. W.; Hong, J.; Cleland, J. L.; Schöneich, C., Metal-catalyzed oxidation of human growth hormone: Modulation by solvent-induced changes of protein conformation. *Journal of Pharmaceutical Sciences* **2001,** *90* (1), 58-69.

109. Chelius, D.; Rehder, D. S.; Bondarenko, P. V., Identification and Characterization of Deamidation Sites in the Conserved Regions of Human Immunoglobulin Gamma Antibodies. *Analytical Chemistry* **2005,** *77* (18), 6004-6011.

110. Kossiakoff, A., Tertiary structure is a principal determinant to protein deamidation. *Science* **1988,** *240* (4849), 191-194.

111. Xie, M.; Shahrokh, Z.; Kadkhodayan, M.; Henzel, W. J.; Powell, M. F.; Borchardt, R. T.; Schowen, R. L., Asparagine deamidation in recombinant human lymphotoxin: Hindrance by three-dimensional structures. *Journal of Pharmaceutical Sciences* **2003,** *92* (4), 869-880.

112. DeLuna, A.; Quezada, H.; Gómez-Puyou, A.; González, A., Asparaginyl deamidation in two glutamate dehydrogenase isoenzymes from Saccharomyces cerevisiae. *Biochemical and Biophysical Research Communications* **2005,** *328* (4), 1083-1090.

113. Liu, H.; Gaza-Bulseco, G.; Sun, J., Characterization of the stability of a fully human monoclonal IgG after prolonged incubation at elevated temperature. *Journal of Chromatography B* **2006,** *837* (1–2), 35-43.

114. Yan, B.; Valliere-Douglass, J.; Brady, L.; Steen, S.; Han, M.; Pace, D.; Elliott, S.; Yates, Z.; Han, Y.; Balland, A.; Wang, W.; Pettit, D., Analysis of post-translational modifications in recombinant monoclonal antibody IgG1 by reversed-phase liquid chromatography/mass spectrometry. *Journal of Chromatography A* **2007,** *1164* (1–2), 153-161.

115. Mozziconacci, O.; Okbazghi, S.; More, A. S.; Volkin, D. B.; Tolbert, T.; Schöneich, C., Comparative evaluation of the chemical stability of four well-defined IgG1 Fc glycoforms. *Journal of Pharmaceutical Sciences*.

116. Kennedy, D. M.; Skillen, A. W.; Self, C. H., Glycation of monoclonal antibodies impairs their ability to bind antigen. *Clinical and Experimental Immunology* **1994,** *98* (2), 245-251.

117. Quan, C.; Alcala, E.; Petkovska, I.; Matthews, D.; Canova-Davis, E.; Taticek, R.; Ma, S., A study in glycation of a therapeutic recombinant humanized monoclonal antibody: Where it is,

how it got there, and how it affects charge-based behavior. *Analytical Biochemistry* **2008,** *373* (2), 179-191.

118. Zhang, B.; Yang, Y.; Yuk, I.; Pai, R.; McKay, P.; Eigenbrot, C.; Dennis, M.; Katta, V.; Francissen, K. C., Unveiling a Glycation Hot Spot in a Recombinant Humanized Monoclonal Antibody. *Analytical Chemistry* **2008,** *80* (7), 2379-2390.

119. Morales, A. A. M.; Núñez-Gandolff, G.; Pérez, N. P.; Véliz, B. C.; Caballero-Torres, I.; Ducongé, J.; Fernández, E.; Crespo, F. Z.; Veloso, A.; Iznaga-Escobar, N., Freeze-dried formulation for direct 99mTc-labeling ior-egf/r3 MAb: additives, biodistribution, and stability. *Nuclear Medicine and Biology* **1999,** *26* (6), 717-723.

120. Kamat MS, T. G., Brown JM, Formulation development of an antifibrin monoclonal antibody radiopharmaceutical. *Pharm Biotechnol* **Pharm Biotechnol. 1996;9:343-64,** *9*, 343-64.

121. W. Jiskoot, E. C. B., A.A. de Koning, J.N. Herron, D.J., Analytical approaches to the study of monoclonal antibody stability. *Pharm Res* **1990,** *7* (12).

122. Usami, A.; Ohtsu, A.; Takahama, S.; Fujii, T., The effect of pH, hydrogen peroxide and temperature on the stability of human monoclonal antibody. *Journal of Pharmaceutical and Biomedical Analysis* **1996,** *14* (8–10), 1133-1140.

123. Cleland, J. L.; Lam, X.; Kendrick, B.; Yang, J.; Yang, T. h.; Overcashier, D.; Brooks, D.; Hsu, C.; Carpenter, J. F., A specific molar ratio of stabilizer to protein is required for storage stability of a lyophilized monoclonal antibody. *Journal of Pharmaceutical Sciences* **2001,** *90* (3), 310-321.

124. Harris, R. J.; Kabakoff, B.; Macchi, F. D.; Shen, F. J.; Kwong, M.; Andya, J. D.; Shire, S. J.; Bjork, N.; Totpal, K.; Chen, A. B., Identification of multiple sources of charge heterogeneity in a recombinant antibody. *Journal of Chromatography B: Biomedical Sciences and Applications* **2001,** *752* (2), 233-245.

125. Cacia, J.; Keck, R.; Presta, L. G.; Frenz, J., Isomerization of an Aspartic Acid Residue in the Complementarity-Determining Regions of a Recombinant Antibody to Human IgE: Identification and Effect on Binding Affinity. *Biochemistry* **1996,** *35* (6), 1897-1903.

126. Lam, X. M.; Oeswein, J. Q.; Ongpipattanakul, B.; Shahrokh, Z.; Wang, S. X.; Weissburg, R. P.; Wong, R. L., Stabilized antibody formulation. Google Patents: 2008.

127. Johnson, R. E.; Qi, H.; Borgmeyer, J. R.; Kessler, R. K.; Zeng, D. L., Stable ph optimized formulation of a modified antibody. Google Patents: 2004.

128. Amphlett G, C. J., Callahan W, Cannova-Davis E, Chang B, Cleland JL, Darrington T, DeYoung L, Dhingra B, Everett R, Foster L, Frenz J, Garcia A, Giltinan D, Gitlin G, Gombotz W, Hageman M, Harris R, Heller D, Herman A, Hershenson S, Hora M, Ingram R, Janes S, Watanabe C, A compendium and hydropathy/flexibility analysis of common reactive sites in proteins:

reactivity at Asn, Asp, Gln, and Met motifs in neutral pH solution. *Pharm Biotechnol* **1996,** *9*, 1-140.

129. Waterman, K. C.; Adami, R. C., Accelerated aging: Prediction of chemical stability of pharmaceuticals. *International Journal of Pharmaceutics* **2005,** *293* (1–2), 101-125.

130. Roberts, C. J., Kinetics of Irreversible Protein Aggregation: Analysis of Extended Lumry−Eyring Models and Implications for Predicting Protein Shelf Life. *The Journal of Physical Chemistry B* **2003,** *107* (5), 1194-1207.

131. Stamper, G. F.; Lambert, W. J., Accelerated Stability Testing of Proteins and Peptides: pH-Stability Profile of Insulinotropin Using Traditional Arrhenius and Non-Linear Fitting Analysis. *Drug Development and Industrial Pharmacy* **1995,** *21* (13), 1503-1511.

132. Goldberg, D. S.; Bishop, S. M.; Shah, A. U.; Sathish, H. A., Formulation Development of Therapeutic Monoclonal Antibodies Using High-Throughput Fluorescence and Static Light Scattering Techniques: Role of Conformational and Colloidal Stability. *Journal of Pharmaceutical Sciences* **2011,** *100* (4), 1306-1315.

133. Sahin, E.; Jordan, J. L.; Spatara, M. L.; Naranjo, A.; Costanzo, J. A.; Weiss, W. F.; Robinson, A. S.; Fernandez, E. J.; Roberts, C. J., Computational Design and Biophysical Characterization of Aggregation-Resistant Point Mutations for γD Crystallin Illustrate a Balance

of Conformational Stability and Intrinsic Aggregation Propensity. *Biochemistry* **2011,** *50* (5), 628-639.

134. Krapp, S.; Mimura, Y.; Jefferis, R.; Huber, R.; Sondermann, P., Structural Analysis of Human IgG-Fc Glycoforms Reveals a Correlation Between Glycosylation and Structural Integrity. *Journal of Molecular Biology* **2003,** *325* (5), 979-989.

Chapter 2

Production, Characterization, and Biological Evaluation of Well-Defined IgG1 Fc Glycoforms as a Model System for Biosimilarity Analysis

2.1 Introduction

Protein therapeutics are inherently structurally complex biological drugs whose active components are not a single, well-defined molecule, but a mixture of similar molecules which can differ by type and extent of post-translational modification,[1-5] chemical modifications,[6-11] and three-dimensional conformations.[12-13] In addition, batch to batch variation of active components and production impurities can further complicate defining of the analytical characteristics of a protein drug.[14] Because of this, the assessment of protein therapeutics in comparability studies or in the regulatory approval of biosimilars is not just a simple exercise in confirming the chemical structure of a single active chemical entity in the presence of excipients. Instead, the primary and higher order structures, physicochemical properties, and biological activities of the protein therapeutics must be analyzed. Often, even after extensive study, the relationship between safety and efficacy of a protein therapeutic and these analytical tests is not entirely clear because of the complexity of the mixtures in protein therapeutics and biological systems involved. In an effort to better understand how *in-vitro* analytical tests can be utilized to determine similarity in biosimilar studies and analysis assessments, we have developed a series of well-defined IgG1 Fc glycoforms as a model system. The use of a series of well-defined glycoproteins in these studies should enable identification of important structural and biological features for comparability and biosimilarity exercise.

A series of IgG1 Fc glycoforms were chosen as the protein model system for biosimilarity analysis because as a fragment of full-length IgG1 it is a simpler system to study but contains the C_H2 and C_H3 constant domains which are present in all human IgG1 based mAb therapeutics. The

Fc region is critical to antibody function in that it mediates effector functions such as antibody-dependent cellular cytotoxicity (ADCC)[15-24] and complement dependent cytotoxicity (CDC)[25-27]. The Fc region of an IgG1 is also important in antibody clearance because binding of the Fc region to the neonatal Fc receptor (FcRn) increases *in-vivo* half-life[28-31]. Also, N-linked glycosylation at asparagine 297 (N297) in the Fc region is known to modulate the biological activity[19, 32-39] and physical properties of IgG1 Fc,[1, 32, 40-48] and this can be used to establish similarities and differences between the members of this model system. A series of sequentially truncated glycoforms of IgG1 Fc (Figure 1), which differ only in the size of the N-linked glycan at N297 or a single conservative amino acid mutation (N297Q), were chosen as a model system. Previous studies have indicated that these glycoforms would display a range of biological activities and physical properties[1, 32, 45] that would be advantageous for our biosimilarity studies.

It was first necessary to develop laboratory production methods to produce sufficient quantities (≈100 mg each) of the well-defined IgG1 Fc glycoforms to conduct the wide range of analytical tests necessary for biosimilarity analysis. Presented here are the methods established to produce the glycoforms shown in Figure 1 through yeast expression, purification, and *in-vitro* enzymatic synthesis. Also presented in this work is the initial biochemical characterization of these glycoforms, the development of binding assays for IgG1 Fc binding to an Fc receptor using biolayer interferometry (BLI), and determination of the affinity of the different IgG1 Fc glycoforms for that Fc receptor as an initial evaluation of biological activity.

2.2 Materials and Methods

2.2.1 Materials

Yeast nitrogen base (YNB) was obtained from Sunrise Biosciences, and Bacto™ Tryptone and Yeast Extract was purchased from Becton Dickinson and Company (Franklin Lakes, NJ). Antifoam 204 was obtained from Sigma-Aldrich (St. Louis, MO). Certified ACS grade crystalline sucrose was purchased from Fisher Scientific (Pittsburg, PA). Boc-triglycine was supplied by Bachem Americas, Inc. (Torrance, CA). The enzymes PNGase F, Sortase, and *B. thetaiotaomicron* α-1,2-mannosidase (BT3990, *B.t.* α-1,2-mannosidase) were produced in-house.[49-52] Endoglycosidase H and restriction enzymes were obtained from New England Biolabs (Ipswich, MA). Protein G resin was produced by coupling protein G (recombinantly expressed in *E. coli*)[53] with Sepharose® CL-4B (Sigma-Aldrich, St Louis, MO) using divinyl sulfone as a coupling reagent.[54] General chemicals were purchased from Sigma-Aldrich and Fisher Scientific unless otherwise noted.

2.2.2 Production and Initial Characterization of IgG1 Fc Glycoforms

2.2.2.1 Expression of High-mannose IgG1 Fc (HM-Fc)

HM-Fc was expressed in a glycosylation-deficient strain of *P. pastoris* (an OCH1 and PNO1 deleted, IgG1 Fc expressing, SMD1168 strain of *P. pastoris* produced by Xiao et.al.[55] was utilized) using glycerol (growth phase) and methanol (induction phase) as carbon sources in a NBS BioFlo 415 fermenter (Eppendorf). The starter culture (2 mL) was allowed to grow at 25°C for about 72 hrs in YPD media (1% yeast extract, 2% peptone, 5% glucose and zeocin 100 μg/mL). This starter culture was then inoculated into 250 mL of YPD media in a baffled shake flask and incubated for about 72 hrs. Before inoculation with the starter culture, the fermenter was filled with 7 liters of fermentation basal salts medium (BSM).[56] The components of BSM per liter are 26.7 mL 85%

phosphoric acid, 18.2 g potassium sulfate, 0.93 g calcium sulfate, 14.9 g magnesium sulphate heptahydrate, 4.13 g potassium hydroxide, and 40.0 g glycerol. Finally, water was added to the appropriate volume and the fermentation media was sterilized. After sterilization and cooling, the temperature was adjusted to 30°C and the pH of the BSM medium was adjusted to 6 with 28% Ammonium hydroxide. Next, PTM_1[56] trace salts solution was prepared by mixing the following components (per L): 6.0 g copper sulfate pentahydrate, 0.08 g sodium Iodide, 3.0 g manganese sulfate monohydrate, 0.2 g Sodium Molybdate dihydrate, 0.02 g boric acid, 0.5 g cobalt(II) chloride, 20.0 g zinc chloride, 65.0 g Iron(II) sulfate heptahydrate, 0.2 g biotin and 5.0 mL sulfuric acid. This step was followed by adding 4.31 mL of filter-sterilized PTM_1 trace salts/liter of BSM. Next, the dense 250 mL starter culture media was added into the fermentor. The culture media was allowed to grow until the batch glycerol was consumed, and an additional 300 mL of glycerol were then added to increase the total cell biomass. Dissolved oxygen was kept ≥ 30% throughout the fermentation processes. Once the added glycerol was consumed and the desired cell biomass was attained, a 100% methanol feeding was initiated to induce the AOX1 promoter for IgG1 Fc expression. The temperature was reduced to 25°C for optimal IgG1 Fc expression prior to induction. Methanol induction was continued for approximately 72 hours. The resulting yeast suspension was pelleted by centrifugation at 12,390 x g for 20 min, and the supernatant was collected. Using this procedure, the amount of HM-Fc obtained after protein G affinity purification was approximately 50 mg/L. Four 7 liter fermentations were conducted to produce sufficient HM-Fc to develop the *in-vitro* enzymatic synthesis used to make the Man5-Fc and GlcNAc-Fc glycoforms, and to generate material for the subsequent experiments described in this and the accompanying papers.

2.2.2.2 Expression of Non-Glycosylated Mutant N297Q-IgG1 Fc (N297Q-Fc)

Spinner flask expression was utilized for the production of N297Q-Fc in a glycosylation-deficient strain of SMD1168 *P. pastoris* (Clone produced in previous study[1]) as follows. A starter culture of 2 mL was inoculated in YPD that contained 100 µg/mL Zeocin. This culture media was incubated at 25 °C for 72 hrs. The 2 mL culture was then used to inoculate a 50 mL of YPD/Zeocin culture, which was incubated with shaking at 25°C for 72 hrs. The 50 mL culture was then used to inoculate 1 L of Buffered Glycerol-complex Media (BMGY)[57] containing 0.00004% biotin and 0.004% histidine. After 48 hours, when the initial glycerol carbon source was metabolized, N297Q-Fc expression was induced by methanol feeding to a final concentration of 1% (by addition of 50 mL of 20% methanol every 24 hrs.) for about 72 hrs. The same protocol used for harvesting HM-Fc was applied for harvesting of the N297Q-Fc supernatant. Using this procedure, the amount of N297Q-Fc obtained after protein G affinity purification was about 20 mg/L. A total of seven 1 L spinner flasks were grown to produce the 130 mg of N297Q-Fc used in the research described in this and the accompanying papers.

2.2.2.3 Purification of IgG1 Fc

Both HM- and N297Q-IgG1 Fc were purified using the same general procedure given below. The supernatant collected from yeast expression was filtered with 0.5 µm filter pads (Buon Vino Manufacturing) to remove particulates prior to protein G affinity chromatography. The protein G column (20 mL bed volume) was equilibrated with 20 mM potassium phosphate pH 6.0 in 10 column bed volumes (CV) and loaded with the filtered supernatant at pH 6.0. The column was subsequently washed with 20 mM potassium phosphate buffer, pH 6.0, containing 0.5 M NaCl (5 CV) and then 20 mM potassium phosphate buffer, pH 6.0, (5 CV). IgG1 Fc was eluted

using 100 mM glycine at pH 2.7. Eluted protein was collected in 20 mL fractions into tubes containing 4 mL of 1 M Tris pH 9.0 (200 µL of 1 M Tris pH 9.0 per mL of elution volume) to neutralize the acidic elution buffer. Fractions of eluted protein detected by UV absorbance at 280 nm were immediately dialyzed in 20 mM sodium phosphate buffer pH 7.0. HIC purification using phenyl sepharose™ high-performance resin (GE Healthcare) with a 125 mL column bed volume (packed in-house) and an ÄKTAmicro chromatographic system (GE Healthcare) were utilized to further purify the IgG1 Fc forms. The phenyl sepharose column was pre-equilibrated with Buffer A (20 mM sodium phosphate, pH 7.0, containing 1M ammonium sulfate) for 5 CV. The protein G purified IgG1 Fc was dialyzed in buffer A and then loaded onto the phenyl sepharose column with a loading volume of 50 mL (concentration, 1 mg/mL). The chromatographic separation was then conducted with three gradient segments from 0 to 50% buffer B (20 mM sodium phosphate, pH 7.0): gradient segment 1 (0-25% B, 3.5 CV), gradient segment 2 (25-30% B, 2.6 CV), and gradient segment 3 (30-50% B, 6.7 CV). Collected fractions (10 mL) were analyzed by SDS-PAGE and mass spectrometry to check for purity and identity. Pure fractions were finally pooled and dialyzed in storage buffer (10% sucrose, 20 mM histidine pH 6.0) and frozen at -80˚C in aliquots. The final collected sample pool was analyzed by SEC, SDS-PAGE, mass spectrometry, and cIEF characterization to confirm overall purity and quality. Samples containing pure fractions were concentrated to 0.2 mg/mL using Vivaflow 50, (10,000 MWCO, Sartorius Stedim Biotech). Using this procedure, approximately 445 mg of the HM-Fc glycoform and 118 mg of the N297Q-Fc non-glycosylated mutant were produced for use in synthesis of other glycoforms and biosimilar analysis studies.

2.2.2.4 In-Vitro Enzymatic Synthesis of the Man5-IgG1 Fc Glycoform (Man5-Fc)

HM-IgG1 Fc was converted to Man5-IgG1 Fc in an *in-vitro* enzymatic reaction using *B.t.* α-1,2-mannosidase (BT3990).[51-52] It was found that the *B.t.* α-1,2-mannosidase used in this study had very low activity in the IgG1 Fc sample storage buffer which contained 10% (w/v) sucrose and 20 mM histidine buffer at pH 6.0. Because of this, prior to the reaction HM-Fc (125 mg) was dialyzed extensively in 10 mM MES buffer pH 6.6 to remove the sucrose and histidine. Next, HM-Fc was dialyzed in a reaction buffer containing 5 mM $CaCl_2$, 150 mM NaCl, and 10 mM MES buffer pH 6.6 for 12 hrs. After dialysis the enzymatic reaction was started by adding 6.7 mg of the bacterial α-1,2-Mannosidase (BT3990). The reaction was incubated at room temperature for 48 hrs. The progress of the reaction was monitored by mass spectrometry, and the percentage of conversion to the Man5-Fc glycoform was estimated from the peak intensity (Table 2). Finally, the reaction mixture was purified using protein G affinity chromatography to remove unwanted impurities and excess enzyme using the same protocol as described in the purification of IgG1 Fc section above. The amount of Man5-Fc produced was 75 mg (60% yield), and the percentage of Man5-Fc in the final product was estimated to be 78% by mass spectrometry.

2.2.2.5 In-Vitro Enzymatic Synthesis of the GlcNAc-IgG1 Fc Glycoform (GlcNAc-Fc)

HM-IgG1 Fc was converted to the GlcNAc-IgG1 Fc glycoform using endoglycosidase H (Endo H). Endo H displayed full activity in the IgG1 Fc storage buffer (10 % (w/v) sucrose, 20 mM histidine pH 6.0). Therefore, it was possible to digest HM-IgG1 Fc directly without a dialysis step. HM-IgG1 Fc (100 mg) at a concentration of 0.2 mg/mL was incubated with Endo H (for every 1 mg of HM-IgG1 Fc, 1000 U of Endo H enzyme were added, which corresponds to approximately 0.1 mg of Endo H per 100 mg HM-Fc) at room temperature for 24 hrs. The progress of the reaction

was monitored by SDS-PAGE and mass spectrometry. The sample was analyzed by mass-spectrometry which showed a nearly quantitative reaction with the percentage of GlcNAc-Fc in the final product ≥99%.

2.2.2.6 LC-MS analysis IgG1 Fc glycoforms

Samples of IgG1 Fc glycoforms at a concentration of 0.2 mg/mL were first reduced with 10 mM dithiothreitol (DTT, Invitrogen) and then 30 µL were injected into the mobile phase of the LC. ESI spectra of the reduced samples were acquired on a Agilent 6520 Quadrupole Time-of-Flight (Q-TOF) system. The instrument was operated in positive ion mode, and a spectrum was acquired covering the mass range from 300-3000 m/z with an acquisition rate of 1 spectra/second. The samples were desalted on a reverse phase C4 column, 50 mm, 4.6 mm I.D. (Vydac 214 MS, 300 A pore size, 5 µm particle size) using a Agilent 1200 series Liquid Chromatography system. The solvents used were A (99.9% H_2O, 0.08% formic acid, 0.02% trifluoroacetic acid (TFA) and B (99.9% acetonitrile, 0.08% formic acid, 0.02% TFA). A gradient was developed from 5% B to 90% B in 7 min with a flow rate of 0.5 mL/min. Data was collected using Agilent MassHunter Acquisition software (Version B.02.00). Protein MW was calculated using the Maximum Entropy Deconvolution function and associated peak intensities of the IgG1 Fc glycoforms were obtained using Agilent MassHunter Qualitative Analysis software (Version B.03.01).

2.2.2.7 Sodium Dodecyl Sulfate-Polyacrylamide Gel Electrophoresis (SDS-PAGE)

For the reduced samples, each of the IgG1 Fc glycoforms (20 µg) were mixed with 2X TrisHCl SDS loading dye containing 100 mM DTT and incubated at 80 °C for 2 min. The reduced IgG1 Fc samples were then separated by sodium dodecyl sulfate-polyacrylamide gel

electrophoresis using NuPAGE 4-12% Bis-Tris gradient gel (Life Technologies, Grand Island, NY) gels and a MES running buffer (Life Technologies). A similar method was followed for non-reduced samples of IgG1 Fc proteins except DTT was omitted during the incubation step. The running time for all the gels was 60 min at 150 V. Protein bands were visualized by staining with Coomassie blue R250 (Teknova, Hollister, CA) and destained with a mixture of 30% methanol, 10% acetic acid, and 60% ultrapure water. Gel images were recorded using an Alphaimager (Protein Simple, Santa Clara, CA) gel imaging system.

2.2.2.8 Size Exclusion High-Performance Liquid Chromatography (SEC)

Experiments were performed using a Shimadzu high-performance liquid chromatography system equipped with a temperature controlled auto sampler and a photodiode array detector capable of recording UV absorbance spectra from 200−400 nm. A Tosoh TSK-Gel Bioassist G3SW$_{XL}$ column (7.8 mm ID x 30.0 cm L) and a corresponding guard column (TOSOH Biosciences, King of Prussia, Pennsylvania) were used for IgG1 Fc glycoform characterization. First, the SEC column was equilibrated for at least 10 CV with a mobile phase containing 200 mM sodium phosphate, pH 6.8 and a flow rate of 0.7 mL/min at 30 °C column temperature. Next, the column was calibrated using gel filtration molecular weight standards (Bio-Rad, Hercules, CA) before and after the runs of IgG1 Fc glycoform to ensure column and HPLC system integrity. All Fc samples were centrifuged at 14,000 g for 5 min before injection to remove insoluble protein aggregates. Protein samples at a concentration of 1 mg/mL were injected in a volume of 25 µL, and a 30 min. run time was used for elution. Peaks quantification was carried out using LC solutions software (Shimadzu, Kyoto, Japan). The error bars for monomer content for all the four

IgG1 Fc samples and soluble dimer aggregates (observed in N297Q IgG1 Fc) represent standard deviation (SD) of triplicate measurements.[58,59]

2.2.2.9 Capillary Isoelectric Focusing (cIEF)

The determination of isoelectric points (pIs) of all the IgG1 Fc glycoforms using capillary isoelectric focusing (cIEF) were performed with an iCE280 analyzer from Convergent Biosciences (now Protein Simple, Toronto, Canada) equipped with a microinjector. A FC Cartridge (Protein Simple, Toronto, Canada) with 50 mm, 100 µm I.D. fluorocarbon-coated capillary and built-in electrolyte tanks was used for focusing. The cartridge was calibrated by a hemoglobin standard (Protein Simple, Toronto, Canada) before and after focusing of IgG1 Fc samples to ensure its integrity. For focusing, a sample mixture was prepared where each of the IgG1 Fc glycoforms were mixed with urea (Fischer Scientific), methyl cellulose (Protein Simple, Toronto, Canada), sucrose (Pfanstiehl Inc., Waukegan, IL), N,N,N',N'-Tetramethylethane-1,2-diamine (Sigma-Aldrich, St Louis, MO) and Pharmalyte 3–10 (GE Healthcare Biosciences, Pittsburgh, PA). The final protein concentration in the sample mixture was 0.2 mg/mL. All the IgG1 Fc glycoforms were resolved using a pre-focusing time of 1 minute at 1500 V and a focusing time of 12,12,7.5 and 7 min. was used for HM-Fc, N297Q-Fc, GlcNAc-IgG1Fc, and Man5-Fc, respectively at 3000 V. Observed peaks were calibrated using two pI markers with values of 5.84 and 8.18. The separation was monitored at 280 nm by a CCD detector. Quantitation of the peaks was done using Chromperfect® software. The error bars for pI values of all the four IgG1 Fc samples represent standard deviation (SD) of triplicate measurements.

2.2.2.10 Experimental Procedures for Synthesis of GGG-linker-Biotin (3)

Synthesis of *tert*-butyl (22-amino-2,5,8-trioxo-13,16,19-trioxa-3,6,9-triazadocosyl) carbamate (1). Boc-triglycine (0.145 g, 0.50 mmol) and N-hydroxy-succinimide (0.079 g, 0.50 mmol) were dissolved in 5 mL DMF followed by the addition of solution of DCC (0.134 g, 0.65 mmol). After being stirred on room temperature with N_2 protection overnight, the mixture was filtered and the filtrate was slowly added to the solution of 4,7,10-Trioxa-1,13-tridecanediamine (0.55 mL, 2.5 mmol). The reaction proceeded at room temperature for 5h. Removal of the solvent under reduced pressure followed by purification of the resulting residue through a silica flash column using EtOAc: MeOH 3:1 and then MeOH as the eluting solvents led to the desired compound (**1**) in a yield of 90 % (0.221 g). ^{1}H-NMR (MeOD, 400 MHz): δ = 3.91 (s, 2H), 3.85 (s, 2H), 3.76 (s, 2H), 3.66-3.64 (m, 5H), 3.61-3.58 (m, 7H), 3.31 (t, *J* = 7.1 Hz, 2H), 2.81 (t, *J* = 6.5 Hz, 2H), 1.81-1.77 (m, 4H), 1.47 (s, 9H); ^{13}C-NMR (MeOD, 100 MHz): δ =24.6, 27.3(x3), 28.9, 36.5, 38.7, 42.1, 68.3, 68.4, 69.0, 69.7, 69.8,69.9, 70.0, 170.0, 170.1, 170.9, 172.3; HRMS (ESI) Calcd for $C_{21}H_{41}N_5O_8Na$ $(M + Na)^+$: 514.2853; Found: 514.2849.

Synthesis of *tert*-butyl(2,5,8,24-tetraoxo-28-(2-oxohexahydro-1H-thieno[3,4-d]imidazol-4-yl)-13,16,19-trioxa3,6,9,23-tetraazaoctacosyl) carbamate (2). Biotin (0.122 g, 0.50 mmol) and N-hydroxy-succinimide (0.079 g, 0.50 mmol) were dissolved in 5 mL DMF followed by the addition of solution of DCC (0.134 g, 0.65 mmol). After being stirred at room temperature with N2 protection overnight, the mixture was filtered and the filtrate was slowly added to the solution of compound **1** (0.221 g, 0.45 mmol). The reaction proceeded at room temperature for 2hrs. Removal of the solvent under reduced pressure followed by purification of the resulting residue through a silica flash column using EtOAc: MeOH 4:1 as the eluting solvent led to the

desired compound (**2**) in a yield of 80 % (0.258 g). ^{1}H-NMR (MeOD, 400 MHz): δ = 4.50 (dd, *J* = 7.8, 4.7 Hz, 1H), 4.50 (dd, *J* = 7.8, 4.4 Hz, 1H), 3.91 (s, 2H), 3.85 (s, 2H), 3.77 (s, 2H), 3.67-3.65 (m, 4H), 3.62-3.60 (m, 4H), 3.54 (t, *J* = 5.7 Hz, 4H), 3.33 (t, *J* = 7.4 Hz, 2H), 3.23-3.23 (m, 1H), 2.94 (dd, *J* = 12.8, 5.0 Hz, 1H), 2.72 (d, *J* = 12.7 Hz, 1H), 2.30 (t, *J* = 7.4 Hz, 2H), 2.03-1.61 (m, 8H), 1.52-1.47 (overlap, 11H); ^{13}C-NMR (MeOD, 100 MHz): δ =24.3, 24.5, 24.7, 24.9(x3), 25.3, 26.8, 27.3, 27.9, 28.0, 28.3, 28.6, 30.6, 33.2, 33.4, 39.6, 47.0, 48.3, 50.6, 50.9, 55.5, 55.6, 164.7, 170.0, 173.5 (overlap), 174.5; HRMS (ESI) Calcd for $C_{31}H_{55}N_7O_{10}SNa$ $(M + Na)^+$: 740.3629; Found: 740.3627.

Synthesis of *N*-(1-amino-2,5,8-trioxo-13,16,19-trioxa-3,6,9-triazadocosan-22-yl)-5-(2-oxohexahydro-1*H*-thieno[3,4-*d*]imidazol-4-yl)pentanamide (3). Compound **2** (0.255 g, 0.355 mmol) was dissolved in 1 mL 95% TFA. After 30 min., 2 mL toluene was added to the solution. Removal of the solvent under reduced pressure led to the desired compound **3**, also referred to as GGG-linker-Biotin, in a yield of around 100 % (0.220 g). ^{1}H-NMR (MeOD, 500 MHz): δ = 4.52 (dd, *J* = 7.8, 4.7 Hz, 1H), 4.33 (dd, *J* = 7.8, 4.4 Hz, 1H), 3.99 (s, 2H), 3.87 (s, 2H), 3.79 (s, 2H), 3.67-3.65 (m, 4H), 3.62-3.60 (m, 4H), 3.54 (t, *J* = 5.7 Hz, 4H), 3.26 (t, *J* = 7.4 Hz, 2H), 3.23-3.20 (m, 1H), 2.95 (dd, *J* = 12.8, 5.0 Hz, 1H), 2.72 (d, *J* = 12.7 Hz, 1H), 2.27 (t, *J* = 7.4 Hz, 2H), 2.03-1.61 (m, 8H), 1.52-1.46 (overlap, 11H); ^{13}C-NMR (MeOD, 125 MHz): δ =25.5, 26.8, 28.4, 29.0, 35.2, 36.4, 43.5, 39.7, 40.1, 42.2, 47.8, 48.1, 53.9, 55.6, 56.9, 58.0, 60.2, 62.0, 68.3, 69.7.

2.2.2.11 FcγRIIIa Binding Assays

Production of a *P. pastoris* strain for Expression of Fc γ receptor IIIa with a C-terminal sortase/histidine tag (FcγRIIIa-ST-H_6). The soluble region of the V158 polymorph of human FcγRIIIa was PCR-amplified from pPICzαA-FcγRIIIa[55] using primers (forward 5'-ggcgccgaattcaaaagaatgcggactgaagatctc and reverse 5'gccgcgcgcgcggccgcttaatgatgatggtggtggtgtccacctccagtttctggcaatccaccaccttgagtgatggtgatgttcac) that added a sortase recognition site (ST) and hexahistidine tag (H_6) to the 3' end of the amplified FcγRIIIa DNA. The FcγRIIIa-ST-H_6 PCR product was inserted into the methanol-inducible Pichia expression vector pPICzαA (Invitrogen, Carlsbad, CA) using the restriction sites EcoR I and Not I. The pPICzαA-FcγRIIIa-ST-H_6 construct was confirmed by DNA sequencing, linearized using Sac I, and transformed into *P. pastoris* OCH1 deleted cells.[55] Ten colonies were screened for levels of secreted FcγRIIIa-ST-H_6 expression by growing the colonies in 2 mL culture tubes containing BMGY[57] media +100 μg/mL Zeocin 100 U at 25°C and 250 rpm. Once they reached density, 0.5% (v/v) methanol was added once per day for three days. Relative levels of FcγRIIIa-ST-H_6 in the media was determined by a dot blot using a mouse Anti-H_6 primary antibody (Thermo Scientific, Rockford, IL) followed by a goat Anti-mouse IgG secondary antibody conjugated with alkaline phosphatase (Thermo Scientific, Rockford, IL). The colony that expressed the highest level of FcγRIIIa-ST-H_6 was selected for 1 L spinner flask expression.

2.2.2.12 Expression and Purification of FcγRIIIa-H_6 and FcγRIIIa-ST-H_6

FcγRIIIa-H_6 and FcγRIIIa-ST-H_6 were expressed in glycosylation-deficient *P. pastoris,* and Ni^{+2}-NTA was used as described previously by Xiao et al.[55] After Ni^{+2}-NTA purification,

approximately 30 mg/L of each receptor was obtained. The receptors were then further purified using hydrophobic interaction chromatography. A Hiprep™ Phenyl FF (high sub) 16/10 column with a 20 mL bed volume was utilized with an ÄKTAmicro (GE Healthcare) to accomplish this. The column was pre-equilibrated with buffer A (1.5 M Ammonium sulfate,100 mM sodium phosphate for 10 CV) prior to loading. The Ni^{+2}-NTA purified receptors were first dialyzed in 100 mM sodium phosphate pH 7.0 buffer for 12 hrs and then adjusted with ammonium sulfate to a final concentration of 1.5 M. The receptors, in 10 mg portions, were loaded onto the column with a loading volume of 5 mL. Due to the capacity of the column, 3 columns were necessary to purify all 30 mg of receptor obtained from Ni^{+2}-NTA chromatography. The chromatographic separation involves three segments from 0 to 100% B (100 mM sodium phosphate pH 7.0): gradient segment 1 (0-25% B, 15 CV), gradient segment 2 (25-33% B, 15 CV), and gradient segment 3 (33-100% B, 12 CV). Collected fractions (5 mL) were characterized using SDS-PAGE to check for purity. Samples containing pure receptor were concentrated to 1 mg/mL using Vivaflow 50, (10,000 MWCO, Sartorius Stedim Biotech) and the amount obtained after purification for each receptor was approximately 18 mg/L.

2.2.2.13 Biotinylation of FcγRIIIa-ST-H_6

Purified FcγRIIIa-ST-H_6 was extensively dialyzed in 50 mM Tris-hydrochloride pH 7.5. Next, this receptor was dialyzed in a reaction buffer containing 50 mM Tris-hydrochloride pH 7.5, 150 mM sodium chloride. The sortase-mediated ligation reaction was carried out using a mixture containing 10 µM FcγRIIIa-ST-H_6, 6 mM $CaCl_2$, 1 mM GGG-linker-Biotin (compound **3**, Fig. 6) and 5 µM sortase at room temperature. The reaction was terminated after 24 hours by adding excess

EDTA to capture the Ca^{+2} required for activity of the sortase. Finally, the receptor was extensively dialyzed in PBS buffer to remove the unreacted GGG-linker-Biotin (**3**).

2.2.2.14 Analysis of the Interaction of Immobilized IgG1 Fc Glycoforms with FcγRIIIa using Biolayer Interferometry (BLI)

The interactions of the different IgG1 Fc glycoforms with the FcγRIIIa-H_6 were studied with biolayer interferometry using a BLITZ instrument (Fortebio, Menlo Park, CA) with protein G biosensor tips. Binding studies using this receptor were conducted as follows. The protein G biosensor tip was hydrated for 10 min with PBS buffer (150 mM NaCl, 50 mM sodium phosphate pH 7.4) and then incubated for 30 min with PBS kinetic buffer (PBS buffer containing 1 mg/mL casein as a blocking agent). Next, an initial baseline (30 sec) was established with PBS kinetics buffer and then the protein G biosensor tips were loaded with the IgG1 Fc glycoforms at a concentration of 0.88 μM (120 sec) to a response level of 2 nm. A new baseline (30 sec) was then established and then the association (180 sec) and dissociation (360 sec) of FcγRIIIa-H_6 was measured by dipping the biosensor into solutions of FcγRIIIa-H_6 and PBS, respectively. To determine the dissociation constant (K_D) for the IgG1 Fc glycoforms, a range of FcγRIIIa-H_6 concentrations from 50 nM-800 nM were tested for HM-Fc and Man5-Fc. For GlcNAc-Fc, the concentration range of FcγRIIIa-H_6 tested was 200 nM to 1600 nM in two-fold serial dilutions. For N297Q-Fc, no binding was observed at 20 μM FcγRIIIa-H_6, the highest concentration of receptor tested. After each assay cycle, the biosensor tip was regenerated using two cycles of 10 mM HCl[60] for 30 sec and each time equilibrated using PBS kinetics buffer for 60 sec Data generated from the binding of the receptor to IgG1 Fc glycoforms were collected six times and globally fitted to a 1:1 binding model and analyzed using BLITZ Pro software.

2.2.2.15 Analysis of the Interaction of IgG1 Fc Glycoforms with Immobilized FcγRIIIa using Biolayer Interferometry (BLI)

The interactions of the different IgG1 Fc glycoforms with the FcγRIIIa were studied with biolayer interferometry using a BLITZ instrument (Fortebio, Menlo Park, CA) with streptavidin (SA) biosensor tips. Prior to the binding experiment, IgG1 Fc samples were dialyzed in PBS buffer to remove the storage buffer (10% sucrose, 20 mM histidine, pH 6.0) and to adjust the pH to 7.4. The concentration of the samples after dialysis was 2.3 µM. Next, a stock solution of each glycoform in PBS kinetic buffer (PBS buffer containing 1 mg/mL casein) were prepared by adding casein (the stock solution of casein used was 10 mg/mL in PBS buffer), and PBS buffer. For HM-Fc and Man5-Fc, stock samples with a concentration of 1.6 µM were prepared and then serially diluted to prepare samples of 800 nM, 400 nM, 200 nM, 100 nM, and 50 nM concentrations by adding PBS kinetics buffer. For subsequent serial dilutions, PBS kinetic buffer containing 1 mg/mL of casein was used. Similarly, for GlcNAc-Fc a stock sample with a concentration of 2.0 µM was prepared and then used to prepare samples of 1600 nM, 800 nM, 400 nM, and 200 nM, by adding PBS kinetic buffer. For N297Q-Fc, after dialysis in PBS buffer, samples were first concentrated to 25 µM using an Amicon® Ultra-15 Centrifugal Filter Device with a molecular weight cutoff of 10 kDa (EMD Millipore, Billerica, MA). Next, a solution containing 20 µM of N297Q-Fc in PBS kinetic buffer was prepared by dilution with PBS buffer and casein (added from a stock solution of 10 mg/mL casein in PBS buffer). This final sample concentration of 20 µM N297Q-Fc was then used for binding experiments without further dilution.

After sample preparation, binding studies were conducted as follows. First, the streptavidin biosensor tip was hydrated for 10 min with PBS buffer and incubated with PBS kinetic

buffer for 30 min. Next, the biotinylated FcγRIIIa-ST-H_6 (0.1 μM) was immobilized onto the streptavidin biosensors to a response level of 0.4 nm and this step was followed by establishing an initial baseline (30 sec) with PBS kinetic buffer. Then the association (180 sec) and dissociation(360 sec) of the IgG1 Fc glycoforms were measured by dipping the biosensor into solutions of IgG1 Fc glycoforms and PBS, respectively. After each assay cycle, the biosensor tip was regenerated using two cycles of 1 mM NaOH[61] for 30 sec and each time equilibrated with PBS kinetic buffer for 60 sec To determine the dissociation constant (K_D), the concentration range tested for HM-Fc and Man5-Fc in solution were 50 nM to 800 nM in two-fold serial dilutions. The concentrations of GlcNAc-Fc tested in solution ranged from 200 nM to 1600 nM in two-fold serial dilutions. For N297Q-Fc, no binding was observed with 20 μM N297Q-Fc in solution. Data generated from the binding of the receptor to IgG1 Fc glycoforms were collected six times and globally fitted to a 1:1 binding model and analyzed using BLItz Pro software.

2.3 Results

2.3.1 Production and Initial Characterization of the Four Well-Defined IgG1 Fc Glycoforms

2.3.1.1 Expression and Purification of High-Mannose IgG1 Fc (HM-Fc) and Non-Glycosylated Mutant N297Q-IgG1 Fc (N297Q-Fc)

Both HM-Fc and N297Q-Fc were recombinantly expressed in glycosylation-deficient strains derived from SMD1168 *P. pastoris* (Invitrogen, Carlsbad, CA). The expression strains were produced as described previously and have the genes OCH1 and PNO1 deleted to reduce the formation of higher order mannan structures and the addition of mannose-phosphorylation.[55,1] The resulting yeast strains produce glycoproteins containing human-like high-mannose N-linked glycans with some additional heterogeneous α-1,2-linked mannose residues added onto an initial

$Man_8GlcNAc_2$ structure. Due to the large amount of HM-Fc required for production of the three glycosylated forms, HM-Fc, Man5-Fc, and GlcNAc-Fc, the HM-Fc was produced in a 10 liter fermentor using basal salts media supplemented with PTM_1 trace salts solution. Protein expression was induced by methanol addition and yeast were harvested after approximately 3 days of induction. Compared to HM-Fc, relatively smaller amounts of N297Q-Fc were required (since it is not used to produce the other Fc glycoforms). Accordingly, N297Q-Fc was expressed in spinner flasks using BMGY media to generate cell mass, and 3 days of methanol induction to produce protein prior to harvest similar to the HM-Fc form. Typical yields from this expression system for the two IgG Fc proteins are summarized in the next section.

The same general purification procedure was utilized for both HM-Fc and N297Q-Fc. Yeast cells were removed by centrifugation, and the resulting supernatant was filtered through 0.5 µm filters to remove remaining particulates prior to chromatography. Secreted IgG1 Fc was then isolated by protein G affinity chromatography. The average yield of HM-Fc from fermenter growth after protein G affinity chromatography was approximately 50 mg/L. The average yield of N297Q-Fc after spinner flask expression was approximately 20 mg/L. After protein G affinity chromatography, there are still some residual yeast proteins remaining in both HM-Fc and N297Q-Fc. In the case of HM-Fc, incomplete glycosylation of the N297 site in yeast also results in microheterogeneity of the glycosylation site.[1-2, 55, 62] Because of this, the disulfide bonded HM-Fc dimer consists of three forms, a completely non-glycosylated form, a form that has glycosylation on only one chain of the dimer (mono-glycosylated), and a form that is glycosylated on both chains of the dimer (di-glycosylated). Hydrophobic interaction chromatography (HIC) using phenyl sepharose resin was utilized to remove residual yeast impurities for both proteins and to

separate the di-glycosylated form of HM-Fc from its mono-glycosylated and non-glycosylated forms. Because protein G purified HM-Fc is distributed between three different forms, the yield of di-glycosylated HM-Fc from HIC purification is lower than that of N297Q-Fc. Nonetheless, after HIC purification 445 mg of HM-Fc and 118 mg of N297Q-Fc were produced for further synthesis and studies. Hereafter HM-Fc will refer to the di-glycosylated form of HM-IgG1 Fc obtained from yeast. Purified protein samples were pooled, dialyzed in storage buffer (10% sucrose, 20 mM histidine pH 6.0), concentrated or diluted to a final concentration of 0.2 mg/mL, and frozen at -80°C in aliquots for future use.

2.3.1.2 In-Vitro Enzymatic Synthesis of Man5-IgG1 Fc (Man5-Fc) and GlcNAc-IgG1 Fc (GlcNAc-Fc)

HM-Fc was converted into the Man5-Fc glycoform using *B.t.* α-1,2-mannosidase (BT3990).[51-52] The outer mannose residues of high-mannose N-linked glycans produced in glycosylation-deficient yeast are α-1,2-linked to a core of five mannose residues that are α-1,3- and α-1,6-linked to one another and β-1,4-linked to the two N-acetylglucosamines attached to asparagine. Because of this, digestion the HM-Fc glycoform with a selective α-1,2-mannosidase will result in the formation of the Man5-Fc glycoform. Unfortunately, initial trial mannosidase reactions revealed that the *B.t.* α-1,2-mannosidase had very little activity in the sucrose containing storage buffer. Hence, before the reaction the starting material (HM-Fc) was extensively dialyzed to remove the storage buffer and exchange it into a buffer the α-1,2-mannosidase had higher activity. Addition of mannosidase (6.7 mg) and incubation at room temperature for 2 days resulted in conversion of the HM-Fc into the Man5-Fc glycoform. Protein G affinity chromatography was utilized to remove the mannosidase enzyme from Man5-Fc, and the protein was dialyzed into storage buffer and adjusted to 0.2 mg/mL concentration. At total

of 75 mg of Man5-Fc was produced from 125 mg of HM-Fc starting material. The low yield of Man5-Fc is likely due to the many extra dialysis steps and the protein G purification in this procedure.

The enzyme endoglycosidase H (Endo H) was utilized to generate further truncation of the high-mannose glycan on HM-Fc. Endo H cleaves at the β-1,4 linkage between the two GlcNAc residues attached to asparagine in high-mannose N-linked glycans. This leaves a single GlcNAc monosaccharide attached at the glycosylation site (Figure 1)**.** Endo H has high activity in the sample storage buffer used to store HM-Fc, and this greatly simplified the production of the GlcNAc-Fc glycoform. A small amount (≈ 0.1 mg) of Endo H added to 100 mg HM-Fc in storage buffer resulted in a quantitative conversion into the GlcNAc-Fc glycoform after incubation at room temperature for 24 hours. Since Endo H was active in storage buffer and only a minute amount was added, GlcNAc-Fc was utilized without any further purification. Approximately 100 mg of GlcNAc-Fc was produced from 100 mg of HM-Fc starting material.

2.3.2 Analytical Characterization of IgG1 Fc Glycoforms

Figure 2 shows intact mass spectrometry data of the four glycoforms, HM-Fc, Man5-Fc, GlcNAc-Fc, and N297Q-Fc, with their respective expected and observed masses. Since the amino acid sequence of HM-Fc, Man5-Fc, and GlcNAc-Fc are identical, the differences in observed masses are mainly due to differences in the attached N-linked glycans. For the HM-Fc glycoform, glycosylation is heterogeneous with high-mannose forms containing between 8 to 12 mannose residues with the major glycoform being the $Man_8GlcNAc_2$ form. The predominant forms of the truncated Man5-Fc and GlcNAc-Fc glycoforms on the other hand are largely one glycosylation state, with estimated abundance of 78% and 99% for the Man5-Fc and GlcNAc-Fc forms

respectively based on peak heights (Table 2). The N297Q-Fc form displays a single major peak corresponding to the non-glycosylated glutamine mutant as would be expected.

The four glycoforms were analyzed by SDS-PAGE under reducing and non-reducing conditions and the results are shown in Figure 3. Purity was estimated to be ~99% for each glycoform and no proteolysis or significant impurities were detected.[63] The shift in migration between the reduced and non-reduced gels indicate intermolecular disulfide bonds are present forming dimers as would be expected in the hinge region. Also, no monomeric IgG1 Fc was detected in the non-reduced gel for any glycoform indicating that all of the IgG1 Fc is present in the dimerized state. Migration of the different glycoforms in both the reduced and non-reduced gels correlates with the size of the N-linked glycans attached, with slower migration occurring for forms with larger N-linked glycans.

Size exclusion chromatography (SEC) was utilized to characterize the size and distribution of high-molecular weight species (HMWS) and low molecular weight species (LMWS) which potentially could be generated during production and purification of IgG1 Fc glycoforms. High molecular weight species could potentially be covalent aggregates, and low molecular weight species are related to fragments from the heavy chains.[64-65] Representative SEC chromatograms of the IgG1 Fc glycoforms are shown in Figure 4 (also see Table 3). All of the IgG1 Fc proteins eluted at ~15 min, which corresponded to a monomer based on the elution pattern of molecular weight standards. As illustrated in Figure 4, the results indicate all the IgG1 Fc glycoforms are monomeric (96-99%) with low levels of aggregates present across the IgG1 Fc samples (1-3 %). No higher molecular weight species (HMWS) were visible in the chromatograms of all the four glycoforms except for the N297Q-Fc, which showed some soluble dimers (~3%). Additionally, the

data indicate no low molecular weight species (LMWS) which is in agreement with SDS-PAGE characterization. All glycoforms were ≥98% monomeric except for the non-glycosylated form, which was greater than 96.4% monomeric. This difference is presumably due to the absence of glycosylation in N297Q-Fc. It has been reported that removal of glycosylation increases the aggregation propensity of IgGs.[47]

The charge distribution profiles of the four IgG1 Fc glycoforms were analyzed using cIEF. Representative electropherograms of HM-Fc, Man5-Fc, GlcNAc-Fc, and N297Q-Fc are shown in Figure 5 (Table 4). All the electropherograms show one major peak, which after resolution gave pI values of 7.0, 6.9, 7.1 and 7.4 for HM-Fc, Man5-Fc, GlcNAc-Fc, and N297Q-Fc, respectively. The theoretical isoelectric points (pI) of IgG1 Fc from the amino acid sequence is 6.9 which is in close agreement with the experimental pI values obtained given assay variability. Nonetheless, the slightly basic shift of the aglycosyated form, compared to other three glycoforms, could be due to the lack of oligosaccharides at the N297 site. Although there are no visible basic variants observed, there are minor acidic peaks/shoulders near the main peaks with the pI values ranging from 5.6-6.8. The observed heterogeneity could potentially be from chemical modifications in IgG1 Fc proteins (e.g., deamidation) during production and/or purification. In summary, these results demonstrate that each of the IgG1 Fc glycoforms is an overall well-defined glycoform species, with some minor charge heterogeneities and soluble aggregates present.

2.3.3 Evaluation of Affinity for IgG1 Fc Glycoforms with FcγRIIIa Using Biolayer Interferometry (BLI)

2.3.3.1 Expression and Purification of two Forms of FcγRIIIa for use in Binding Assays

We have previously produced an expression strain for the production of the soluble domain of FcγRIIIa in yeast with a C-terminal histidine tag for affinity purification, reported in Xiao et al.[55], and this strain was utilized to produce FcγRIIIa-H_6 used in the binding assays with IgG1 Fc-immobilized on protein G biosensors. To reverse the immobilization format and have the receptor-immobilized, a new expression strain was also constructed that produces the soluble domain of FcγRIIIa in yeast with a combined C-terminal histidine and sortase tag. This new receptor form, FcγRIIIa-ST-$H_{6,}$ allows for affinity purification and the attachment of synthetic molecules, such as the synthetic biotin derivative used in this study, selectively to the C-terminus using sortase-mediated ligation.[50, 66-68] Both receptors were expressed in a glycosylation-deficient strain of *P. pastoris* with glycerol and methanol as carbon sources. After centrifugation and filtration to remove yeast, Ni^{+2}-NTA affinity chromatography was utilized to isolate the FcγRIIIa forms. The receptors were further purified by phenyl sepharose chromatography, and after isolation and concentration approximately 18 mg/L of purified protein were obtained for both forms of FcγRIIIa.

2.3.3.2 Selective C-terminal Biotinylation of FcγRIIIa-ST-H_6 Using Sortase-Mediated Ligation

Sortase mediated ligation[50, 66-68] was utilized to attach biotin to the C-terminus of FcγRIIIa. Bacterial sortases, such as the SrtA of *S. aureus*, are enzymes that catalyze transpeptidase reactions to attach proteins containing sortase recognition sites to the peptidoglycan of bacterial cell walls. Sortases have been adapted for biotechnology applications using the sortase reaction

for immobilization and to attach synthetic molecules and labels selectively to the N- or C-termini of recombinant proteins. The requirements for sortase ligations are N-terminal poly-glycine containing peptides, such as those found in peptidoglycan, and C-terminal recognition peptide motifs such as LPETG, as in the SrtA mediated ligation used in this study.[50, 66-68] The C-terminal peptide is cleaved between threonine and glycine and a new peptide bond is formed between the N-terminal poly-glycine containing molecule and the C-terminal threonine. Accordingly, in order to selectively biotinylate FcγRIIIa-ST-H_6 it was necessary to synthesize a form of biotin containing an N-terminal poly-glycine. In addition, to ensure strong binding to streptavidin and prevent steric hindrance with streptavidin interfering with the interaction of FcγRIIIa with IgG1 Fc, a long hydrophilic diamine linker was used to separate biotin from the C-terminus of FcγRIIIa. The synthesis of GGG-linker-Biotin (compound **3**) is described in the Supporting information for this paper (Figure 10), and the ligation of GGG-linker-Biotin to FcγRIIIa-ST-H_6 is shown in Figure 6. The sortase reaction proceeded efficiently to attach biotin to the C-terminus of FcγRIIIa-ST-H_6, and the resulting biotinylated FcγRIIIa was immobilized in binding assays with streptavidin biosensors.

2.3.4 Analysis of Binding of Immobilized IgG1 Fc Glycoforms to FcγRIIIa Using Biolayer Interferometry (BLI)

The affinity of FcγRIIIa in solution for immobilized IgG1 Fc glycoforms was studied using BLI with protein G biosensors. The format for this binding study is shown in Figure 7A. Protein G biosensors were first loaded with IgG1 Fc glycoforms to a response level of 2 nm using 0.8 μM solutions of the various IgG1 Fc glycoforms. Then a baseline was established and the association of FcγRIIIa was observed by dipping the biosensor into solutions of different concentrations of FcγRIIIa. After the Fc-FcγRIIIa complex had formed on the biosensor, dissociation of FcγRIIIa was

observed by placing the biosensor in a solution of PBS kinetic buffer. The kinetic rate constants for association, k_a, and dissociation, k_d, were then obtained by fitting the resulting curves to a 1:1 binding model which is consistent with previous biochemical and structural studies of this interaction.[69] The equilibrium dissociation constant was determined by dividing k_d by k_a for each glycoform. Representative sensorgrams for each glycoform (HM-Fc, Man5-Fc, GlcNAc-Fc, and N297Q-Fc) are displayed in Figure 8, and the results for these binding experiments are given in Table 1 (Figure 13 also displays representative sensograms with curve fits added). HM-Fc and Man5-Fc have similar high affinity for FcγRIIIa as would be expected for high-mannose IgG1 Fc glycoforms, with K_D's of 27.7 nM and 31.8 nM, respectively.[1-2, 70] In contrast, the GlcNAc-Fc glycoform has significantly weaker binding to FcγRIIIa with a K_D of 1115 nM, and this agrees with recent studies of this glycoform.[71] Interestingly, the association rate constants (k_a) are very similar for HM-Fc, Man5-Fc, and GlcNAc-Fc, such that the driving factor behind the GlcNAc-Fc's weaker affinity for FcγRIIIa is its significantly faster dissociation rate (k_d). This similarity in k_a values and significant differences in k_d and K_D values is illustrated in Figure 12. No interaction was observed between FcγRIIIa and the non-glycosylated N297Q-Fc form at the highest concentration of receptor tested (20 μM).

2.3.5 Analysis of Binding of IgG1 Fc Glycoforms to Immobilized FcγRIIIa Using Biolayer Interferometry (BLI)

The affinity of the IgG1 Fc glycoforms in solution for immobilized FcγRIIIa was studied using BLI with streptavidin biosensors. The format for this binding study is shown in Figure 7B. Streptavidin biosensors were first loaded with C-terminally biotinylated FcγRIIIa to a response level of 0.4 nm using 0.1 μM biotinylated FcγRIIIa. Next a baseline was established and the association of IgG1 Fc glycoforms was observed by dipping the biosensors into solutions of

different concentrations of IgG1 Fc glycoforms. After the complex had formed on the biosensor, dissociation of the IgG1 Fc glycoforms was observed by dipping the biosensor into of PBS kinetic buffer. Kinetic rate constants and equilibrium dissociation constants were determined as described for the protein G method above. Representative sensorgrams for each glycoform (HM-Fc, Man5-Fc, GlcNAc-Fc, and N297Q-Fc) are displayed in Figure 9, and the results for these binding experiments are given in Table 1 (Figure 14 also displays representative sensograms with curve fits added). Perhaps not surprisingly, the affinities determined for this receptor-immobilized binding format were very similar to the results observed for the IgG1 Fc-immobilized binding format. HM-Fc and Man5-Fc showed similar high affinity for FcγRIIIa with K_D's of 26.4 nM and 32.8 nM, respectively.[1-2, 70] Also, the GlcNAc-Fc glycoform displayed much weaker binding with a K_D of 995 nM, and this weak affinity was again due to a larger dissociation rate constant (k_d) for GlcNAc-Fc relative to the other glycoforms. Finally, the N297Q-Fc form displayed no affinity for immobilized FcγRIIIa even at 20 μM N297Q-Fc.

2.4 Discussion

2.4.1 Production and Initial Characterization of Well-Defined IgG1 Fc Glycoforms

As a first step to develop a model system for biosimilar analysis studies, it was desirable to not only have a group of related well-defined proteins that differ from one another in specific attributes, but also to be able to produce relatively large amounts of those proteins, on an academic laboratory scale, to provide sufficient material to conduct biosimilarity assessments through a combination of biochemical, physicochemical and biological tests. To achieve this, glycosylation-deficient yeast (OCH1/PNO1 deleted *P. pastoris* derived from strain SMD1168) that express human-like, high-mannose type N-linked glycosylation were utilized to produce the IgG1

Fc glycoproteins and the non-glycosylated mutant used in this study. IgG1 Fc was secreted into culture media, and after centrifugation and filtration the IgG1 Fc was captured and purified using protein G affinity chromatography. Residual yeast impurities and, in the case of HM-Fc, removal of mono- and non-glycosylated IgG1 Fc forms was accomplished using HIC chromatography. The non-glycosylated N297Q-Fc mutant (Figure 1) was utilized directly as a negative control for the effects of glycosylation in these studies. The glycosylated HM-Fc glycoform (Figure 1) is a member of this model system and also serves as the starting material for the production of the remaining two glycoforms of the model system. The HM-Fc glycoform was treated with *B.t.* α-1,2-mannosidase and Endo H to produce the Man5-Fc and GlcNAc-Fc glycoforms respectively (Figure 1). The HM-Fc, Man5-Fc, and GlcNAc-Fc glycoforms form a well-defined series where HM-Fc contains the largest N-linked glycan and the remaining glycoforms are sequentially truncated to give the intermediate glycosylation state of Man5-Fc, and the minimally glycosylated state of GlcNAc-Fc. This series of glycoproteins with decreasing N-linked glycan size all derived from the same precursor should be useful in elucidating effects of glycosylation on the biological and physicochemical properties of IgG1 Fc.

In terms of ease of production, the HM-Fc and N297Q-Fc are both derived directly from fermentation, and therefore more easily accessed than the other two glycoforms. Because N297Q-Fc has no glycosylation site occupancy heterogeneity, its HIC purification is simplified compared to the HM-Fc form which requires separation of di-, mono-, and non-glycosylated forms. After HIC purification of both forms, 445 mg of HM-Fc and 118 mg of N297Q-Fc were produced for this study from approximately 28 and 7 liters of growth media, respectively. Conversion of 100 mg of HM-Fc into GlcNAc-Fc using Endo H (approximately 0.1 mg) was

straightforward and nearly quantitative, allowing relatively easy access to 100 mg of the GlcNAc-Fc glycoform. Production of the Man5-Fc glycoform was more problematic since it was discovered that the *B.t.* α-1,2-mannosidase had little activity in sucrose containing storage buffer after the HM-Fc had been transferred into the storage buffer. This required additional dialysis steps to transfer the HM-Fc into a different buffer to conduct the *B.t.* α-1,2-mannosidase reaction. In addition, a larger amount of *B.t.* α-1,2-mannosidase (6.7 mg) relative to Endo H (0.1 mg) was required for the reaction to produce Man5-Fc, and this made it necessary to purify the Man5-Fc glycoform by an additional protein G affinity chromatography step after the mannosidase reaction. All of these factors combined to result in a 60% yield for conversion of HM-Fc into Man5-Fc and only 75 mg of the Man5-Fc glycoform being produced. The amount of Man5-Fc produced was sufficient to conduct this and the accompanying studies, but the procedure to produce this glycoform could be optimized in the future to produce more of this glycoform in a higher yield. Taken together, these methods allow easy access to the four well-defined glycoforms from Figure 1 in quantities sufficient to enable a wide range of biosimilar analysis and stability studies.

Initial characterization of the glycosylation state of the model glycoforms was conducted using intact protein mass spectrometry. Mass spectrometry was used to confirm the type of glycosylation on each glycoform and determine if there were any significant proteolytic products present (Figure 2). None of the IgG1 Fc glycoforms showed any evidence of internal proteolysis, and all were found to be in forms containing their complete amino acid sequences including C-terminal lysine residues. The intact protein mass spectra also allowed evaluation of the glycosylation state of the IgG1 Fc glycoforms. The N297Q-Fc and GlcNAc-Fc glycoforms were

highly homogeneous with single peaks corresponding to no glycosylation with a glutamine mutation and a single GlcNAc attached to asparagine, respectively. The HM-Fc glycoform obtained directly from yeast was heterogeneously glycosylated with high-mannose type glycans ranging in size from $Man_8GlcNAc_2$ to $Man_{12}GlcNAc_2$, with the form containing $Man_8GlcNAc_2$ being the major form at approximately 49% of its glycosylation sites based on peak intensities (Table 2). The mannosidase treated Man5-Fc glycoform is much more homogeneous and estimated to contain $Man_5GlcNAc_2$ on 78% of its glycosylation sites based on peak intensities (Table 2). The remainder of the glycoform peaks observed in the Man5-Fc mass spectra correspond to small amounts of incompletely cleaved high-mannose glycosylated forms, indicating the mannosidase reaction could be further optimized in the future. The mass spectrometry results demonstrate well-defined differences between the model IgG1 Fc glycoforms based on the size or absence of N-linked glycosylation.

Additional biochemical characterization was conducted using SDS-PAGE, size exclusion chromatography (SEC), and capillary isoelectric focusing (cIEF). This was done to further define the chemical state and purity of the IgG1 Fc glycoforms and to establish a baseline prior to the chemical and physical stability studies described in other works.[72-73] Reducing and non-reducing SDS-PAGE (Figure 3) display an absence of proteolytic fragments and show high purity for each glycoform. In addition, the non-reduced SDS-PAGE indicated complete intermolecular disulfide bond formation corresponding to 100% dimerized form for all glycoforms. Analysis of the glycoforms by SEC (Figure 4) revealed that all members of the model system were largely in the monomeric state with the amount of monomer ranging from 96-99%. The non-glycosylated N297Q-Fc form displayed the most amount of soluble dimers present in SEC at 3%, which may

be a consequence of the absence of glycosylation to stabilize protein folding and prevent aggregation. Analysis of the isoelectric points for the four glycoforms also identified a difference between the N297Q-Fc form and the other forms, with the N297Q-Fc form having a pI of 7.4 compared to 7.0, 6.9, and 7.1 for HM-Fc, Man5-Fc, and GlcNAc-Fc, respectively (Figure 5). The significance and cause of this difference in the pIs between the non-glycosylated form and the others is not clear at this time since none of the N-linked glycans present on the glycoforms are charged and neither is glutamine or asparagine. Interestingly, it has been noted by our laboratory and others that cation exchange chromatography can be used to separate glycosylated and non-glycosylated proteins from one another even when only neutral oligosaccharides are present on the glycosylation sites. The elution order observed from cation exchange chromatography in the cases of separation of glycosylated and non-glycosylated IL-1ra and di-glycosylated IgG from mono- and non-glycosylated IgG are consistent with the non-glycosylated forms having higher isoelectric points.[2-3, 74]

2.4.2 Biological Evaluation of Well-Defined IgG1 Fc Glycoforms

Potential biological activities of the IgG1 Fc glycoforms in our model system were assessed using binding to an activating Fc receptor, FcγRIIIa, as a measure of the potential to activate antibody dependent effector functions. In full-length antibodies, simultaneous binding of the antigen binding regions of an antibody to a polyvalent antigen and the antibody Fc region to FcγRIIIa can activate antibody dependent cell-mediated cytotoxicity (ADCC).[75] FcγRIIIa is also important in the function of natural killer cells, since it is the only Fc receptor expressed on natural killer cells (NK cells).[76] ADCC and NK cells are both believed to be important in the function of many therapeutic mAbs.[76-77] Additionally, FcγRIIIa is sensitive to the type of glycosylation

present on the Fc region of antibodies, having high affinity to antibodies that do not contain core-linked fucose, and like most Fc receptors, lower affinity for truncated N-linked glycans.[77] This makes FcγRIIIa useful in distinguishing the different IgG1 Fc glycoforms in our model system.

The interactions of the IgG1 Fc glycoforms with FcγRIIIa were assessed with kinetic binding studies using biolayer interferometry (BLI). Observation of binding using surface techniques such as BLI or surface plasmon resonance (SPR) generally do not require large amounts of material to conduct binding studies, and this is an advantage for biosimilarity analysis studies where many samples may be required to be analyzed. Kinetic binding studies using BLI or SPR allow determination of kinetic rate constants for association (k_a) and dissociation (k_d), and by taking the ratio of the kinetic rate constants, equilibrium dissociation constants (K_D) can be determined. One drawback of surface binding techniques is that one binding partner, receptor or ligand, needs to be immobilized to conduct the experiment (Figure 7). Choice of which component, receptor or ligand, to immobilize and method of immobilization can both affect the outcome of the experiment. In addition, from the perspective of conducting experiments with samples of formulated drug products, the format of binding assays can have practical effects on how the assays are conducted and what kind of information is obtained. To gain a better understanding of how binding format affects the results of binding studies, we developed two formats for studying the interaction of IgG1 Fc glycoforms with FcγRIIIa (Figure 7), one with the IgG1 Fc-immobilized and one with the receptor-immobilized.

For a BLI binding format where the IgG1 Fc glycoforms were immobilized (Figure 7A), we decided to use protein G biosensors for immobilization of IgG1 Fc glycoforms. Protein A and/or protein G have previously been used in SPR binding studies of IgG interactions with Fc receptors,

and immobilization using these proteins have many advantages.[78-79] Since protein G binds tightly to IgGs over a wide pH range (≈ pH 5-8), protein G biosensor tips can be loaded under a variety of formulation conditions without having to adjust the buffer conditions of samples to promote immobilization. In addition, once IgG1 Fc (or full-length IgG) has been immobilized onto a protein G biosensor, binding experiments can be conducted in buffers optimized for receptor binding by simply dipping the IgG1 Fc loaded protein G biosensor into receptor solutions with optimized buffer conditions. Also, protein G biosensors can be regenerated by acidic treatment much the way protein A and protein G affinity resins are eluted during affinity chromatography, allowing for relatively easy reuse of protein G biosensors. A disadvantage of using protein G biosensors to immobilize IgG1 Fc in binding studies may arise during stability studies when there is the potential of the formation of damaged forms of IgG1 Fc which would no longer be capable of binding to protein G, but which could still retain the ability to bind to Fc receptors. Such proteins would not be measured in this assay format. Also, this assay format is relatively insensitive to the actual concentration of IgG1 Fc glycoforms in samples, since to obtain reproducible binding curves the biosensors are loaded to the same approximate level, and because of this changes in concentrations in the samples may be difficult to detect. Nevertheless, this assay format provides valuable information about the kinetics and thermodynamics of the interaction of IgG1 Fc glycoforms with FcγRIIIa.

Figure 8 shows representative binding curves and Table 1 summarizes the resulting rate constants and dissociation constants obtained for the interaction of immobilized IgG1 Fc glycoforms with FcγRIIIa in solution using this binding format. As can be seen in Table 1, both HM-Fc and Man5-Fc have high affinity for FcγRIIIa (K_D's of 28 and 32 nM respectively), GlcNAc-Fc

showed a much lower affinity (K_D of 1115 nM), and N297Q-Fc had no observable affinity for FcγRIIIa (all measurements were conducted at 25˚C). Examination of the rate constants for the different interactions reveals that the main factor in the GlcNAc-Fc glycoform's lower affinity is due to significantly faster dissociation of the complex once it forms relative to HM-Fc and Man5-Fc, and this can be seen in the magnitudes of the dissociation rate constants, k_d (Table 1), and the ratios of kinetic and thermodynamic values when compared to HM-Fc values (Figure 12).

For a BLI binding format where FcγRIIIa is immobilized and IgG1 Fc glycoforms were in solution (Figure 7B), we utilized selectively biotinylated FcγRIIIa and streptavidin biosensors. Streptavidin biosensors were chosen for immobilization of FcγRIIIa because the high affinity of non-fucosylated IgG1 Fcs, such as HM-Fc and Man5-Fc ($K_D \approx 30$ nM), required either covalent or significantly higher affinity immobilization to prevent artifacts related to dissociation of receptors during binding measurements. The high affinity of streptavidin for biotin ($K_D \approx 10^{-14}$ M)[80] was appropriate for this application, therefore we developed a novel method to selectively biotinylate the C-terminus of FcγRIIIa using sortase-mediated ligation. This required constructing an expression strain of FcγRIIIa which contained a C-terminal sortase tag, expression and purification of the sortase tagged FcγRIIIa, synthesis of a triglycine containing biotin derivative (compound **3**, Figure 10), and sortase-mediated ligation to produce the C-terminally biotinylated FcγRIIIa, and these methods are described in the supporting information. An advantage of using an immobilized FcγRIIIa binding format such as that shown in Figure 7B is that binding measurements can be made directly in solutions of IgG1 Fc glycoforms. This type of format is also potentially more sensitive to changes in IgG1 Fc concentration since measurements are done with the samples directly in solution rather than in an immobilized format.

A disadvantage of this binding format is that buffer conditions present in samples must be compatible with receptor binding measurements. The affinity of many receptors is pH dependent, so formulation pH could affect binding measurements. In addition, high concentrations of sugars, such as the 10% sucrose in our sample storage buffer, can have significant effects on the kinetics and thermodynamics of binding measurements. Because of these factors, in our experiments it was necessary to transfer the IgG1 Fc glycoforms from storage buffer (10% sucrose, 20 mM histidine pH 6.0) to kinetics buffer (PBS buffer containing 1 mg/mL casein as a blocking agent) by dialysis, prior to binding measurements. This added a step to the binding measurements and has the potential to skew results if there is loss of sample or changes in concentration during the transfer of samples to the new buffer. The results of the receptor-immobilized binding format are shown in Figure 9 and Table 1. The binding results for the receptor-immobilized format (Figure 7B) are highly similar to the IgG1 Fc-immobilized format (Figure 7A), suggesting the extra dialysis step in the receptor-immobilized format did not affect the binding measurement significantly. Both HM-Fc and Man5-Fc displayed high affinity for FcγRIIIa with K_D's of 26 and 33 nM respectively, while the GlcNAc-Fc had lower affinity at 995 nM, and the N297Q-Fc form had no observable affinity (all measurements were conducted at 25˚C). The driving factor in the difference between the high affinity HM-Fc and Man5-Fc and the lower affinity GlcNAc-Fc was again faster dissociation of the complex (Table 1 and Figure 12). These results suggest that these two different binding formats are complementary in these experiments using well-defined IgG1 Fc glycoforms. These model IgG1 Fc glycoforms are also utilized to assess how glycosylation alters the chemical stability and physical stability.[72-73]

In summary, we have presented here the production and biological evaluation of four well-defined IgG1 Fc glycoforms as the initial steps of developing a model system for biosimilarity analysis. The methods developed here allow relatively easy access to the four well-defined IgG1 Fc glycoforms (HM-Fc, Man5-Fc, GlcNAc-Fc and N297Q-Fc) on a laboratory scale in quantities sufficient to enable a wide variety of biosimilarity analyses. Initial characterization of the glycoforms demonstrate that they are well-defined glycoproteins which vary significantly only in their glycosylation state, or in the case of non-glycosylated N297Q-Fc, in the presence of a conservative N to Q amino acid mutation. The four IgG1 Fc glycoforms form a set of sequentially truncated glycoproteins which can be used to assess the effects of glycosylation on biological activity and protein physicochemical stability. Potential biological activity of the IgG1 Fc glycoforms was evaluated using BLI to study the interaction of the glycoforms with the activating Fc receptor FcγRIIIa. Two BLI binding formats were developed, one utilizing protein G biosensors to immobilize IgG1 Fc, and one utilizing C-terminally biotinylated FcγRIIIa produced by a novel method to immobilize FcγRIIIa on streptavidin biosensors. The two assay formats resulted in complementary information about the affinity of the IgG1 Fc glycoforms for FcγRIIIa (Table 1). From the perspective of developing a model system for biosimilarity analysis, the binding studies also identified members of the model system that exhibited highly similar biological activity and those with distinct differences. The HM-Fc and Man5-Fc glycoforms exhibited highly similar affinity for FcγRIIIa (approximate K_D*'s* of 27 and 32 nM respectively), while GlcNAc-Fc had much weaker affinity (K_D of around 1000 nM), and N297Q-Fc displayed no affinity at the highest concentrations (20 μM) tested. These similarities and distinct differences in biological activity

may be useful in identifying physical and chemical features that correlate with changes in biological activity.

2.5 Figures

Figure 1. Production of homogenous IgG1 Fc glycoforms. HM-Fc was expressed in glycoengineered *P. pastoris* and utilized as a precursor for generation of GlcNAc-Fc and Man5-Fc. N297Q-Fc was recombinantly expressed in a different yeast strain.

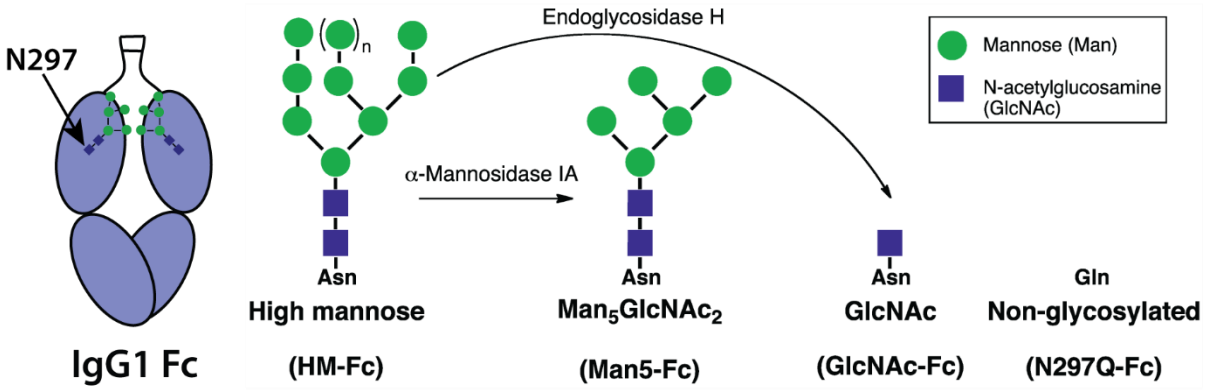

Figure 2. Intact protein MS analysis of IgG1 Fc glycoforms under reducing conditions**.**

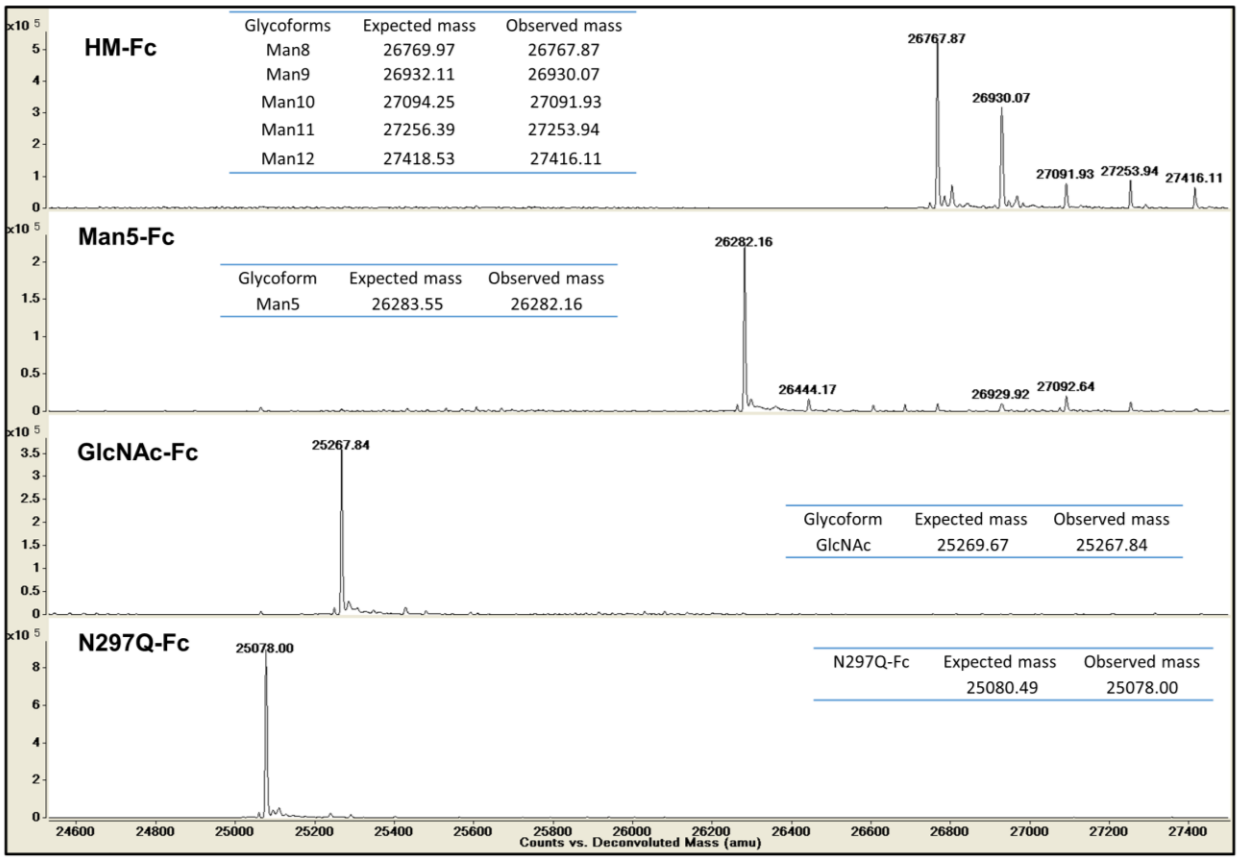

Figure 3. SDS-PAGE analysis of the four different IgG1 Fc glycoforms (1. HM; 2. Man5; 3. GlcNAc; 4. N297Q) under reduced and non-reduced conditions. The purified IgG1 Fc glycoforms showed ~99% purity under both conditions. The HM-Fc glycoform that has the highest molecular weight runs slowest among the four types followed by the Man5-Fc, GlcNAc-Fc, and N297Q-Fc.

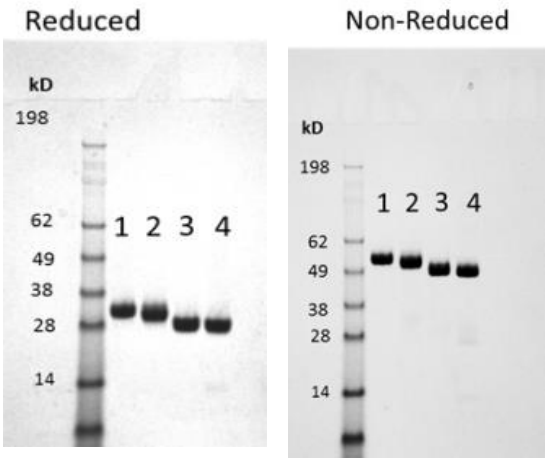

Figure 4. Representative size exclusion chromatograms of the IgG1 Fc glycoforms. Results showed the following total monomer content (n=3; SD ~1.0%): HM-Fc 98.0% for HM-Fc, >99% purity for Man5-Fc and GlcNAc-Fc showed, and 96.7% for N297Q-Fc.

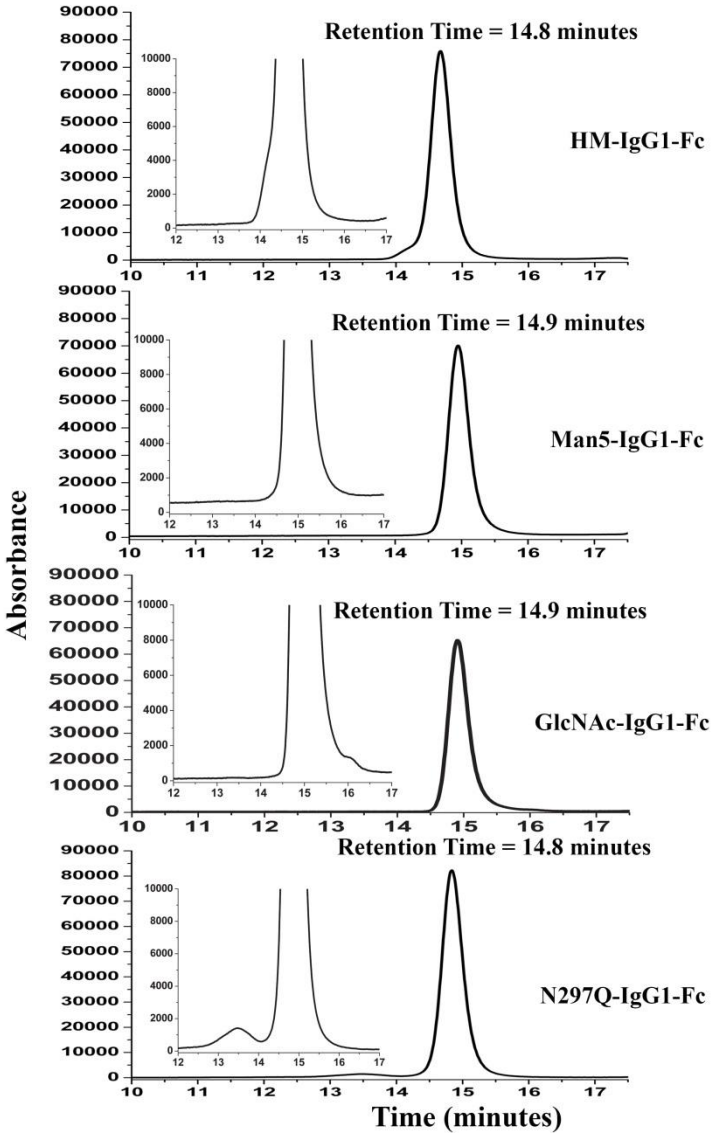

Figure 5. Representative charge heterogeneity profiles of IgG1 Fc glycoforms as measured by capillary isoelectric focusing (cIEF). The isoelectric point (pI) of the main peak (n=3; SD ~0.1 pI units): pI of 7.0 for HM-Fc, pI of 6.9 for Man_5-IgG1Fc, , pI of 7.1 for GlcNAc-Fc, and pI of 7.4 for N297Q-Fc.

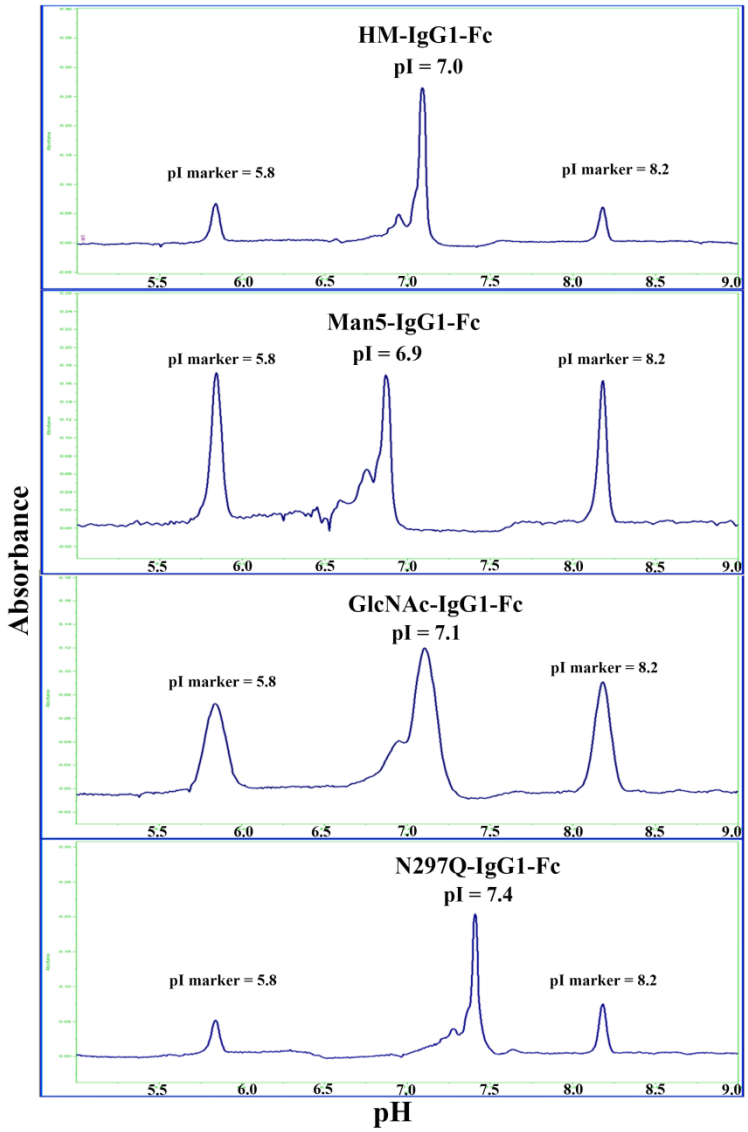

Figure 6. Production of biotinylated FcγRIIIa using sortase-mediated ligation between FcγRIIIa-ST-H_6 and GGG-linker-Biotin (compound **3** in the supporting information).

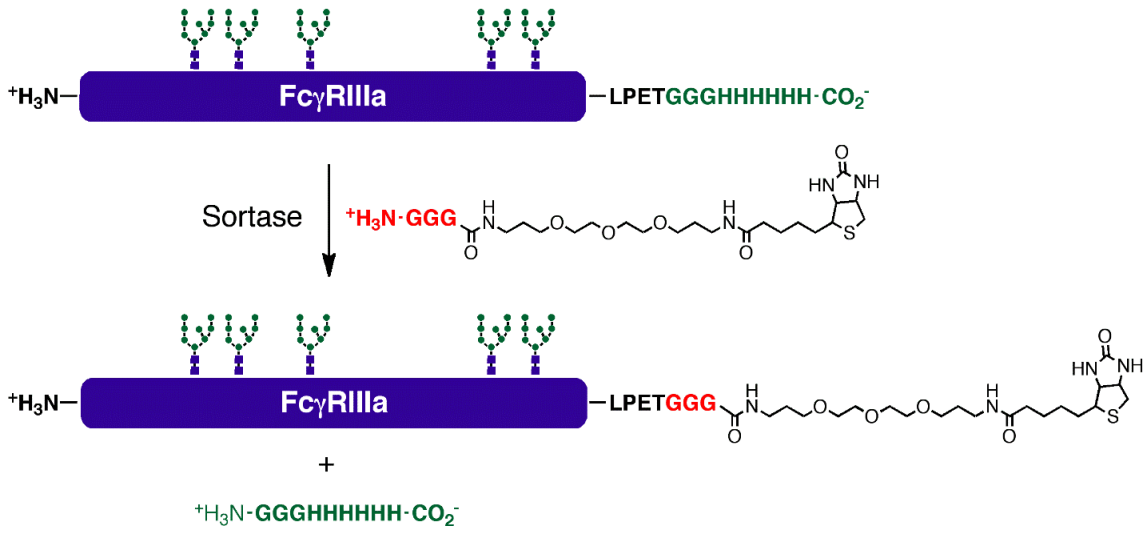

Figure 7. Steps followed in kinetic binding experiments using biolayer interferometry. A) Top panel shows steps followed for measuring binding kinetics using protein G biosensors (Fc-immobilized format), where IgG1 Fc glycoforms were immobilized and FcγRIIIa-H_6 was present in solution. B) Bottom panel shown steps involved in binding kinetics using streptavidin biosensor (receptor-immobilized format), where biotinylated FcγRIIIa was immobilized and IgG1 Fc glycoforms were present in solution.

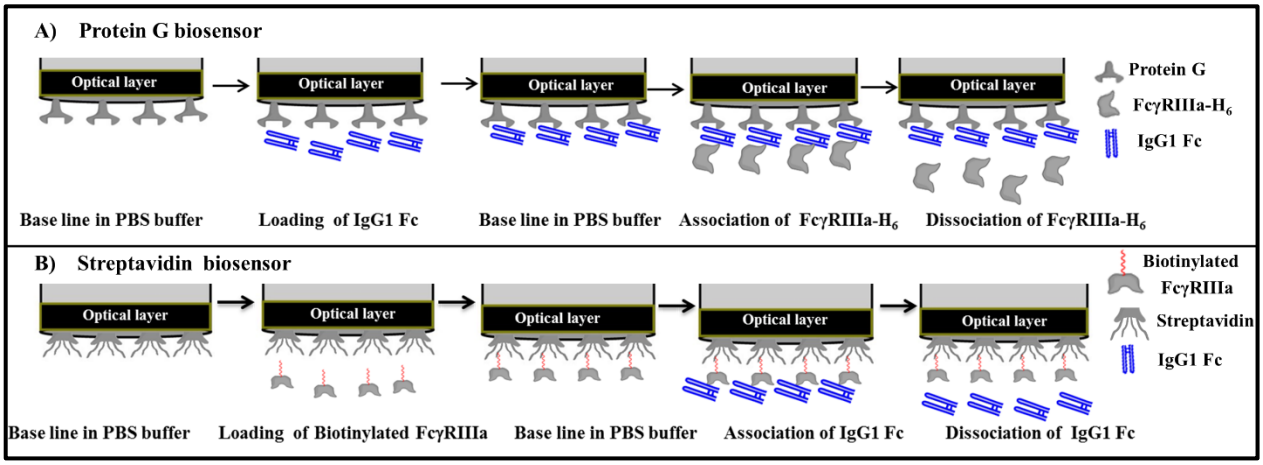

Figure 8. Representative BLI binding data for the interaction of FcγRIIIa with IgG1 Fc glycoforms immobilized on protein G biosensors (Fc-immobilized format). The binding curves correspond to a range of receptor concentrations in solution. For HM-Fc and Man5-Fc data is shown for FcγRIIIa at concentrations of 800 nM, 400 nM, 200 nM, and 100 nM, which corresponds with the curves from top to bottom. For GlcNAc-Fc data is shown for FcγRIIIa at concentrations of 1600 nM, 800 nM, 400 nM, and 200 nM, which corresponds with the binding curves from top to bottom. For N297Q-Fc a single concentration of 20 µM was tested and no binding was observed.

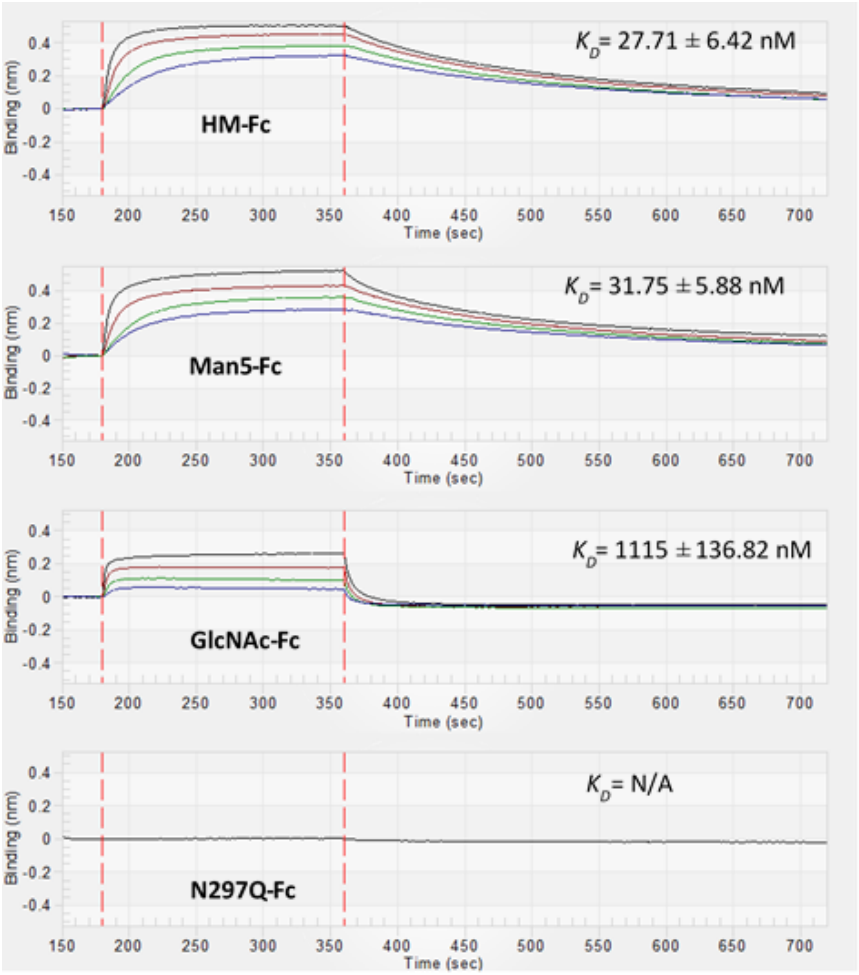

Figure 9. Representative BLI binding data for the interaction of IgG1 Fc glycoforms with FcγRIIIa immobilized on streptavidin biosensors (receptor-immobilized format). The binding curves correspond to a range of IgG1 Fc glycoform concentrations in solution. For HM-Fc and Man5-Fc data is shown at concentrations of 800 nM, 400 nM, 200 nM, and 100 nM, which corresponds with the curves from top to bottom. For GlcNAc-Fc data is shown at concentrations of 1600 nM, 800 nM, 400 nM, and 200 nM, which corresponds with the binding curves from top to bottom. For N297Q-Fc a single concentration of 20 µM was tested and no binding was observed.

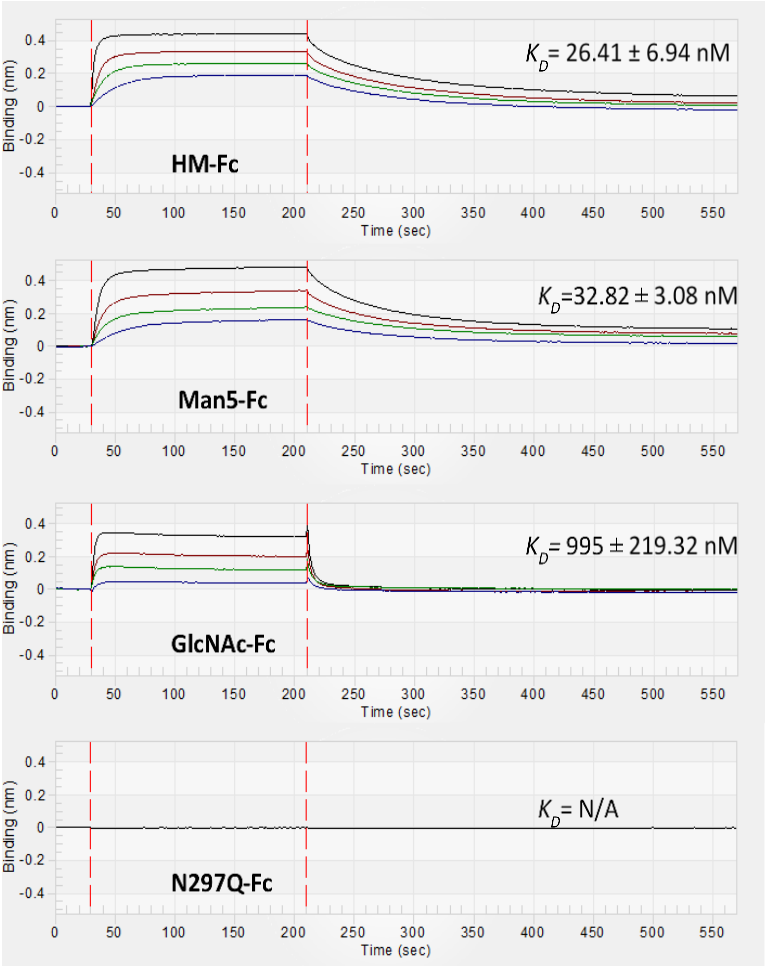

Figure 10. Scheme showing synthesis of GGG-linker-Biotin

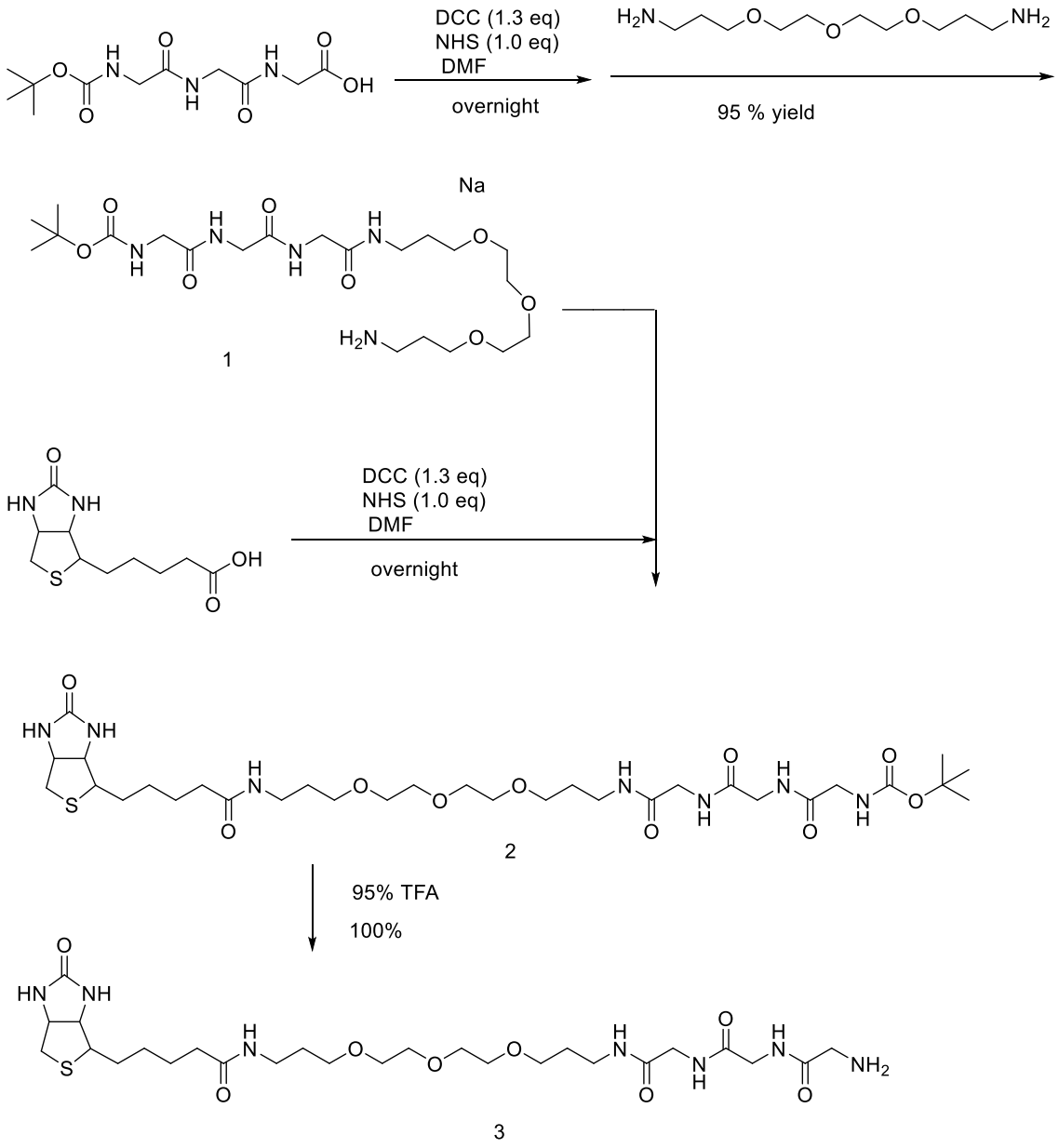

Figure 11. ESI-MS analysis of IgG1 Fc glycoform after protein G affinity chromatography purification. The mass spectrometry data shows the molecular weight of the Fc monomer and its N-linked glycan at Asn297. The peaks represent $Man_8GlcNAc_2$, $Man_9GlcNAc_2$, $Man_{10}GlcNAc_2$, $Man_{11}GlcNAc_2$, and $Man_{12}GlcNAc_2$ with MWs of 26767.53, 26926.67, 27091.99, 270253.68, and 27416.33Da, respectively. The peak with MW 25063.7Da is a nonglycosylated Fc monomer containing asparagine at the glycosylation site.

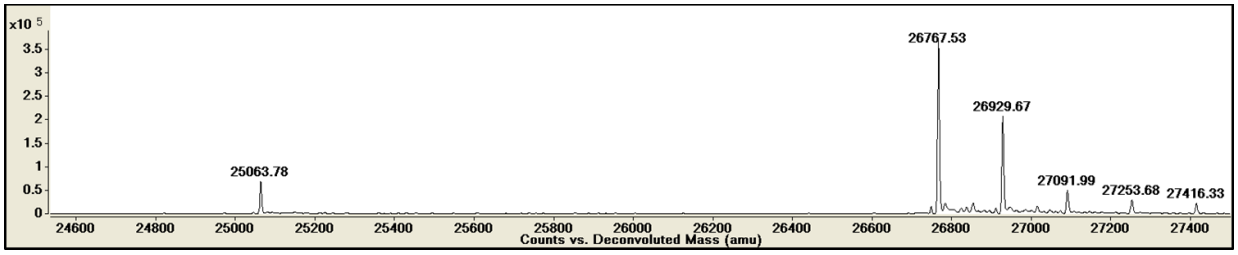

Figure 12. Bar graphs show ratios of k_a, k_d, and K_D for the IgG1 Fc glycoforms obtained by dividing with k_a, k_d, and K_D of HM-Fc for A, B, and C, respectively. The data indicates a slight difference in the ratio of k_a values (A), but significant difference in the ratio of k_d and K_D as shown in panels B and C, respectively. Streptavadin immobilization represents the receptor-immobilized format, while the protein G immobilization represents the Fc-immobilized format

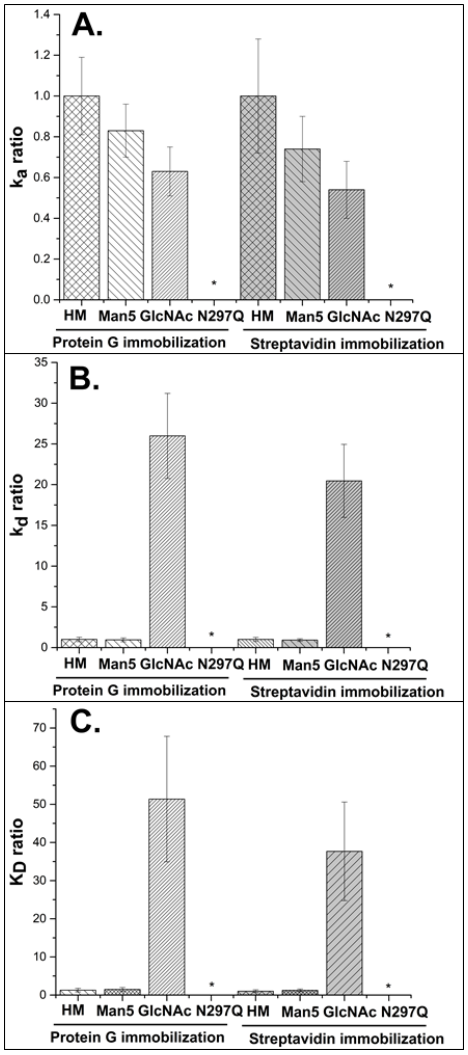

Figure 13. Representative BLI binding curves (fitted) for the interaction of FcγRIIIa with IgG1 Fc glycoforms immobilized on protein G biosensors (Fc-immobilized). The binding curves correspond to a range of receptor concentrations in solution. For HM-Fc and Man5-Fc data is shown for FcγRIIIa at concentrations of 800 nM, 400 nM, 200 nM, and 100 nM, which corresponds with the curves from top to bottom. For GlcNAc-Fc data is shown for FcγRIIIa at concentrations of 1600 nM, 800 nM, 400 nM, and 200 nM which corresponds with the binding curves from top to bottom. For N297Q-Fc a single concentration of 20 µM was tested and no binding was observed.

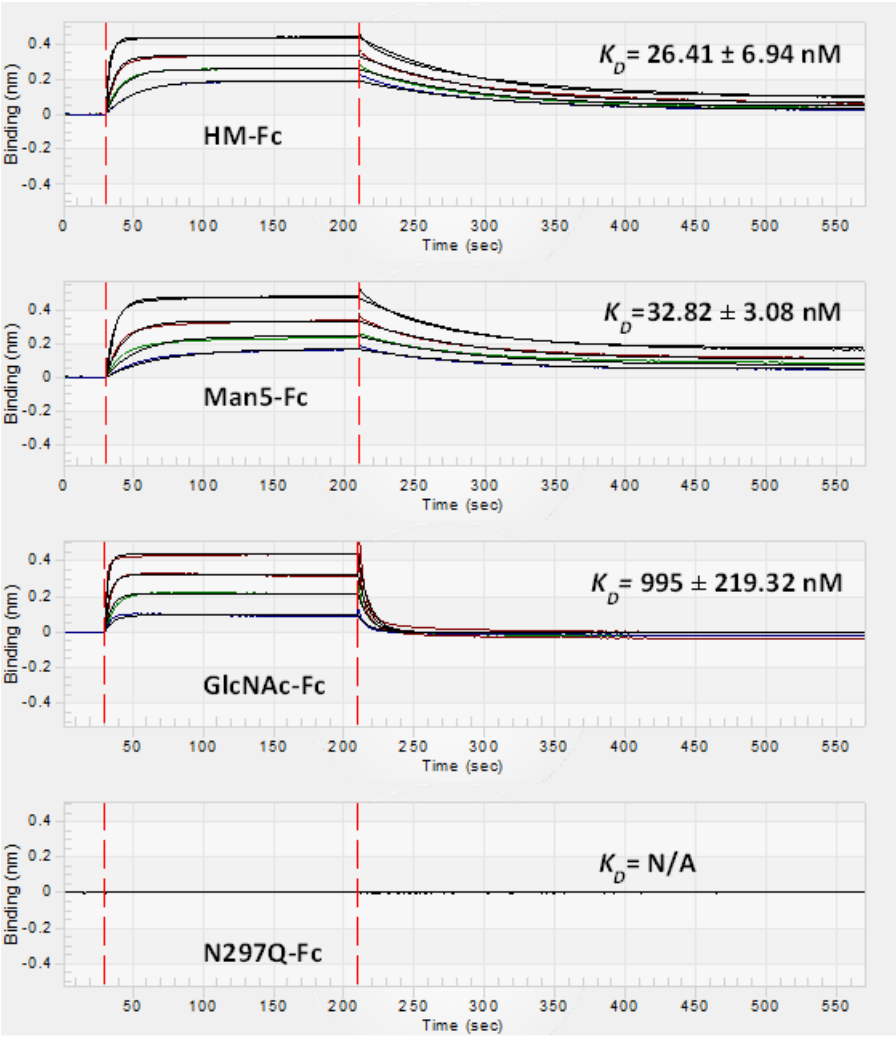

Figure 14. Representative BLI binding curves (fitted) for the interaction of IgG1 Fc glycoforms with FcγRIIIa immobilized on streptavidin biosensors (receptor-immobilized format). The binding curves correspond to a range of IgG1 Fc glycoform concentrations in solution. For HM-Fc and Man5-Fc data is shown for IgG1 Fc glycoforms at concentrations of 800 nM, 400 nM, 200 nM, and 100 nM, which corresponds with the curves from top to bottom. For GlcNAc-Fc data is shown at concentrations of 1600 nM, 800 nM, 400 nM, and 200 nM, which corresponds with the binding curves from top to bottom. For N297Q-Fc a single concentration of 20 µM was tested and no binding was observed.

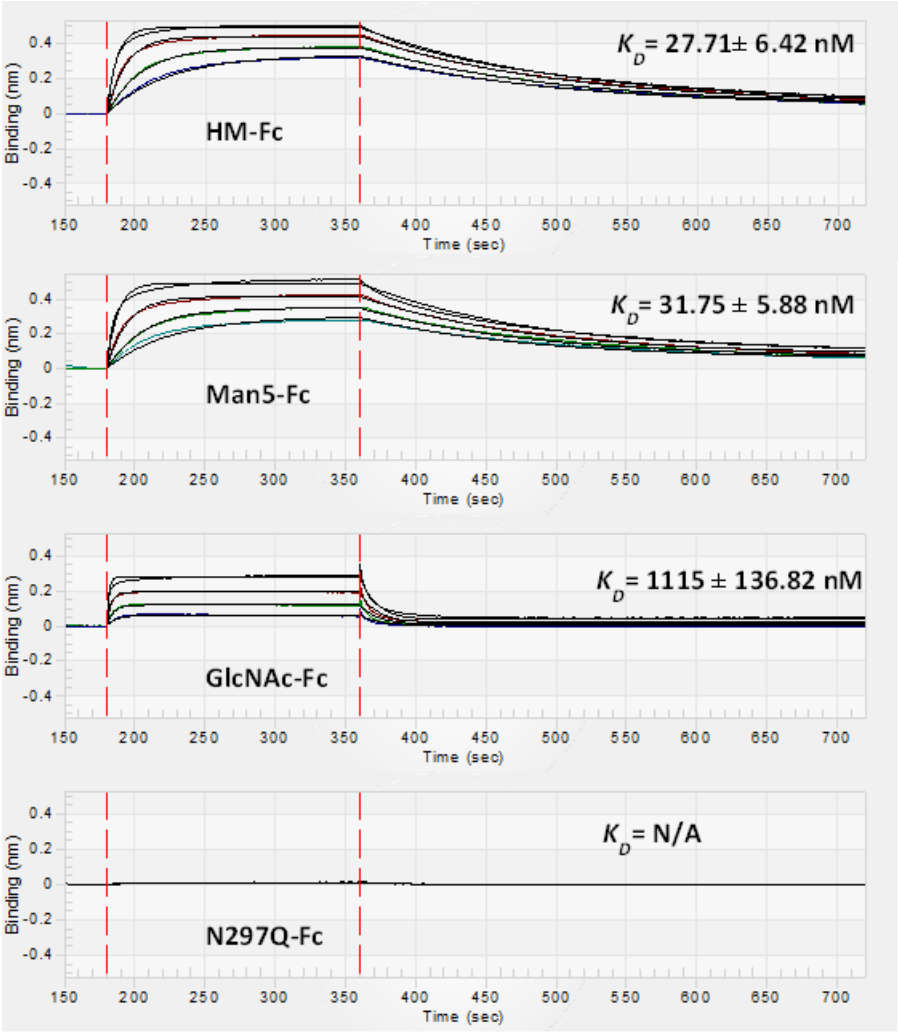

2.6 Tables

Table 1. Kinetic parameters obtained for binding of FcγRIIIa with IgG1 Fc glycoforms. Binding kinetics were measured at 25˚C. The data shows kinetic association rate k_a, kinetic dissociation rate k_d, and equilibrium dissociation constant K_D. These data are averaged values of six independent experiments. *For N297Q, there was no detectable binding at the highest concentration tested (20 μM) for both methods.

Glycoforms	Immobilized protein	Biosensor	Avg k_a x 10^{-5} (1/Ms)	Avg. k_d x 10^3 (1/s)	Avg.K_D (nM)
HM-Fc	IgG1 Fc	Protein G	1.94 ± 0.26	5.37 ± 1.02	27.71± 6.42
	FcγRIIIa	Streptavidin	3.00 ± 0.59	7.93 ± 1.38	26.41 ± 6.94
Man5-Fc	IgG1 Fc	Protein G	1.61 ± 0.12	5.10 ± 0.86	31.75 ± 5.88
	FcγRIIIa	Streptavidin	2.23 ± 0.18	7.31 ± 0.32	32.82 ± 3.08
GlcNAc-Fc	IgG1 Fc	Protein G	1.23 ± 0.18	139.53 ±9.15	1115 ± 136.82
	FcγRIIIa	Streptavidin	1.62 ± 0.28	161.27 ± 21.75	995 ± 219.32
N297Q-Fc	IgG1 Fc / FcγRIIIa	Protein G / Streptavidin	*	*	*

Table 2. Expected mass, observed mass, and peak intensity for each glycoform as observed by MS. Peak intensity was obtained using Agilent Masshunter qualitative analysis software and estimated percent abundance for each glycoform was calculated using all glycoform peaks present in a given spectra.

Glycoform		Expected mass	Observed mass	Δ Mass	Peak intensity	Est. Abund. (%)
HM-IgG1 Fc	Man8	26769.97	26767.87	2.10	370000	49
	Man9	26932.11	26930.01	2.1	250000	33
	Man10	27094.25	27091.93	2.32	50000	7
	Man11	27256.39	27253.94	2.45	40000	5
	Man12	27418.53	27416.00	2.53	40000	5
Man5-IgG1 Fc	Man5	26283.55	26282.16	1.39	92940	78
	Man6	26445.69	26444.17	1.52	5970	5
	Man8	26769.97	26767.92	2.05	3600	3
	Man9	26932.11	26929.92	2.19	4032	3
	Man10	27094.25	27092.64	1.61	7573	6
	Man11	27256.39	27254.67	1.72	4766	4
GlcNAc-IgG1 Fc	GlcNAc	25269.67	25267.84	1.83	136433	≥ 99
N297Q-IgG1 Fc	Non-glycosylated	25080.49	25078.01	2.48	25240	≥ 99

Table 3. Percentage of monomers for IgG1 Fc glycoforms measured using SEC

	Percentage of monomer			
Number of runs	HM-Fc	Man5-Fc	GlcNAc-Fc	N297Q-Fc
1	99.0	>99.0	>99.0	96.4
2	99.0	>99.0	>99.0	97.3
3	99.0	>99.0	>99.0	96.3
4	97.0			
5	97.3			
6	96.9			
Average	98.0	>99.0	>99.0	96.7
Std Dev	1.1	0.0	0.0	0.6

Table 4. pI values of the main peak for IgG1 Fc glycoforms measured using cIEF.

	PI of the main peak			
Number of runs	HM-Fc	Man5-Fc	GlcNAc-Fc	N297Q-Fc
1	7.1	6.9	7.1	7.4
2	7.1	6.9	7.1	7.4
3	7.1	6.9	7.1	7.4
4	7.0			
5	6.9			
6	6.9			
Average	7.0	6.9	7.1	7.4
Std Dev	0.1	0.0	0.0	0.0

Table 5. Raw data for the protein G immobilization technique (Fc-immobilized format) for six independent runs. * For N297Q-Fc, no binding was observed at the highest concentration tested (20µM).

Glycoforms	k_a x 10^{-5} (1/Ms)	k_d x 10^{3} (1/s)	K_D (nM)
HM-Fc	3.42	8.93	26.1
	3.64	9.33	25.66
	3.54	9.24	26.09
	2.41	6.28	26.05
	2.57	6.97	27.17
	2.43	6.80	28.03
Man5-Fc	2.28	7.54	32.99
	2.28	7.04	30.88
	2.44	7.83	32.1
	2.18	7.03	32.25
	1.89	7.10	37.58
	2.29	7.31	31.91
GlcNAc-Fc	1.53	1.53	996
	1.36	1.51	1112
	1.45	1.33	9191
	1.48	1.64	1110
	2.11	1.97	935
	1.80	1.70	946
N297Q-Fc	*	*	*

Table 6. Raw data for the streptavidin immobilization technique (receptor-immobilized format) for six independent runs. *For N297Q-Fc, no binding was observed at the highest concentration tested (20

Glycoforms	k_a x 10^{-5} (1/Ms)	k_d x 10^{3} (1/s)	K_D (nM)
HM-Fc	3.42	8.93	26.1
	3.64	9.33	25.66
	3.54	9.24	26.09
	2.41	6.28	26.05
	2.57	6.97	27.17
	2.43	6.80	28.03
Man5-Fc	2.28	7.54	32.99
	2.28	7.04	30.88
	2.44	7.83	32.1
	2.18	7.03	32.25
	1.89	7.10	37.58
	2.29	7.31	31.91
GlcNAc-Fc	1.53	1.53	996
	1.36	1.51	1112
	1.45	1.33	9191
	1.48	1.64	1110
	2.11	1.97	935
	1.80	1.70	946
N297Q-Fc	*	*	*

Table 7. The amount of IgG1 Fc glycoforms produced using a combination of expression, enzymatic reaction, and purification.

Glycoforms	Amount expressed (Protein G purified)	Amount after phenyl sepharose purification (HIC)	HM-Fc used for reaction (HIC purified)	Enzymatic reaction Product	Yield
HM-Fc	1000 mg	445 mg	---------	-------	--------
Man5-Fc	----------	--------	125 mg	75 mg	60 %
GlcNAc-Fc	-------	--------	100 mg	100 mg	≥ 99%
N297Q-Fc	130 mg	118 mg	-----	-----	------

2.7 References

1. Alsenaidy, M. A.; Okbazghi, S. Z.; Kim, J. H.; Joshi, S. B.; Middaugh, C. R.; Tolbert, T. J.; Volkin, D. B., Physical Stability Comparisons of IgG1-Fc Variants: Effects of N-Glycosylation Site Occupancy and Asp/Gln Residues at Site Asn 297. *Journal of Pharmaceutical Sciences* **2014,** *103* (6), 1613-1627.

2. Ha, S.; Ou, Y.; Vlasak, J.; Li, Y.; Wang, S.; Vo, K.; Du, Y.; Mach, A.; Fang, Y.; Zhang, N., Isolation and characterization of IgG1 with asymmetrical Fc glycosylation. *Glycobiology* **2011,** *21* (8), 1087-1096.

3. Wang, S.; Ionescu, R.; Peekhaus, N.; Leung, J.-y.; Ha, S.; Vlasak, J., Separation of post-translational modifications in monoclonal antibodies by exploiting subtle conformational changes under mildly acidic conditions. *Journal of Chromatography A* **2010,** *1217* (42), 6496-6502.

4. Walsh, C. T.; Garneau-Tsodikova, S.; Gatto, G. J., Protein Posttranslational Modifications: The Chemistry of Proteome Diversifications. *Angewandte Chemie International Edition* **2005,** *44* (45), 7342-7372.

5. Farley, A. R.; Link, A. J., Chapter 40 Identification and Quantification of Protein Posttranslational Modifications. In *Methods in Enzymology*, Richard, R. B.; Murray, P. D., Eds. Academic Press: 2009; Vol. Volume 463, pp 725-763.

6. Fischer, S.; Hoernschemeyer, J.; Mahler, H.-C., Glycation during storage and administration of monoclonal antibody formulations. *European Journal of Pharmaceutics and Biopharmaceutics* **2008,** *70* (1), 42-50.

7. Mozziconacci, O.; Kerwin, B. A.; Schöneich, C., Exposure of a Monoclonal Antibody, IgG1, to UV-Light Leads to Protein Dithiohemiacetal and Thioether Cross-Links: A Role for Thiyl Radicals? *Chemical Research in Toxicology* **2010,** *23* (8), 1310-1312.

8. Gaza-Bulseco, G.; Faldu, S.; Hurkmans, K.; Chumsae, C.; Liu, H., Effect of methionine oxidation of a recombinant monoclonal antibody on the binding affinity to protein A and protein G. *Journal of Chromatography B* **2008,** *870* (1), 55-62.

9. Cohen, S. L.; Price, C.; Vlasak, J., β-Elimination and Peptide Bond Hydrolysis: Two Distinct Mechanisms of Human IgG1 Hinge Fragmentation upon Storage. *Journal of the American Chemical Society* **2007,** *129* (22), 6976-6977.

10. Xiang, T.; Lundell, E.; Sun, Z.; Liu, H., Structural effect of a recombinant monoclonal antibody on hinge region peptide bond hydrolysis. *Journal of Chromatography B* **2007,** *858* (1–2), 254-262.

11. Hambly, D. M.; Banks, D. D.; Scavezze, J. L.; Siska, C. C.; Gadgil, H. S., Detection and Quantitation of IgG 1 Hinge Aspartate Isomerization: A Rapid Degradation in Stressed Stability Studies. *Analytical Chemistry* **2009,** *81* (17), 7454-7459.

12. Houde, D.; Peng, Y.; Berkowitz, S. A.; Engen, J. R., Post-translational Modifications Differentially Affect IgG1 Conformation and Receptor Binding. *Molecular & Cellular Proteomics* **2010,** *9* (8), 1716-1728.

13. Berkowitz, S. A.; Engen, J. R.; Mazzeo, J. R.; Jones, G. B., Analytical tools for characterizing biopharmaceuticals and the implications for biosimilars. *Nat Rev Drug Discov* **2012,** *11* (7), 527-540.

14. Kuhlmann, M.; Covic, A., The protein science of biosimilars. *Nephrology Dialysis Transplantation* **2006,** *21* (suppl 5), v4-v8.

15. Putnam, W. S.; Prabhu, S.; Zheng, Y.; Subramanyam, M.; Wang, Y.-M. C., Pharmacokinetic, pharmacodynamic and immunogenicity comparability assessment strategies for monoclonal antibodies. *Trends in Biotechnology* **2010,** *28* (10), 509-516.

16. Jones, A. J. S.; Papac, D. I.; Chin, E. H.; Keck, R.; Baughman, S. A.; Lin, Y. S.; Kneer, J.; Battersby, J. E., Selective clearance of glycoforms of a complex glycoprotein pharmaceutical caused by terminal N-acetylglucosamine is similar in humans and cynomolgus monkeys. *Glycobiology* **2007,** *17* (5), 529-540.

17. Shinkawa, T.; Nakamura, K.; Yamane, N.; Shoji-Hosaka, E.; Kanda, Y.; Sakurada, M.; Uchida, K.; Anazawa, H.; Satoh, M.; Yamasaki, M.; Hanai, N.; Shitara, K., The Absence of Fucose but Not the Presence of Galactose or Bisecting N-Acetylglucosamine of Human IgG1 Complex-

type Oligosaccharides Shows the Critical Role of Enhancing Antibody-dependent Cellular Cytotoxicity. *Journal of Biological Chemistry* **2003,** *278* (5), 3466-3473.

18. Raju, T. S., Terminal sugars of Fc glycans influence antibody effector functions of IgGs. *Current Opinion in Immunology* **2008,** *20* (4), 471-478.

19. Okazaki, A.; Shoji-Hosaka, E.; Nakamura, K.; Wakitani, M.; Uchida, K.; Kakita, S.; Tsumoto, K.; Kumagai, I.; Shitara, K., Fucose Depletion from Human IgG1 Oligosaccharide Enhances Binding Enthalpy and Association Rate Between IgG1 and FcγRIIIa. *Journal of Molecular Biology* **2004,** *336* (5), 1239-1249.

20. Yamane-Ohnuki, N.; Kinoshita, S.; Inoue-Urakubo, M.; Kusunoki, M.; Iida, S.; Nakano, R.; Wakitani, M.; Niwa, R.; Sakurada, M.; Uchida, K.; Shitara, K.; Satoh, M., Establishment of FUT8 knockout Chinese hamster ovary cells: An ideal host cell line for producing completely defucosylated antibodies with enhanced antibody-dependent cellular cytotoxicity. *Biotechnology and Bioengineering* **2004,** *87* (5), 614-622.

21. Mori, K.; Kuni-Kamochi, R.; Yamane-Ohnuki, N.; Wakitani, M.; Yamano, K.; Imai, H.; Kanda, Y.; Niwa, R.; Iida, S.; Uchida, K.; Shitara, K.; Satoh, M., Engineering Chinese hamster ovary cells to maximize effector function of produced antibodies using FUT8 siRNA. *Biotechnology and Bioengineering* **2004,** *88* (7), 901-908.

22. Schuster, M.; Umana, P.; Ferrara, C.; Brünker, P.; Gerdes, C.; Waxenecker, G.; Wiederkum, S.; Schwager, C.; Loibner, H.; Himmler, G.; Mudde, G. C., Improved Effector Functions of a Therapeutic Monoclonal Lewis Y-Specific Antibody by Glycoform Engineering. *Cancer Research* **2005,** *65* (17), 7934-7941.

23. Niwa, R.; Natsume, A.; Uehara, A.; Wakitani, M.; Iida, S.; Uchida, K.; Satoh, M.; Shitara, K., IgG subclass-independent improvement of antibody-dependent cellular cytotoxicity by fucose removal from Asn297-linked oligosaccharides. *Journal of Immunological Methods* **2005,** *306* (1–2), 151-160.

24. Shields, R. L.; Lai, J.; Keck, R.; O'Connell, L. Y.; Hong, K.; Meng, Y. G.; Weikert, S. H. A.; Presta, L. G., Lack of Fucose on Human IgG1 N-Linked Oligosaccharide Improves Binding to Human FcγRIII and Antibody-dependent Cellular Toxicity. *Journal of Biological Chemistry* **2002,** *277* (30), 26733-26740.

25. Raju, T. S., Impact of Fc Glycosylation on Monoclonal Antibody Effector Functions and Degradation by Proteases. In *Current Trends in Monoclonal Antibody Development and Manufacturing*, Shire, S. J.; Gombotz, W.; Bechtold-Peters, K.; Andya, J., Eds. Springer New York: 2010; Vol. XI, pp 249-269.

26. Hodoniczky, J.; Zheng, Y. Z.; James, D. C., Control of Recombinant Monoclonal Antibody Effector Functions by Fc N-Glycan Remodeling in Vitro. *Biotechnology Progress* **2005,** *21* (6), 1644-1652.

27. Raju, T. S.; Jordan, R. E., Galactosylation variations in marketed therapeutic antibodies. *mAbs* **2012,** *4* (3), 385-391.

28. Suzuki, T.; Ishii-Watabe, A.; Tada, M.; Kobayashi, T.; Kanayasu-Toyoda, T.; Kawanishi, T.; Yamaguchi, T., Importance of Neonatal FcR in Regulating the Serum Half-Life of Therapeutic Proteins Containing the Fc Domain of Human IgG1: A Comparative Study of the Affinity of Monoclonal Antibodies and Fc-Fusion Proteins to Human Neonatal FcR. *The Journal of Immunology* **2010,** *184* (4), 1968-1976.

29. Wang, W.; Vlasak, J.; Li, Y.; Pristatsky, P.; Fang, Y.; Pittman, T.; Roman, J.; Wang, Y.; Prueksaritanont, T.; Ionescu, R., Impact of methionine oxidation in human IgG1 Fc on serum half-life of monoclonal antibodies. *Molecular Immunology* **2011,** *48* (6–7), 860-866.

30. Wang, W.; Lu, P.; Fang, Y.; Hamuro, L.; Pittman, T.; Carr, B.; Hochman, J.; Prueksaritanont, T., Monoclonal Antibodies with Identical Fc Sequences Can Bind to FcRn Differentially with Pharmacokinetic Consequences. *Drug Metabolism and Disposition* **2011,** *39* (9), 1469-1477.

31. Vaccaro, C.; Zhou, J.; Ober, R. J.; Ward, E. S., Engineering the Fc region of immunoglobulin G to modulate in vivo antibody levels. *Nat Biotech* **2005,** *23* (10), 1283-1288.

32. Mimura, Y.; Church, S.; Ghirlando, R.; Ashton, P. R.; Dong, S.; Goodall, M.; Lund, J.; Jefferis, R., The influence of glycosylation on the thermal stability and effector function

expression of human IgG1-Fc: properties of a series of truncated glycoforms. *Molecular Immunology* **2000,** *37* (12–13), 697-706.

33. Kaneko, Y.; Nimmerjahn, F.; Ravetch, J. V., Anti-Inflammatory Activity of Immunoglobulin G Resulting from Fc Sialylation. *Science* **2006,** *313* (5787), 670-673.

34. Anthony, R. M.; Nimmerjahn, F.; Ashline, D. J.; Reinhold, V. N.; Paulson, J. C.; Ravetch, J. V., Recapitulation of IVIG Anti-Inflammatory Activity with a Recombinant IgG Fc. *Science* **2008,** *320* (5874), 373-376.

35. Okazaki, A.; Shoji, E.; Nakamura, K.; Wakitani, M.; Uchida, K.; Kakita, S.; Tsumoto, K.; Kumagai, I.; Shitara, K., Thermodynamic and kinetic effects of human IgG1 defucosylation on IgG1-FcγRIIIa interaction. In *Animal Cell Technology: Basic & Applied Aspects*, Iijima, S.; Nishijima, K.-I., Eds. Springer Netherlands: 2006; Vol. 14, pp 47-53.

36. Mori, K.; Iida, S.; Yamane-Ohnuki, N.; Kanda, Y.; Kuni-Kamochi, R.; Nakano, R.; Imai-Nishiya, H.; Okazaki, A.; Shinkawa, T.; Natsume, A.; Niwa, R.; Shitara, K.; Satoh, M., Non-fucosylated therapeutic antibodies: the next generation of therapeutic antibodies. *Cytotechnology* **2007,** *55* (2-3), 109-114.

37. Yamane-Ohnuki, N.; Satoh, M., Production of therapeutic antibodies with controlled fucosylation. *mAbs* **2009,** *1* (3), 230-236.

38. Böhm, S.; Schwab, I.; Lux, A.; Nimmerjahn, F., The role of sialic acid as a modulator of the anti-inflammatory activity of IgG. *Semin Immunopathol* **2012,** *34* (3), 443-453.

39. Mimura, Y.; Sondermann, P.; Ghirlando, R.; Lund, J.; Young, S. P.; Goodall, M.; Jefferis, R., Role of Oligosaccharide Residues of IgG1-Fc in FcγRIIb Binding. *Journal of Biological Chemistry* **2001,** *276* (49), 45539-45547.

40. Zheng, K.; Bantog, C.; Bayer, R., The impact of glycosylation on monoclonal antibody conformation and stability. *mAbs* **2011,** *3* (6), 568-576.

41. Ghirlando, R.; Lund, J.; Goodall, M.; Jefferis, R., Glycosylation of human IgG-Fc: influences on structure revealed by differential scanning micro-calorimetry. *Immunology Letters* **1999,** *68* (1), 47-52.

42. Solá, R. J.; Griebenow, K., Effects of glycosylation on the stability of protein pharmaceuticals. *Journal of Pharmaceutical Sciences* **2009,** *98* (4), 1223-1245.

43. Yamaguchi, Y.; Nishimura, M.; Nagano, M.; Yagi, H.; Sasakawa, H.; Uchida, K.; Shitara, K.; Kato, K., Glycoform-dependent conformational alteration of the Fc region of human immunoglobulin G1 as revealed by NMR spectroscopy. *Biochimica et Biophysica Acta (BBA) - General Subjects* **2006,** *1760* (4), 693-700.

44. Liu, D.; Ren, D.; Huang, H.; Dankberg, J.; Rosenfeld, R.; Cocco, M. J.; Li, L.; Brems, D. N.; Remmele, R. L., Structure and Stability Changes of Human IgG1 Fc as a Consequence of Methionine Oxidation. *Biochemistry* **2008,** *47* (18), 5088-5100.

45. Alsenaidy, M. A.; Kim, J. H.; Majumdar, R.; Weis, D. D.; Joshi, S. B.; Tolbert, T. J.; Middaugh, C. R.; Volkin, D. B., High-Throughput Biophysical Analysis and Data Visualization of Conformational Stability of an IgG1 Monoclonal Antibody After Deglycosylation. *Journal of Pharmaceutical Sciences* **2013,** *102* (11), 3942-3956.

46. Li, C. H.; Narhi, L. O.; Wen, J.; Dimitrova, M.; Wen, Z.-q.; Li, J.; Pollastrini, J.; Nguyen, X.; Tsuruda, T.; Jiang, Y., Effect of pH, Temperature, and Salt on the Stability of Escherichia coli- and Chinese Hamster Ovary Cell-Derived IgG1 Fc. *Biochemistry* **2012,** *51* (50), 10056-10065.

47. Kayser, V.; Chennamsetty, N.; Voynov, V.; Forrer, K.; Helk, B.; Trout, B. L., Glycosylation influences on the aggregation propensity of therapeutic monoclonal antibodies. *Biotechnology Journal* **2011,** *6* (1), 38-44.

48. Krapp, S.; Mimura, Y.; Jefferis, R.; Huber, R.; Sondermann, P., Structural Analysis of Human IgG-Fc Glycoforms Reveals a Correlation Between Glycosylation and Structural Integrity. *Journal of Molecular Biology* **2003,** *325* (5), 979-989.

49. Loo, T.; Patchett, M. L.; Norris, G. E.; Lott, J. S., Using Secretion to Solve a Solubility Problem: High-Yield Expression in Escherichia coli and Purification of the Bacterial Glycoamidase PNGase F. *Protein Expression and Purification* **2002,** *24* (1), 90-98.

50. Mao, H.; Hart, S. A.; Schink, A.; Pollok, B. A., Sortase-Mediated Protein Ligation: A New Method for Protein Engineering. *Journal of the American Chemical Society* **2004,** *126* (9), 2670-2671.

51. Cuskin, F.; Lowe, E. C.; Temple, M. J.; Zhu, Y.; Cameron, E. A.; Pudlo, N. A.; Porter, N. T.; Urs, K.; Thompson, A. J.; Cartmell, A.; Rogowski, A.; Hamilton, B. S.; Chen, R.; Tolbert, T. J.; Piens, K.; Bracke, D.; Vervecken, W.; Hakki, Z.; Speciale, G.; Munoz-Munoz, J. L.; Day, A.; Pena, M. J.; McLean, R.; Suits, M. D.; Boraston, A. B.; Atherly, T.; Ziemer, C. J.; Williams, S. J.; Davies, G. J.; Abbott, D. W.; Martens, E. C.; Gilbert, H. J., Human gut Bacteroidetes can utilize yeast mannan through a selfish mechanism. *Nature* **2015,** *517* (7533), 165-169.

52. Zhu, Y.; Suits, M. D. L.; Thompson, A. J.; Chavan, S.; Dinev, Z.; Dumon, C.; Smith, N.; Moremen, K. W.; Xiang, Y.; Siriwardena, A.; Williams, S. J.; Gilbert, H. J.; Davies, G. J., Mechanistic insights into a Ca2+-dependent family of α-mannosidases in a human gut symbiont. *Nat Chem Biol* **2010,** *6* (2), 125-132.

53. Xiao, J.; Tolbert, T. J., Synthesis of Polymerizable Protein Monomers for Protein-Acrylamide Hydrogel Formation. *Biomacromolecules* **2009,** *10* (7), 1939-1946.

54. Porath, J., General methods and coupling procedures. . *Methods in Enzymology* **1974,** *34*, 13-30.

55. Xiao, J.; Chen, R.; Pawlicki, M. A.; Tolbert, T. J., Targeting a Homogeneously Glycosylated Antibody Fc To Bind Cancer Cells Using a Synthetic Receptor Ligand. *Journal of the American Chemical Society* **2009,** *131* (38), 13616-13618.

56. Zhang, W.; Inan, M.; Meagher, M., Fermentation strategies for recombinant protein expression in the methylotrophic yeastPichia pastoris. *Biotechnol. Bioprocess Eng.* **2000,** *5* (4), 275-287.

57. Choi, B.-K.; Bobrowicz, P.; Davidson, R. C.; Hamilton, S. R.; Kung, D. H.; Li, H.; Miele, R. G.; Nett, J. H.; Wildt, S.; Gerngross, T. U., Use of combinatorial genetic libraries to humanize N-linked glycosylation in the yeast Pichia pastoris. *Proceedings of the National Academy of Sciences* **2003,** *100* (9), 5022-5027.

58. Manikwar, P.; Majumdar, R.; Hickey, J. M.; Thakkar, S. V.; Samra, H. S.; Sathish, H. A.; Bishop, S. M.; Middaugh, C. R.; Weis, D. D.; Volkin, D. B., Correlating excipient effects on conformational and storage stability of an IgG1 monoclonal antibody with local dynamics as measured by hydrogen/deuterium-exchange mass spectrometry. *J Pharm Sci* **2013,** *102* (7), 2136-51.

59. Alsenaidy, M. A.; Okbazghi, S. Z.; Kim, J. H.; Joshi, S. B.; Middaugh, C. R.; Tolbert, T. J.; Volkin, D. B., Physical stability comparisons of IgG1-Fc variants: effects of N-glycosylation site occupancy and Asp/Gln residues at site Asn 297. *J Pharm Sci* **2014,** *103* (6), 1613-27.

60. Cooper, M. A., Label-Free Biosensors: Techniques and Applications. *Cambridge University Press* **2009,** *first edition*.

61. Bruhns, P.; Iannascoli, B.; England, P.; Mancardi, D. A.; Fernandez, N.; Jorieux, S.; Daëron, M., Specificity and affinity of human Fcγ receptors and their polymorphic variants for human IgG subclasses. *Blood* **2009,** *113* (16), 3716-3725.

62. Choi, B.-K.; Warburton, S.; Lin, H.; Patel, R.; Boldogh, I.; Meehl, M.; d'Anjou, M.; Pon, L.; Stadheim, T.; Sethuraman, N., Improvement of N-glycan site occupancy of therapeutic glycoproteins produced in Pichia pastoris. *Appl Microbiol Biotechnol* **2012,** *95* (3), 671-682.

63. Liu, H.; Gaza-Bulseco, G.; Chumsae, C.; Newby-Kew, A., Characterization of lower molecular weight artifact bands of recombinant monoclonal IgG1 antibodies on non-reducing SDS-PAGE. *Biotechnology Letters* **2007,** *29* (11), 1611-1622.

64. Franey, H.; Brych, S. R.; Kolvenbach, C. G.; Rajan, R. S., Increased aggregation propensity of IgG2 subclass over IgG1: Role of conformational changes and covalent character in isolated aggregates. *Protein Science* **2010,** *19* (9), 1601-1615.

65. Vlasak, J.; Ionescu, R., Fragmentation of monoclonal antibodies. *mAbs* **2011,** *3* (3), 253-263.

66. Tsukiji, S.; Nagamune, T., Sortase-Mediated Ligation: A Gift from Gram-Positive Bacteria to Protein Engineering. *ChemBioChem* **2009,** *10* (5), 787-798.

67. Pritz, S.; Wolf, Y.; Kraetke, O.; Klose, J.; Bienert, M.; Beyermann, M., Synthesis of Biologically Active Peptide Nucleic Acid−Peptide Conjugates by Sortase-Mediated Ligation. *The Journal of Organic Chemistry* **2007,** *72* (10), 3909-3912.

68. Proft, T., Sortase-mediated protein ligation: an emerging biotechnology tool for protein modification and immobilisation. *Biotechnology Letters* **2010,** *32* (1), 1-10.

69. Zhang, Y.; Boesen, C. C.; Radaev, S.; Brooks, A. G.; Fridman, W.-H.; Sautes-Fridman, C.; Sun, P. D., Crystal Structure of the Extracellular Domain of a Human FcγRIII. *Immunity* **2000,** *13* (3), 387-395.

70. Kanda, Y.; Yamada, T.; Mori, K.; Okazaki, A.; Inoue, M.; Kitajima-Miyama, K.; Kuni-Kamochi, R.; Nakano, R.; Yano, K.; Kakita, S.; Shitara, K.; Satoh, M., Comparison of biological activity among nonfucosylated therapeutic IgG1 antibodies with three different N-linked Fc oligosaccharides: the high-mannose, hybrid, and complex types. *Glycobiology* **2007,** *17* (1), 104-118.

71. Subedi, Ganesh P.; Hanson, Quinlin M.; Barb, Adam W., Restricted Motion of the Conserved Immunoglobulin G1 N-Glycan Is Essential for Efficient FcγRIIIa Binding. *Structure* **2014,** *22* (10), 1478-1488.

72. Mozziconacci, O.; Okbazghi, S.; More, A. S.; Volkin, D. B.; Tolbert, T.; Schöneich, C., Comparative evaluation of the chemical stability of four well-defined IgG1 Fc glycoforms. *Journal of Pharmaceutical Sciences*.

73. More, A. S.; Toprani, V. M.; Okbazghi, S. Z.; Kim, J. H.; Joshi, S. B.; Middaugh, C. R.; Tolbert, T. J.; Volkin, D. B., Correlating the impact of well-defined oligosaccharide structures on physical stability profiles of IgG1-Fc glycoforms. *Journal of Pharmaceutical Sciences*.

74. Hamilton, B. S.; Brede, Y.; Tolbert, T. J., Expression and characterization of human glycosylated interleukin-1 receptor antagonist in Pichia pastoris. *Protein expression and purification* **2008,** *59* (1), 64-68.

75. Presta, L. G.; Shields, R. L.; Namenuk, A. K.; Hong, K.; Meng, Y. G., Engineering therapeutic antibodies for improved function. *Biochemical Society transactions* **2002,** *30* (4), 487-490.

76. Seidel, U. J. E.; Schlegel, P.; Lang, P., Natural killer (NK) cell mediated antibody-dependent cellular cytotoxicity (ADCC) in tumour immunotherapy with therapeutic antibodies. *Frontiers in Immunology* **2013,** *4*.

77. Abès, R.; Teillaud, J.-L., Impact of Glycosylation on Effector Functions of Therapeutic IgG. *Pharmaceuticals* **2010,** *3* (1), 146-157.

78. Kuramochi, T.; Igawa, T.; Tsunoda, H.; Hattori, K., Humanization and Simultaneous Optimization of Monoclonal Antibody. In *Human Monoclonal Antibodies*, Steinitz, M., Ed. Humana Press: 2014; Vol. 1060, pp 123-137.

79. Champion, T.; Beck, A., Capture of the Human IgG1 Antibodies by Protein A for the Kinetic Study of h-IgG/Fc?R Interaction Using SPR-Based Biosensor Technology #. In *T Glycosylation Engineering of Biopharmaceuticals*, 2013; Vol. 988, pp 331-343.

80. Holmberg, A.; Blomstergren, A.; Nord, O.; Lukacs, M.; Lundeberg, J.; Uhlén, M., The biotin-streptavidin interaction can be reversibly broken using water at elevated temperatures. *ELECTROPHORESIS* **2005,** *26* (3), 501-510.

Chapter 3

Comparative Evaluation of Well-Defined Mixtures of IgG1 Fc Glycoforms as a Model for Biosimilar Comparability Analysis

3.1 Introduction

The patents of several best-selling biologic therapeutic products are expiring soon; consequently, the interest in developing biosimilar products is growing. The exact chemical structure of small-molecule drugs and their purities can be well-established. This gives an opportunity for generic manufacturers to produce a generic product without clinical trials by demonstrating bioequivalence in pharmacokinetics studies. Unlike small-molecule drugs, protein molecules are structurally complex, often containing a mixture of different species produced after posttranslational modification. In fact, most of the heterogeneity of protein molecules is attributed to variably complete N-linked glycosylation.[1]

For a protein-based product, it is nearly impossible to produce identical products from two different manufacturing plants.[2] Moreover, it is even difficult to produce an identical product by the innovator from lot-to-lot as there is always inherent variability. In general, protein therapeutics are mixtures because of posttranslational modifications, chemical modifications, and potentially multiple conformations or aggregated forms. In fact, as the definition of biosimilar indicates, it is unlikely that all the structure and function aspects of the biosimilar will be identical to the originator. However, the innovator should demonstrate consistency in manufacturing the therapeutic product within a set of defined and acceptable criteria for the critical quality attributes.[2] The other challenge is that the manufacturing process and criteria are not disclosed, and the sponsor of a biosimilar is required to perform extensive characterization to show that the originator and biosimilar candidate are highly similar.[2] In addition, a biosimilar sponsor can never exactly replicate the complex bioprocess of the originator, and it is well known that “the process defines the product” with regard to the structural and functional aspects of a

biologic product.[3] Therefore, protein therapeutics contain a mixture of structurally similar molecules, which differ by the type and extent of posttranslational modifications. These modifications include glycosylation, deamidation, oxidation, phosphorylation, and C-terminal lysine variability. Because of this structural complexity, even after extensive characterization, the safety and efficacy of protein therapeutics cannot be guaranteed. Hence, the need to have sensitive and robust analytical methods to demonstrate the similarity and differences between a biosimilar candidate with the originator is urgently needed.[2, 4]

Monoclonal antibodies are the most prevalent type of biologic therapeutic products used today.[5] Among the four IgG subclasses (IgG1, IgG2, IgG3, and IgG4), IgG1 is the most widely used antibody in the treatment of various diseases, such as cancer, inflammation, and rheumatoid arthritis.[6-9] IgG1 has a conserved N-linked glycosylation site at Asn297,[10-11] and the glycosylation can vary with production condition, media composition, cell-line used, and duration of expression.[12-16] It is well studied that the type of glycosylation at Asn297 can have a significant impact on the effector function, stability, solubility, pharmacokinetics, and immunogenicity.[4, 12-13, 17-24] Therefore, monitoring glycosylation during production is critical for safety and efficacy of therapeutic proteins. This is particularly important during comparability and biosimilarity exercises since a shift in glycosylation caused by a change in the manufacturing process and/or cell line can have a detrimental effect on the biological activity and physical stability of mAb therapeutics.[2, 25-26] Monoclonal antibodies are inherently heterogeneous with respect to their N-linked glycosylation on the Fc region.[27] Therefore, glycosylation is a critical quality attribute that requires close monitoring during biosimilarity exercises.[28]

Glycosylation of mAbs modulates interaction to the Fc-receptors and plays a key role in complement dependent-cytotoxicity (CDC) and antibody-dependent cell-mediated cytotoxicity (ADCC).[12, 29-30] Thus, comparability assessments of the Fc-mediated effector functions (CDC and ADCC) is an integral component of the data package during a biosimilar exercise.[31] Fc-mediated effector functions include binding with Fc gamma RIIIa (FcγRIIIa), which can be measured accurately using biolayer interferometry (BLItz), surface plasmon resonance (SPR), and flow cytometry techniques.[31] Although there is an inherent variability in bioassays, there is a continuous effort to develop robust analytical methods.[26, 31] Most mAb therapeutics rely on specific binding interaction of the Fc region to target receptors to achieve desired clinical outcomes.[32-33] Hence, comparing the binding activities of a biosimilar to an innovator product using a reliable binding assay can yield valuable information about similarity and potential biological activity.[31, 34]

A functional activity assay provides valuable information about the characteristics related to a product's functional activity and conformational stability, and it is critical in demonstrating similarity. These assays complement the physicochemical analysis by demonstrating potential effects of observed structural difference between the originator and the biosimilar candidate.[26, 31] In addition to their use in demonstrating biosimilarity, functional assays are utilized for candidate selection, product release, and stability assessment.[25-26, 31] A functional assay can potentially predicts how a biosimilar may behave *in-vivo,* and such assays may provide, together with other analytical data, evidence about clinical outcomes.[26, 31] Biosimilar sponsors conduct biological activity tests to examine the impact of process changes on the potency of the product in development. In addition, functional tests are used as a surrogate to confirm a protein's higher-

order structure in parallel to the physical techniques. However, if the physicochemical and functional tests are inconclusive or not enough to confirm the higher-order structure of the originator and biosimilar, then further clinical and nonclinical studies may be necessary for regulatory approval.[2, 26]

Biosimilarity exercises are performed in a step-wise fashion where the level of similarity demonstrated by multifaceted analytical techniques guides the pre-clinical and clinical evaluation required to demonstrate biosimilarity.[31, 35] If higher similarity is demonstrated by the analytical techniques, then a reduced clinical test may be required for regulatory approval. In other words, demonstrating a high level of similarity using a battery of analytical techniques is critical for achieving a biosimilar development process with a reduced clinical package.[29, 31, 36-37] Hence, the first goal is to achieve analytical similarity between the originator and the biosimilar; then the biosimilar sponsor can partially rely on the previous findings of safety, purity, and potency of the originator.[31] This is because biosimilars are developed to be used at the same dose and dosing regime as the originator product. Consequently, a phase II finding study may not be a requirement.[2, 37-38] Therefore, a biosimilar can be approved with a reduced clinical data package, compared with the one required for the originator product.[37]

During biosimilar development, a biosimilar candidate is expected to have similar glycosylation pattern and the same sequence as the originator.[27] Therefore, it is important to understand how a change in glycosylation of a therapeutic mAb impacts its functional, physical, and chemical quality attributes in the development processes.[25] The role of analytical techniques in comparing a biosimilar with the originator is getting significant interest in biosimilar assessments. The three most important characteristics of a protein molecule for establishing

similarity are: post-translational modifications, three-dimensional structure, and protein aggregation. However, no single analytical method can fully demonstrate the similarity between a biosimilar and the originator.[25] Thus, a battery of analytical techniques is employed to demonstrate molecular equivalence.[31] Moreover, it is time- and cost-demanding to demonstrate all aspects of the biosimilar that are necessary for evaluating the critical quality attributes.[31] In general, the type of comparison between the originator and biosimilars should include primary and higher order structures. In addition, post-translational modifications, such as glycosylation, oxidation, and deamidation, should be examined. For instance, analytical techniques, such as mass spectrometry, play a vital role in the identification of post-translational modifications.[35] Other analytical techniques, such as circular dichroism, fourier transformation infrared spectroscopy, and differential scanning calorimetry, are used to demonstrate higher-order structure similarity between the originator and the biosimilar.[26]

In this study, a combination of recombinant expression of the human IgG1 Fc in *P. pastoris*, coupled with *in-vitro* enzymatic reaction and site-directed mutagenesis, was used to produce well-defined homogeneous glycoforms: HM-Fc, Man5-Fc, GlcNAc-Fc, and N297Q-Fc.[4, 21] Our previous studies have shown that the HM-Fc and Man5-Fc glycoforms both exhibited similar high receptor binding affinities (FcγRIIIa) and physical stabilities, whereas the GlcNAc-Fc showed minimal functional activity and physical stability. The non-glycosylated IgG1 Fc (N297Q-Fc) showed the least physical stability as well as no detectable binding affinity to FcγRIIIa and was used as a negative control for the effects of glycosylation in these functional and physical stability characterizations.[4, 24] These four control glycoforms with decreasing N-linked glycan size and the same amino acid sequence were found to be useful in examining the effect of glycosylation on

the functional activity and physicochemical characteristics of IgG1 Fc.[4, 21, 24, 39] Therefore, these glycoforms were selected to make well-defined mixtures as a model for biosimilar comparability analysis. For example, these mixtures can model the impact of change in glycosylation during a biosimilar product development. In this work, the functional and physical assay methods were tested for their ability to differentiate between mixtures of IgG1 Fc glycoforms. Moreover, the pre-defined mixtures of glycoforms were investigated to mimic more heterogeneous glycoforms typically present in monoclonal antibodies. The study of glycoform mixtures prepared in this work will help to understand the contribution of the individual glycoforms to the overall functional activity.

3.2 Materials and Methods

3.2.1 Material

Yeast nitrogen base (YNB) was supplied by Sunrise Biosciences. Bacto TM tryptone and yeast extract were obtained from Beckman, Dickinson and company (Franklin Lakes, NJ). Casein was purchased from Sigma-Aldrich (St. Louise, MO). The enzymes, B. Thetaiotaomicron α-1,2-mannosidase (BT3990, B.t. α-1,2-mannosidase) was produced in-house.[4, 40-42] Endoglycosidase HF (Endo HF) was purchased from New England Biolabs (Ipswich, MA). The components of all buffers including, sodium phosphate, sodium chloride, and PEG-10,000, were purchased from Sigma-Aldrich (St Louis, MO), while citric acid monohydrate and citric acid anhydrous were purchased from Fisher Scientific at the highest purity grade. All other general chemicals were supplied by Sigma-Aldrich and Fisher Scientific unless otherwise noted.

3.2.2 Expression of High-Mannose IgG1 Fc (HM-Fc)

HM-Fc was expressed using a glycosylation-deficient strain of *P. pastoris*[43] using the same protocol as previously described elsewhere.[4] One minor change to the expression protocol was a mixture of methanol and sorbitol were utilized during the induction phase to increase the yield of HM-Fc.

3.2.3 Expression of Non-Glycosylated Mutant N297Q-IgG1 Fc (N297Q-Fc)

Fermentor expression was utilized to produce N297Q-Fc in a glycosylation-deficient *P. pastoris*. The cDNA plasmid for N297Q produced from previous work was linearized with Sac I endonuclease and transformed into a strain of *P. pastoris* (an OCH1 and PNO1 deleted, N297Q-IgG1 Fc expressing, SMD1168 strain containing sttd3) by electroporation. The yeast colonies were selected on YPD plates containing 100 µg/mL Zeocin. Following this step, colonies were tested for N297Q-IgG1 Fc expression using SDS-PAGE. Additionally, the molecular weight of the expressed protein was confirmed by mass spectrometry after expression trial from 1 L spinner flask. A single colony with higher N297Q-IgG1 Fc expression was selected for further protein production. A starter culture of 2 mL was inoculated in Yeast extract-Peptone-Dextrose (YPD) media that contained 100 µg/mL Zeocin. This culture media was incubated at 25°C for 72 hrs. The 2 mL culture media was then inoculated into a 250 mL of YPD/Zeocin, which was incubated with shaking for 72 hrs. The 250 mL culture was then used to inoculate 7 L of Buffered Glycerol-complex Media (BMGY) containing 0.00004% biotin. N297Q-IgG1 Fc expression was induced by methanol feeding with the addition of sorbitol as a carbon source to maximize the yield for about 72 hrs. The cell pellets were harvested, and the N297Q-IgG1 Fc was purified from the

supernatant using protein G affinity chromatography in a similar protocol as described above for HM-IgG1 Fc.

3.2.4 Purification of IgG1 Fc

Both HM- and N297Q-IgG1 Fc were purified using the same general procedure given below. The supernatant collected from yeast expression was filtered with 0.5 µm filter pads (Buon Vino Manufacturing) to remove particulates before protein A affinity chromatography. The protein A column (100 mL bed volume) was equilibrated with 20 mM potassium phosphate pH 6.0 in 10 column bed volumes (CV) and loaded with the filtered supernatant culture medium at pH 6.0. The column was then washed with 20 mM potassium phosphate buffer, pH 6.0, containing 0.5 M NaCl (5 CV) and then 20 mM potassium phosphate buffer, pH 6.0, (5 CV). HM-Fc or N297Q-Fc was eluted using 50 mM citrate buffer pH 3.0. Eluted protein was collected in 20 mL fractions into tubes containing four mL of 1 M Tris pH 9.0 (200 µL of 1 M Tris pH 9.0 per mL of elution volume) to neutralize the acidic elution buffer. Fractions of eluted protein detected by UV absorbance at 280 nm were immediately dialyzed in 20 mM sodium phosphate buffer pH 7.0 (4 L exchanged twice every eight hours). After protein A, the samples were purified using hydrophobic interaction chromatography (HIC) in a similar protocol as described previously.[4] After HIC purification, approximately 940 mg of the HM-Fc glycoform and 400 mg of the N297Q-Fc non-glycosylated mutant were produced. HM-Fc was used in the synthesis of Man5-Fc and GlcNAc-Fc.

3.2.5 Production of Man5-Fc

HM-Fc was converted to Man5-Fc in an *in-vitro* enzymatic reaction using B.t. α-1,2-mannosidase (BT3990).[4] Initially, the sample was at a concentration of 0.6 mg/mL in 20 mM histidine pH 6.0. Before the reaction, HM-Fc (175 mg) was dialyzed extensively in 10 mM MES buffer pH 6.6 to remove the traces of phosphate buffer, and adjust the pH for maximum enzyme activity. Next, HM-Fc was dialyzed in a reaction buffer containing 5 mM $CaCl_2$, 150 mM NaCl, and 10 mM MES buffer pH 6.6 for 12 hrs. After dialysis, the enzymatic reaction was started by adding 10 mg of the bacterial α-1,2-Mannosidase (BT3990) in a 6000 MWCO dialysis bag. The reaction was kept at room temperature for about 48 hrs. Mass spectrometry was utilized to monitor the progress of the reaction, and the percentage of conversion to the Man5-Fc glycoform was estimated from the peak intensity. Finally, the reaction mixture was purified using protein A affinity chromatography to remove unwanted impurities, salts, and excess enzyme using the same protocol as described previously in the purification of HM-Fc.[4] The amount of Man5-Fc produced was 140 mg (85% yield) and the percentage of conversion to Man5-Fc in the final product was estimated to be 81%. The percentage of conversion to Man5-Fc was determined from the MS peak intensity.

3.2.6 Production of GlcNAc-Fc

Treatment of HM-Fc with endoglycosidase HF (Endo HF) under mild conditions (20 mM histidine, pH 6.0) provides an efficient conversion to GlcNAc-Fc. Endo HF displayed full activity in the IgG1 Fc storage buffer (20 mM histidine pH 6.0); therefore, it was possible to digest HM-Fc directly without a dialysis step. Samples of HM-Fc were at 0.65 mg/mL and for every 1mg of protein, 800 U of Endo HF enzyme was added (which corresponds to approximately 0.08 mg of

Endo H per 100 mg HM-Fc). The mixture was incubated at room temperature for 24 hours, and the reaction progress was monitored by mass spectrometry and SDS-PAGE. Finally, the reaction mixture was purified using protein A (Using the same protocol mentioned in the purification of HM-Fc) to remove unwanted impurities and excess enzyme. The sample was dialyzed in a 4L of 20 mM Histidine buffer pH 6.0 (exchanged three times in 16 hrs). The percentage of conversion from HM-Fc to the GlcNAc-Fc glycoform was calculated from the peak intensity obtained from mass spectrometry, which showed a nearly quantitative reaction with the percentage of GlcNAc-Fc in the final product ≥ 95%. The percentage of yield from the reaction was > 60%.

3.2.7 Preparation of Control and Mixtures of Glycoforms for Functional Study

The four control glycoforms (HM, Man5, GlcNAc, and N297Q) were first extensively characterized using mass spectrometry and SDS-PAGE to test for purity. Enzymes used to digestion the glycoforms were removed using protein A affinity chromatography. Before preparing the mixture, control glycoforms were buffer exchanged into 20 mM citrate-phosphate pH 6.0 containing 150 mM NaCl. Each control glycoform concentration was adjusted to 0.5 mg/mL.

3.2.8 Preparation of IgG1 Fc glycoform Mixtures

The four control glycoforms (HM-Fc, Man5-Fc, GlcNAc-Fc, and N297Q-Fc) were first extensively characterized using mass spectrometry, and SDS-PAGE to test for purity. Enzymes used to digestion the glycoforms were removed using protein A affinity chromatography purification. Before preparing the mixture, control glycoforms were dialyzed at 4°C overnight in a 20 mM citrate phosphate buffer with ionic strength adjusted to 0.15 by NaCl at pH 6.0. Dialysis was performed at 4°C using Slide-A-Lyzer dialysis cassettes (Life Technologies, Grand Island, NY)

with a 10 kDa molecular weight cutoff with three buffer exchanges, two exchanges at 4h intervals and one overnight. After dialysis, the final concentrations of the control IgG1 Fc glycoforms were adjusted to 0.5 mg/mL and were mixed in different ratios as seen in Figure 1 to obtain seven different mixtures. The final concentration of protein in the mixtures was 0.5 mg/mL, and the seven mixtures and 4 controls were stored in aliquots of 5 mL at -80°C for further analysis.

3.2.9 Intact protein MS

Samples of control and mixture IgG1 Fc glycoforms at a concentration of 0.5 mg/mL were first incubated with 10 mM dithiothreitol (DTT, Invitrogen) and then 60 µL was injected into the mobile phase of the LC. ESI spectra of the reduced samples was acquired on an Agilent 6520 Quadrupole Time-of-Flight (Q-TOF) system. The same protocol was followed for running the experiment and data collection as described previously.[4] Data was collected in triplicates and, based on the peak intensities, the percentages of the compositions of the mixtures and control glycoforms were analyzed.

3.2.10 Sodium Dodecyl Sulfate Polyacrylamide Gel Electrophoresis (SDS-PAGE)

The experiment was performed under reducing and non-reducing conditions using the Bio-Rad MiniPROTEAN® electrophoresis. Samples containing 10 µg proteins were mixed with an equal volume of loading buffer (62.5 mM Tris-HCl, 2% w/v SDS, 0.01% Bromophenol blue, 25% glycerol) with and without DTT for reducing and non-reducing conditions, respectively. The Fc glycoforms were kept in a boiling-water bath for 2 min before loading. Samples and molecular weight markers were loaded into pre-cast 4-20% gradient gels with a running buffer containing 25 mM Tris, 192 mM glycine, and 0.1% SDS at constant 200V for about 45 min. Gels were then

stained with a staining solution containing 0.05% Coomassie brilliant blue, 10% acetic acid, 40% water, and 50% methanol for one hour. Next, the gels were destained with 30% methanol, 10% acetic acid, 60% methanol. Band densitometry measurement was performed using the Image J program (NIH) as described in detail elsewhere.[21, 44] The percentage of the total area in a band was determined and used to calculate the percentage of the composition of the mixtures.

3.2.11 Production of Fcγ Receptors

FcγRIIIa was expressed and purified in the same manner as described in detailed elsewhere.[4] The cDNA of pGAP-FcγRIIb was linearized using Bgl II and transformed into P pastoris OCH1 deleted cells. Expression and purification of FcγRIIb were conducted similarly to the expression of FcγRIIIa as described in detail elsewhere.[4] The histidine-tagged protein was first affinity isolated from yeast media by Ni^{+2}-NTA and then extensively buffer exchanged in 20 mM sodium phosphate, pH 7.0, for a further HIC purification outlined below. A hydrophobic interaction chromatography (HIC) method using phenyl sepharose™ high-performance resin (GE Healthcare) with a 75 mL CV (packed in-house) and an AKTAmicro chromatographic systems (GE Healthcare) were used to purify FcγRIIB. First, the HIC column was equilibrated with Buffer A (20 mM sodium phosphate, 1.5 M ammonium sulfate pH 7.0) for 10 CV. Next, Ni^{+2}-NTA purified FcγRIIB (dialyzed in buffer A) was loaded onto the pre-equilibrated column. The chromatographic purification was then performed with a linear gradient from 1.5 to 0 M ammonium sulfate (15 CV) using Buffer B (20 mM sodium phosphate, pH 7.0). Fractions (5 mL) containing pure FcγRIIB was collected and concentrated to 1 mg/mL using Vivaflow 50 (10,000 MWCO; Sartorius Stedim Biotech). The total amount of protein produced using this technique was 20 mg. After that, the sample was dialyzed against PBS buffer, and frozen at -80°C for further use.

3.2.12 Interaction of Immobilized Fc Glycoforms with FcγRIIIa Using Biolayer Interferometry

The interactions of the different controls and mixtures of IgG1 Fc glycoforms with the FcγRIIIa was studied with biolayer interferometry using a BLItz instrument (Fortebio, Menlo Park, CA) with protein G biosensor tips. Samples for the binding study were prepared in different compositions (Figure 1) as follows: The first set of samples includes control glycoforms (HM-Fc, Man5-Fc, GlcNAc-Fc, and N297Q-Fc). The second set contains a mixture of HM-Fc with a small percentage of the other glycoforms, which includes 90%HM:10%Man5, 90%HM:10GlcNAc, and 90%HM:10%N297Q. The third set of samples are 50% composition as follows: 50%HM:50%Man5, 50%HM:50GlcNAc, and 50%HM:50%N297Q. The fourth set is a mixture of the four glycoforms 25%HM-Fc:25%Man5:25%GlcNAc:25%N297Q. The binding of controls and mixtures of the IgG1 Fc glycoforms with FcγRIIIa were performed as described previously.[4] The concentration range of the FcγRIIIa in solution was 50 nM to 800 nM in a two-fold serial dilution. Briefly, the binding progress was monitored, which is proportional to the surface bound protein. At the end of the association phase, the unbound analyte in the cuvette was removed from the vicinity of the biosensor, and the dissociation of the complex formed was monitored by dipping in an analyte-free PBS kinetic buffer. The formation of the complex during incubation followed a typical binding profile, with the exponential increase in signal. After dipping the biosensor into Fc-free PBS buffer, the dissociation was monitored with a signal eventually returning close to the baseline. Data generated from the binding of the receptor to IgG1 Fc glycoforms were collected in triplicates and globally fitted to a 1:1 using the first-order rate equation binding model in

BLItz® Pro software. The same binding method as described for FcγRIIIa above was used for studying the interaction of FcγRIIb with mixtures of IgG1 Fc glycoforms, except the concentration range of the receptor in solution was 200 nM to 10,000 nM in a two-fold serial dilution. Similarly, data were collected in triplicates and globally fitted to a 1:1 binding model using BLItz® Pro software.

3.2.13 Interaction of Immobilized FcγRIIIa with Fc Glycoforms Using Biolayer Interferometry

The interactions of the different pure and mixtures of IgG1 Fc glycoforms with biotinylated FcγRIIIa was studied with biolayer interferometry using a BLItz instrument (Fortebio, Menlo Park, CA) with streptavidin (SA) biosensor tips. The concentration range of the Fc in solution was 50 nM to 800 nM in a two-fold serial dilution.

Before the binding experiment, the mixture of glycoforms were dialyzed in PBS buffer to remove the storage buffer (20 mM Histidine, pH 6.0) and to adjust the pH to 7.4. The same protocol was followed as described in detail elsewhere.[4]

3.2.14 Binding Response Measurements

The responses of the controls and mixtures of IgG1 Fc glycoforms with the FcγRIIIa were studied with biolayer interferometry using a Blitz instrument (Fortebio, Menlo Park, CA) using protein G biosensor tips. One protein G biosensor was used for each of the mixtures including its reference for generating the sensorgrams. The biosensor was regenerated after each cycle of runs. Response measurements using FcγRIIIa were conducted as follows. The protein G biosensor tip was hydrated for 10 min with PBS buffer (150 mM NaCl, 50 mM sodium phosphate pH 7.4) and incubated for 30 min with PBS kinetic buffer (PBS buffer containing 1 mg/mL casein as a blocking agent). Next, an initial baseline (30 sec) was established with PBS kinetic buffer and the

protein G biosensor tips were loaded with the IgG1 Fc glycoforms (control and mixtures) at a concentration of 0.8 μM (120 sec). The Fc concentration was based on the total of all glycoform component's concentration in the mixture. The Fc concentration was based on the total of all glycoform component's concentration. Next, a new baseline (30 sec) was established, and the association (180 sec) and dissociation (360 sec) of FcγRIIIa were measured by dipping the biosensor into solutions of FcγRIIIa (0.8 μM) and PBS, respectively. The response curves were then reference subtracted and exported into Microsoft excel. The last five points at the end of the association phases were averaged to measure the response for each curve. These responses obtained from the three curves were averaged to measure the response for each sample. The same protocol was followed for all the controls and the mixtures of glycoforms to determine their responses. The same protocol was also followed for measuring the binding responses for all of the interactions between the glycoforms and FcγRIIb. The concentration of the FcγRIIb used was 3.2 μM.

3.3 Results

3.3.1 Characterization of Control and Mixture of IgG1-Fc Glycoforms

A large amount of HM-Fc was required as a starting material to produce GlcNAc Fc, and Man5-Fc using *in-vitro* enzymatic digestion. Additionally, HM-Fc is a common component of the mixture of IgG1 Fc glycoforms. Hence, to make a large quantity, HM-Fc was expressed in a 10 L fermenter using a glycosylation-deficient strain of *P. pastoris*. Using fermenter expression, 940 mg of the HM-Fc and 400 mg of the N297Q-Fc glycoforms were produced for this study. Several attempts to produce N297Q-Fc in expression media containing BSM and PTM_1 salts resulted in low yields. Thus, BMGY media was used to generate higher yields. Man5-Fc was produced using

an *in-vitro* enzymatic reaction by treating HM-Fc with *B.t.* α-1, 2-mannosidase (BT3990),[4] and the percentage of conversion was 81% calculated from the mass spectrometry peak intensity. The amount of Man5-Fc produced was 140 mg with 86% yield.

Characterization was performed to establish baseline characteristics of the controls and mixtures of glycoforms. Thus, rigorous analytical characterizations were conducted on the controls and mixtures of glycoforms to identify aggregation level, glycosylation state, chemical modification, and intact protein mass. In biosimilarity and comparability studies, extensive characterization is performed on the structure and function of the originator and biosimilar to identify the critical quality attributes.[2, 25] Thus, SEC, cIEF, mass spectrometry, SDS-PAGE, and densitometry were used to characterize the controls and mixtures of glycoforms. These characterizations include the following: glycosylation profile, the percentage of composition, purity, aggregation, and charge heterogeneity. The size exclusion high-performance liquid chromatography (SEC) was used (under nondenaturing condition) to determine if aggregates were present in the controls and mixtures of glycoforms. Table 6 showed average monomer percent results indicated that the controls and mixtures glycoforms were present as monomers with small levels of aggregates across the samples (1-3%). Next, characterization of the isoelectric pH (pI) range by capillary isoelectric focusing was done to monitor charge heterogeneity, and the (Table 6) showed similar pI values of the major species for all the samples tested. This initial characterization demonstrated the homogeneity and purity of the samples prepared. Thus, any difference observed in their functional and physical characteristics was mainly attributed to differences in their glycosylation profile.

Next, mass spectrometry was used to characterize the controls and mixtures of IgG1 Fc glycoforms. Mass spectrometry is used to characterize post-translational modifications, such as oxidation, phosphorylation, truncation, proteolysis, glycosylation state. Mass spectrometry is increasingly becoming an important tool in biosimilarity and comparability studies to establish structural similarities for the proteins under test.[2] In this work, the control and mixture of glycoforms were well-characterized using mass spectrometry with regard to their glycosylation profiles and purities. Figure 3 shows intact mass spectrometry data for HM-Fc, Man5-Fc, N297Q-Fc, and GlcNAc-Fc, under reducing conditions. These four glycoforms were used as controls in this study. As shown from the mass spectrometry data, the differences observed in mass were mainly due to the differences in their glycosylation profile because the same precursor (HM-Fc) was used to produce GlcNAc-Fc and Man5-Fc glycoforms, except N297Q-Fc in which there was a single amino acid mutation (i.e., N297Q).

On mass spectrometry, a shift to a lower molecular weight was observed in the order of HM-Fc>Man5-Fc>GlcNAc-Fc>N297Q-Fc. Moreover, the mass spectrometry data showed the purity and relative homogeneity of the IgG1 Fc glycoforms produced after protein A and HIC purifications. The peak intensities of the intact mass spectra of the control glycoforms under reducing conditions were shown in Table 2. The estimated abundances of the control glycoforms were >81% for Man5, ≥ 96% for GlcNAc-Fc and ≥ 97% for N297Q-Fc, which were consistent with our previously reported data.[4] The predominant forms of the truncated Man5-Fc and GlcNAc-Fc contained a single major peak as would be expected. For N297Q-Fc, a single major peak was observed, which corresponded to the non-glycosylated Fc monomer containing glutamine at the 297 position. HM-Fc contained high-mannose glycans ranging from $Man_8GlcNAc_2$ to

$Man_{12}GlcNAc_2$ with their corresponding percentages ranging from 45% to 5% as shown in Figure 3. All these glycosylation profiles agreed with our previously reported work.[4] Next, the glycosylation profiles and compositions of the mixtures were examined using mass spectrometry. For instance, the mass spectrometry data for the first set of the mixtures of HM-Fc and N297Q-Fc, Mix6 was shown in Figure 3; the N297Q-Fc (25078 Da) showed a smaller peak intensity, which corresponded to its proportion present in the sample. The sum of the intensities of $Man_8GlcNAc_2$, $Man_9GlcNAc_2$, $Man_{10}GlcNAc_2$, and $Man_{11}GlcNAc_2$ was considered when comparing the intensities of HM-Fc with N297Q-Fc. To determine the percentage of composition of these mixtures, each intensity of the glycoforms (N297Q-Fc and HM-Fc) was divided by the total intensities of both components. The mass spectrometry characterizations were run in triplicates, and the estimated percentage of compositions were the average of these triplicate runs (Table 2). The estimated compositions from the peak intensities were 89.6±0.1% and 10.4±0.1% for HM-Fc and N297Q-Fc, respectively. The calculated values agreed with the percentage of components present in the mixture. Moreover, the data suggested that the mass spectrometry data can be utilized for estimation of the percentage compositions consistently.

The second mixture of HM-Fc and N297Q-Fc contained an equal amount of each glycoform (i.e., 50% of each glycoform). The peak intensity of N297Q-Fc significantly increased, which was proportional to its amount present in this particular mix (Figure 3). The percentage of compositions of HM-Fc and N297Q-Fc in the mixture were 48.2±0.6% and 51.8±0.6%, respectively, as shown in Table 2. Again, these values indicated that the mass spectrometry data could be utilized to differentiate or identify both the subtle as well as obvious differences in glycosylation profiles and compositions of the mixtures. The second set of the mixtures contained

HM-Fc and GlcNAc-Fc with proportions of the Mix2 and Mix5. A smaller peak of GlcNAc-Fc at 25265 Da compared to HM-Fc was observed, which corresponded to its proportion present in the sample. The estimated percentage of compositions from the peak intensities were 89.6±0.4% and 10.4±0.4% for HM-Fc and GlcNAc-Fc, respectively. Similarly, with Mix2 mixture, the percentage of compositions calculated from the peak intensities were 54.7±2.9% for HM-Fc and 45.3±2.9% for GlcNAc-Fc, which agreed with the composition of the samples prepared.

The third mixture contained HM-Fc and Man5-Fc mixed in a similar proportion to the previous two mixtures described above. The mass spectrometry data for Mix4 showed a lower peak intensity at 26280 Da for Man5-Fc, as expected from the percentages of the composition. The estimated percentages of composition were 90.5±0.3% and 10±0.3% for HM-Fc and Man5-Fc, respectively. Similarly, the percentages of composition for Mix1 mixture were 55.5±0.4% and 44.4±0.4% for HM-Fc and Man5-Fc, respectively. These values corresponded to the percentages of the composition of the glycoforms in the mixture. The fourth set of the mixtures contained a combination of HM-Fc, Man5-Fc, GlcNAc-Fc, and N297Q-Fc. This mixture contained an equal proportion (i.e., 25% each glycoform) of the four glycoforms as indicated from their peak intensities (Figure 3 and Table 2). The calculated percentages of the composition from the peak intensities were 32.0±2.1%, 21.3±0.8%, 25.8±0.6%, and 20.8±2.0% for HM-Fc, Man5-Fc, GlcNAc-Fc, and N297Q-Fc, respectively. These percentages of the glycoforms were close to their compositions in the mixture. Overall, the mass spectrometry tool demonstrated the ability to differentiate the mixtures and provided accurate percentages of composition of the different mixtures tested.

Next, SDS-PAGE was used to examine the purity, presence of covalent aggregation, and fragments of the control and mixture of glycoforms. In addition, the SDS-PAGE was conducted to examine if the mixtures with an evident and subtle difference in molecular weight could be differentiated. The SDS-PAGE (Figure 2) shows reducing and non-reducing conditions for the control and mixture of glycoforms. The control glycoforms (Lanes 8, 9, 10, and 11) each showed a single band, suggesting purity of the glycoforms prepared. Also, no fragment of the glycoforms tested was observed when tested under reducing and non-reducing conditions. Furthermore, the SDS-PAGE under non-reducing condition showed no heavy chain monomer, which again, indicated that the samples prepared were homogenous, containing no trace of monomers or fragments. For instance, a mixture of HM-Fc and N297Q-Fc (i.e., Mix6) under non-reducing conditions (Lane 4) showed a major and a minor band. The intensities of the bands were proportional to the amount of HM-Fc and N297Q-Fc present in the mixture. Likewise, the non-reducing condition showed a major band for HM-Fc and minor band for the N297Q-Fc.

The second mixture of HM-Fc and N297Q-Fc (50% of each glycoform) was also examined by SDS-PAGE, and as shown in lane 5 (reducing and non-reducing), the band intensities were nearly equivalent, reflecting the composition of the sample. A similar pattern was observed for the mixture of HM-Fc and GlcNAc-Fc, in which the band intensities indicated the nature of the composition. Equal band intensities were observed in the 50% composition, whereas for the Mix6, a faint band for the 10% GlcNAc-Fc and a major band for the 90%HM-Fc were observed (Lane 6). The reducing and non-reducing SDS-PAGE for the control glycoforms showed migration according to their molecular weights (HM-Fc>Man5-Fc>GlcNAc-Fc>N297Q-Fc) as illustrated in Figure 2. The difference between GlcNAc-Fc and N297Q-Fc was only a single glycan. Hence, their

difference was not obvious from the band migrations, suggesting that the mass spectrometry characterization might be the best choice in such mixture of glycoforms.

The SDS-PAGE bands of the mixture of HM-Fc and Man5-Fc were shown in Figure 2. The molecular weight difference between these two glycoforms was small, and thus, no resolution was achieved as expected. Therefore, there was less information that can be obtained from the SDS-PAGE that indicated a difference in their glycosylation state. The last set of the mixtures was 25% composition of the four control IgG1-Fc glycoforms. Two bands were observed; the upper band was a combination of Man5-Fc and HM-Fc, and the lower band corresponds to GlcNAc-Fc and N297Q-Fc (Figures 2, Lane 3). This data suggested that, even for a complex mixture, SDS-PAGE can be helpful in identifying differences in glycosylation profile and estimating the percentages of the composition as shown below.

The mixture of glycoforms were further characterized using densitometry as shown in Table 3. The densitometry analysis includes a combination of HM-Fc with GlcNAc-Fc and N297Q-Fc glycoforms at different proportions that showed band resolution. In the Mix6 mixture, the percentages of compositions determined by densitometry were 89.5% HM-Fc and 10.5% N297Q-Fc, respectively. These percentages of composition were in close agreement with the estimated percentages calculated from the mass spectrometry intensities. Likewise, with the Mix3 mixture, the percentages of composition from the densitometry analysis were 48.0% HM-Fc and 51. 6% N297Q-Fc. Again, these percentages of the composition were in close agreement with percentages calculated from the mass spectrometry peak intensities. In the Mix5 mixture, the percentages of the composition were 89.3% and 10.7%, for HM-Fc and GlcNAc-Fc, respectively. A similar characterization with the Mix2 mixture indicated the following percentages of

composition: 54.7% HM-Fc and 45.3% GlcNAc-Fc. All these percentages were in close agreement with the percentages calculated from the mass spectrometry peak intensities. However, less information can be obtained from the mixture of HM-Fc and Man5-Fc regarding their composition because they have similar molecular weight. Therefore, the bands were not resolved on the gel. A more sensitive method, such as mass spectrometry, could be used as the method of choice to characterize the percentage of these particular glycoforms.

3.3.2 Binding of Control IgG1 Fc Glycoforms with FcγRIIIa

The binding interactions of immobilized controls and mixtures of glycoforms to FcγRIIIa were performed using biolayer interferometry with protein G biosensors. First, the biosensors were loaded with Fc glycoforms to a response level of 2 nm. The association (k_{on}) and dissociation (k_{off}) phases were measured, which corresponded to the formation and dissociation of the complex formed between the immobilized Fc glycoforms and FcγRIIIa. The k_{on} and k_{off} were utilized to calculate the equilibrium dissociation constant (K_D). The k_{on}, k_{off}, and K_D values for the Fc-immobilized format were given in Table 1. The K_D values were 26.6±2.1 nM, 30.7±5.6 nM, 1073.6±240.2 nM for HM-Fc, Man5-Fc, and GlcNAc-Fc, respectively. These K_D values were consistent with previously reported data.[4] In addition, no binding was observed for N297Q-Fc at the highest concentration tested (10 μM). The comparison in K_D values between the four control glycoforms was demonstrated in Figure 4F. Similarly, representative binding curves were given in Figure 9A. As shown from the bar graphs, HM-Fc and Man5-Fc bound to FcγRIIIa similarly, whereas GlcNAc-Fc bound weakly. Furthermore, no detectable binding was observed for N297Q-Fc. In these studies, significant differences in the k_{off} values of these glycoforms were found as shown in Table 1 and illustrated in Figure 4B. These large differences in binding affinities make

the glycoforms prepared in this work an excellent model to study the behavior of mixtures during binding to Fc-receptors.

3.3.3 Binding of Control IgG1 Fc Glycoforms with Immobilized FcγRIIIa

This technique was the reverse of the above method in which FcγRIIIa was selectively immobilized to streptavidin biosensors.[4] A linker between streptavidin and FcγRIIIa was expected to avoid steric hindrance. In addition, the level of immobilization was kept < 0.4 nm to prevent any crowding effect since streptavidin is a tetrameric protein.

The interactions of control IgG1 Fc glycoforms were measured with streptavidin biosensors. In this format, the FcγRIIIa was selectively immobilized onto the biosensor, whereas the Fc glycoforms were kept in solution. A range of concentrations of the controls and mixtures of glycoforms were used to determine the K_D values of the interactions. FcγRIIIa was loaded onto the streptavidin biosensors to a response level of 0.4 nm and then incubated with the Fc glycoforms in solution. For dissociation, the biosensor was incubated with analyte-free PBS buffer and monitored for the rate of dissociation of the complex formed. From the binding curves generated, the association (k_{on}) and dissociation (k_{off}) rate constants were obtained and utilized to calculate the equilibrium dissociation constant (K_D) values. As shown in Table 1, the K_D values were 27.7±2.7 nM, 31.5±4.7 nM, and 1079.5±109.9 nM for HM-Fc, Man5-Fc, and GlcNAc-Fc, respectively. These results demonstrated a range of binding affinities and were in agreement with our previous work.[4] The Fc-immobilized (FγRIIIa in solution) and receptor-immobilized (Fc glycoform in solution) formats provided nearly the same K_D values for the control IgG1 Fc glycoforms as shown in Table 1. These data suggested that both methods were equally sensitive and behaved similarly at detecting changes in glycosylation state, which consequently, changes

the binding affinities to FcγRIIIa. Figure 4 shows a comparison of the K_D values of control Fc-glycoforms generated using the immobilized Fc and receptor (Table 1). Overall, the data indicated that the same K_D values were obtained from both formats for HM-Fc, Man5-Fc, and GlcNAc-Fc control glycoforms. Representative binding curves generated for the association and dissociation of the control glycoforms were given in Figure 9. Fast kinetic dissociation rate constants (k_{off}) was observed for GlcNAc-Fc and, consequently, weaker binding affinity. Comparatively, slow kinetic dissociation rate constants (k_{off}) were observed for HM-Fc and Man5-Fc. No signal was observed for N297Q-Fc, which underlined the significance of the N-linked glycan (N297) for maintaining the functional activity. The control glycoforms were used to optimize both methods and demonstrated that the two formats were complementary. Thus, any difference between the mixtures could be identified based on the individual glycoforms they were made of (components of the mix) and attributed to the characteristics of the mixture.

3.3.4 Interaction of Mixture Fc Glycoforms with FcγRIIIa

3.3.4.1 Mixtures of HM-Fc and N297Q-Fc

HM-Fc and N297Q-Fc were combined to make two mixtures with the compositions as follows: Mix3 and Mix6. These two mixtures were prepared to observe the behavior of the mixtures during association and dissociation phases using both the Fc-immobilized and receptor-immobilized formats. Furthermore, the Mix6 mixture was designed to observe any subtle change that can be detected using the binding assays. The Mix3 mixture was designed to represent a major shift in the composition, and understand how this mixture with equal proportion behaves using the two binding assay formats. In other words, the main goal was to test whether the methods can identify both subtle and major changes in binding affinities in a given sample with

either a subtle or a major change in composition. Thus, in this work, the interactions were measured using the two immobilization techniques as described below.

3.3.4.2 Binding of Immobilized Mixtures of N297Q-Fc and HM-Fc to FcγRIIIa

Mixtures of N297Q-Fc and HM-Fc were prepared and loaded onto the biosensor; both mixtures (i.e., Mix3 and Mix6) were tested and analyzed. The formation and dissociation of the complex formed were measured in the same protocol used for the control glycoforms. Interestingly, N297Q-Fc in these mixtures was functionally inactive and does not bind with the FcγRIIIa. Thus, it is relevant to monitor how the effect of this inactive protein affects the overall apparent equilibrium dissociation constant. The K_D values for Mix6 and Mix3 were 24.9±1.3 nM and 24.9±1.1 nM, respectively, as shown in Table 1.

The results indicated that regardless of the amount of N297Q-Fc present in the mixture, no differences in apparent K_D were detected using the Fc-immobilized format. Moreover, the data demonstrated the presence of inactive protein (N297Q-Fc) has no effect on the apparent equilibrium dissociation constant measured. This phenomenon was observed because the level of immobilization (active or inactive) did not influence the kinetic parameters (k_{on} and k_{off}) used for determination of the K_D values. In other words, the K_D determined by kinetic parameters was dependent on the k_{on} and k_{off} values and independent of the amount of immobilized Fc proteins. The other factor that contributed to the K_D values was the concentration of protein in solution: in this case, the Fc receptor. The concentration of the Fc receptor used for both sets of mixtures was the same. As a result, this technique was not able to detect the presence of the inactive protein (N297Q-Fc) present in the mixture. This result highlights the need to carefully analyze binding experiments performed with the Fc-immobilized format since the technique is blind to

inactive proteins. A typical example of inactive protein could be a denatured protein (physical and chemical) or non-native aggregates caused by various stress factors.

3.3.4.3 Binding of N297Q-Fc and HM-Fc Mixtures with Immobilized FcγRIIIa

The receptor-immobilized format was used to test the two mixtures of N297Q-Fc and HM-Fc. Mixture with different concentrations of HM-Fc and N297Q-Fc was prepared and kept in solution, whereas FcγRIIIa was immobilized selectively onto the streptavidin biosensors. The K_D value obtained for Mix6 was 31.5±2.9 nM, showing subtle change compared to the control HM-Fc K_D value measured, which was 27.7 ±2.7 nM. Next, the second mixture of HM-Fc and N297Q-Fc (50% each) was examined, and the K_D value increased by two-fold. Unlike the Fc-immobilized format, the inactive protein (N297Q-Fc) was included in the total concentration of Fc used for determination of the K_D value. In other words, in the 50% mixture of HM-Fc and N297Q-Fc, the K_D value increased by two-fold, which was due to the presence of 50% inactive protein (N297Q-Fc) in the solution. This inactive protein accounted for 50% of the concentration of Fc used for determination of the K_D value. Thus, when 50% N297Q-Fc (inactive protein) was present, the K_D value increased by two-fold. From the kinetic parameters, the association rate constant was concentration dependent and showed a significant reduction when the proportion of N297Q-Fc increased. However, the dissociation constant (k_{off}) was independent of concentration, so the differences observed were attributed to the k_{on} values. In other words, the dissociation rate constant value was independent of the concentration, and no change was observed as shown in Table 1. Representative binding curves for this mixture were shown in Figure 9B. The k_{on}, k_{off} ,and K_D values were illustrated in Figure 4.

Unlike the the dissociation rate constant, the association rate constant (k_{on}) and the equilibrium dissociation constant (K_D) were dependent upon the concentration. To prove our concept that the change in K_D value was only due to the presence of N297Q-Fc (functionally inactive), the data was re-processed by adjusting the actual concentration of the HM-Fc present in the mixture without accounting for the N297Q-Fc concentration. As shown in Table 1, the k_{on} values showed a significant increase from (1.7± 0.1)x10^5 $M^{-1}s^{-1}$to (3.1±0.4)x10^5 $M^{-1}s^{-1}$, and the K_D value decreased from 52.7±3.7 nM to 29.0±4.2 nM as expected for pure HM-Fc control glycoform measured (Table 1). The re-processed K_D values were similar to the pure HM-Fc values, indicating that the changes were mainly due to the apparent concentration. Overall significant differences in K_D values were observed between the two immobilization formats, highlighting the impact of the sample composition and immobilization technique on the binding outcome.

The K_D values from the 50% mixture of HM-Fc and N297Q-Fc measured using the Fc-immobilized and receptor-immobilized formats were 24.9±1.1 nM and 52.7±3.7 nM, respectively. As shown above, the difference in K_D values between the two formats was nearly two-fold. The result demonstrated that care must be exercised when designing an experiment and analyzing the data since the selected immobilization technique could have a significant impact on the equilibrium dissociation constant. Overall, the receptor-immobilized method successfully determined the presence of inactive protein in the samples and must be the method of choice when the sample is expected to have impurities or inactive protein.

3.3.4.4 Mixtures of Man5-Fc and HM-Fc Glycoforms

HM-Fc and Man5-Fc controls showed a similar high affinity to FcγRIIIa, as would be expected for high-mannose IgG glycoforms. Two sets of mixtures of HM-Fc and Man5-Fc were

prepared with subtle and major differences in composition, Mix1 and Mix4, respectively. These two Fcs model mixture of non-fucosylated glycoforms with differences in the α-1,2-linked high mannose-terminal glycans. The HM-Fc glycoforms contained high-mannose glycans consisting primarily of 8 mannoses ($Man_8GlcNAc_2$), whereas the Man5-Fc contained high-mannose glycans consisting primarily five mannoses ($Man_5GlcNAc_2$). The binding studies for both immobilizations were conducted with the same protocol as described above. In the Fc-immobilized, the K_D values were 25.9±1.2 nM and 26.9±1.4 nM for Mix4 and Mix1, respectively. No change in K_D values between the mixtures was observed. For the immobilized FcγRIIIa binding with the mixture, the K_D values for Mix4 and Mix1 were 27.03±1.1 nM and 25.74±2.9 nM, respectively. Similar to the Fc-immobilized, no change in K_D values was observed regardless of composition of the mixture or immobilization technique used. Likewise, no change in K_D values was found between the two immobilization technique.

The similarity in K_D values was presumably due to both HM-Fc, and Man5-Fc binding similarly to FcγRIIIa. Mixing the glycoform did not seem to change the apparent binding affinity. Additionally, both glycoforms behaved similarly with regard to their interaction with the FcγRIIIa in both formats, suggesting the α-1,2 glycans have minimum effect on the binding affinities. This result indicates that when the components of the mixture have the same binding affinity, then neither the percentage of composition nor the immobilization technique influences the apparent binding affinities. See Table 1 for kinetic data and Figures 9A and 9B for representative binding curves and illustration of the kinetic parameters in Figure 4.

3.3.4.5 Mixtures of HM-Fc and GlcNAc-Fc Glycoforms

HM-Fc and GlcNAc-Fc have a slight difference in their kinetic association rate constants (k_{on}) but a significant difference in their kinetic dissociation rate constants (k_{off}). The differences in k_{off} values ultimately give differences in equilibrium dissociation constants (K_D). Two mixtures, namely: Mix2 and Mix5, were prepared and determined using both immobilization format. The K_D values generated from the Fc-immobilized technique for HM-Fc and GlcNAc-Fc control glycoforms were 26.6±2.1 nM and 1073.6±240 nM, respectively. Similarly, using the receptor-immobilized technique, the K_D values were 27.7±2.7 nM for HM-Fc and 1079.5±109.9 nM for GlcNAc-Fc. There was a 40-fold difference between the two K_D values, mainly attributed to their differences in kinetic dissociation rate constant (k_{off}) values as shown in Table 1. The K_D values obtained using the Fc-immobilized technique were 44.4±2.8 nM and 76.7±5.6 nM for Mix5 and Mix2, respectively. This decrease in binding affinity was due to the presence of a weak binding component (GlcNAc-Fc) in the mixtures. The result demonstrated that the Fc-immobilized technique was able to detect the contribution of the weak binding components (i.e., GlcNAc-Fc) in the mixture.

For Mix2, in which there was a higher proportion of GlcNAc-Fc, the kinetic dissociation constant (k_{off}) values increased as shown in Table 1. Hence, there was a significant increase in k_{off} compared to the second set of the mixture (Mix5). This result indicated that when there was a weak binding component in the mixture that can still bind to FcγRIIIa, the Fc-immobilized technique could pick up the contribution, and thus the K_D values reflect the nature of the mixture composition. This was important, specifically when compared to the previous sets of mixtures (N297Q-Fc and HM-Fc) on which the Fc-immobilized method was blind to the inactive protein

(N297Q-Fc) but sensitive to partially active protein (GlcNAc-Fc) present in the mixture. Again, this highlights the complexity of directly interpreting the K_D value without looking at the composition of the sample. It is well known that mAbs contain heterogeneous glycoforms that can bind differently to FcγRIIIa.[45] Thus the selected binding assay method has a significant impact on the measured binding affinities. Next, to see how this partially active component might affect the kinetic values and apparent dissociation constant, the FcγRIIIa immobilization technique was tested. The K_D values obtained for this reverse immobilization technique (immobilized FcγRIIIa) were 31.7±1.0 nM and 43.3±4.1 nM for Mix5, and Mix2, respectively. The kinetic values from this immobilization were significantly different from the Fc-immobilized format as shown in Table 1.

The difference in K_D values in this mixture was presumably due to the difference in the mechanism of complex formation between Fc glycoforms and FcγRIIIa, which was dependent on the immobilization platform used. When the two mixtures (GlcNAc-Fc and HM-Fc) were immobilized, there was a single component in the solution (FcγRIIIa), which interacted with both components independently (heterogeneous ligand binding model) as illustrated in Figures 5 and 6. When the receptor was immobilized, the two Fcs in the solution were competing for a single binding site (FcγRIIIa). Thus, there was a competition for a single binding site during the association phase leading to the enrichment of the high binding component (i.e., HM-Fc) compared to GlcNAc-Fc at the end of the association phase as demonstrated in Figures 5 and 6. The competition continued during the association phase leading to the displacement of the weak binding component, and consequently, resulted in the enrichment of HM-Fc at the end of the association phase. This made the dissociation phase to behave more like HM-Fc than reflecting the percentages of the components present in the sample. As a result of this phenomenon, the

dominant component of the dissociation phase was HM-Fc, which was evident from the k_{off} values obtained. As shown in Table 1, the k_{off} values for HM-Fc control was (7.1±0.5)x10^{-3} $M^{-1}s^{-1}$ and for Mix2 the k_{off} value was (8.5±0.6)X10^{-3} $M^{-1}s^{-1}$. Given the standard deviation, there was no significant difference between these two k_{off} values, indicating that the major component of the dissociation phase was enriched HM-Fc glycoform.

Furthermore, for the Fc-immobilized format, the k_{off} values of Mix2 was (14.1±1.0)x10^{-3} $M^{-1}s^{-1}$ and HM-Fc control was (5.5±0.0)x10^{-3} $M^{-1}s^{-1}$. This k_{off} value showed a nearly three-fold difference, suggesting there was a significant contribution of GlcNAc-Fc on the dissociation phase. Once the Fc was immobilized, there was no competitive displacement since the two sites were independent, and a single component (FcγRIIIa) was in the solution. The result demonstrated that when there was a weak binding component, the immobilized Fc was the method of choice and reflected the composition of the mixture. Additionally, this result demonstrated that the binding kinetic results should be carefully interpreted since the binding results depend on the immobilization selected. Moreover, knowing the sample composition before the experiment gives important clues about the expected binding result. Therefore, care must be exercised not to make a conclusion based on the K_D values without looking into the sample composition. This is because the result may not represent the actual K_D value or could be skewed due to the presence of a high binding affinity component present in the sample. The binding results of both immobilization formats were illustrated in Figure 4.

3.3.4.6 Time Course Binding Assessment

To prove our concept of the complex binding as well as displacement of GlcNAc-Fc by HM-Fc observed in the receptor immobilized format, a time course binding experiment was

performed. The dissociation curves were measured at different incubation times for the mixtures of GlcNAc-Fc and HM-Fc control glycoforms (Figure 6A). The control HM-Fc showed the slowest dissociation phase, whereas GlcNAc-Fc showed the fastest dissociation phase at 180 sec association time. Next, we monitored the dissociation phase at different incubation times ranging from 30 sec to 180 sec As shown from the dissociation phases, it was evident that the incubation time influences the shape of the dissociation curve. This was because of the competitive displacement of GlcNAc-Fc by HM-Fc as the incubation time increased. In addition, as the incubation time increases, the k_{off} values decreased, which was also evident from the % dissociation curves (Figure 6B). Even at the lowest incubation time of 30 sec, the dissociation curve behaved more like HM-Fc dissociation than GlcNAc-Fc. This event demonstrated the impact of the difference in their binding interaction, which ultimately leads to the fast displacement of GlcNAc-Fc by HM-Fc on the surface of the biosensor. For ease of comparison, a similar % dissociation was examined for the Mix2, using both immobilization formats as shown in Figure 6C, and the shape of the dissociation curve behaved more like HM-Fc when the Fc-immobilized technique was used. In the Fc-immobilized, however, the dissociation curve reflected both HM-Fc and GlcNAc-Fc, indicating the contribution of both components. This was because the two binding events were independent, and no competitive displacement existed. Again, these events prove the differences observed between the two formats.

3.3.4.7 A mixture of HM-Fc, Man5-Fc, GlcNAc-Fc, and N297Q-Fc glycoforms

A four component mixture containing an equal proportion of four glycoforms (Mix7) was prepared to represent a more complex system. The K_D value obtained from the Fc-immobilized technique was 52.5±4.0 nM. Since both HM-Fc and Man5-Fc bind with high affinity similarly and

N297Q-Fc has no effect on the binding affinity, this change in K_D value was presumably due to the contribution of the GlcNAc-Fc present in the sample. In the receptor-immobilized format, the K_D value obtained was 35.6±1.3 nM, which was significantly lower than the K_D value measured by the Fc-immobilized technique. This lower K_D value was presumably due to competitive displacement described previously for HM-Fc and GlcNAc-Fc mixtures. Representative binding curves for both immobilization techniques are shown in Figures 9A and 9B.

3.3.5 Binding of Control IgG1 Fc Glycoforms with FcγRIIb

FcγRIIb is the only inhibitory Fcγ receptor produced in humans and specifically expressed in B-cells.[46] Hence, it is relevant in many clinical effects of mAb therapeutics that exert their effect through the Fc region.[47] The K_D values obtained for HM-Fc and Man5-Fc were 3419.8±288.4 nM and 3274.5±957.4 nM, respectively. This result indicated that the HM-Fc and Man5-Fc have similar binding affinities to FcγRIIb. For the N297Q-Fc and GlcNAc-Fc control glycoforms, no detectable binding affinities were observed at the highest concentration of FcγRIIb tested (10 μM). See Table 4 for kinetic data and Figure 9C for the binding curve of the control glycoforms.

3.3.5.1 Mixtures of Glycoforms Binding with FcγRIIb

HM-Fc and Man5-Fc glycoforms have similar binding affinities to FcγRIIb; no difference was observed between Mix4 and Mix1. This was in agreement with the previously observed phenomenon when a mixture of HM-Fc and Man5-Fc were examined using FcγRIIIa (Figure 4 and Table 4). The N297Q-Fc and GlcNAc-Fc glycoforms have no contribution to the observed apparent equilibrium dissociation constant. As a result, all the mixtures showed no significant difference in apparent equilibrium dissociation constant (K_D) values. The data indicated that the K_D values provided less information about the nature of the sample composition, but since the GlcNAc-Fc

glycoform interacted differently to FcγRIIb than FcγRIIIa, this might be utilized to differentiate mixtures containing it. Representative binding curves for the mixture and control glycoforms are given in Figure 9C.

3.3.6 Response Comparison for Controls and Mixtures of Glycoforms

The kinetic (k_{on} and k_{off}) and the equilibrium dissociation constant were not related to the response of the complex formed. In this case, the response was monitored for the control and mixture of glycoforms using the Fc-immobilized method. Interestingly, the responses as shown from the bar graphs (Figure 8A and Table 5) were able to detect the presence of inactive or weak binding component (i.e., N297Q-Fc). For instance, the decrease in response was proportional to the presence of inactive protein (N297Q-Fc) or a low-affinity binding protein. This result indicated that although the K_D values for a mixture of HM-Fc and N297Q-Fc does not show any difference regardless of their composition, the proportional decrease in response does indicate the presence of the inactive component. Hence, it is important to look not only at the K_D values but also at the response as critical quality attributes of the sample under test. For instance, the response value for Mix6 was approximately 9% less than the HM-Fc control, which was in agreement with the amount of inactive protein (N297Q-Fc) present in the mixture. Similarly, the response value for Mix3 was approximately 52% of control HM-Fc glycoform, indicating that half of the mixture was an inactive component (i.e., N297Q-Fc). A similar pattern was observed for mixtures of GlcNAc-Fc and HM-Fc, in which a high proportion of GlcNAc (50%) gave a lower response. However, unlike the N297Q-Fc, the GlcNAc-Fc contributes to the observed response of the mixture, and the decrease in response was proportional to its contribution to the binding response. Mixtures of Man5-Fc and HM-Fc (Mix4 and Mix1) showed a comparable response in

agreement with their close K_D values. Compared to all sample components that can potentially bind with FcγRIIIa, GlcNAc-Fc showed the lowest response, which was in agreement with its weak binding affinity. No response of N297Q-Fc binding to FcγRIIIa was observed as described previously.

The binding response comparison was performed using the immobilized Fc technique as shown in Figures 7, 8A and Table 5. The data clearly demonstrated the difference in binding responses between the different sets of mixtures. Hence, the response measured can be used in evaluating critical quality attributes because it showed a trend with the percentage of the composition and the nature of the components in the mixtures. Furthermore, it was evident from the data that subtle as well as obvious differences were observed, suggesting response measurement could differentiate different mixtures. The same method was also used to determine the response using FcγRIIb. The response showed that the glycoforms bind differently, and both N297Q-Fc and GlcNAc-Fc showed no binding response. Also, mixtures containing GlcNAc-Fc and N297Q-Fc showed the lowest responses.

The surface capacity (loading) of a biosensor could significantly affect the binding response. Hence, these binding response measurements were performed by carefully monitoring the loading capacity and loading level of the Fc glycoforms. Any defective and low surface capacity biosensors were excluded from the experiment. Multiple regenerations can also decrease the loading capacity of a biosensor and, consequently, reduce the binding response. Therefore, the regeneration cycles were kept minimum (three cycles), and one biosensor was used for each sample. The response measurements were conducted in triplicates at a single concentration. To minimize day-to-day variability in response, the samples were run head-to-

head. The above protocol ensures that the differences in binding responses observed among the glycoforms were mainly attributed to the differences in their receptor binding affinity.

3.4 Discussion

The structure of an IgG comprises the Fc and Fab portions, linked by the disulfide bond at the hinge region.[11] Unlike the Fab region, which is variable in sequence among different IgGs, the Fc is homologous and constant in sequence across all IgGs in the same subclass.[10] By studying the constant Fc portion of IgG1 Fc, rather than a single full-length mAb with variable regions, it should be possible to apply the assays developed in this study to differentiate the critical quality attributes of the mAbs. The Fc portion is a simpler system to study but contains the C_H3 and glycosylated C_H2 domains, which are present across all human IgG1 mAbs.[4] Thus, in this study, the human IgG1 Fc was used as a model that can potentially represent all monoclonal antibodies. It is well known that the glycan profile in monoclonal antibodies varies with the type of cell line and expression conditions. Thus, it is important to study the effect of changes in the glycan profile on the biological activity using comparability studies.[48-49] Such variations in glycosylation profile include the following: core fucosylation, terminal sialic acid, N-acetylglucosamine, and high mannose, which are known to affect binding affinity to Fc receptors.[50] Therefore, the effect of glycosylation on the functional activity of the mAbs is often examined, even if the Fc functionality is not part of the mAbs mechanism of action.[25] Due to these reasons the Fc region is critical for the safety and structural integrity of mAbs.[51] In addition to their use in demonstrating biosimilarity, functional assays are utilized for candidate selection, product release, and stability assessment.[26, 31] The biological assay examinations, which include potency form the backbone of

the quality control (QC) testing scheme. The biological test used for QC testing needs to be sensitive to relevant structural changes with a potential effect on product safety and efficacy.[25]

These four glycoforms were selected in this study as controls because they exhibit a broad range of biological and physicochemical quality attributes. Hence, these control glycoforms are suitable to use as a model for typical changes in quality attributes encountered during biosimilar comparability assessments. The mixtures of IgG1 Fc glycoforms were prepared by combining the homogeneous glycoforms to make well-defined mixtures with differences in biological and physical quality attributes. An advantage of producing homogeneous glycoforms is that it allows for developing comparative assays with well-known differences in functional and physicochemical quality attributes. Then the assay can be optimized with well-defined mixtures that exhibit subtle differences.

Previously, we developed two functional assay formats: an Fc-immobilized and a receptor-immobilized format. Moreover, we demonstrated that the two methods were complementary, providing the same K_D values for the well-defined homogeneous glycoforms (utilized as controls in this study).[4] In this study, our goal is to examine how the immobilization formats impact the binding outcome of the mixture of IgG1 Fc glycoforms. Also, we want to gain a better understanding of which format efficiently differentiates the mixtures with subtle and major differences in critical quality attributes. Functional activity assessments are needed because physicochemical tests alone cannot provide full information on the structure of the molecule necessary for potency. Hence, the functional activity can be used as a surrogate of the protein conformational integrity, which is required for activity.[25] To achieve our goal, we first

tested the control glycoforms and then we used optimized assays to evaluate the mixture of glycoforms prepared with the different composition of these glycoforms.

In biosimilarity studies, the assessment of similarity requires multiple orthogonal analytical approaches to adequately define the characteristics of the original biotherapeutics and their potential biosimilarity.[2] Therefore, as an initial characterization, the purity profiles of the control and mixture of glycoforms were assessed using SDS-PAGE, mass spectrometry (MS), capillary isoelectric focusing (cIEF), and size exclusion chromatography (SEC). In addition, the overall glycosylation profiles of the glycoforms were examined using mass spectrometry to confirm their identity and homogeneity. Mass spectrometry plays a vital role in the identification of posttranslational modifications, such as oxidation, reduction, deamidation, fragmentation and N-linked glycosylation, which can be examined at the protein levels.[29, 35] Thus, initial characterization of the glycosylation profiles of the control glycoforms was examined using intact protein mass spectrometry. In addition, mass spectrometry was utilized to identify the presence of proteolytic fragment, C-terminal lysine variability, and oxidation that could arise during expression and purification steps. These control glycoforms were found to be highly pure with no evidence of chemical modifications, and their glycosylation profiles were consistent with our previously reported work.[4] Next, we used the intact mass of the control glycoforms and their glycosylation profiles as a base characterization to evaluate the composition of the mixture of glycoforms. Moreover, the percentage of composition of the mixture of glycoforms was examined using the mass spectrometry peak intensity, and the results demonstrated that the estimated percentages of the components were accurately determined as shown in Table 2. Therefore, the mass spectrometry can be used efficiently to not only identify the glycosylation

profiles but also in the estimation of the composition of the mixture of glycoforms. This approach could be applied when measuring glycoform composition in mAb therapeutics.

In general, the mass spectrometry demonstrated distinct differences between the control glycoforms based on the size and absence of N-linked glycosylation. Furthermore, the mixtures were differentiated based on the size, type and percentages of the glycoform in the mixture used in preparing them. For instance, in the mixture containing the four control glycoforms (i.e., HM-Fc, Man5-Fc, GlcNAc-Fc, and N297Q-Fc), the mass spectrometry demonstrated distinct differences as well as the percentage composition of each glycoform as shown in Table 2 and Figure 3. This data illustrates the importance of mass spectrometry in characterizing complex mixtures, a tool highly needed in biosimilarity assessments.

We also performed further characterization using SDS-PAGE, size exclusion chromatography (SEC), and capillary isoelectric focusing (cIEF). These characterizations were carried out to evaluate the presence of dimers, fragments, and charge variants of the control and mixture of glycoforms of IgG1 Fc. The SDS-PAGE under reducing condition confirmed an absence of any proteolytic and fragment of the control and mixture of glycoforms, consistent with mass spectrometry data. In addition, the non-reducing SDS-PAGE confirmed intact Fc homodimer (i.e., an intramolecular disulfide bond) in all the samples tested. Furthermore, the percentages of mixture compositions were examined using densitometry, and the results agreed with the percentages estimated using mass spectrometry as shown in Table 3. The SEC data (Table 6) confirmed the absence of low molecular species and showed low levels of dimers across all the samples (1-3%). Further characterization with ciEF (Table 6) indicated no charge heterogeneity with the major peak being the same across all the control and mixtures of glycoforms. In mAbs,

differences in the relative proportions of charge variants are usually observed during production or process changes and present a challenging task in demonstrating product comparability. Chemical modifications that result in charge variants include deamidation, isomerization, fragmentation, and oxidation. Thus, these charge variants ultimately lead to modification of their isoelectric pH (p*I*) values.[52]

In the biosimilarity assessment, extensive characterizations are performed, which includes physical, chemical, and biological on the originator; then this characterization is used as a base characteristic to compare with their corresponding biosimilar molecule and thereby to establish molecular equivalence.[31] In our work, all these initial characterizations were conducted to establish baseline characteristics of the control and mixture of glycoforms prior to their functional and physical stability studies. Therefore, any differences observed between these different mixtures during functional and physical characterizations were attributed to the differences in their glycosylation profiles as well as their percentages of composition in the mixture.

In this study, binding measurements were first conducted on the control glycoforms (i.e., HM-Fc, Man5-Fc, GlcNAc-Fc, and N297Q-Fc) to characterize binding differences and to identify critical quality attributes that could help differentiate mixtures. Furthermore, mixtures of IgG1 Fc glycoforms were then analyzed for binding to two receptors: the activating receptor (FcγRIIIa) and the inhibitory receptor (FcγRIIb), using biolayer interferometry (BLI). We selected FcγRIIIa because of its functional relevance, and it is known to bind to the Fc portion of mAbs. Furthermore, FcγRIIIa is the only activating receptor expressed in natural killer cells and linked to antibody-dependent cellular cytotoxicity (ADCC).[53-54] Previously, we demonstrated this receptor

could differentially bind to Man5-Fc, HM-Fc, and GlcNAc-Fc and showed no detectable binding affinity to N297Q-Fc.[4] Also, we employed FcγRIIb because of its functional relevance to the mechanism of action of mAbs therapeutics it being the only inhibitory receptor expressed in B-cells.[47] In addition to having opposite effects on antibody-dependent effector functions, FcγRIIIa and FcγRIIb have different binding specificity for IgG1 Fc glycoforms, allowing the receptors to be utilized to differentiate particular glycoforms. To further characterize the IgG1 Fc glycoform mixtures and to investigate the effect of binding assay format on biological characterization, the two BLI binding formats were utilized for FcγRIIIa binding assays.

The two binding assay formats produced remarkably different results for the mixtures of glycoforms. Our result demonstrated that the advantage of using the Fc-immobilized format is its ability to detect the presence of a low-affinity glycoform mixed with a high-affinity glycoform in binding to FcγRIIIa (i.e., a mixture of HM-Fc and GlcNAc-Fc). In mAb therapeutics, a mix of high and low-affinity glycoforms could be the non-fucosylated and fucosylated glycoforms, respectively, which are known to bind differentially to FcγRIIIa.[55] Since protein G is not sensitive to changes in Fc glycosylation, both HM-Fc and GlcNAc-Fc can be immobilized equally, and their interaction with the FcγRIIIa is evident in the biphasic nature of the dissociation phases. This type of dissociation phase is attributed to the fast dissociation of GlcNAc-Fc and slow dissociation of HM-Fc, ultimately resulting in a biphasic dissociation curve. In the Fc-immobilized method, the association phase is monophasic given the fact that both HM-Fc and GlcNAc-Fc have similar kinetics of association (k_{on}). The dissociation phase shows a biphasic behavior, suggesting the two-components (HM-Fc and GlcNAc-Fc) have a different dissociation rate. Although 5% dissociation could be enough to describe the dissociation phase as explained elsewhere,[56] it is

necessary to follow a longer dissociation phase to fully define the biphasic or monophasic behavior of the curve, specifically for samples containing mixtures of glycoforms with differential binding to FcγRIIIa.

In the mixtures of HM-Fc and GlcNAc-Fc glycoforms, competitive displacement was observed in the receptor immobilized format. This competitive displacement of GlcNAc-Fc by HM-Fc exists because the two binding events were dependent on each other. Also, GlcNAc-Fc has a low binding affinity to FcγRIIIa compared to HM-Fc, and this leads to the enrichment of HM-Fc during the association phase (incubation time). Thus, the dissociation phase behaves more like HM-Fc than the dissociation behavior of the mixture of components. Therefore, during competitive displacement, slow dissociating component (HM-Fc) displaced fast dissociating (GlcNAc-Fc). Hence, the dissociation phase was strongly influenced by the incubation time. Data collected over different incubation times can be utilized to understand the behavior of components present in the sample. In general, as the contact time increases, there is less and less information about the dissociation phases to describe the nature of the composition.

The ratio of the k_{off} values of GlcNAc-Fc to HM-Fc was estimated to be about 27.2. This data indicated the differences in k_{off} values were significant and controlled the binding interaction to the receptor. For instance, the half-life of GlcNAc-Fc complex with the receptor was 5 sec, which indicated the residence time on the biosensor surface was short. Similarly, the half-life of HM-Fc was 100 sec, which was significantly higher residence time than GlcNAc-Fc. These differences in half-life explained the displacement of GlcNAc-Fc by HM-Fc in the association phase, which was observed when the receptor-immobilized format was used. Consequently, this displacement resulted in the enrichment of HM-Fc at the end of the association phase in

agreement with their half-life. Therefore, the dissociation phase behaves more like HM-Fc. The competitive binding model at equilibrium can explain the displacement of GlcNAc-Fc by HM-Fc observed in the receptor immobilized format. For instance, with the Mix2 the complex formed between HM-Fc and the immobilized receptor was 40-fold higher than the complex formed between the GlcNAc-Fc and the receptor. Since both HM-Fc and GlcNAc-Fc are at the same concentration, the ratio of the complex formed at equilibrium is simply the ratio of their equilibrium dissociation constant (K_D). Although no displacement of GlcNAc-Fc by HM-Fc was anticipated in the Fc-immobilized format, the fast dissociation phase was attributed to the short half-life of GlcNAc-Fc whereas the slower dissociation phase was attributed to the longer half-life of HM-Fc.

The association and dissociation phases of HM-Fc and Man5-Fc were very similar, and the ratio of k_{off} value of Man5-Fc to HM-Fc was estimated to be about 1.23. In addition, the half-life of HM-Fc and Man5-Fc were 100 sec and 87 sec, respectively. The similarity in k_{on}, k_{off}, and half-life of HM-Fc and Man5-Fc indicated their binding to the immobilized receptor was competitive. Therefore, no displacement was anticipated in the mixture of HM-Fc and Man5-Fc, unlike the mixtures of GlcNAc and HM-Fc. Furthermore, the ratio of the K_D values of HM-Fc and Man5-Fc is estimated to be about 1.13, which indicated their similar binding affinities to the immobilized receptor.

The receptor-immobilized technique is a widely-used method to characterize protein interaction quantitatively. Our data indicates that this approach is less sensitive when mixtures of glycoforms with different affinities are present in the sample. This data suggests that different binding protocols can result in different K_D values, which will eventually lead to a wide range of

reported values in the literature. Moreover, this variability in K_D value can potentially create difficulty in correlating with *in-vitro* cell-based assays. This binding displacement was not observed in the Fc-immobilized format because the two immobilized mixture components bind independently to FcγRIIIa and no competition was observed. As a result, the dissociation phase represents both elements of the mixtures.

In the mixture of HM-Fc and N297Q-Fc, the Fc-immobilized method was not able to detect the presence of inactive protein (i.e., N297Q-Fc). Moreover, no change in K_D value was obtained regardless of the percentage of composition of these two glycoforms (50%HM vs. 90%HM). This event is observed because in the Fc immobilized format the concentration of IgG1 Fc is not relevant for the determination of K_D value. In other words, the concentration of the FcγRIIIa in solution is used in determining the K_D value, not the immobilized Fc (HM-Fc and N297Q-Fc). Additionally, N297Q-Fc was not contributing to the association and dissociation phases, and the binding interaction was purely controlled by the immobilized HM-Fc present in the mixture (Mix3 or Mix6) and FcγRIIIa. Thus, this binding interaction behaves similarly to the interaction of 100%HM-Fc (control) and FcγRIIIa, generating the same K_D value, except the response was higher in the latter as discussed below. In practice, the inactive protein could be non-native aggregates, fragmented, and chemically degraded protein, with the capacity to be immobilized into protein G. However, it would be unable to bind with FcγRIIIa. Also, the inactive protein could be the presence of non-glycosylated IgG, typically observed in the yeast expression system.[21, 57] One way to overcome this issue is to monitor the binding response by comparing it head-to-head with a well-characterized reference product, and a decrease in response will indicate a change in the quality of the sample under examination.

We performed the binding response measurement of the controls and mixtures of glycoforms. Therefore, the binding response measurements in this experiment were able to differentiate the controls as well as the mixtures of glycoforms with subtle and major changes in composition (Figure 7). For instance, in the mixture containing 90%HM and 10%N297Q, the response measurement showed 10% decrease compared to 100% HM-Fc, indicating the amount of inactive protein present (i.e., N297Q-Fc) was a 10% in the mixture. Similarly, with the mixture containing a 50%N297Q, the response decreased nearly two-fold, which is proportional to the amount of inactive protein present in the mixture. These results demonstrated that in addition to measuring the K_D value, monitoring the binding response as a measure of critical quality attributes of the sample under test is necessary.

Unlike the Fc-immobilized, the receptor-immobilized format could detect and differentiate mixtures of N297Q-Fc and HM-Fc. This is because the concentrations of the mixtures in the solution containing both glycoforms were used in determining the K_D values (i.e., receptor was immobilized). Furthermore, the change in the K_D value was proportional to the amount of N297Q-Fc present in the mixture. For example, in the Mix6 mixture, a subtle decrease in binding affinity was observed. However, with the Mix3 mixture, a two-fold decrease in binding affinity was observed, which was proportional to the amount of N297Q-Fc present in the mixture.

We noticed remarkable differences between the two immobilization formats in differentiating the mixtures. Using well-defined mixtures, we uncovered the importance of sample composition and selection of immobilization platforms in achieving accurate and reliable binding affinity results. Furthermore, understanding the binding event is important as mAbs therapeutics are heterogeneous with respect to their glycosylation on N297.[25] It is also well

known that glycosylation could shift upon a change in a cell line, manufacturing sites, and scale up; hence, a sensitive method is required to monitor batch- to-batch variation. Thus, this study contributes to developing the analytical aspects of biosimilar comparability analysis.[25]

Analysis of a complex mixture of glycoforms is not a trivial assessment, specifically if there is no prior knowledge of the composition of the sample to be examined. Knowledge of the glycoform composition of the sample using mass spectrometry can be helpful to achieve unambiguous data. Hence, a combination of in-depth glycan characterization, coupled with knowledge of the individual glycan contribution to binding, can be useful to analyze the data more accurately. In this work, we illustrated the complexity of the methods and analysis of the data for mixtures with different affinities. The data highlights the extra care required to get a reliable biological activity with samples containing mixtures of glycoforms. Additionally, this work demonstrates the need to monitor the response of a sample in comparison to a well-characterized control when measuring the quality of the protein. In addition, our data highlights the importance of analytical techniques in biosimilar comparability analysis, and both functional assay formats could differentiate the mixture of glycoforms with different sensitivity depending on the immobilization format selected and type of mixture composition. The methods and concepts developed in this work can be applied during a biosimilar comparability assessment. Today similar challenges exist in comparing products after processes change or in the development of a biosimilar candidate.[25]

In summary, the four control glycoforms and seven mixtures were evaluated with their functional activities using to the two assay platforms. To examine how a functional activity test can be used in assessing similarity in biosimilar comparability exercises, we compared the two

assay platforms. These assay platforms were tested with a series of homogeneous and well-defined IgG1 Fc glycoforms (controls). Next, the two-assay platform was tested in a mixture of IgG1 Fc glycoforms with subtle and major differences in functional and physical properties. Future work should address to correlate *in-vivo* activity assay with the *in-vitro* binding assay. These functional characterization techniques generated large amount and different type of data. Thus, raw characterization data will be utilized to develop a mathematical model for determining the level of similarity in biosimilar comparability analysis.

3.5 Figures

Figure 1. HM-Fc and N297Q-Fc were recombinantly expressed in glycoengineered *P.pastoris*. Man5-Fc and GlcNAc-Fc were produced using *in-vitro* enzymatic reaction. The four glycoforms HM-Fc, Man5-Fc, GlcNAc-Fc, and N297Q-Fc were used as a control and to prepare the mixtures. Fifty percent mixtures were prepared to monitor for obvious differences. Mixtures containing 90% HM with 10% of the other glycoforms were prepared to study for a subtle difference. The 25% mixture of the four glycoforms represents a more

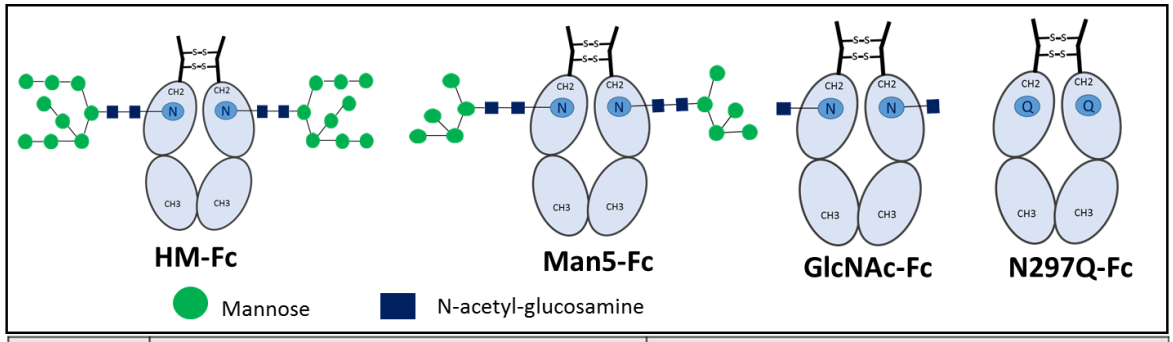

Glycoform	Controls				Mixture						
	100%HM	100%Man5	100%GlcNAc	100%N297Q	Mix1	Mix2	Mix3	Mix4	Mix5	Mix6	Mix7
HM-Fc	100				50	50	50	90	90	90	25
Man5-Fc		100			50			10			25
GlcNAc-Fc			100			50			10		25
N297Q-Fc				100			50			10	25
Mixture type	Obvious differences							Subtle differences			

Figure 2. SDS-PAGE characterizations of control and mixture glycoforms under reduced (A) and non-reduced (B) conditions. The SDS-PAGE bands represent: (1) 90%HM:10%Man5; 2) 50%HM:50%Man5; 3) 25%HM:25Man5:25GlcNAc:25%N297Q; 4) 90%HM:10%N297Q; 5) 50%HM:50%N297Q; 6) 90%HM:10%GlcNAc; 7) 50%HM:50%GlcNAc. The bands 8, 9, 10, and 11 represent N297Q-Fc, GlcNAc-Fc, Man5-Fc, and HM-Fc control glycoforms, respectively.

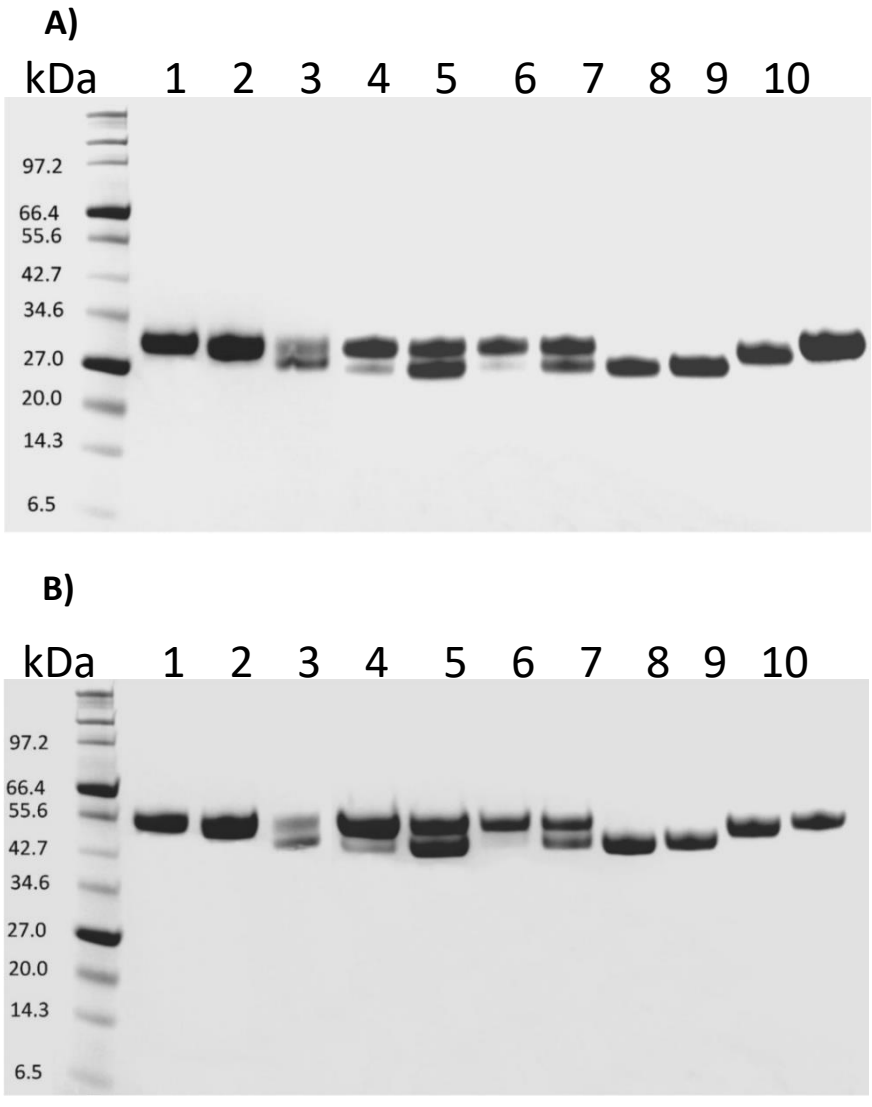

Figure 3: Intact protein ESI-MS analysis of IgG1 Fc control and mixture of glycoforms under reducing conditions. About ten µg of each glycoform was loaded into the LC-MS, and the data was acquired on an Agilent 6250 quadrupole time-of-flight system. No fragment or degradation was observed. The percentage of composition was calculated from the peak intensities.

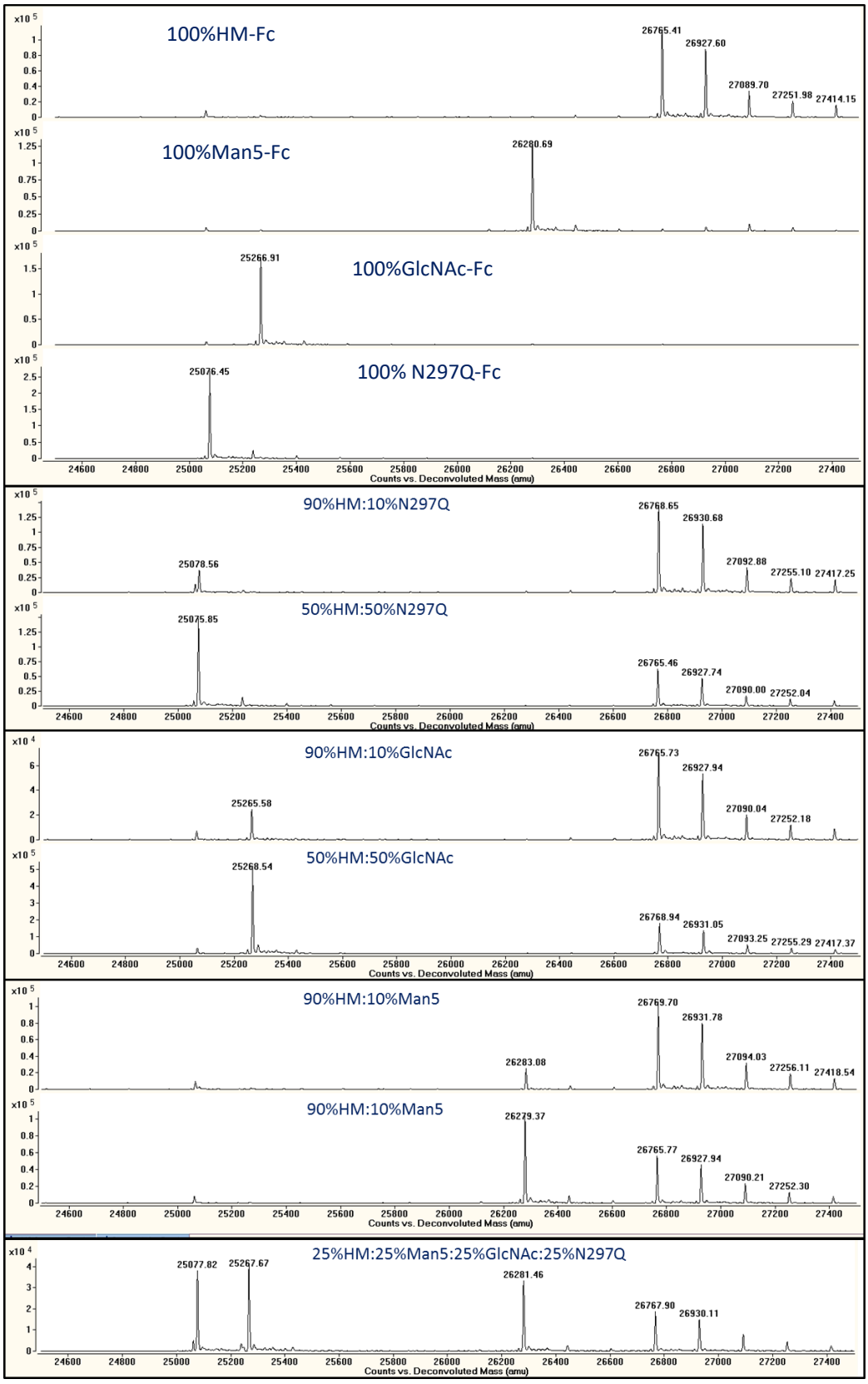
100%HM-Fc
26765.41
26927.60
27089.70
27251.98
27414.15
100%Man5-Fc
26280.69
100%GlcNAc-Fc
25266.91
100% N297Q-Fc
25076.45
Counts vs. Deconvoluted Mass (amu)
90%HM:10%N297Q
26768.65
26930.68
27092.88
27255.10
27417.25
25078.56
50%HM:50%N297Q
25075.85
26765.46
26927.74
27090.00
27252.04
Counts vs. Deconvoluted Mass (amu)
90%HM:10%GlcNAc
26765.73
26927.94
27090.04
27252.18
25265.58
50%HM:50%GlcNAc
25268.54
26768.94
26931.05
27093.25
27255.29
27417.37
Counts vs. Deconvoluted Mass (amu)
90%HM:10%Man5
26769.70
26931.78
27094.03
27256.11
27418.54
26283.08
90%HM:10%Man5
26279.37
26765.77
26927.94
27090.21
27252.30
Counts vs. Deconvoluted Mass (amu)
25%HM:25%Man5:25%GlcNAc:25%N297Q
25077.82
25267.67
26281.46
26767.90
26930.11
Counts vs. Deconvoluted Mass (amu)

Figure 3

Figure 4. Bar graphs show k_{on}, k_{off}, and K_D for the control and mixture of IgG1 Fc glycoforms. The top panel is data for the receptor-immobilized format (FcγRIIIa immobilized), and the middle panel is for the Fc-immobilized format (FcγRIIIa in solution). The bottom panel represents data for binding of FcγRIIb with IgG1 Fc glycoforms using protein G immobilization method. A significant difference in the equilibrium dissociation constants was observed between the mixtures, depending on their percentage of composition. Additionally, a substantial difference was found between the two immobilization techniques, indicating that the two binding formats differ in their capacity to distinguish the mixtures. For the interaction of the controls and mixtures of IgG1 Fc glycoforms with FcγRIIb, no significant difference in biological activity was obtained. For N297Q-Fc and GlcNAc-Fc, no binding was observed at the highest concentration tested (10 μM). N.B: no binding.

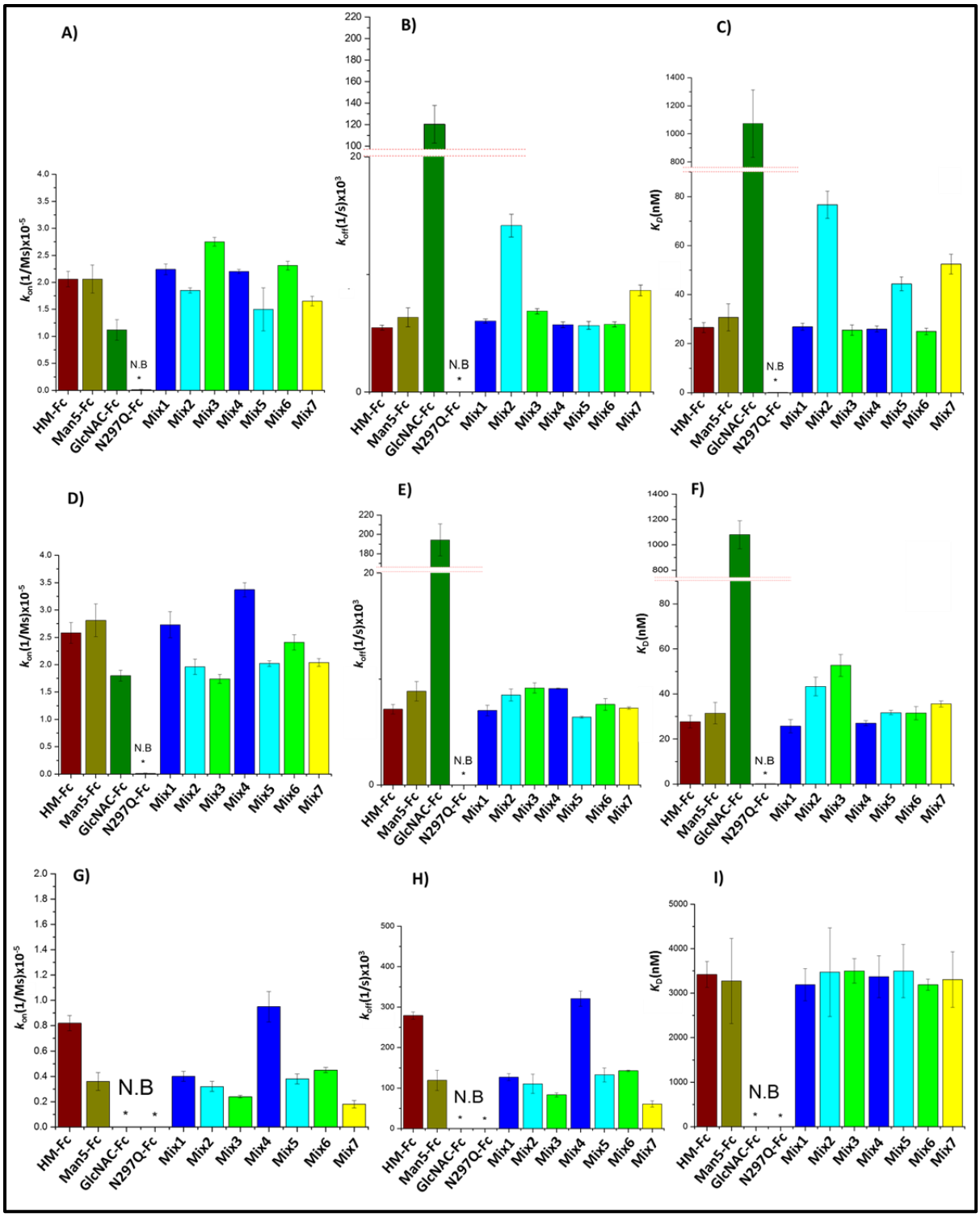
A)
B)
C)
D)
E)
F)
G)
H)
I)
k_{on}(1/Ms)x10^{-5}
k_{off}(1/s)x10^{3}
K_D(nM)
N.B
HM-Fc
Man5-Fc
GlcNAC-Fc
N297Q-Fc
Mix1
Mix2
Mix3
Mix4
Mix5
Mix6
Mix7

Figure 4

Figure 5. The diagram shows the binding events on the surface of the streptavidin (top) and protein G (bottom) for 50%HM:50%GlcNAc binding with FcγRIIIa. The receptor was immobilized onto streptavidin biosensors and 50%HM:50%GlcNAc mixture was in solution. During the early phase of the association phase, both GlcNAc-Fc and HM-Fc binds onto FcγRIIIa. However, as incubation time increases, HM-Fc displaces GlcNAc-Fc. Therefore, slowly dissociating HM-Fc is shown in the dissociation phase. For the Fc-immobilized format, the two binding events are independent of each other, and no displacement is expected during the association phase. Therefore, the dissociation phase reflects the contribution of GlcNAc and HM-Fc.

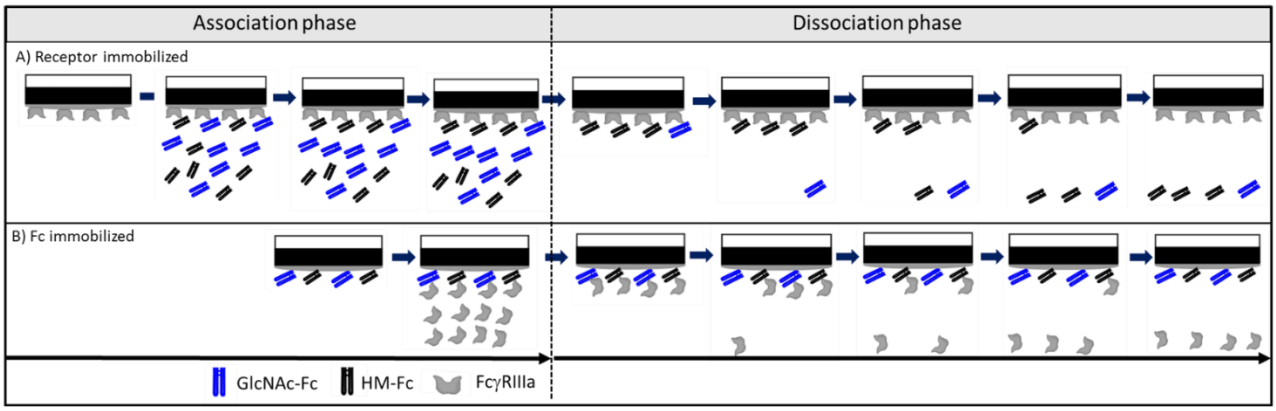

Figure 6. Dissociation curves (A) measured at different incubation times for 50%HM:50%GlcNAc. HM-Fc control (100%HM-Fc) showed the slowest dissociation phase, while GlcNAc-Fc control (100% GlcNAc-Fc) showed the fastest dissociation phases. As incubation time increases, the rate of dissociation gets slower. The k_{off} for each curve is represented in the bar graph (B). Comparison between receptor-immobilized and Fc-immobilized formats is represented in Figure C and D, respectively.

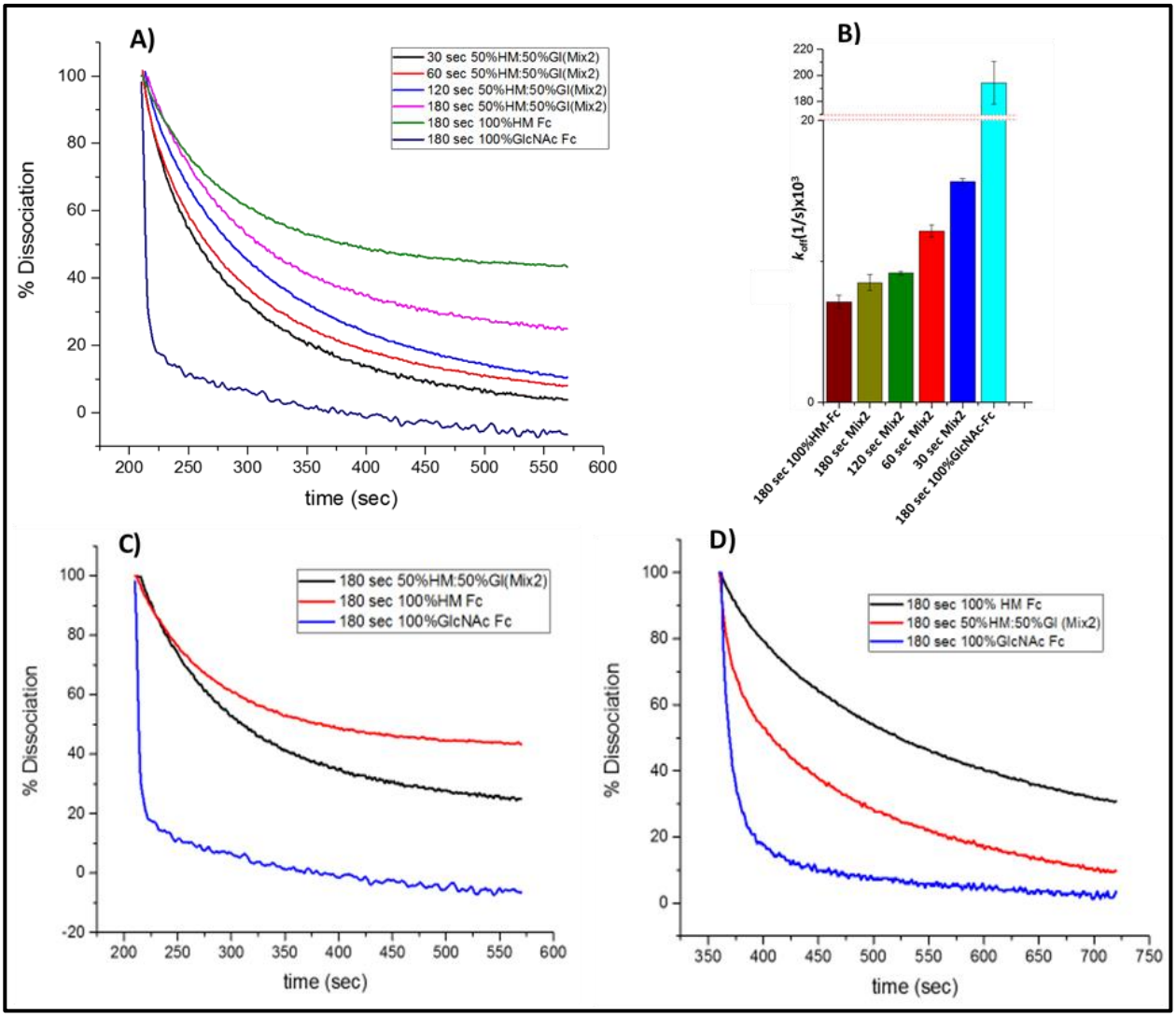
A)
30 sec 50%HM:50%Gl(Mix2)
60 sec 50%HM:50%Gl(Mix2)
120 sec 50%HM:50%Gl(Mix2)
180 sec 50%HM:50%Gl(Mix2)
180 sec 100%HM Fc
180 sec 100%GlcNAc Fc
% Dissociation
time (sec)
B)
$k_{off}(1/s)x10^3$
180 sec 100%HM-Fc
180 sec Mix2
120 sec Mix2
60 sec Mix2
30 sec Mix2
180 sec 100%GlcNAc-Fc
C)
180 sec 50%HM:50%Gl(Mix2)
180 sec 100%HM Fc
180 sec 100%GlcNAc Fc
% Dissociation
time (sec)
D)
180 sec 100% HM Fc
180 sec 50%HM:50%Gl (Mix2)
180 sec 100%GlcNAc Fc
% Dissociation
time (sec)

Figure 6

Figure 7. Representative BLI binding curves for the interaction of FcγRIIIa with control and mixture of IgG1 Fc glycoforms using the Fc immobilization technique. The binding curve shown is for FcγRIIIa in solution at a concentration of 800 nM.

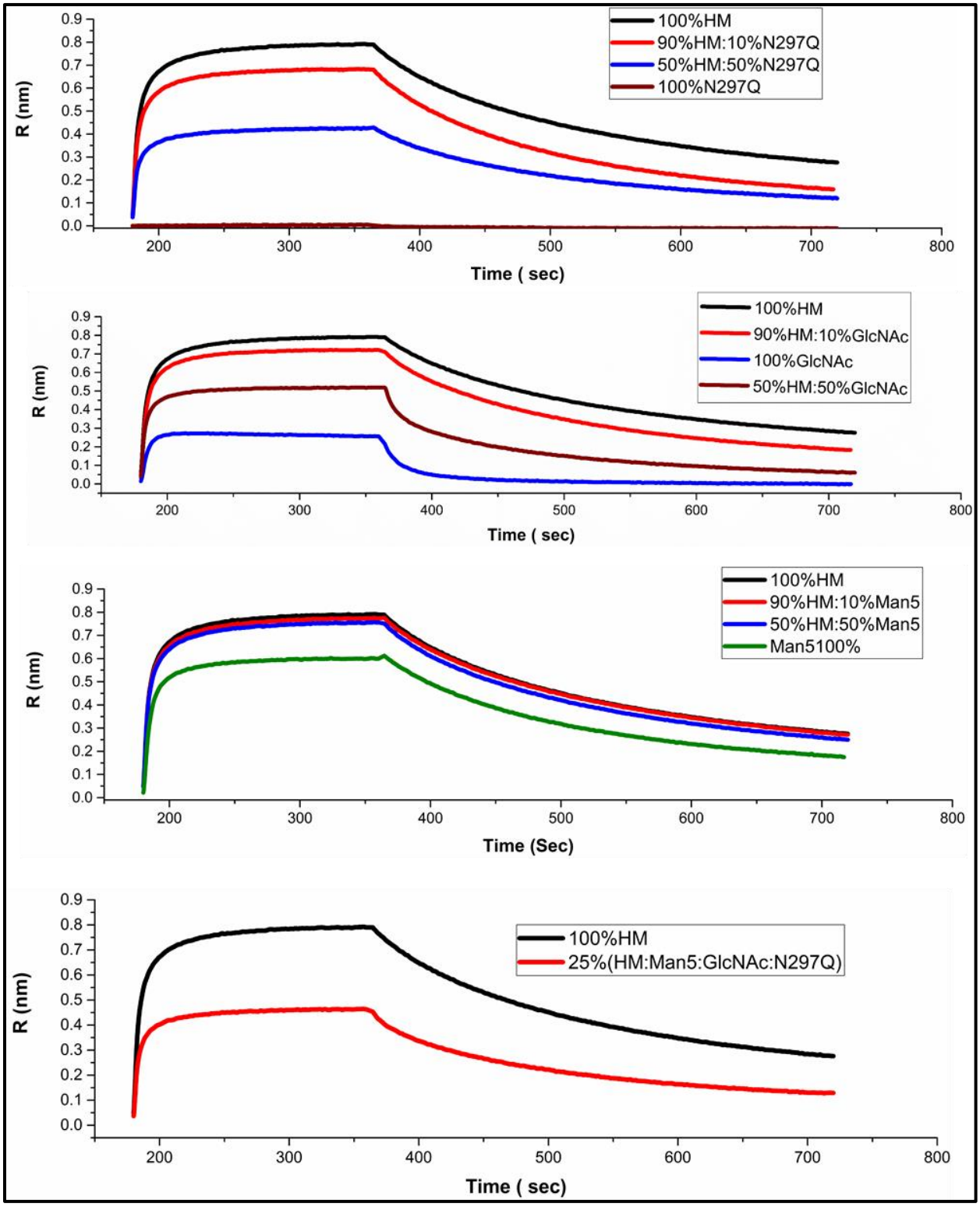
100%HM
90%HM:10%N297Q
50%HM:50%N297Q
100%N297Q
R (nm)
Time (sec)
100%HM
90%HM:10%GlcNAc
100%GlcNAc
50%HM:50%GlcNAc
R (nm)
Time (sec)
100%HM
90%HM:10%Man5
50%HM:50%Man5
Man5100%
R (nm)
Time (Sec)
100%HM
25%(HM:Man5:GlcNAc:N297Q)
R (nm)
Time (sec)

Figure 7

Figure 8. Bar graphs showing a binding response to the interaction of FcγRIIIa (A) and FcγRIIb (B) with control and mixture of IgG1 Fc glycoforms measured using Fc immobilization technique. A difference in response was observed, depending on the percentage of the composition and nature of the components.

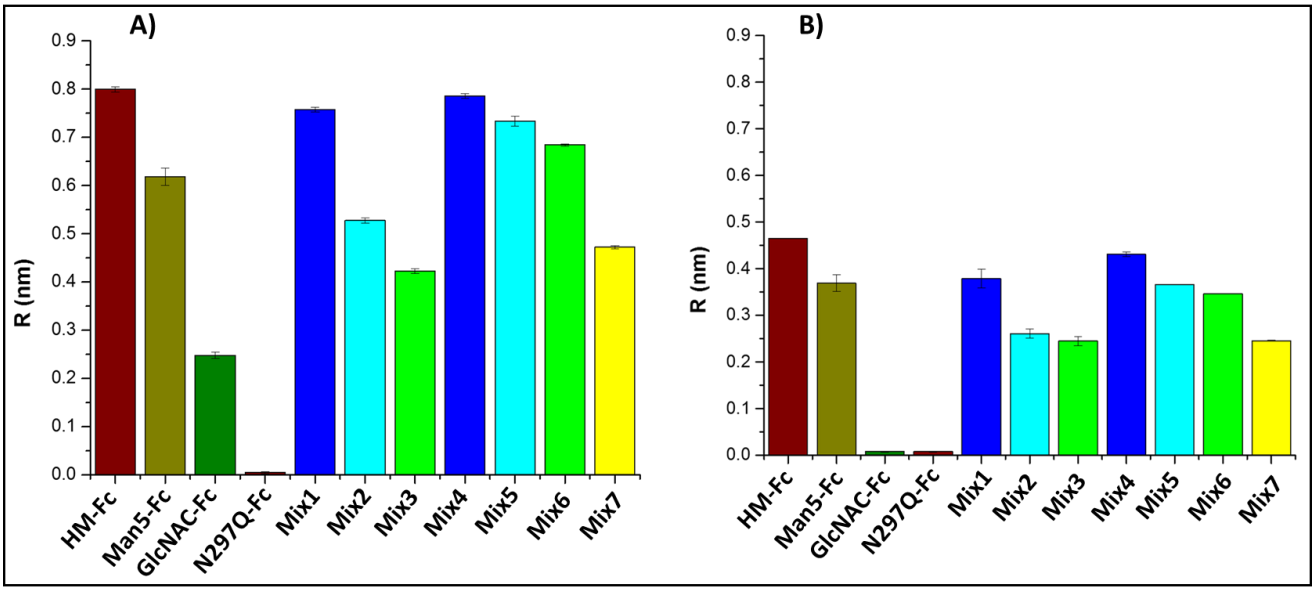

Figure 9. Representative BLI binding curves for the interaction of FcγRIIIa with a mixture of IgG1 Fc glycoforms using the Fc immobilization technique (Figure 1A) and the receptor immobilization technique (Figure 1B). Data shown is for the protein in solution (FcγRIIIa or Fc) at concentrations of 800 nM, 400 nM, 200 nM, 100 nM, and 50 nM, which corresponds with the curves from top to bottom. For Figure 1C**,** the data shown is for the protein in solution (FcγRIIb) at concentrations of 10000 nM, 5000 nM, 2500 nM, 1250 nM, and 625 nM, which corresponds with the curves from top to bottom. For GlcNAc and N297Q-Fc, no binding was observed at the highest concentration tested (10 μM).

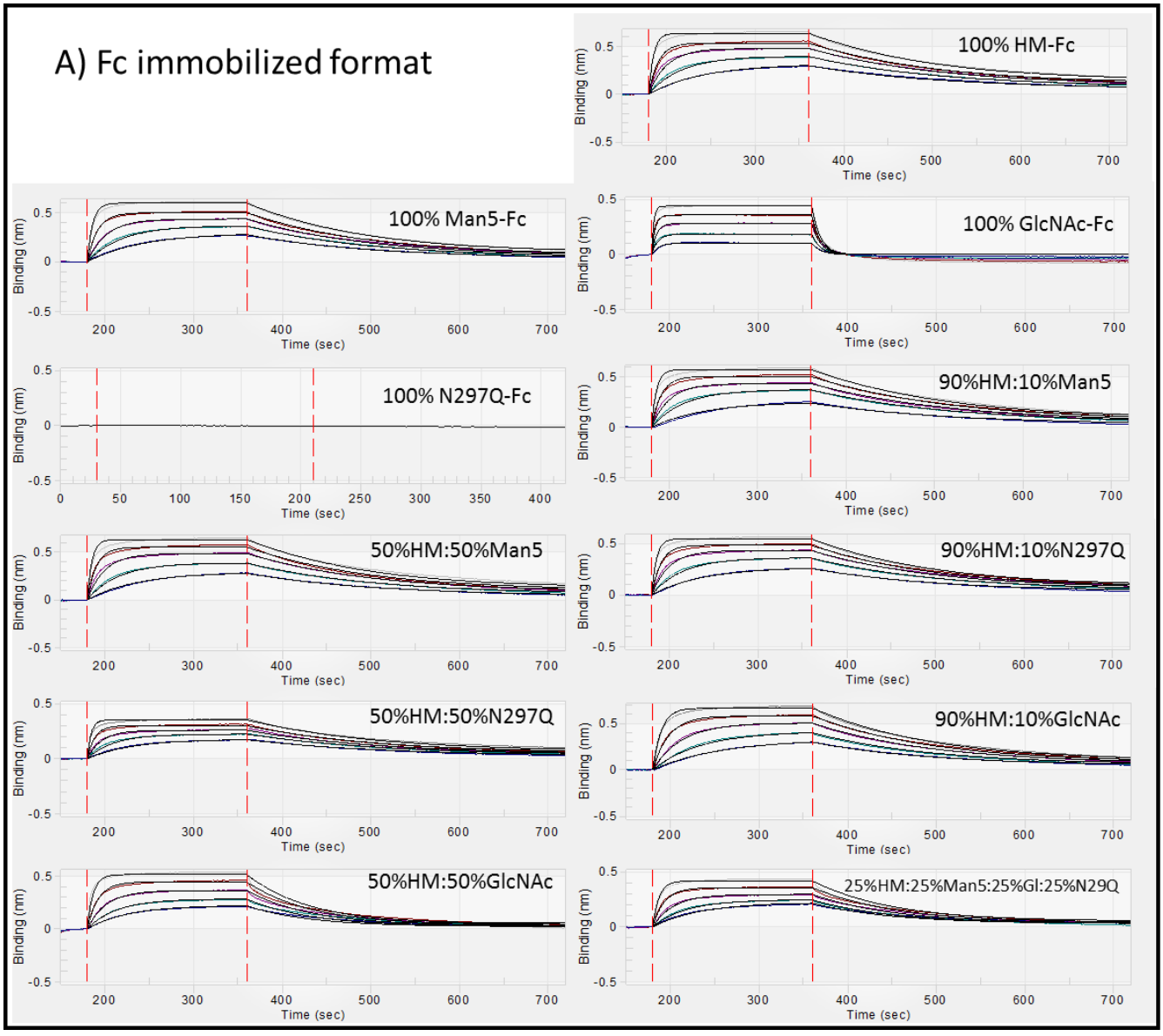
A) Fc immobilized format
100% HM-Fc
100% Man5-Fc
100% GlcNAc-Fc
100% N297Q-Fc
90%HM:10%Man5
50%HM:50%Man5
90%HM:10%N297Q
50%HM:50%N297Q
90%HM:10%GlcNAc
50%HM:50%GlcNAc
25%HM:25%Man5:25%Gl:25%N29Q
Binding (nm)
Time (sec)

Figure 9A

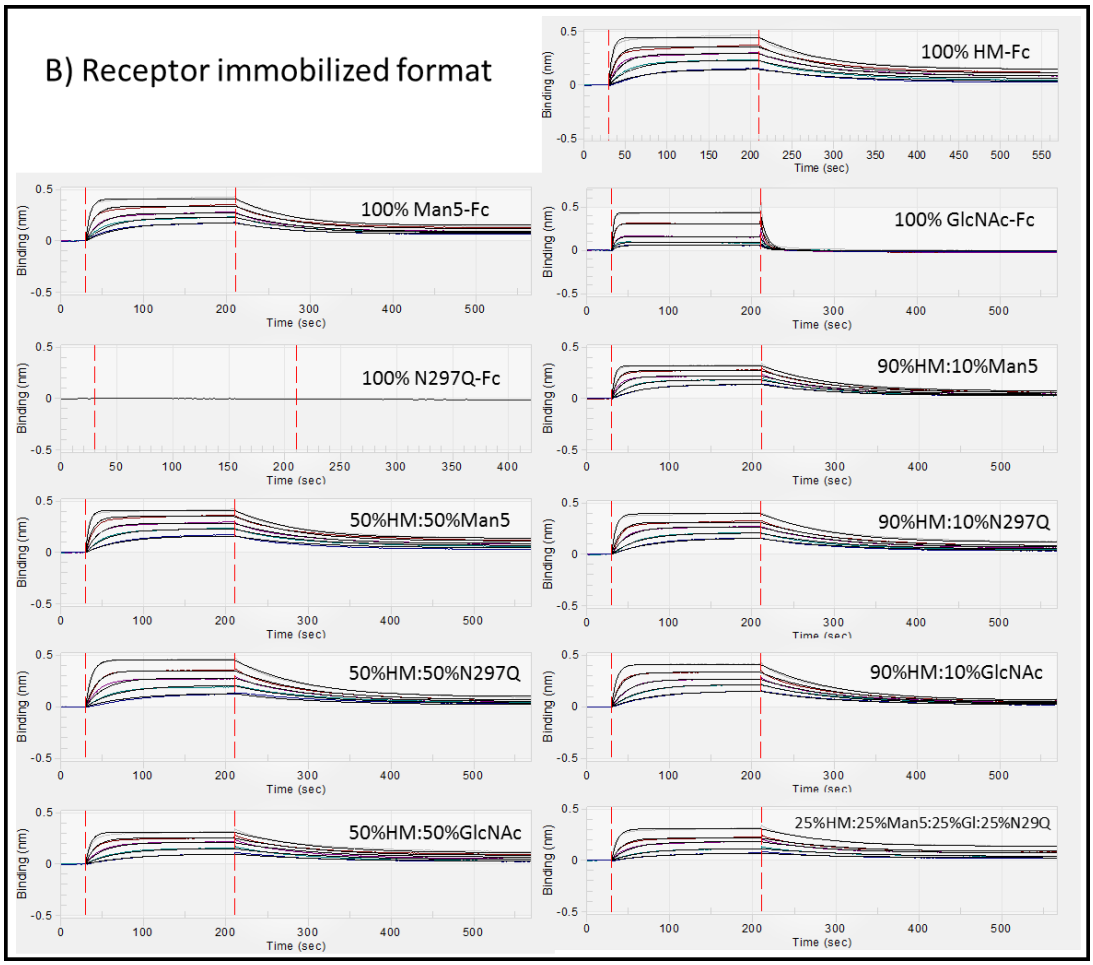
B) Receptor immobilized format
100% HM-Fc
100% Man5-Fc
100% GlcNAc-Fc
100% N297Q-Fc
90%HM:10%Man5
50%HM:50%Man5
90%HM:10%N297Q
50%HM:50%N297Q
90%HM:10%GlcNAc
50%HM:50%GlcNAc
25%HM:25%Man5:25%Gl:25%N29Q
Binding (nm)
Time (sec)

Figure 9B

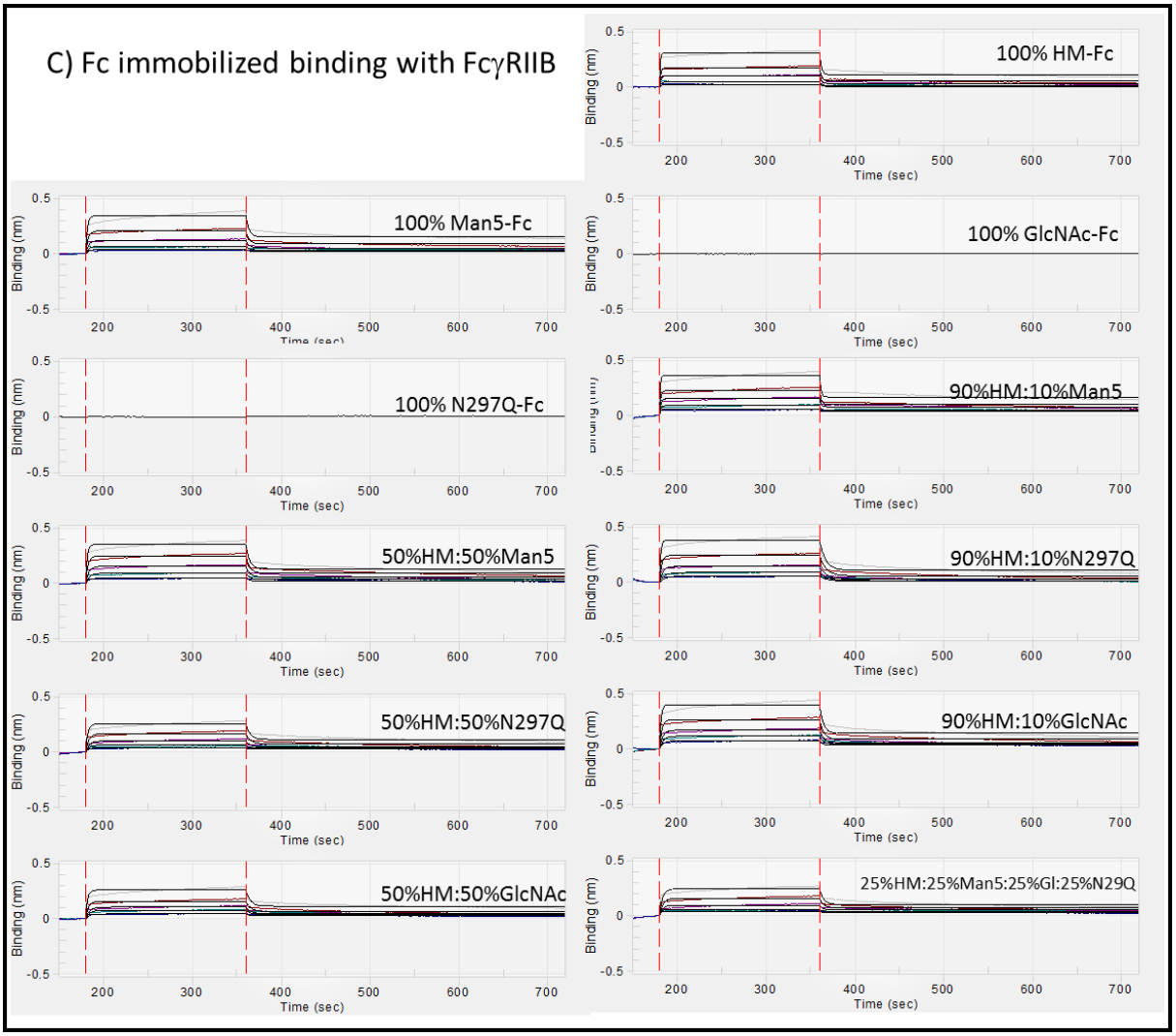
C) Fc immobilized binding with FcγRIIB
100% HM-Fc
100% Man5-Fc
100% GlcNAc-Fc
100% N297Q-Fc
90%HM:10%Man5
50%HM:50%Man5
90%HM:10%N297Q
50%HM:50%N297Q
90%HM:10%GlcNAc
50%HM:50%GlcNAc
25%HM:25%Man5:25%Gl:25%N29Q
Binding (nm)
Time (sec)

Figure 9C

3.6 Tables

Table 1. Kinetic parameters obtained for binding of FcγRIIIa with control and mixture of IgG1 Fc glycoforms using Fc and receptor immobilization techniques. Binding kinetics were performed at 25˚C. The data shows kinetic association rate (k_{on}), kinetic dissociation rate (k_{off}), and the equilibrium dissociation constant (K_D). The entries are averaged values of three independent experiments. For N297Q-Fc, there was no detectable binding at the highest concentration tested (10 µM) from both techniques. * Only active component concentration (HM-Fc) was used in calculating the K_D values.

Glycoforms	Method	k_{on} (1/Ms)x10^5	k_{off} (1/s)X10^{-3}	K_D (nM)
100% HM-Fc	PG	2.1±0.1	5.5±0.2	26.7±2.1
100% HM-Fc	SA	2.6±0.2	7.2 ±0.5	27.7±2.7
100% Man5-Fc	PG	2.1±0.3	6.3± 0.8	30.7±5.6
100% Man5-Fc	SA	2.8±0.3	8.9 ± 0.9	31.7±4.7
100% GlcNAc-Fc	PG	1.1±0.2	120.3±17.4	1073.6±240.2
100% GlcNAc-Fc	SA	1.8±0.1	194.2±16.5	1079.5±109.9
90%HM:10%Man5 (Mix4)	PG	2.2±0.0	5.7±0.3	25.9± 1.2
90%HM:10%Man5 (Mix4)	SA	3.4±0.1	9.1 ±0.2	27.0 ±1.1
50%HM:50%Man5 (Mix1)	PG	2.2±0.1	6.0±0.2	26.9 ±1.4
50%HM:50%Man5 (Mix1)	SA	2.7±0.2	7.0 ±0.5	25.7±2.9
90%HM:10%N297Q (Mix6)	PG	2.3 ±0.1	5.7±0.2	24.9 ±1.2
90%HM:10%N297Q (Mix6)	SA	2.4±0.1	7.6±0.6	31.5±2.9
50%HM:50%N297Q (Mix3)	PG	2.7±0.1	6.9± 0.2	24.9± 1.1
50%HM:50%N297Q (Mix3)	SA	1.7±0.1	9.2±0.5	52.7±3.7
90%HM:10%GlcNAc (Mix5)	PG	1.5±0.4	5.7±0.3	44.4 ±2.8
90%HM:10%GlcNAc (Mix5)	SA	2.0±0.1	6.4±0.1	31.7±1.0
50%HM:50%GlcNAc (Mix2)	PG	1.6±0.1	14.2±1.0	76.7±5.6
50%HM:50%GlcNAc (Mix2)	SA	2.0±0.1	8.50±0.56	43.3 ±4.1
25%HM:25%GlcNAc:25%Man5:25%N297Q (Mix7)	PG	1.7±0.1	8.6±0.5	52.5 ± 4.00
25%HM:25%GlcNAc:25%Man5:25%N297Q (Mix7)	SA	2.0±0.1	7.3±0.1	35.6±1.3
90%HM:10%N297Q* (Mix6)	SA	2.9±0.3	7.6±0.6	28.3±2.4
50%HM:50%N297Q* (Mix3)	SA	3.1 ± 0.4	9.1± 0.5	29.0 ± 4.2

Table 2. Estimated percentage of composition for each glycoform observed by intact protein mass spectrometry. The percentage of composition in the mixtures was calculated using all glycoform peaks in a given spectrum. The result shown was the averaged values of triplicate runs.

Glycoforms composition	Glycoform	Percentage of composition
90%HM:10%N29Q (Mix6)	HM	89.6 ± 0.1
	N297Q	10.4 ± 0.1
50%HM:50%N297Q (Mix3)	HM	48.2 ± 0.6
	N297Q	51.8 ± 0.6
90%HM:10%Man5 (Mix4)	HM	90.5 ± 0.3
	Man5	9.5 ± 0.3
50%HM:50%Man5 (Mix1)	HM	55.6 ± 0.4
	Man5	44.5 ± 0.4
90%HM:10%GlcNAc (Mix5)	HM	89.6 ± 0.4
	GlcNAc	10.4 ± 0.4
50%HM:50%GlcNAc (Mix2)	HM	54.7 ± 2.9
	GlcNAc	45.3 ± 2.9
25%HM:25%Man5:25%GlcNAc:25N297Q (Mix7)	HM	32.0 ± 2.1
	Man5	21.4 ± 0.8
	GlcNAc	25.8 ± 0.6
	N297Q	20.8 ± 2.0

Table 3. Estimated percentage of composition of the mixtures determined from SDS-PAGE band intensities.

Glycoforms composition	Glycoform	Band intensity	Percentage of composition
90%HM:10%N29Q (Mix6)	HM	127009	89.5
	N297Q	14852.9	10.5
50%HM:50%N297Q (Mix3)	HM	80274.7	48.4
	N297Q	85447.5	51.6
90%HM:10%GlcNAc (Mix3)	HM	66603.0	89.3
	GlcNAc	8003.2	10.7
50%HM:50%GlcNAc (Mix2)	HM	77413.6	54.7
	GlcNAc	64146.9	45.3

Table 4. Kinetic parameters obtained for binding of FcγRIIb with control and mixture of IgG1 Fc glycoforms using Fc immobilization method. Binding kinetics were performed at 25˚C. The data shows kinetic association rate (k_{on}), kinetic dissociation rate (k_{off}), and the equilibrium dissociation constant (K_D). These data entries are the average of three independent experiments. * For N297Q-Fc and GlcNAc-Fc, there was no detectable binding at the highest concentration tested (10 µM).

Glycoforms	Method	k_{on} (1/Ms)x10^5	k_{off} (1/s)x10^{-3}	K_D (nM)
100% HM-Fc	PG	0.8±0.1	279.2±9.0	3419.8±288.4
100% Man5-Fc	PG	0.4 ±0.1	119.0 ±25.1	3274.5±957.4
90%HM-Fc:10%Man5 (Mix4)	PG	0.9±0.1	321.0±19.0	3368.6±469.3
50%HM-Fc:50%Man5 (Mix1)	PG	0.4±0.0	127.0±8.9	3187.1±361.2
90%HM-Fc:10%N297Q (Mix6)	PG	0.4 ±0.0	142.9 ±2.0	3190.4±124.0
50%HM-Fc:50%N297Q (Mix3)	PG	0.2±0.0	83.3±4.9	3500.3±272.8
90%HM-Fc:10%GlcNAc (Mix5)	PG	0.4±0.0	132.6±17.1	3496.9±598.6
50%HM-Fc:50%GlcNAc (Mix2)	PG	0.3 ±0.0	110.6 ±23.9	3471.7 ±993.6
25%HM:25%GlcNAc:25%Man5:25%N297Q(Mix7)	PG	0.2±0.0	60.5±7.7	3307.5±624.1
N297Q-Fc and GlcNAc-Fc*	PG			

Table 5. Raw data for the response to FcγRIIIa and FcγRIIb interaction with control and mixture Fc glycoforms using Fc-immobilized format. The concentration of FγRIIIa and FγRIIb in solution was 800 nM and 10,000 nM, respectively. The data was the averaged values of triplicates runs. The response measurement was able to differentiate all of the samples tested.

Glycoforms	Response for FcγRIIIa	Response for FcγRIIb
100%HM	0.799 ± 0.005	0.465± 0.001
90%HM:10%N297Q	0.684 ± 0.003	0.346 ± 0.000
50%HM:50%N297Q	0.422 ± 0.005	0.245 ± 0.007
100%N297Q	0.005 ± 0.001	0.001 ± 0.001
90%HM:10%Man5	0.786 ± 0.005	0.431 ± 0.005
50%HM:50%Man5	0.758 ± 0.005	0.379 ± 0.020
100%Man5	0.618 ± 0.018	0.369 ± 0.018
90%HM:10%GlcNAc	0.734 ± 0.010	0.366 ± 0.000
50%HM:50%GlcNAc	0.527 ± 0.005	0.2615 ± 0.009
100%GlcNAc	0.248 ±0.006	0.001 ± 0.001
25%(HM:Man5:GlcNAc:N297Q)	0.472 ±0.003	0.246 ± 0.001

Table 6. Average monomer percent and pI values measured using size exclusion chromatography (SEC) and capillary isoelectric focusing (cIEF), respectively.

Mixture	Average Monomer Percent	Average pI
HM-Fc control	99.7±0.0	7.2±0.0
Man5-Fc Control	99.7±0.1	7.2±0.0
GlcNAcFc-Control	99.8±0.1	7.2±0.0
N297Q-Fc Control	97.8±0.0	7.2±0.0
Mix 1	99.7±0.0	7.2±0.0
Mix 2	99.6±0.1	7.2±0.0
Mix 3	98.9±0.1	7.2±0.0
Mix 4	99.6±0.1	7.2±0.0
Mix 5	99.6±0.0	7.2±0.0
Mix 6	99.4±0.1	7.2±0.0
Mix 7	99.3±0.0	7.2±0.0

3.7 References

1. Higel, F.; Seidl, A.; Sörgel, F.; Friess, W., N-glycosylation heterogeneity and the influence on structure, function and pharmacokinetics of monoclonal antibodies and Fc fusion proteins. *European Journal of Pharmaceutics and Biopharmaceutics* **2016,** *100*, 94-100.

2. Berkowitz, S. A.; Engen, J. R.; Mazzeo, J. R.; Jones, G. B., Analytical tools for characterizing biopharmaceuticals and the implications for biosimilars. *Nat Rev Drug Discov* **2012,** *11* (7), 527-540.

3. Falconer, R. J.; Jackson-Matthews, D.; Mahler, S. M., Analytical strategies for assessing comparability of biosimilars. *Journal of Chemical Technology & Biotechnology* **2011,** *86* (7), 915-922.

4. Okbazghi, S. Z.; More, A. S.; White, D. R.; Duan, S.; Shah, I. S.; Joshi, S. B.; Middaugh, C. R.; Volkin, D. B.; Tolbert, T. J., Production, Characterization, and Biological Evaluation of Well-Defined IgG1 Fc Glycoforms as a Model System for Biosimilarity Analysis. *Journal of Pharmaceutical Sciences* **2016,** *105* (2), 559-574.

5. Ecker, D. M.; Jones, S. D.; Levine, H. L., The therapeutic monoclonal antibody market. *mAbs* **2015,** *7* (1), 9-14.

6. Nimmerjahn, F.; Ravetch, J. V., The antiinflammatory activity of IgG: the intravenous IgG paradox. *The Journal of Experimental Medicine* **2007,** *204* (1), 11-15.

7. Scott, A. M.; Wolchok, J. D.; Old, L. J., Antibody therapy of cancer. *Nat Rev Cancer* **2012,** *12* (4), 278-287.

8. Bossaller, L.; Rothe, A., Monoclonal antibody treatments for rheumatoid arthritis. *Expert Opinion on Biological Therapy* **2013,** *13* (9), 1257-1272.

9. John G. Allen, M. M., Michael J. Frohn, Alex J. Pickrell, Paul Kodama, Facile Modulation of Antibody Fucosylation with Small Molecule Fucostatin Inhibitors and Cocrystal Structure with GDP-Mannose 4,6-Dehydratas. *ACS Chem. Biol.* **2016**.

10. Vidarsson, G.; Dekkers, G.; Rispens, T., IgG Subclasses and Allotypes: From Structure to Effector Functions. *Frontiers in Immunology* **2014,** *5*, 520.

11. Wang, W.; Singh, S.; Zeng, D. L.; King, K.; Nema, S., Antibody structure, instability, and formulation. *Journal of Pharmaceutical Sciences* **2007,** *96* (1), 1-26.

12. Jefferis, R., Glycosylation as a strategy to improve antibody-based therapeutics.

13. Liu, L., Antibody Glycosylation and Its Impact on the Pharmacokinetics and Pharmacodynamics of Monoclonal Antibodies and Fc-Fusion Proteins. *Journal of Pharmaceutical Sciences* **2015**, n/a-n/a.

14. Mimura, Y.; Sondermann, P.; Ghirlando, R.; Lund, J.; Young, S. P.; Goodall, M.; Jefferis, R., Role of Oligosaccharide Residues of IgG1-Fc in FcγRIIb Binding. *Journal of Biological Chemistry* **2001,** *276* (49), 45539-45547.

15. Schiestl, M.; Stangler, T.; Torella, C.; Cepeljnik, T.; Toll, H.; Grau, R., Acceptable changes in quality attributes of glycosylated biopharmaceuticals. *Nat Biotech* **2011,** *29* (4), 310-312.

16. Sethuraman, N.; Stadheim, T. A., Challenges in therapeutic glycoprotein production. *Current Opinion in Biotechnology* **2006,** *17* (4), 341-346.

17. Krapp, S.; Mimura, Y.; Jefferis, R.; Huber, R.; Sondermann, P., Structural Analysis of Human IgG-Fc Glycoforms Reveals a Correlation Between Glycosylation and Structural Integrity. *Journal of Molecular Biology* **2003,** *325* (5), 979-989.

18. Hristodorov, D.; Fischer, R.; Linden, L., With or without sugar? (A)glycosylation of therapeutic antibodies. *Mol Biotechnol* **2013,** *54* (3), 1056-68.

19. Anthony, R. M.; Wermeling, F.; Ravetch, J. V., Novel roles for the IgG Fc glycan. *Annals of the New York Academy of Sciences* **2012,** *1253* (1), 170-180.

20. Li, H.; d'Anjou, M., Pharmacological significance of glycosylation in therapeutic proteins. *Current Opinion in Biotechnology* **2009,** *20* (6), 678-684.

21. Alsenaidy, M. A.; Okbazghi, S. Z.; Kim, J. H.; Joshi, S. B.; Middaugh, C. R.; Tolbert, T. J.; Volkin, D. B., Physical Stability Comparisons of IgG1-Fc Variants: Effects of N-Glycosylation Site Occupancy and Asp/Gln Residues at Site Asn 297. *Journal of Pharmaceutical Sciences* **2014,** *103* (6), 1613-1627.

22. Mozziconacci, O.; Okbazghi, S.; More, A. S.; Volkin, D. B.; Tolbert, T.; Schöneich, C., Comparative evaluation of the chemical stability of four well-defined IgG1 Fc glycoforms. *Journal of pharmaceutical sciences* **2016,** *105* (2), 575-587.

23. Pisupati, K.; Tian, Y.; Okbazghi, S.; Benet, A.; Ackermann, R.; Ford, M.; Saveliev, S. V.; Hosfield, C. M.; Urh, M.; Carlson, E.; Becker, C.; Tolbert, T. J.; Schwendeman, S. P.; Ruotolo, B. T.; Schwendeman, A., A Multidimensional Analytical Comparison of Remicade and the Biosimilar Remsima. *Analytical Chemistry* **2017**.

24. More, A. S.; Toprani, V. M.; Okbazghi, S. Z.; Kim, J. H.; Joshi, S. B.; Middaugh, C. R.; Tolbert, T. J.; Volkin, D. B., Correlating the impact of well-defined oligosaccharide structures on physical stability profiles of IgG1-Fc glycoforms. *Journal of Pharmaceutical Sciences*.

25. Federici, M.; Lubiniecki, A.; Manikwar, P.; Volkin, D. B., Analytical lessons learned from selected therapeutic protein drug comparability studies. *Biologicals* **2013,** *41* (3), 131-147.

26. Tsuruta, L. R.; Lopes dos Santos, M.; Moro, A. M., Biosimilars advancements: Moving on to the future. *Biotechnology Progress* **2015,** *31* (5), 1139-1149.

27. Mellstedt, H., Clinical considerations for biosimilar antibodies. *EJC Supplements* **2013,** *11* (3), 1-11.

28. Reusch, D.; Tejada, M. L., Fc glycans of therapeutic antibodies as critical quality attributes. *Glycobiology* **2015**.

29. Xie, H.; Chakraborty, A.; Ahn, J.; Yu, Y. Q.; Dakshinamoorthy, D. P.; Gilar, M.; Chen, W.; Skilton, S. J.; Mazzeo, J. R., Rapid comparison of a candidate biosimilar to an innovator monoclonal antibody with advanced liquid chromatography and mass spectrometry technologies. *mAbs* **2010,** *2* (4), 379-394.

30. Zheng, K.; Bantog, C.; Bayer, R., The impact of glycosylation on monoclonal antibody conformation and stability. *mAbs* **2011,** *3* (6), 568-576.

31. Al-Sabbagh, A.; Olech, E.; McClellan, J. E.; Kirchhoff, C. F., Development of biosimilars. *Seminars in Arthritis and Rheumatism* **2016,** *45* (5, Supplement), S11-S18.

32. Chames, P.; Van Regenmortel, M.; Weiss, E.; Baty, D., Therapeutic antibodies: successes, limitations and hopes for the future. *British Journal of Pharmacology* **2009,** *157* (2), 220-233.

33. LK, H., Post-Translational Structural Modifications of Immunoglobulin G and Their Effect on Biological Activity. . *Anal. Bioanal. Chem.* **2015,** *407* (1), 79–94.

34. ICH Q6B: specifications — test procedures and acceptance criteria for biotechnological/biological products. *Fed Regist* **1999,** *64*.

35. Beck, A.; Debaene, F.; Diemer, H.; Wagner-Rousset, E.; Colas, O.; Dorsselaer, A. V.; Cianférani, S., Cutting-edge mass spectrometry characterization of originator, biosimilar and biobetter antibodies. *Journal of Mass Spectrometry* **2015,** *50* (2), 285-297.

36. Schneider, C. K.; Vleminckx, C.; Gravanis, I.; Ehmann, F.; Trouvin, J.-H.; Weise, M.; Thirstrup, S., Setting the stage for biosimilar monoclonal antibodies. *Nat Biotech* **2012,** *30* (12), 1179-1185.

37. Weise, M.; Bielsky, M.-C.; De Smet, K.; Ehmann, F.; Ekman, N.; Narayanan, G.; Heim, H.-K.; Heinonen, E.; Ho, K.; Thorpe, R.; Vleminckx, C.; Wadhwa, M.; Schneider, C. K., Biosimilars[mdash]why terminology matters. *Nat Biotech* **2011,** *29* (8), 690-693.

38. Weise, M.; Bielsky, M.-C.; De Smet, K.; Ehmann, F.; Ekman, N.; Giezen, T. J.; Gravanis, I.; Heim, H.-K.; Heinonen, E.; Ho, K.; Moreau, A.; Narayanan, G.; Kruse, N. A.; Reichmann, G.; Thorpe, R.; van Aerts, L.; Vleminckx, C.; Wadhwa, M.; Schneider, C. K., Biosimilars: what clinicians should know. *Blood* **2012,** *120* (26), 5111-5117.

39. Mozziconacci, O.; Okbazghi, S.; More, A. S.; Volkin, D. B.; Tolbert, T.; Schöneich, C., Comparative evaluation of the chemical stability of four well-defined IgG1 Fc glycoforms. *Journal of Pharmaceutical Sciences*.

40. Loo, T.; Patchett, M. L.; Norris, G. E.; Lott, J. S., Using Secretion to Solve a Solubility Problem: High-Yield Expression in Escherichia coli and Purification of the Bacterial Glycoamidase PNGase F. *Protein Expression and Purification* **2002,** *24* (1), 90-98.

41. Cuskin, F.; Lowe, E. C.; Temple, M. J.; Zhu, Y.; Cameron, E. A.; Pudlo, N. A.; Porter, N. T.; Urs, K.; Thompson, A. J.; Cartmell, A.; Rogowski, A.; Hamilton, B. S.; Chen, R.; Tolbert, T. J.; Piens, K.; Bracke, D.; Vervecken, W.; Hakki, Z.; Speciale, G.; Munoz-Munoz, J. L.; Day, A.; Pena, M. J.; McLean, R.; Suits, M. D.; Boraston, A. B.; Atherly, T.; Ziemer, C. J.; Williams, S. J.; Davies, G. J.; Abbott, D. W.; Martens, E. C.; Gilbert, H. J., Human gut Bacteroidetes can utilize yeast mannan through a selfish mechanism. *Nature* **2015,** *517* (7533), 165-169.

42. Zhu, Y.; Suits, M. D. L.; Thompson, A. J.; Chavan, S.; Dinev, Z.; Dumon, C.; Smith, N.; Moremen, K. W.; Xiang, Y.; Siriwardena, A.; Williams, S. J.; Gilbert, H. J.; Davies, G. J., Mechanistic insights into a Ca2+-dependent family of α-mannosidases in a human gut symbiont. *Nat Chem Biol* **2010,** *6* (2), 125-132.

43. Xiao, J.; Chen, R.; Pawlicki, M. A.; Tolbert, T. J., Targeting a Homogeneously Glycosylated Antibody Fc To Bind Cancer Cells Using a Synthetic Receptor Ligand. *Journal of the American Chemical Society* **2009,** *131* (38), 13616-13618.

44. Schneider CA, R. W., Eliceiri KW., NIH Image to ImageJ: 25 years of image analysis. *Nat Methods* **july 2012,** *9* (7), 671-5.

45. Chung, S.; Quarmby, V.; Gao, X.; Ying, Y.; Lin, L.; Reed, C.; Fong, C.; Lau, W.; Qiu, Z. J.; Shen, A.; Vanderlaan, M.; Song, A., Quantitative evaluation of fucose reducing effects in a humanized antibody on Fcγ receptor binding and antibody-dependent cell-mediated cytotoxicity activities. *mAbs* **2012,** *4* (3), 326-340.

46. Bjorn Tackenberga, Ilijas Jelc ˇic ´b,1, Anne Baerenwaldtc,1, Wolfgang H. Oertela, Norbert Sommera, Falk Nimmerjahnc,2,3, and Jan D. Lu ¨nemannd, Impaired inhibitory Fc receptor IIB expression on B cells in chronic inflammatory demyelinating polyneuropath. *PNAS* **2009** *112* (31), 4788–4792

47. Ravetch2, F. N. J. V., Fcbig gamma receptors as regulators of immune responses. **2008**.

48. Raju, T. S., Glycosylation variations with expression systems and their impact on biological activity of therapeutic immunoglobulins. *BioProcess Int* **2013**, 44–53.

49. Walsh, G.; Jefferis, R., Post-translational modifications in the context of therapeutic proteins. *Nat Biotech* **2006,** *24* (10), 1241-1252.

50. Raju, T. S., Terminal sugars of Fc glycans influence antibody effector functions of IgGs. *Current Opinion in Immunology* **2008,** *20* (4), 471-478.

51. Jiang, X.-R.; Song, A.; Bergelson, S.; Arroll, T.; Parekh, B.; May, K.; Chung, S.; Strouse, R.; Mire-Sluis, A.; Schenerman, M., Advances in the assessment and control of the effector functions of therapeutic antibodies. *Nat Rev Drug Discov* **2011,** *10* (2), 101-111.

52. Khawli, L. A.; Goswami, S.; Hutchinson, R.; Kwong, Z. W.; Yang, J.; Wang, X.; Yao, Z.; Sreedhara, A.; Cano, T.; Tesar, D. B.; Nijem, I.; Allison, D. E.; Wong, P. Y.; Kao, Y.-H.; Quan, C.; Joshi, A.; Harris, R. J.; Motchnik, P., Charge variants in IgG1. *mAbs* **2010,** *2* (6), 613-624.

53. Seidel, U. J. E.; Schlegel, P.; Lang, P., Natural killer (NK) cell mediated antibody-dependent cellular cytotoxicity (ADCC) in tumour immunotherapy with therapeutic antibodies. *Frontiers in Immunology* **2013,** *4*.

54. Abès, R.; Teillaud, J.-L., Impact of Glycosylation on Effector Functions of Therapeutic IgG. *Pharmaceuticals* **2010,** *3* (1), 146-157.

55. Oganesyan, V.; Damschroder, M. M.; Leach, W.; Wu, H.; Dall'Acqua, W. F., Structural characterization of a mutated, ADCC-enhanced human Fc fragment. *Molecular Immunology* **2008,** *45* (7), 1872-1882.

56. Tobias, R., Biomolecular Binding Kinetics Assay on the Octet platform.

57. Ha, S.; Ou, Y.; Vlasak, J.; Li, Y.; Wang, S.; Vo, K.; Du, Y.; Mach, A.; Fang, Y.; Zhang, N., Isolation and characterization of IgG1 with asymmetrical Fc glycosylation. *Glycobiology* **2011,** *21* (8), 1087-1096.

Chapter 4

Characterization of IgG1 Fc Glycoforms After Prolonged Storage at Low and Elevated Temperatures: A Model System for Biosimilar Comparability Analysis

4.1 Introduction

The stability of monoclonal antibodies is a critical component of a product development to ensure safety and efficacy. The most reliable information regarding the stability of the monoclonal antibody can be achieved by monitoring the normal storage conditions throughout its shelf-life. However, to obtain the most susceptible degradation pathway, the stability of the glycoforms can be tested at an elevated temperature. Valuable information about the functional difference between samples stored at high and low temperatures can be obtained. In addition, stress conditions can be used for formulation screening, accumulation of degraded products, and evaluation of molecular entity. In one study, a mouse IgG1 and a IgG2a monoclonal antibodies were examined at different pHs and temperatures, and the results indicated that these antibodies were more prone to degradation at 37˚C than at 4˚C. Moreover, peptide bond cleavage was found to be the primary degradation pathway at 37˚C, while irreversible aggregation was the dominant degradation pathway at 4˚C.[1] Furthermore, an acidic shift at a higher pH was also observed, which could be due to deamidation. Similarly, it has been reported that the stability of mouse monoclonal IgG2a antibody acidic shift was observed by cation-exchange and cIEF after incubation at 37˚C for six weeks.[2-3]

In another study, deamidation of an asparagine residue in the constant region was found to be the primary degradation pathway when stored at 37˚C, while aggregation was the major degradation pathway when it was at 2-8˚C after long-term storage (>14 months). In addition, oxidation of methionine, tryptophan, and non-disulfide linked cysteine (Cys) residue was also

observed in different sites of the antibody.[4] Similar studies indicated that with a chimeric mouse-human monoclonal antibody incubated at 60˚C at a higher pH, fragmentation was the major degradation pathway, while at the lower pH range, aggregation was the primary degradation pathway. Furthermore, deamidation and disulfide bond cleavage were observed at a high pH range.[4] In other similar reports, significant chemical degradation of antibody was found among the stability samples, including peptide bond cleavage, Asn deamidation, Gln deamidation, and pyroglutamate formation (i.e., N-terminal Glu cyclization).[4] In general, deamidation is a major degradation pathway in proteins, and it has been reported for several monoclonal antibodies.[3,5-10] Furthermore, deamidation is a commonly observed chemical modification during storage, and it is well known that the three-dimensional structure of the protein affects the deamidation rate of Asn residue.[5-10] Formation of pyroglutamic acid has been reported for several antibodies, which was formed from N-terminal Gln. Moreover, formation of pyroglutamine from Glu is less common than from Gln.[11-13] Other reports indicate +16 Da in the protein mass during storage, presumably due to the oxidation of methionine and other residues.[1-2, 14]

Stability testing is required to establish shelf life of therapeutic products. It is well known that environmental factors, such as pH, temperature, ionic strength, and the presence of stabilizers, can impact the conformational stability of the product. Therefore, the stability of the biosimilar in the formulation should be studied.[15] Accelerated stability studies are based on the underlying assumption that the degradation profile follows Arrhenius behavior. This is true in small molecules where studies performed at a higher temperature can predict stability during longer and lower temperature storage.[16] However, in proteins, the degradation profile at high and low temperature may be different and uncorrelated. Thus, to address such issues, a non-

Arrhenius behavior was introduced to account for protein aggregation where the rate depends on equilibrium (for the formation of aggregation-prone state) and the rate of irreversible aggregation.[17] However, using Arrhenius equation to fit protein stability data can be very difficult[18] because there are potentially multiple degradation pathways involved. Therefore, long-term stability is required for protein biologics to achieve regulatory approval.[15] Protein aggregates can have a detrimental effect by inducing an unwanted immune reaction in patients treated with the products. Because of this reason, extensive characterization using multifaceted analytical techniques and clinical studies are required to achieve marketing approval of a biosimilar product.[15]

Forced degradation studies include a set of analytical tests applied to a protein molecule to examine the physicochemical mechanism of degradation. On the other hand, the accelerated stability study measures the rate of a given degradation process over time at a different temperature in a specific formulation conditions. Examining the effect of storage time and excipients on the accelerated and long-term stabilities of biologic drug products is an important part of formulation development and comparability evaluation.[19] Protein drug products may encounter many environmental stresses during expression, purification, processing, storage, and shipment. Therefore, forced degradation and accelerated stability studies are required to examine the degradation profile of a biologic drug by applying various stress conditions, such as elevated temperature, freeze-thaw, agitation, oxidation environment, light, and the presence of different interfaces and pH changes.[19] The design and outcome of successfully forced degradation and accelerated stability studies depend on the analytical techniques employed to identify and characterize the degradants generated.[19]

Forced degradation studies play a critical role in the development of biological drug products. For instance, forced degradation is used in the selection of candidate molecule, characterization, formulation development, stability indicating assay development, and comparability studies. The robustness of a protein formulation against environmental stress factors is essential since biologic products are exposed to various types of stress during production, fill-finish, shipment, storage and final administration.[4, 20] Examples of these stress factors are elevated temperature, freeze-thawing, and light exposure. Forced degradation (or stress testing) is a general term, which includes all forms of stress to drug substances or drug product that exceeds the condition used for stability testing. On the other hand, stability testing refers to studies performed to examine the stability of a formulation according to the general requirement; in particular, international conference on harmonization (ICH) guidelines Q5C (specific for biotech products).[21] In accelerated testing, stability testing was conducted at elevated temperature under the quiescent condition, according to ICH Q5C.[19, 21]

Forced degradation studies are an integral part of the development of therapeutic proteins. The purpose of forced degradation studies may vary depending on the phase of the therapeutic drug development.[19] In general, according to ICH Q5C,[21] the first purpose of the forced degradation studies is to examine how accidental exposure to conditions other than those proposed is harmful to the product. The second purpose is to assess the stability indicating analytical methods. In addition, the accelerated stability may provide useful data for establishing shelf-life.[22,23] The data generated during an accelerated stability study can provide product stability information for future product development. An example would be initial assessment of proposed production changes, which includes changes in formulation or scale-up. Furthermore,

the data can be used in developing and validating of analytical methods for stability studies. In addition, the stability study can be used to generate information that will help to uncover the degradation profile of the drug substance or drug product.[19] Forced degradation studies go hand-in-hand with the analytical characterization techniques, since the result of these studies depend not only on the stress applied but also on the analytical methods used to evaluate them. Hence, selected analytical methods that are sensitive in detecting and quantifying the degradation products formed are necessary. Multiple degradation products can be generated during forced degradation.[24-25] Therefore, a combination of complementary methods is required to cover the degradation products.[26-29]

Upon changes in the manufacturing processes of the marketed products or during product development phases, such as scale-up, manufacturing site change, and cell-line change, the potential effect of the changes on the product quality needs to be examined. Typically, such comparability exercise includes characterization of the product and product-related impurities. Thus, the stability profiles of the pre- and post-change products are compared by studying at the real time and accelerated storage conditions. If significant differences are obtained during analysis of potential impact on the efficacy or safety of the drug product, further studies may be necessary, including clinical and non-clinical studies. The comparability evaluation is performed case-by-case, depending on the product, its mechanism of action, and type of change made during production processes. Therefore, accelerated and stress stability studies are usually applied to determine the degradation profile and establish a head-to-head comparison of pre-change and post-change products.[19]

Unlike the stability testing, which is well-regulated and established in the guidelines (i.e., CHQ1A and ICHQ5C), there are no standard procedures for forced degradation biologic products. The guidelines provide a rough concept on forced degradation studies, but detailed information on how and to which extent these studies should be conducted are not given.[30] However, the condition for photostability test is outlined in the ICH guidelines QIB.[25] Biologic products can be exposed to a temperature higher than the recommended storage temperature during production, shipment, storage, and final administration. Elevated temperature is the most common method to apply stress and generate degraded therapeutic proteins, which are developed to be stored under non-refrigerated conditions (2-8°C). When the temperature increases, proteins may undergo conformational changes, such as unfolding and partial unfolding. These physical changes may lead to further degradation reactions, such as aggregation and denaturation. Starting from the onset temperature of unfolding (T_{onset}) towards the melting point (T_m) of the protein, gradual destabilization of the native protein becomes a more visible state, which leads to irreversible aggregation.[30-32] In addition, diffusion becomes faster at a higher temperature, resulting in a more energetic collision, as well as with reactive chemicals, thereby favoring both physical and chemical degradation. Chemical reactions may be apparent in the unfolded state. An example would be if buried amino acids are exposed for the chemical reactions in solution.[19]

In particular cases, the T_m value has been used to predict the stability of liquid formulations at the planned storage conditions. This was demonstrated by some examples in the literature, which suggest a correlation between the measured T_m values and storage stability. This correlation eventually allowed to select more robust formulation for these cases.[33-38]

However, T_m measurements can not replace stability assessment under real time and temperature conditions. For instance, if the dominant degradation processes or the rate limiting step is not related to the (potential) unfolding of the protein, then T_m can not be used as a predictive tool for the storage stability.[38] In other studies, it has been shown that the extent of refolding upon lowering the temperature below the T_m value can be used to predict the stability of proteins.[53] The specific temperature for thermal stress testing needs to be chosen depending on the thermal behavior of the protein. An example would be a drug product for storage at 2-8°C; accelerated stability assessment is generally conducted at 25°C, as outlined in ICHQ1A.[39] In addition, the effect of heat is recommended to be tested in increments of 10°C the selected accelerated testing temperature. The best approach is that during thermal stress testing, it is a good idea to stay below T_{onset} and at least 10-20°C below the T_m. Studies performed at the T_m value can not be used for stability evaluation because the protein will be predominantly unfolded under these conditions, and the degradation product may not hold relevant information to the "real-life'' storage conditions.[19] Therefore, the prediction of real-time aggregation rates and shelf life from accelerated data may become feasible only if aggregate formation under accelerate and real-time temperature are qualitatively controlled by the same physicochemical factors.[19]

A typical example of these conditions is the formation of a conformationally altered intermediate or a chemical modification that triggers aggregation.[40] Thus, it is critical to understand the degradation mechanism at high temperature and compare it to that occurring at the storage condition (2-8°C). The evaluation of degradation kinetics can also aid in comparing degradation pathways for the pre-change and post-change products in comparability studies. Besides high temperature, for several proteins it has been described that the freeze-thawing may

trigger the formation of a larger aggregation with characteristics of a higher degree of native-like protein structure.[41-44] One should be very cautious in extrapolating the outcome of thermal stress studies to real-life storage conditions, because the conditions during forced degradation studies generally differ from the real-life storage conditions. Therefore, forced degradation studies cannot substitute the stability test under real-time and real temperature conditions. Besides selection of stress conditions, analytical characterization of degradation products is an integral part of the forced degradation studies.[19]

In this study, well-defined homogeneous IgG1 Fc glycoforms (i.e., HM-Fc, Man5-Fc, GlcNAc-Fc, and N297Q-Fc) were studied after incubating at 40˚C, 4˚C, and -80˚C for two, four, and twelve weeks. The samples were characterized head-to-head using bio-layer interferometry which includes the following: An Fc-immobilized format and a receptor-immobilized format. In addition, mass spectrometry was used to monitor chemical modifications during the storage. The data collected includes binding affinities, binding response, potency assay (concentration measurement) and intact protein mass. To our best knowledge, the impact of storage temperature on the functional activity of IgG1 Fc glycoforms with the concept of biosimilar comparability has not been addressed in prior studies. Hence, we examined the effect of storage temperature on the functional activity of IgG1 Fc glycoforms as a model system for biosimilar comparability analysis.

4.2 Materials and Methods

4.2.1 Materials

Yeast nitrogen base (YNB) was used for expression purchased from Sunrise Biosciences. Bacto™ Tryptone and Yeast Extract were obtained from Becton Dickinson and Company (Franklin

Lakes, N.J.). Antifoam 204 utilized in the fermenter was obtained from Sigma-Aldrich (St. Louis, MO.). Certified ACS grade crystalline sucrose was obtained from Fisher Scientific (Pittsburg, PA.). *B. thetaiotaomicron* α-1,2-mannosidase (BT3990, *B.t.* α-1,2-mannosidase) was expressed in-house.[45-48] Endoglycosidase H was purchased from New England Biolabs (Ipswich, MA). The protein G resin was prepared by conjugating protein G (recombinantly expressed in *E. coli*)[49] with Sepharose® CL-4B (Sigma-Aldrich, St Louis, MO) using divinyl sulfone as a coupling reagent.[50] All other general chemicals were obtained from Sigma-Aldrich and Fisher Scientific unless otherwise noted.

4.2.2 Preparation of Fc Glycoforms

HM-Fc was expressed using a glycosylation-deficient strain of *P. pastoris* by following the same protocol as described in our previous work.[51] A large quantity of HM-Fc was expressed using a fermenter for the physical and chemical stability studies as well as for the storage stability studies. Fermenter media used for expression of HM-Fc was fermentation basal salts medium (BSM) and PTM_1 trace salts. The non-glycosylated mutant N297Q-IgG1 Fc (N297Q-Fc) was designed using site-directed mutagenesis as described in our previous work[51] and expressed in a spinner flask containing 1 L of Buffered Glycerol-complex Media (BMGY) and 0.00004% biotin. After maximum cell growth, the protein expression was induced by methanol feeding for about 72 hrs. Next, the cell pellets were harvested, and the Fc protein was purified from the supernatant using protein G in a similar protocol as described in chapter two. Both N297Q-Fc and HM-Fc were purified using HIC and dialyzed in the storage buffer, which was a 20 mM histidine buffer pH 6.0, containing 10% sucrose for further analysis. Man5-Fc and GlcNAc-Fc were produced using an *in-vitro* enzymatic reaction using HM-Fc as a precursor. Man5-Fc was

generated by treating HM-Fc with B.t. α-1,2-mannosidase (BT3990),[51] while GlcNAc-Fc was produced by digesting of HM-Fc with endoglycosidase H. All of the Fc glycoforms were initially dialyzed in 20 mM Histidine buffer pH 6.0, 10% sucrose and stored at -80˚C for further analysis. For this study, the Fc glycoforms were extensively dialyzed in 20 mM citrate-phosphate buffer pH 6.0, containing 150 mM NaCl. Next, samples of 2 mL were sealed in vials and incubated at -80˚C, 4˚C, and 40˚C, and samples were collected at two, four, and twelve weeks as shown in Table 1. After the incubation periods, the samples were stored at -80˚C for further study.

4.2.3 Liquid Chromatography-Mass Spectrometry (LC-MS)

Samples at a concentration of 0.2 mg/mL were first reduced with 10 mM dithiothreitol (DTT); 30 µL was injected into the mobile phase of the liquid chromatography (LC). ESI spectra of the stressed samples were collected on an Agilent 6520 Quadrupole Time-of-Flight (Q-TOF) system. The same procedure was used for conducting the experiment and data analysis as described in our previous work.[51] Furthermore, the percentages of chemical modification were estimated based on the peak intensities using Agilent MassHunter Qualitative Analysis Software. Intact protein mass of the samples stored at -80˚C were used as a reference to identify potential chemical modifications of the incubated Fc glycoforms.

4.2.4 Binding Assays

4.2.4.1 Fc-Immobilized Assay

The interactions of the stressed IgG1 Fc glycoforms with the Fc receptor (FcγRIIIa) were performed with biolayer interferometry (a Blitz instrument Fortebio, Menlo Park, CA). In this immobilization technique, protein G biosensor tips were used to measure the interaction. The binding of stressed IgG1 Fc glycoforms with FcγRIIIa was conducted as described below. Briefly, the protein G biosensor was hydrated for about 10 min with PBS buffer (150 mM NaCl, 50 mM

sodium phosphate pH 7.4) to remove the coating on the surface of the biosensor. This step was followed by incubation of the biosensor for 30 min with PBS kinetic buffer (PBS buffer containing 1 mg/mL casein as a blocking agent) to block non-specific interactions. For kinetic measurement, an initial baseline (30 sec) was performed with PBS kinetics buffer followed by loading (120 sec) of the Fc glycoforms (0.8 μM) onto the biosensor. After loading, a new baseline (30 sec) was established, followed by the association (180 sec) and dissociation (360 sec) of FcγRIIIa to measure the kinetics. To determine the K_D value, a range of concentrations of the receptor (50-800 nM) were tested for interaction with the Fc glycoforms (eg., HM-Fc and Man5-Fc). For GlcNAc-Fc, the concentration range of the receptor was 200 nM to 1600 nM prepared in a two-fold serial dilution. To examine the kinetics of interaction in the dissociation phase, the biosensor was dipped into an analyte-free PBS kinetic buffer. The dissociation was monitored for 360 sec until the signal eventually returning close to the baseline. The data for the binding of the stressed samples with the receptor was collected in triplicated and globally fitted to a 1:1 using the first-order rate equation binding model in Blitz® Pro software.

4.2.4.2 Receptor-Immobilized Assay

The interactions of the different stressed samples of Fc glycoforms with the immobilized receptor were examined with biolayer interferometry (Blitz instrument Fortebio, Menlo Park, CA). In this immobilization technique, streptavidin (SA) biosensor tips were used to measure the interactions. Before the binding experiment, the glycoforms were dialyzed in PBS buffer to remove the storage buffer (20 mM citrate-phosphate buffer, 150 mM NaCl, pH 6.0) and to adjust the pH to 7.4. The same procedure was followed as described in detail in our previous work.[51]

4.2.5 Binding Response Measurements

The response of the stressed IgG1 Fc glycoforms with the FcγRIIIa was examined with biolayer interferometry using a Blitz instrument (Fortebio, Menlo Park, CA). In this experiment, protein G biosensor tips were used for each of the samples, including their references for generating the sensorgrams. The response experiment was conducted as follows. Briefly, the protein G biosensor tip was hydrated for about 10 min in PBS buffer (150 mM NaCl, 50 mM sodium phosphate pH 7.4) to remove sucrose coating from the surface. This step was followed by incubation for 30 min with PBS kinetic buffer (PBS buffer containing 1 mg/mL casein as a blocking agent) to block any non-specific interaction during binding. For response measurement, an initial baseline (30 sec) was performed with PBS kinetics buffer, followed by loading (120 sec) of the IgG1 Fc glycoforms onto the biosensor. The concentration of Fc glycoform during loading was 0.8 μM. In the next step, a new baseline (30 sec) was performed, followed by the association (180 sec) and dissociation (360 sec) of the receptor. The concentration of the receptor during the association was kept at 0.8 μM. The dissociation phase was monitored by dipping the biosensor in analyte-free PBS buffer for 360 sec To calculate the binding responses, the curves were reference subtracted and exported into Microsoft Excel. The last five points at the end of the association phases were averaged from triplicate measurements for each Fc glycoform.

4.2.6 Concentration Measurements

A standard curve was generated before running a quantitative assay on the stability samples. The standard curve with a known concentration of a reference sample was developed for each Fc glycoform. The samples were in a formulation buffer (20 mM citrate-phosphate, 150 mM NaCl-pH 6.0). Protein G biosensors were used to develop the standard curve and measure

the concentration of the stressed Fc glycoform. The protein G biosensor was pre-rehydrated with the formulation buffer for about 15 min. Next, the “Create a standard curve module” was selected in Blitz Pro data analysis software, and 4 µL of each concentration was run for 30 sec with shaker enabled. A reference containing a formulation buffer was used to subtract background response. After collecting the data, the software calculated binding rates and generated a standard curve fitted by a linear model. To determine the concentration, a 4 µL of the stressed Fc glycoforms was used, and “quantitate sample module” was selected. After acquiring the data, unknown concentrations of the stressed Fc glycoforms were automatically fitted to the standard curve and their concentrations calculated.

4.3 Results

4.3.1 Chemical Modification of IgG1 Fc Glycoforms at Low and Elevated Temperatures

Initial characterizations were conducted using mass spectrometry to identify any chemical modifications that occurred after incubating the four Fc-glycoforms (Figure 1 in Chapter 2) at -80°C, 4°C, and 40°C for two, four, and twelve weeks. First, the samples stored at -80°C were examined for any chemical modifications and utilized as controls to compare with the samples incubated at 4°C and 40°C. For the HM-Fc, the intact protein mass showed the Fc monomer with high mannose glycoforms containing between $Man_8GlcNAc_2$ to $Man_{12}GlcNAc_2$ residues. As shown in Figure 1, the major peak of the HM-Fc was attributed to the $Man_8GlcNAc_2$ glycoform, followed by decreasing intensity of the peaks as follows: $Man_9GlcNAc_2$, $Man_{10}GlcNAc_2$, and $Man_{11}GlcNAc_2$. The control HM-Fc stored at -80°C showed no chemical modifications as shown in the intact protein mass (Figure 1) as well as the percentage of chemical modification (Table 2). As shown in Figure 1A, HM-Fc stored at -80°C showed a peak of +16 Da, presumably oxidation. The estimated percentage of the oxidation was 8.7%, and the percentage of chemical modification was calculated from the peak intensities of the intact protein mass. This level of oxidation was comparable to the sample before incubation, indicating the chemical modification occurred during protein production. Besides oxidation, no other chemical modifications were observed, suggesting the HM-Fc was stable when stored at -80°C. The HM-Fc glycoforms incubated for two weeks at 4°C showed an estimated level of oxidation about 8.7%, and this extent of chemical modification was comparable to the control sample stored at -80°C. Thus, this data demonstrated the HM-Fc samples remained stable for two weeks at 4°C with no further chemical degradation as shown in Figure 1 and Table 2. However, samples of HM-Fc stored at 4°C for four weeks

showed a slight increase in the level of oxidation (9.8%). This data demonstrated a slow increase in oxidation during storage at 4°C. Further storage of HM-Fc for twelve weeks at 4°C resulted in a significant increase in oxidation, which was estimated at about 11.6%. Therefore, this sample showed approximately a 3% increase in oxidation level compared to the control sample stored at -80°C. Overall, a slight increase in oxidation was observed in samples of HM-Fc incubated at 4°C for four and twelve weeks.

The HM-Fc samples stored at the elevated temperature (40°C) for two, four and twelve weeks were examined using mass spectrometry. For instance, the HM-Fc stored at 40°C for two weeks showed a significant oxidation levels, which were estimated to be about 13.4%. An increase of 4.7% compared to the control samples stored at -80°C. This data illustrated the effect of elevated storage temperature on the extent of chemical modification of the Fc glycoforms. Obviously, higher temperature storage resulted in significant chemical modifications as expected. Similarly, samples stored at 40°C for four weeks showed 14.1% oxidation, suggesting a slight increase in the chemical modification. However, after an extended storage time (i.e., twelve weeks), a significant oxidation was observed, which was estimated at about 28.6%. This major degradation of the HM-Fc compared to the similar sample stored at 4°C for twelve weeks again, which showed the instability of this glycoform at elevated temperature. Moreover, about 20% increase in oxidation was observed compared to the control samples frozen at -80°C. This trend of increasing chemical modification with incubation period was more apparent for samples stored at 40°C compared to the same samples stored at 4°C.

For the Man5-Fc, the intact protein mass showed the Fc monomer containing five mannose residues. As shown in Figure 1B, the main peak of Man5-Fc was attributed to the

$Man_5GlcNAc_2$ and showed a predominantly single peak at 26280 Da, consistent with our previous work.[51] Like the HM-Fc, the Man5-Fc samples stored at -80°C showed 9.5% oxidation, which was an initial oxidation level generated during protein production. This percentage of oxidation was not surprising because HM-Fc was used as a precursor to produce Man5-Fc. Hence, any chemical modification that originated from the HM-Fc was expected to appear in the Man5-Fc glycoform. Samples of Man5-Fc stored for two weeks at 4°C showed significant modifications compared to the same sample of HM-Fc, indicating the impact of glycosylation on the chemical degradation. The percentage of chemical modification remained unchanged for Man5-Fc stored at 4°C for four weeks. However, a slight increase in chemical modification was observed for the samples stored at the same temperature for twelve weeks as shown in Figure 1B and Table 2.

The chemical modification of the Man5-Fc glycoform at an elevated temperature was similar to the HM-Fc glycoform. For instance, samples stored at 40°C showed an estimated 13.5% oxidation and slightly increased during incubation for four weeks at 40°C, which was estimated to be 13.7%. However, storage of Man5-Fc at 40°C for twelve weeks resulted in a significant oxidation, which was estimated to be 26.1%. The pattern and the level of chemical modification observed in both HM-Fc and Man5-Fc glycoforms were similar as shown in Figures 1A, B, C, and Table 2. In general, the increase in peak intensity of the oxidized product was more apparent at 40°C compared to 4°C incubation for both Man-Fc and HM-Fc glycoforms.

For the GlcNAc-Fc, the intact protein mass showed the Fc monomer containing a single N-Acetylglucosamine residue as shown in Figure 1C. The GlcNAc-Fc glycoform showed a single peak at 25267 Da, and this glycosylation profile was consistent with our previously reported work.[51] Characterization of GlcNAc-Fc samples stored at -80°C showed an estimated oxidation

level of 8.0%, which was similar to the control Man5-Fc and HM-Fc glycoforms. Since HM-Fc was used as a precursor to generate GlcNAc-Fc, any chemical modification that existed in the HM-Fc samples was expected to appear in the intact mass of GlcNAc-Fc glycoform. The chemical modifications of GlcNAc-Fc at 4°C were 8.0%, 8.1%, and 8.1% for two, four and twelve weeks, respectively. Therefore, GlcNAc-Fc incubated at 4°C showed no significant chemical modification compared to the same reference sample stored at -80°C. This was a unique stability profile compared to the HM-Fc and Man5-Fc glycoforms samples studied at the same storage period and temperature. However, for GlcNAc-Fc samples incubated at 40°C, a significant chemical degradation was noticed. The oxidation levels at 40°C were 10.3%, 14.4%, and 27.2% for two, four, and twelve weeks, respectively. This pattern of chemical degradation was similar to the HM-Fc and Man5-Fc glycoforms incubated at the same temperature as well as the same incubation time.

The non-glycosylated N297Q-Fc showed a single peak for the Fc monomer, consistent with its non-glycosylated state as shown in Figure 1D. The asparagine residue at the 297-position was mutated to glutamine to prevent glycosylation during biosynthesis. The N297Q-Fc samples stored at -80°C showed an estimated percentage of modification at about 7.1%, calculated based on the peak intensities. Compared to other glycoforms studied in this work, the initial oxidation level was relatively lower. Samples of N297Q-Fc stored at 4°C for two weeks showed a 10.2% oxidation level, higher than any of the other glycoforms tested (HM-Fc, Man5-Fc, and GlcNAc-Fc). The degradation of N297Q-Fc incubated at 4°C for four and twelve weeks were 10.7% and 11.1%, respectively. This data demonstrated rapid deterioration in the first two weeks, but remained stable over the period of four to twelve weeks. The chemical modifications of N297Q-

Fc incubated at 40°C for two, four, and twelve weeks were 12.5%, 15.3%, and 30.1%, respectively. This increasing trend of chemical modification with N297Q-Fc was higher compared to the other glycoforms examined in this study.

4.3.2 Concentrations of IgG1 Fc Glycoforms Incubated at Low and Elevated Temperatures

The concentration of the Fc glycoform was examined using protein G biosensors as shown in Figures 2 as well as the raw values in Table 3. First, a well-characterized reference standard was employed for each glycoform to develop a standard curve. The concentration of the Fc glycoform was then measured. The HM-Fc showed a slightly lower concentration when stored at -80°C which was about 170 µg/mL. The original concentration of the Fc glycoforms studied in this work was 200 µg/mL. Furthermore, the concentration of the HM-Fc was decreased to 152 µg/mL during incubation at 4°C for four weeks. Similarly, the concentration of HM-Fc further decreased to 148 µg/mL during the incubation period of twelve weeks at 4°C. On the other hand, the concentration of HM-Fc stored at 40°C for two weeks was 147 µg/mL, indicating a significant decrease in concentration compared to the same samples and duration of period when stored at 4°C (163 µg/mL). A further decrease in concentration was noticed during the incubation period of four and twelve weeks, which were 146 µg/mL and 139 µg/mL, respectively. This data illustrated the differences in concentration between the three storage conditions, in which higher concentration was noticed at -80°C, followed by 4°C and 40°C incubation temperatures. Moreover, the trend of decreasing concentration profile of the HM-Fc was faster at 40°C than at 4°C storage condition. The concentrations of HM-Fc were similar during the two-week incubation at -80°C and 4°C as shown in Table 3.

For Man5-Fc, the concentration of the samples stored at -80°C was 167 µg/mL. Similarly, the concentration of the samples stored at 4°C for two, four, and twelve weeks were 175 µg/mL, 166 µg/mL, and 168 µg/mL, respectively. This data showed that the concentration remained stable throughout the storage time. This stability trend of concentration was visible from the concentration curve in Figure 2A as well as the concentration data in Table 3. Furthermore, the data highlighted the physical stability of Man5-Fc at a lower temperature, which was comparable to the control sample stored at -80°C. However, samples of Man5-Fc stored at 40°C showed a significant decrease in concentration as shown in Figure 2B. The measured concentrations at 40°C for two, four, and twelve weeks were 158 µg/mL, 152 µg/mL, and 143 µg/mL, respectively. This data demonstrated a clear difference in stability between the samples stored at low and elevated temperatures.

Next, the concentration of the GlcNAc-Fc at the three storage conditions was examined. For instance, the concentration measured for samples stored at -80°C was 167 µg/mL. Similarly, the concentration of the GlcNAc-Fc stored at 4°C for two weeks was 163 µg/mL, suggesting a slight decrease in concentration. Furthermore, the concentrations of GlcNAc-Fc incubated at 4°C for two and four weeks were 149 µg/mL and 132 µg/mL, respectively. This data showed a significant decrease in the concentration of GlcNAc-Fc at 4°C during the extended period of incubation. The concentration of GlcNAc-Fc stored at 40°C showed a relatively lower trend in decreasing concentration profile compared to the lower temperature storage conditions (i.e., 4°C). The concentrations of GlcNAc-Fc incubated at 40°C were 166 µg/mL, 151 µg/mL, and 146 µg/mL, for storage periods of two, four, and twelve weeks (Table 3 and Figure 2B). This decrease

in concentration was apparent from the reduction in concentration curve profile as shown in Figure 2B.

A similar concentration measurement was conducted for the non-glycosylated N297Q-Fc, and the concentration of the samples stored at -80°C was 133 µg/mL. Thus, N297Q-Fc showed the lowest concentration at -80°C, presumably due to aggregation and precipitation. The concentration of N297Q-Fc incubated for two, four, and twelve weeks at 4°C was 134 µg/mL, 134 µg/mL, and 123 µg/mL, respectively. This data demonstrated that there was no significant change in concentration when stored at the low temperature after the initial drop in concentration. This was presumably due to the significant decrease in the concentration of N297Q-Fc (the protein was diluted) and, consequently, no further aggregation was possible. The concentration of the sample incubated at 40°C for two weeks was 123 µg/mL. This concentration was the lowest compared to the other glycoforms stored at the same temperature and incubation time. The concentrations of the N297Q-Fc samples incubated at 40°C for four and twelve weeks were 118 µg/mL and 115 µg/mL, respectively. Overall, this result indicated the reduction in the concentration profile of N297Q-Fc was higher compared to the other glycoforms. Moreover, significant differences between the two storage conditions (4°C and 40°C) were observed as shown in the major reduction in concentration at 40°C compared to the 4°C storage condition. Overall, a higher concentration decrease was observed for samples stored at 40°C compared to the same samples stored at 4°C and -80°C. N297Q-Fc showed the lowest concentration at all storage conditions tested.

4.3.3 Binding Interaction of Stressed IgG1 Fc Glycoforms with FcγRIIIa

4.3.3.1 Fc-immobilized Format

The binding interaction of the Fc glycoforms with the FcγRIIIa was examined using the Fc-immobilized format. This binding interaction was performed for samples stored at 4°C, 40°C, and -80°C incubated for two, four, and twelve weeks. The Fc glycoforms stored at -80°C were used as a reference for measuring any change in K_D values of the samples stored at 4°C and 40°C. The interaction was first evaluated using the Fc-immobilized format, in which the glycoforms were immobilized onto the protein G biosensor, and the receptor was kept in solution. The k_{on}, k_{off}, and K_D values for this format were shown in Table 4 and illustrated in Figure 3. The associations (k_{on}) and dissociations (k_{off}) were evaluated and used to calculate the equilibrium dissociation constant (K_D) values. The HM-Fc K_D value stored at -80°C was 29.8±1.8 nM, which was consistent with values for non-stressed samples. No significant increase in K_D value was observed for HM-Fc samples incubated at 4°C for two weeks (31.0±1.7 nM). The HM-Fc sample stored at 4°C for four weeks showed further decrease in K_D value, suggesting that there was a reduction in functional activity. Similarly, for samples stored at 4°C for twelve weeks, the K_D value was 37.0±1.1 nM, indicating a further deterioration of the sample upon incubation. Overall, a trend of decreasing functional activity of HM-Fc was observed at 4°C after two, four, and twelve weeks of storage.

The binding interaction for samples of HM-Fc stored at 40°C was also examined, using the Fc-immobilized format. The K_D values for HM-Fc stored at 40°C for two, four, and twelve weeks were 31.7±1.5 nM, 37.1±1.8 nM, and 37.0±1.1 nM, respectively as shown in Table 4A. In comparison to the 4°C storage condition, the 40°C incubation showed a significant reduction in

binding affinities, demonstrating deterioration of the sample at the elevated temperature. This difference in binding affinities between the low and elevated temperatures was more apparent at twelve weeks of storage period as shown in Table 4 and Figure 3.

Likewise, the K_D values of Man5-Fc were evaluated after incubation at -80°C, 4°C, and 40°C for two, four, and twelve weeks. No significant change in binding affinities was observed for the samples incubated at 4°C, and the value is comparable to the samples stored -80°C. However, the K_D values of the samples stored at 40°C for two, four, and twelve weeks were 40.9±0.8 nM, 43.8±1.9 nM, and 52.8±2.5 nM, respectively as shown in Table 4B and illustrated in Figure 3. Therefore, Man5-Fc showed a significant decrease in binding affinities at the elevated temperature (increase in K_D values). This data indicated the effect of temperature as evidenced by the decreasing trend in binding affinities.

The interaction of GlcNAc-Fc with the FcγRIIIa was also evaluated after the samples were incubated at 4°C and 40°C for two, four, and twelve weeks. The samples stored at -80°C were used as a reference to evaluate any decrease in binding affinities for the samples stored at elevated and low temperatures. A slight increase in K_D values (decrease in binding affinities) was observed for samples incubated at 4°C as shown in Table 4C. The K_D values of the samples stored at 4°C for two, four, and twelve weeks were 1111±166 nM, 1333±181 nM, and 1675±45 nM, respectively as shown in Figure 3. Similarly, samples of HM-Fc stored at 40°C showed reduced binding affinities with the lowest being 2236±596 nM after twelve weeks of storage. The increase in K_D value was almost two-fold compared to the sample stored at -80°C as well as the samples stored at 4°C for two weeks. Thus, the result highlighted the effect of temperature in binding affinities and the kinetic binding as shown in Table 4C and Figures 3 and 4.

4.3.3.2 Receptor-immobilized Format

The change in K_D values of the stressed samples after prolonged storage at the elevated and low temperatures was evaluated using the receptor-immobilized format. In addition, the result was compared with the Fc-immobilized format for further analysis. The samples incubated at 4°C and 40°C for twelve weeks were examined using the receptor immobilized format. The twelve weeks' samples were selected because that change in K_D values was more apparent after an extended storage time. Also, samples stored at -80°C were used as a reference to assess the change in binding affinities of the samples stored at the low and elevated temperatures.

The K_D value for HM-Fc stored at 4°C for twelve weeks was 65.2±2.0 nM. This K_D value was significantly higher compared to the value measured using the Fc-immobilized format. Thus, this result demonstrated the difference between the two immobilization techniques regarding their sensitivity in detecting a change in binding affinities upon stress conditions. Likewise, the HM-Fc stored at 40°C for twelve weeks was also evaluated, and the K_D value was 136.3±9.2 nM. Again, this data demonstrated that the functional activity of HM-Fc significantly decreased compared to the same sample incubated at 4°C. Moreover, the receptor-immobilized format demonstrated significant differences between the two incubation conditions compared to the differences observed when using the Fc-immobilized format. Comparatively, the sample stored at 4°C for twelve weeks showed a decrease in k_{off} values. The decreased k_{off} was presumably due to the presence of a weak binding component in the sample. For HM-Fc, the k_{off} measured after incubation at 40°C and 4°C was similar. However, the k_{on} value after incubation at 40°C decreased significantly, suggesting an inactive component present in the sample. The kinetic data were shown in Table 5 and illustrated in Figures 5 and 6.

Like HM-Fc, samples of Man5-Fc stored at 4°C and 40°C for twelve weeks were evaluated using the receptor-immobilized format. First, the samples stored at -80°C were evaluated, and the K_D value was 34.3±1.9 nM, which was consistent with our previous work reported for the same non-stressed samples.[51] The K_D value for Man5-Fc stored at 4°C for twelve weeks was 65.2±1.9 nM. This increase in K_D value was attributed to the faster dissociation rate. Moreover, the k_{off} value measured was significantly faster compared to the same sample stored at -80°C. Furthermore, the k_{on} values of the samples stored at 4°C and -80°C were similar (2.1±0.0)x10^5 $M^{-1}s^{-1}$ and (2.4±0.0)10^5 $M^{-1}s^{-1}$, respectively. Again, this data suggested a significant proportion of the protein was partially active. For samples of Man5-Fc stored at 40°C for twelve weeks, the K_D value was 121.9±7.1 nM. Thus, a significant decrease in K_D value was observed, which was attributed to the increase in k_{off} rate and a reduction in the association rate as shown in Table 5. The k_{off} values of the samples incubated at 4°C and 40°C for twelve weeks were similar, whereas significant differences in k_{on} values were observed as shown in Table 5 and Figures 5 and 6.

Similarly, samples of GlcNAc-Fc stored at 4°C, 40°C, and -80°C for twelve weeks were examined using the receptor-immobilized format. The K_D value for the GlcNAc-Fc stored at -80°C was 988.8±21.8 nM, which was consistent with our previous work for the non-stressed samples.[51] The data suggested the samples stored at -80°C were stable with no change in K_D values expected. However, GlcNAc-Fc stored at 4°C for twelve weeks showed a significantly lower binding affinity (8779.3±143.4 nM) compared to the same sample stored at -80°C. Again, this decrease in K_D value was attributed to the increase in k_{off} value and a reduction in the association rate, in which both contributed to the lower binding affinity. One difference observed with the GlcNAc-Fc compared to the other glycoforms was that the k_{on} value at 4°C was significantly lower compared to the k_{on}

value of the same sample stored at -80°C. The GlcNAc-Fc stored at 40°C for twelve weeks showed a significantly lower K_D value, again attributed to the decrease in association and increase in dissociation rates.

4.3.4 Binding Responses of Stressed IgG1 Fc Glycoforms

The binding response of the Fc glycoforms with FcγRIIIa was also evaluated using the Fc-immobilized format. HM-Fc samples stored at -80°C showed a higher response compared the same samples stored at 4°C and 40°C (Figures 7 and 8A , Table 6). Also, the samples stored at 4°C for two, four, and twelve weeks showed similar binding responses. However, samples of HM-Fc stored at 40°C showed a significant decrease in binding response compared to the same samples stored at -80°C. Moreover, differences in response were observed for samples incubated at 40°C, in which the trend in response was as follows: two weeks> four weeks> twelve weeks. Representative response binding curves were given in Figure 8A, and the raw values were shown in Table 6. For ease of comparison, the response values were further illustrated in Figure 7. In general, a similar pattern was observed for HM-Fc, Man5-Fc, and GlcNAc-Fc. Furthermore, differences in response were more apparent when the samples stored at -80°C, 4°C, and 40°C for twelve weeks were compared. This data illustrates the need to monitor the stability for an elongated period of time to observe major differences in functional activity in a biosimilar comparability analysis.

4.4 Discussion

During manufacturing, shipping, and storage, antibodies are subjected to various degradation pathways, which can potentially affect their potency.[14] In one study, it has been demonstrated that chemical degradation in the antigen binding site decreased the binding affinity.[4] However, the effect of physical and chemical degradations of the Fc fragment on the functional activity as well as binding affinity to Fc receptors is less known.

The mass spectrometry data demonstrate a significant chemical modification at 40°C compared to the samples incubated at 4°C and -80°C. This could be either due to the physical degradation that accelerates the chemical degradation or the impact of temperature on the rate of chemical deterioration. Nevertheless, the difference in chemical degradation between the storage conditions was apparent as shown in Table 2 and Figure 1. Samples were tested for chemical modification using intact protein mass spectrometry under reducing conditions. A significant chemical modification (+16), presumably due to oxidation was observed for samples stored at 40˚C and showed a trend with the incubation time (twelve weeks>four weeks>two weeks). This trend in chemical modification was observed in all glycoforms tested as shown in Figure 1 and Table 2. Samples stored at -80˚C and 4˚C showed a modest change in the chemical modification, indicating a stable storage temperature. Moreover, the data showed the Fc glycoforms were more stable when stored at -80˚C and 4˚C than at 40˚C. Unlike the elevated temperature, no significant chemical modification (+16) was observed for samples stored at 4˚C.

Several reports demonstrated deamidation of asparagine residue and oxidation of methionine sulfoxide after prolonged storage at an elevated temperature. IgG1 contains two conserved Met residues: Met ^{252} and Met ^{428} (EU numbering).[52] Methionine oxidation can be

induced by oxidizing agents, such as Ter-butyl hydro-peroxide, H_2O_2, UV, and an elevated temperature. In one study, Met oxidation was found to affect binding to protein A, protein G, and FcRn; however, binding to FcγRIIIa was not affected.[53] Oxidation has been shown in samples stored at an elevated temperature, whereas a sample kept at a low-temperature aggregation was found to be the major degradation pathway. Another study reported the oxidation of tryptophan and methionine during storage at a high temperature.[4] These samples incubated at low and elevated temperatures were examined for chemical modification using peptide mapping. Minor oxidation of Met and deamidation of asparagine was observed.[54]

The concentration of the samples was measured using BLI by binding with the protein G on the surface of the biosensors. The concentration decreased more rapidly in samples incubated at 40˚C. The concentration corresponds to the rate of binding of the Fc glycoforms to the protein G biosensors. A significant drop in concentration was observed for N297Q-Fc, presumably due to aggregation and precipitation as shown in Figures 2A and 2B. Samples stored at 4˚C showed a modest change in concentration, except N297Q-Fc in which a significant decrease was observed, presumably due to aggregation and precipitation**.** As shown in Figures 2A and 2B, a significant decrease in concentration was observed, indicating the presence of degraded protein generated during stress. For instance, HM-Fc stored at 40°C for twelve weeks showed about a 30% decrease in concentration, presumably due to the inactive protein present in the sample (i.e., protein unable to bind protein G). Similarly, HM-Fc stored at 4°C for twelve weeks showed a 26% decrease in concentration, likely due to the presence of inactive protein (Table 2). Therefore, the decrease in concentration measurement agreed to the reduction in binding affinities measured in the samples incubated at 4°C and 40°C for twelve weeks. Furthermore, these samples showed

similar levels of inactive protein, resulting in a similar decrease in the association rates as shown in Table 5.

In this study, a reduction in binding affinities, which corresponded with the storage times, was observed for samples incubated at 40˚C and 4˚C. A decrease in association rate and an increase in dissociation rate was noted for the Fc-glycoforms incubated at 40˚C tested as shown in Figure 3 and Table 4. Samples stored at 4˚C for two, four, and twelve weeks showed modest changes in binding affinities when tested using the Fc-immobilized format. This data demonstrated the Fc glycoforms remained relatively stable at the low-temperature incubation, which agreed with the binding responses and chemical modifications examined. A trend of decreasing binding affinities was observed for all glycoforms tested, except N297Q-Fc in which no binding was observed.

In addition to the Fc-immobilized format, the glycoforms were examined using the receptor-immobilized format to assess the binding affinities as well as to compare the two immobilization formats. Differences in equilibrium dissociation constants were noticed between the Fc glycoforms incubated at 4˚C and 40˚C for twelve weeks, as shown in Figure 6 and Table 5. The HM-Fc samples incubated at 4˚C showed a minor decrease in association rate compared to the control sample stored at -80˚C. This data indicated the absence of inactive protein during the twelve weeks of incubation period at 4˚C. However, the dissociation phase showed a significant increase, presumably due to the presence of a partially active protein in the sample. Therefore, the HM-Fc data suggested a substantial amount of partially active protein, but a minor inactive protein in the sample generated during the incubation period of twelve weeks at 4˚C. Likewise, samples of HM-Fc incubated at 40˚C for twelve weeks showed a significantly lower association

rate compared to the same samples stored at -80˚C and 4˚C. This significant decrease in association rate was presumably due to the presence of a large amount of inactive protein present in the sample generated during incubation at 40˚C.

A significant increase in dissociation rate was noted, presumably due to the presence of a substantial amount of partially active protein in the sample. Thus, the data of the HM-Fc samples incubated at 40˚C for twelve weeks indicated a substantial presence amount of inactive and a partially active protein generated during twelve weeks of incubation. Moreover, both samples incubated at 4˚C and 40˚C showed a similar increase in the dissociation rate, which was attributed to the comparable amount of a partially active protein in the samples. However, a major decrease in association rate was observed only in the samples incubated at 40˚C, indicating a significant amount of inactive protein was present in this sample compared to the same samples incubated at 4˚C. Furthermore, this data demonstrated that the differences in the binding kinetics between the samples incubated at low and elevated temperatures were attributed to the differences in the type of degradation products generated during storage. These degraded products could be due to chemical modifications, aggregates, or conformational. A similar binding profile was observed for Man5-Fc compared to HM-Fc incubated at a low and elevated temperature for twelve weeks. This similarity is not surprising because Man5-Fc and HM-Fc have similar glycosylation profiles, binding activity, and physical stability.

Similarly, GlcNAc-Fc samples incubated for twelve weeks at 4˚C, 40˚C, and -80˚C were examined using the receptor-immobilized format. A significant decrease in association rates was observed for both the samples incubated at 4˚C and 40˚C for twelve weeks. This data suggested the comparable amount of inactive protein present in both storage conditions. Moreover, the

data indicated GlcNAc-Fc was unstable at 4˚C and 40˚C incubation, presumably due to its truncated N-linked glycan at Asn297. Therefore, this work demonstrated the application of stress conditions to differentiate glycoforms based on their stability attributed to their difference in glycosylation size and state. The instability ultimately resulted in the significant loss of functional activity for the samples containing shorter or no glycans. In other words, this data demonstrated that the effect of glycosylation not only modulates the binding affinity to FcγRIIIa but also affects stability and, consequently, affects the activity.

Like the receptor-immobilized format, the Fc-immobilized format showed a decrease in association rate and an increase in dissociation rate after twelve weeks of the incubation period. However, the difference in binding kinetics (k_{on}, k_{off}, and K_D) between the low and elevated incubation temperature were more apparent when measured using the receptor-immobilized format. Also, lower binding affinities were observed when the receptor-immobilized format was utilized. Nevertheless, both methods demonstrated differences in binding affinities for all the samples examined, which could be helpful in a biosimilar assessment. Therefore, these glycoforms were found to be a useful model for biosimilar comparability analysis.

The impact of physically and chemically degraded products generated during the incubation at a low and elevated temperature on the binding affinities cannot be easily assigned. However, the differences in K_D values observed between the two immobilization formats for the stress samples in this study can be deconvoluted using the mixtures of glycoforms examined in chapter 3. These mixtures contain N297Q-Fc (inactive) and GlcNAc-Fc (partially active) combined with HM-Fc in different proportions. In the mixture study, using the receptor-immobilized format, a decrease in association rate was observed that was proportional to the amount of

N297Q-Fc present in the mix. However, no change in dissociation rate was observed. Also, using the Fc-immobilized format, a decrease in dissociation rate was noted due to the presence of a weak binding component (i.e., GlcNAc-Fc). Therefore, N297Q-Fc and GlcNAc-Fc can potentially mimic the inactive and partially active proteins present in the stressed samples of the Fc glycoforms generated during storage. In this study, the differences in K_D, k_{on} , and k_{off} between the samples incubated at low and elevated temperatures were similar to the differences observed between the mix1 (a mixture of N297Q-Fc and HM-Fc) and Mix2 (a mix of GlcNAc-Fc and HM-Fc) studied in chapter 3.

For all of the stressed samples incubated for twelve weeks, a decrease in association rate and an increase in dissociation rate was observed when the receptor-immobilized format was utilized. The reduction in association rate was an indication of an inactive protein (i.e., unable to bind to a receptor) present in the sample (i.e., unable to bind receptor). However, an increase in the dissociation rate was likely due to the presence of the partially inactive component (i.e., weakly binding to a receptor) present in the sample (i.e., binds to receptor weakly). Moreover, in the mixture of HM-Fc and GlcNAc-Fc, we observed displacement of the weak binding GlcNAc-Fc by HM-Fc during the association phase. Thus, the dissociation phase behaved more like HM-Fc. Overall, no significant change in dissociation rate was noted in the mixture containing HM-Fc and GlcNAc when compared to the 100% HM-Fc. However, for the incubated samples, we have seen major changes in dissociation rate, presumably due to the presence of a partially active protein. In order for this partially active protein to exert contribution in the dissociation phase, it needs to have a higher binding affinity than GlcNAc-Fc to withstand displacement by HM-Fc. The presence of this partially active protein was similar to the samples of HM-Fc incubated at 4°C and

40°C, as shown in their similar dissociation rates. However, the amount of inactive protein was higher in the samples incubated at 40°C, as demonstrated by the significant drop in association phase. This data was also in agreement with the concentration measured using Bio-Layer Interferometry (BLI) as shown in Table 2.

A significant difference in binding response between samples incubated at 40˚C was observed in which the samples stored for two weeks showed the highest binding responses followed by the samples stored at four weeks and twelve weeks. Therefore, the binding responses showed a decreasing trend with increasing incubation times, indicating a loss of functional activity. This reduction in binding responses could be due to the chemical or physical degradation of the samples incubated at 40˚C for extended storage time. Moreover, this decrease in binding response with an increase in storage time at the elevated temperature was observed in all glycoforms, except N297Q-Fc in which no binding with FcγRIIIa was observed.

Samples stored at 4˚C showed no significant change in responses, indicating the samples remained relatively stable (native state) during the incubation time. The loading level of HM-Fc to protein G was examined and found to be the same regardless of the incubation time. Moreover, no significant difference in the loading level of Fc to protein G was observed between two, four, and twelve weeks, in all the samples tested. Thus, the difference in binding responses indicates that there was a protein loaded onto the protein G that binds weakly with FcγRIIIa (partially active). Therefore, the Fc-immobilized format successfully differentiated the samples stored at low and elevated temperatures. This binding response measurement can be utilized to monitor the activity of the mAbs during stability study and formulation development of a biosimilar.

In general, the samples incubated at 4°C showed a similar response, suggesting the protein remained relatively stable during the incubation period. However, the samples stored at 40°C showed a decrease in binding response, in which a higher response was observed in the samples stored for two weeks and the lowest response in the samples stored for twelve weeks. Furthermore, the difference in response (i.e., measured using Fc immobilized format) was more visible when the samples incubated at 4°C, 40°C, and 80°C were compared at twelve weeks of storage (Figures 8A, 8B, and 8C). In addition, the data demonstrated the use of stress (40°C) to observe differences in response, which was not visible at low temperatures (4°C and -80°C). For instance, HM-Fc incubated at 4°C showed a decrease in response compared to the same samples incubated at 40°C for twelve weeks. The estimated decrease in response of HM-Fc incubated at 4°C for twelve weeks was 28.3% compared to the same samples stored at -80°C. Similarly, the samples of HM-Fc incubated at 40°C for twelve weeks showed a 52.4 % decrease in response compared to the control samples of HM-Fc stored at -80°C. A further decrease in response at an elevated temperature illustrated the instability of HM-Fc, presumably due to chemical and physical degradations. Man5-Fc showed a similar binding response profile to HM-Fc at the low and elevated temperatures. Compared to the GlcNAc-Fc stored at -80°C, the GlcNAc-Fc samples stored at 4°C and 40°C for twelve weeks showed 36.0% and 73.14% decrease in binding response, respectively. This higher percentage of decrease in binding response of the GlcNAc-Fc compared to HM-Fc and Man5-Fc was presumably due to the differences in the glycosylation state. In other words, GlcNAc-Fc contained a more truncated glycan (single N-Acetylglucosamine), potentially leading to aggregation and further physical degradation.

Overall the data highlights the use of longer incubation time to compare samples incubated at low and high temperatures to observe apparent differences, which were not possible to differentiate at a lower temperature and shorter incubation time. This stress condition and techniques developed in this study can be applied when comparing the originator with its biosimilar product, in the biosimilar comparability analysis.

4.5 Conclusion

The functional activities of homogeneous glycoforms were characterized after incubating at elevated and low temperatures. The data indicated samples stored at the elevated temperature showed a significant decrease in binding affinities. Additionally, a reduction in binding response to receptor (i.e., measured using the Fc immobilized format) was observed for the samples stored at the elevated temperature. Samples stored at -80˚C and 4˚C showed a moderate change in binding affinities as well as binding response to FcγRIIIa. Mass spectrometry characterization indicated significant chemical modification for samples incubated at the elevated temperature, presumably due to oxidation, while samples stored at a low temperature showed a moderate change in the chemical modification. Concentration measurement using BLI for all glycoforms demonstrated a decreasing trend when stored at low and elevated temperatures. N297Q-Fc showed the lowest concentration, presumably due to precipitation and aggregation during storage. When the two immobilization formats were compared (Fc-immobilized vs. receptor-immobilized), a significant difference in binding affinities was observed. This was due to the differences in the mechanism of binding between the two formats as described in chapter 3. Moreover, the data collected showed significant differences between the two formats in detecting a change in binding affinities attributed to the stress condition. The low

and elevated temperatures generated physical and chemical degradation products after incubation of the samples for twelve weeks, which ultimately resulted in lower binding affinities to FcγRIIIa. More studies are required in the future to understand further if the decrease in binding affinities was because of chemical modification, aggregation and/or a combination of both.

4.6 Figures

Figure 1. Intact protein ESI-MS analysis of tested IgG1 Fc glycoforms under reducing conditions. Samples were incubated at -80˚C, 4˚C, and 40˚C for two, four and twelve weeks. Figure 1A, 1B, 1C, and 1D are for HM-Fc, Man5-Fc, GlcNAc-Fc, and N297Q-Fc, respectively.

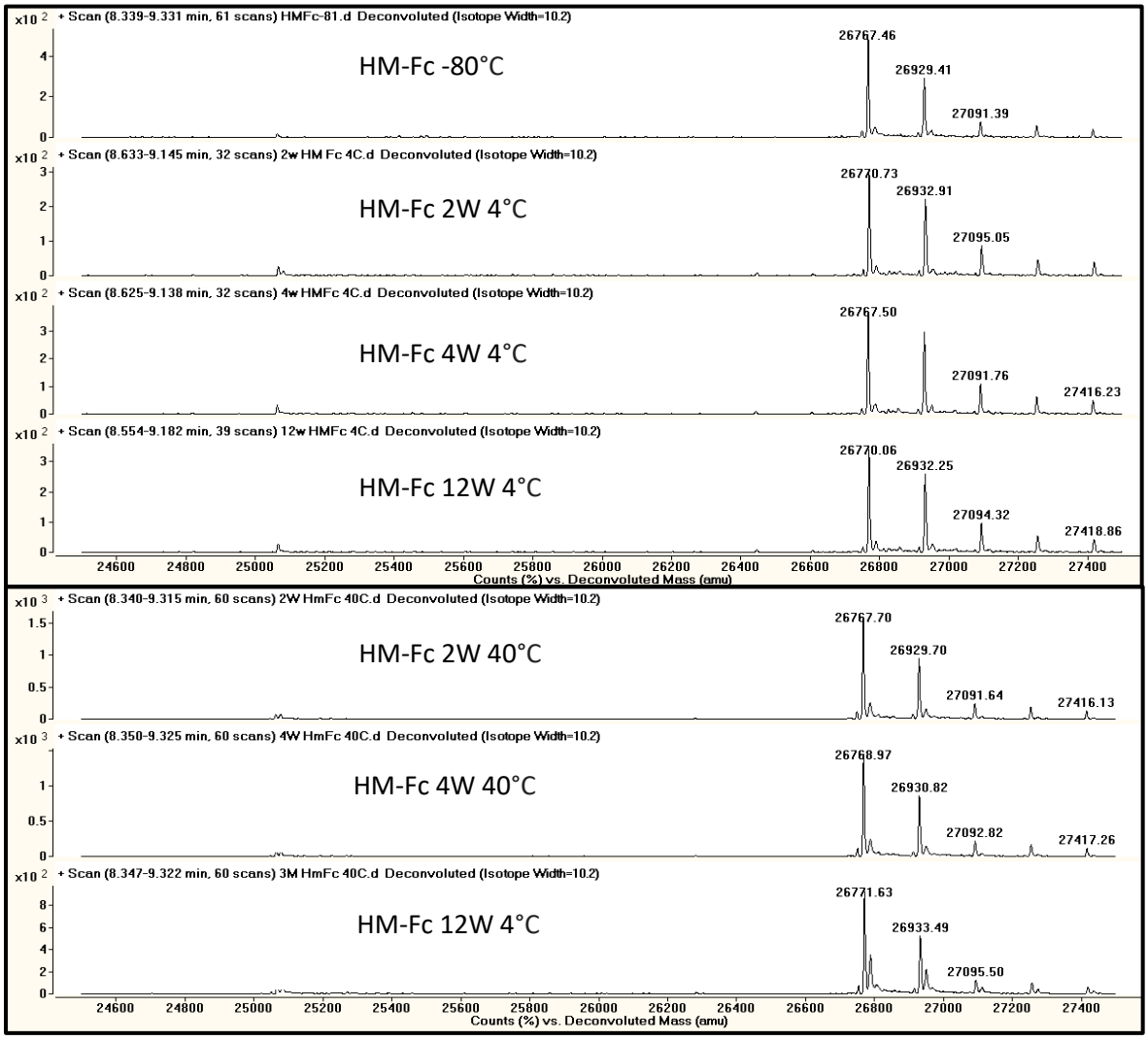

Figure 1A

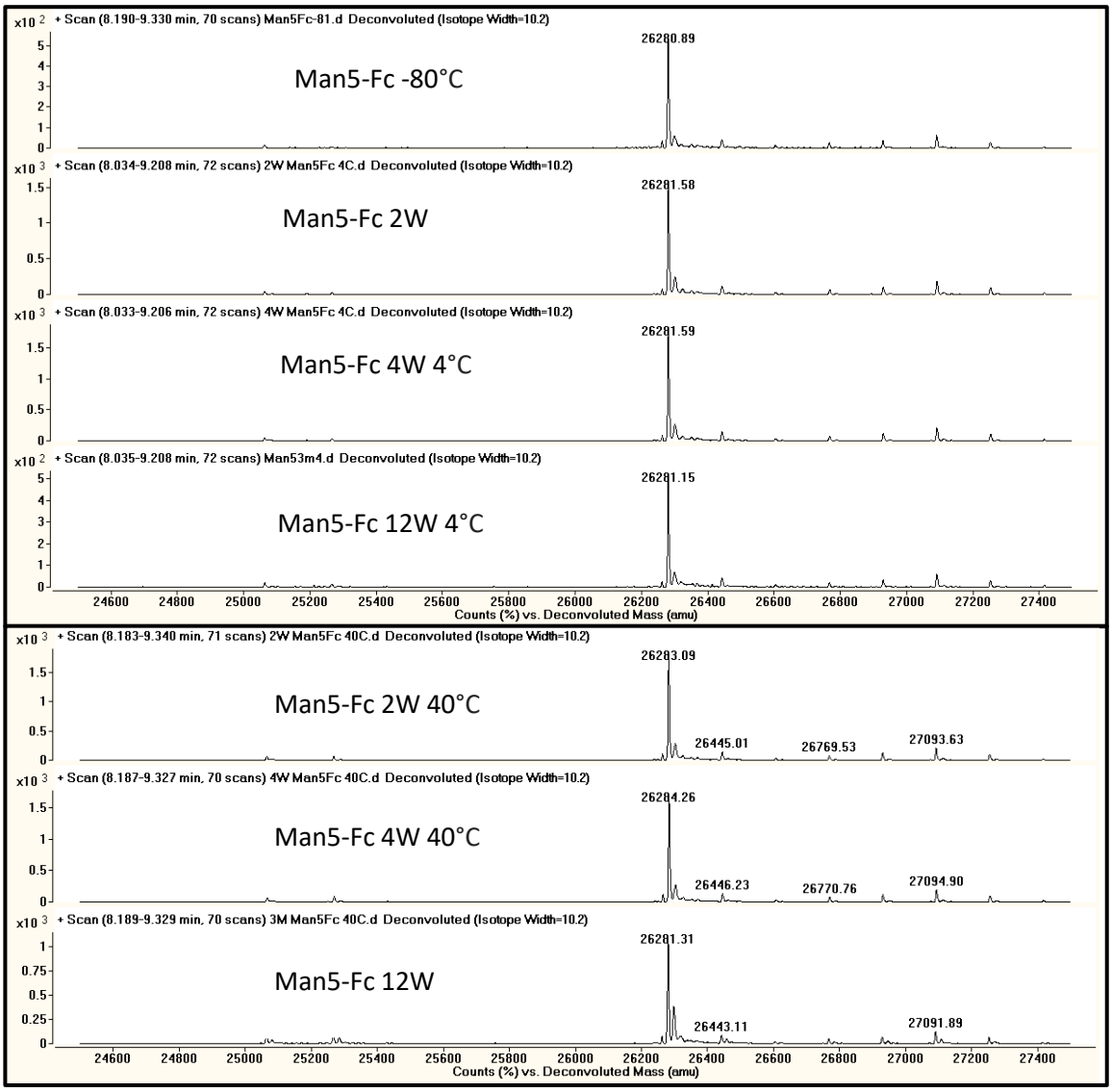
+ Scan (8.190-9.330 min, 70 scans) Man5Fc-81.d Deconvoluted (Isotope Width=10.2)
26280.89
Man5-Fc -80°C
+ Scan (8.034-9.208 min, 72 scans) 2W Man5Fc 4C.d Deconvoluted (Isotope Width=10.2)
26281.58
Man5-Fc 2W
+ Scan (8.033-9.206 min, 72 scans) 4W Man5Fc 4C.d Deconvoluted (Isotope Width=10.2)
26281.59
Man5-Fc 4W 4°C
+ Scan (8.035-9.208 min, 72 scans) Man53m4.d Deconvoluted (Isotope Width=10.2)
26281.15
Man5-Fc 12W 4°C
Counts (%) vs. Deconvoluted Mass (amu)
+ Scan (8.183-9.340 min, 71 scans) 2W Man5Fc 40C.d Deconvoluted (Isotope Width=10.2)
26283.09
26445.01
26769.53
27093.63
Man5-Fc 2W 40°C
+ Scan (8.187-9.327 min, 70 scans) 4W Man5Fc 40C.d Deconvoluted (Isotope Width=10.2)
26284.26
26446.23
26770.76
27094.90
Man5-Fc 4W 40°C
+ Scan (8.189-9.329 min, 70 scans) 3M Man5Fc 40C.d Deconvoluted (Isotope Width=10.2)
26281.31
26443.11
27091.89
Man5-Fc 12W
Counts (%) vs. Deconvoluted Mass (amu)

Figure 1B

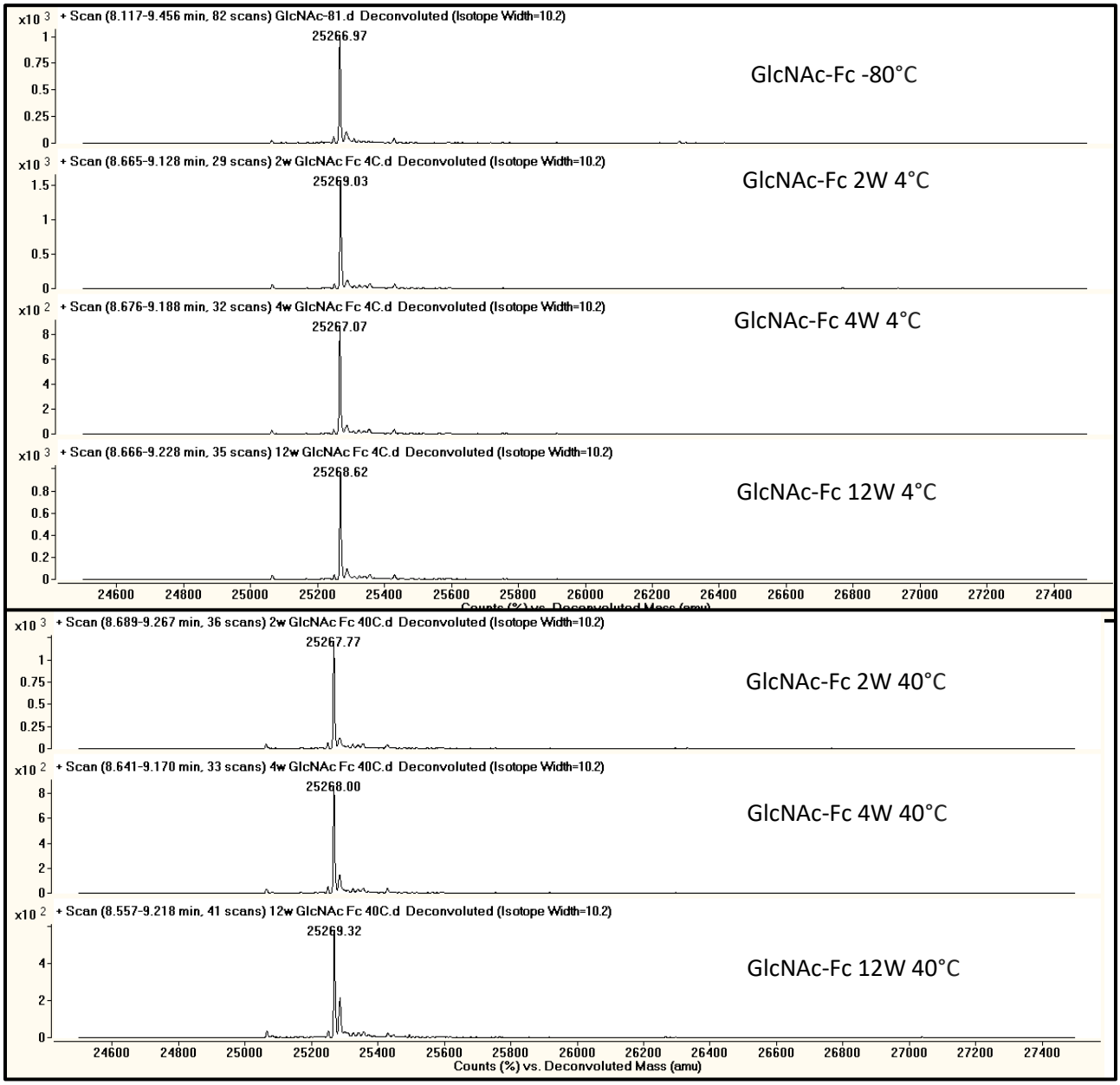
+ Scan (8.117-9.456 min, 82 scans) GlcNAc-81.d Deconvoluted (Isotope Width=10.2)
25266.97
GlcNAc-Fc -80°C
+ Scan (8.665-9.128 min, 29 scans) 2w GlcNAc Fc 4C.d Deconvoluted (Isotope Width=10.2)
25269.03
GlcNAc-Fc 2W 4°C
+ Scan (8.676-9.188 min, 32 scans) 4w GlcNAc Fc 4C.d Deconvoluted (Isotope Width=10.2)
25267.07
GlcNAc-Fc 4W 4°C
+ Scan (8.666-9.228 min, 35 scans) 12w GlcNAc Fc 4C.d Deconvoluted (Isotope Width=10.2)
25268.62
GlcNAc-Fc 12W 4°C
+ Scan (8.689-9.267 min, 36 scans) 2w GlcNAc Fc 40C.d Deconvoluted (Isotope Width=10.2)
25267.77
GlcNAc-Fc 2W 40°C
+ Scan (8.641-9.170 min, 33 scans) 4w GlcNAc Fc 40C.d Deconvoluted (Isotope Width=10.2)
25268.00
GlcNAc-Fc 4W 40°C
+ Scan (8.557-9.218 min, 41 scans) 12w GlcNAc Fc 40C.d Deconvoluted (Isotope Width=10.2)
25269.32
GlcNAc-Fc 12W 40°C
24600 24800 25000 25200 25400 25600 25800 26000 26200 26400 26600 26800 27000 27200 27400
Counts (%) vs. Deconvoluted Mass (amu)

Figure 1C

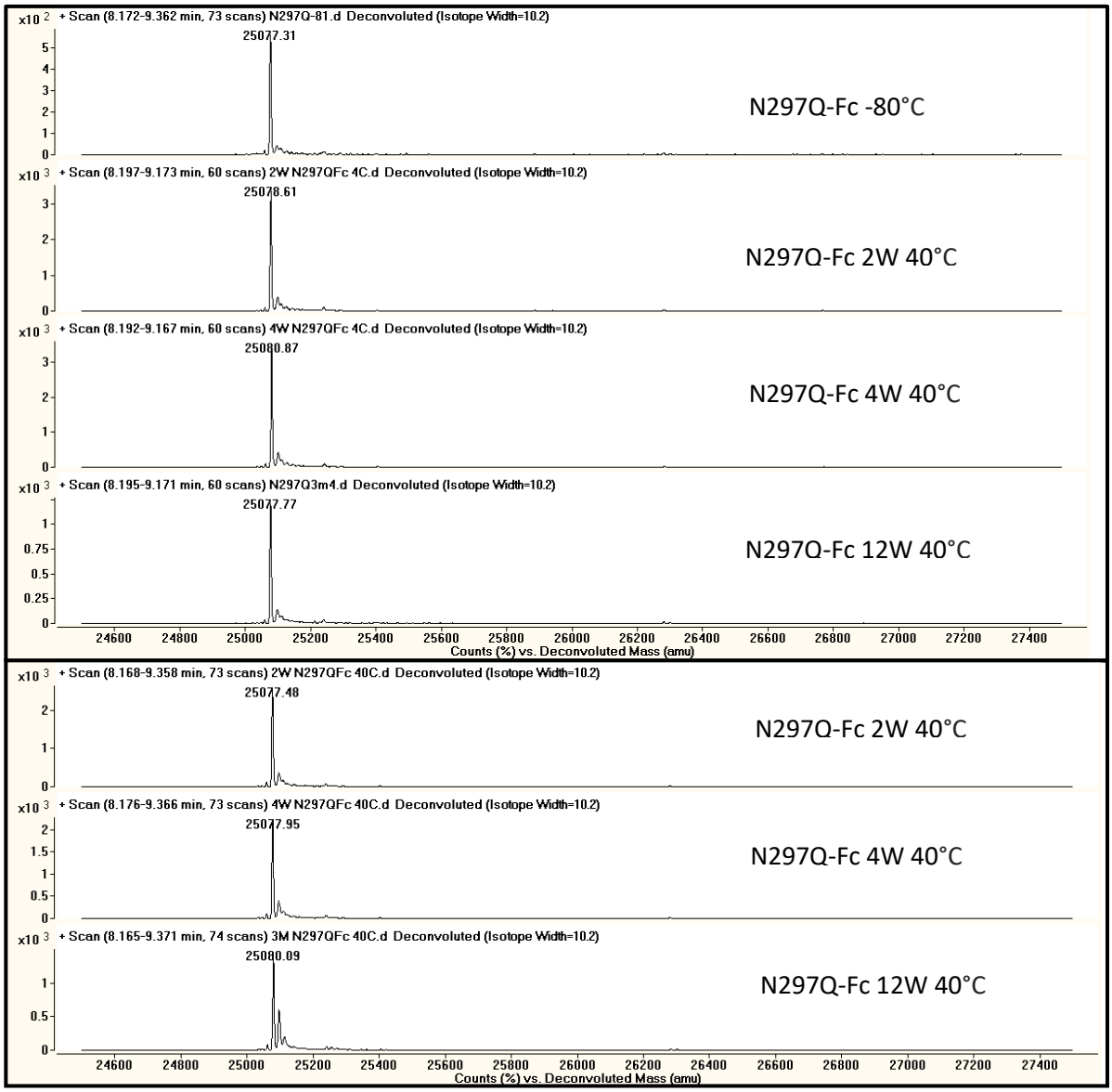
x10 2 + Scan (8.172-9.362 min, 73 scans) N297Q-81.d Deconvoluted (Isotope Width=10.2)
25077.31
N297Q-Fc -80°C
x10 3 + Scan (8.197-9.173 min, 60 scans) 2W N297QFc 4C.d Deconvoluted (Isotope Width=10.2)
25078.61
N297Q-Fc 2W 40°C
x10 3 + Scan (8.192-9.167 min, 60 scans) 4W N297QFc 4C.d Deconvoluted (Isotope Width=10.2)
25080.87
N297Q-Fc 4W 40°C
x10 3 + Scan (8.195-9.171 min, 60 scans) N297Q3m4.d Deconvoluted (Isotope Width=10.2)
25077.77
N297Q-Fc 12W 40°C
24600 24800 25000 25200 25400 25600 25800 26000 26200 26400 26600 26800 27000 27200 27400
Counts (%) vs. Deconvoluted Mass (amu)
x10 3 + Scan (8.168-9.358 min, 73 scans) 2W N297QFc 40C.d Deconvoluted (Isotope Width=10.2)
25077.48
N297Q-Fc 2W 40°C
x10 3 + Scan (8.176-9.366 min, 73 scans) 4W N297QFc 40C.d Deconvoluted (Isotope Width=10.2)
25077.95
N297Q-Fc 4W 40°C
x10 3 + Scan (8.165-9.371 min, 74 scans) 3M N297QFc 40C.d Deconvoluted (Isotope Width=10.2)
25080.09
N297Q-Fc 12W 40°C
24600 24800 25000 25200 25400 25600 25800 26000 26200 26400 26600 26800 27000 27200 27400
Counts (%) vs. Deconvoluted Mass (amu)

Figure 1D

Figure 2. The concentration of IgG1 Fc glycoforms measured using Bio-Layer Interferometry (BLI). Protein G biosensors were used to determine the concentration of samples incubated for two, four, and twelve weeks at -80˚C, 4˚C, and 40˚C. Figure 1A and Figure 2A and 2B represent for the samples incubated at 4˚C and 40˚C, respectively.

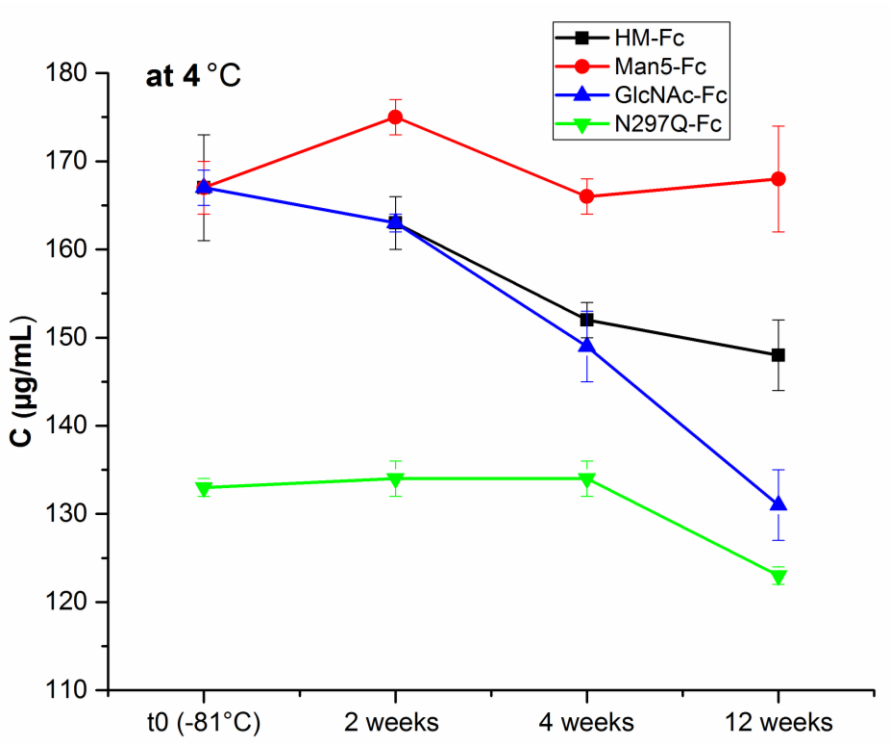

Figure 2A

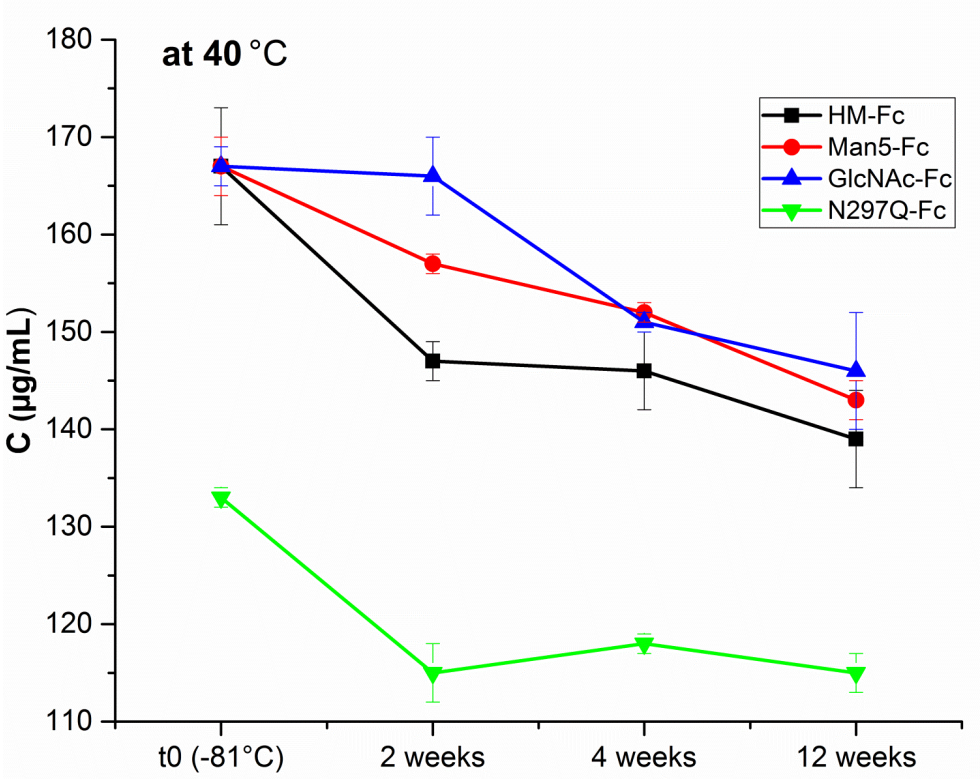
at 40 °C
HM-Fc
Man5-Fc
GlcNAc-Fc
N297Q-Fc
C (µg/mL)
180
170
160
150
140
130
120
110
t0 (-81°C)
2 weeks
4 weeks
12 weeks

Figure 2B

Figure 3. Bar graphs show K_D values for samples of IgG1 Fc incubated at low and elevated temperatures for two, four, and twelve weeks. The K_D values were determined using the Fc-Immobilized format.

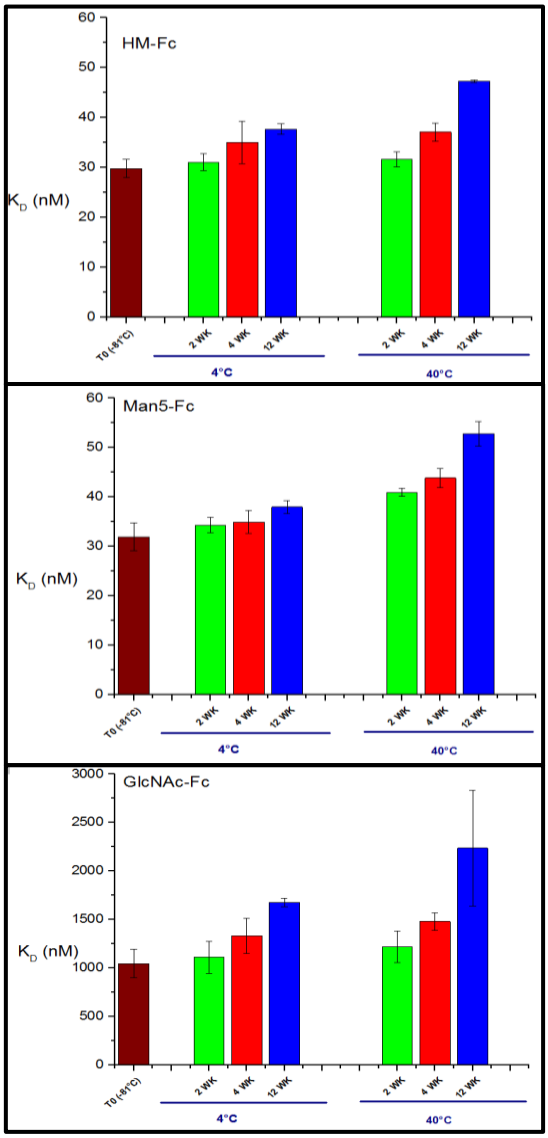

Figure 4. Bar graphs show the k_{on}, and k_{off} values for IgG1 Fc glycoforms measured using the Fc-Immobilized format.

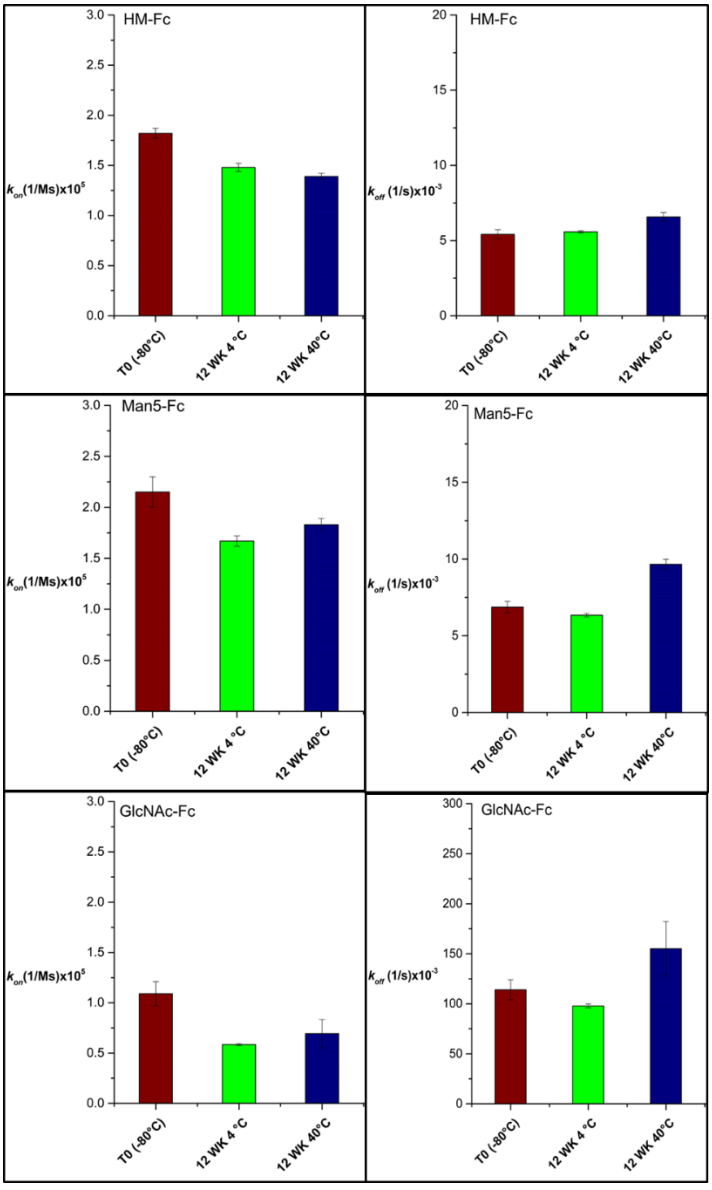

Figure 5. The bar graph show K_D values for samples of IgG1 Fc incubated at -80˚C, 4˚C, and 40˚C for twelve weeks measured using the receptor-Immobilized format.

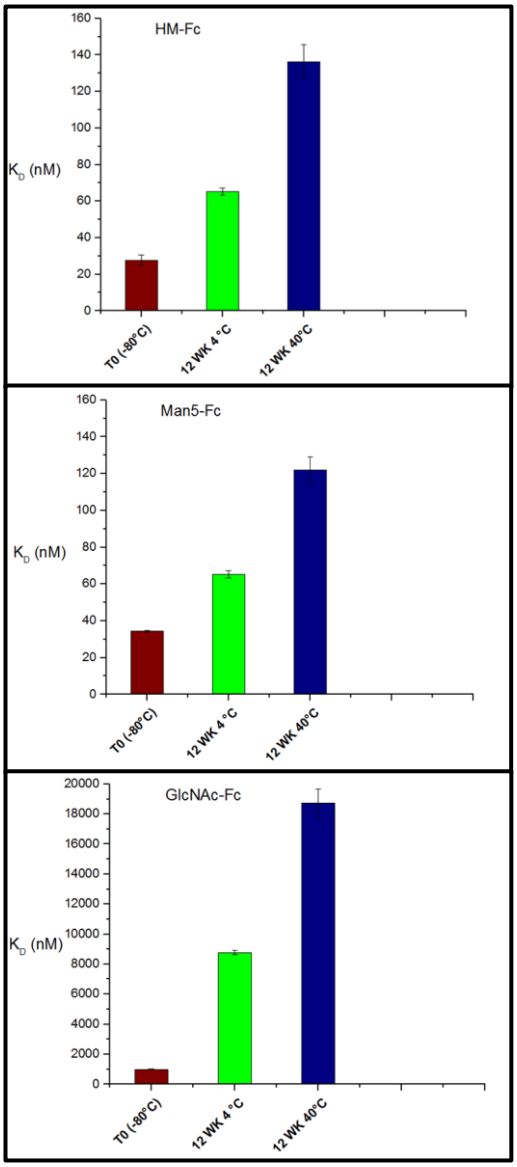

Figure 6. Bar graphs of the k_{on} and k_{off} values for samples of IgG1 Fc incubated at -80˚C, 4˚C, and 40˚C for twelve weeks measured using the receptor-Immobilized format.

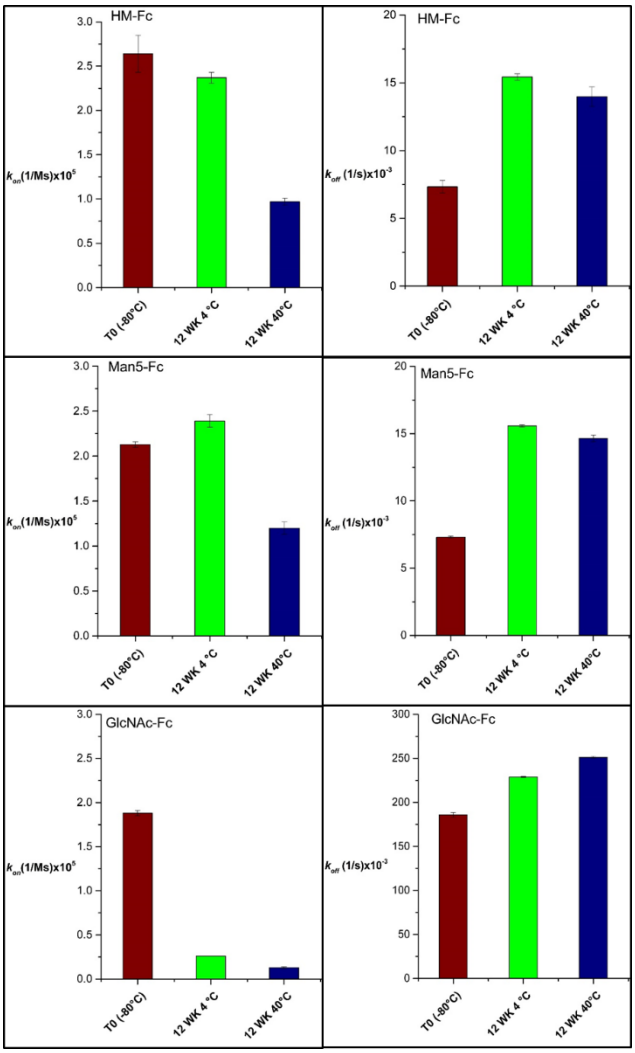

Figure 7. The binding responses of IgG1 Fc glycoform to FcγRIIIa measured the Fc-immobilized format. The samples were incubated at -80˚C, 4˚C, and 40˚C for two, four, and twelve weeks.

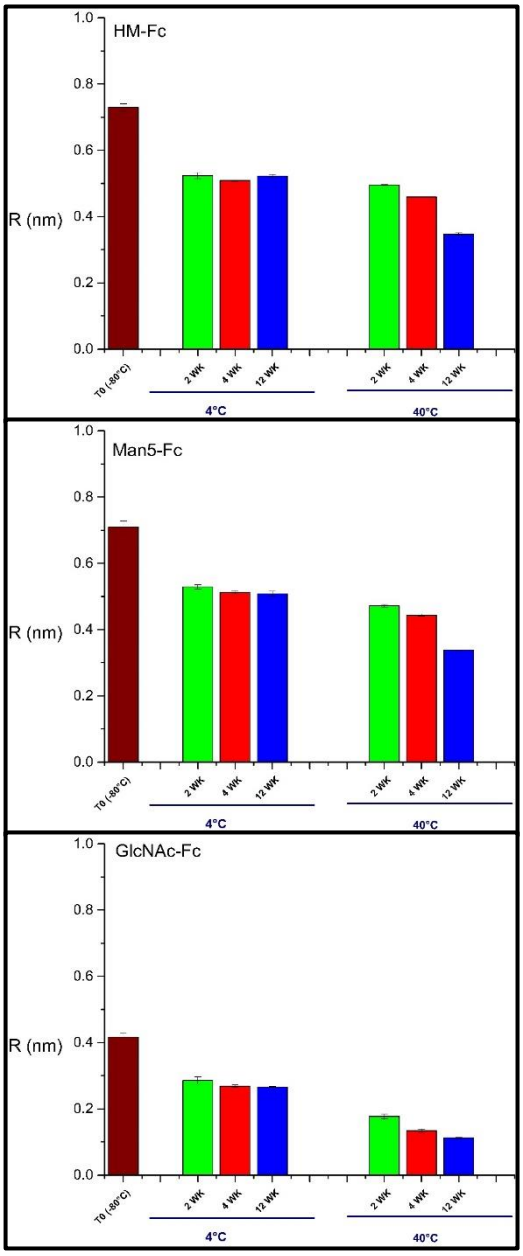

Figure 8. Representative binding response curves measured using the Fc-immobilized format. Figure 8A, 8B, and 8C represent for HM-Fc, Man5-Fc, and GlcNAc-Fc, respectively.

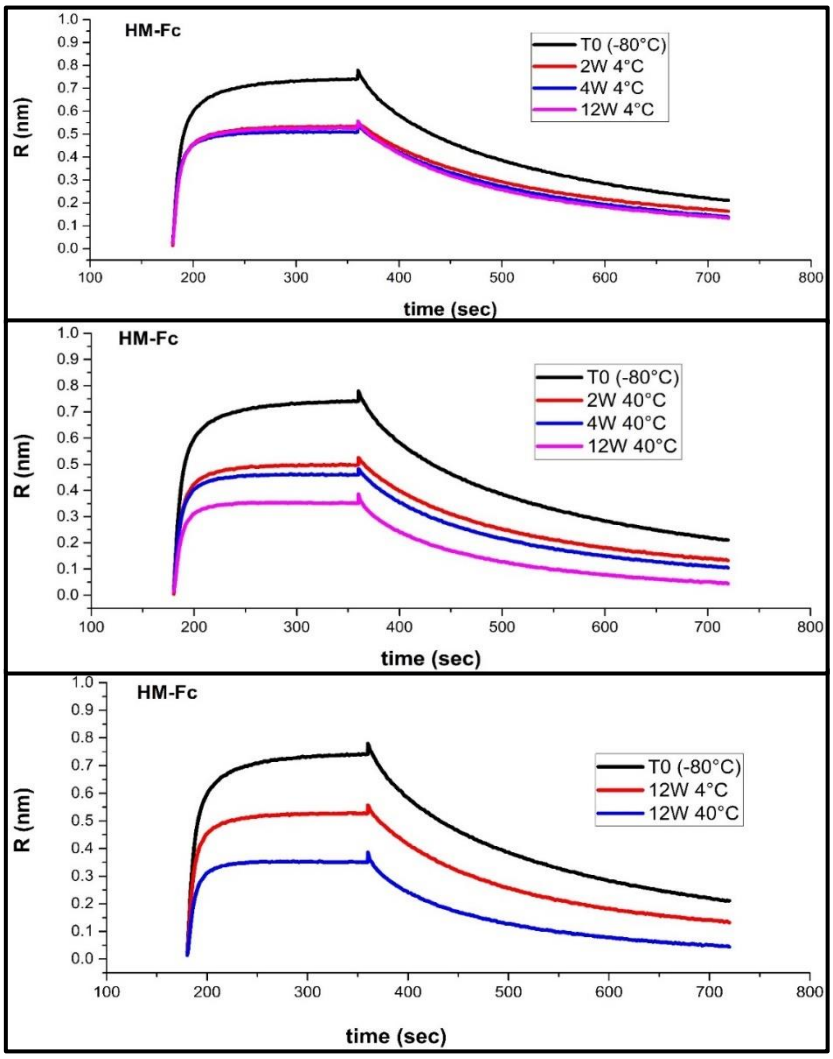

Figure 8A

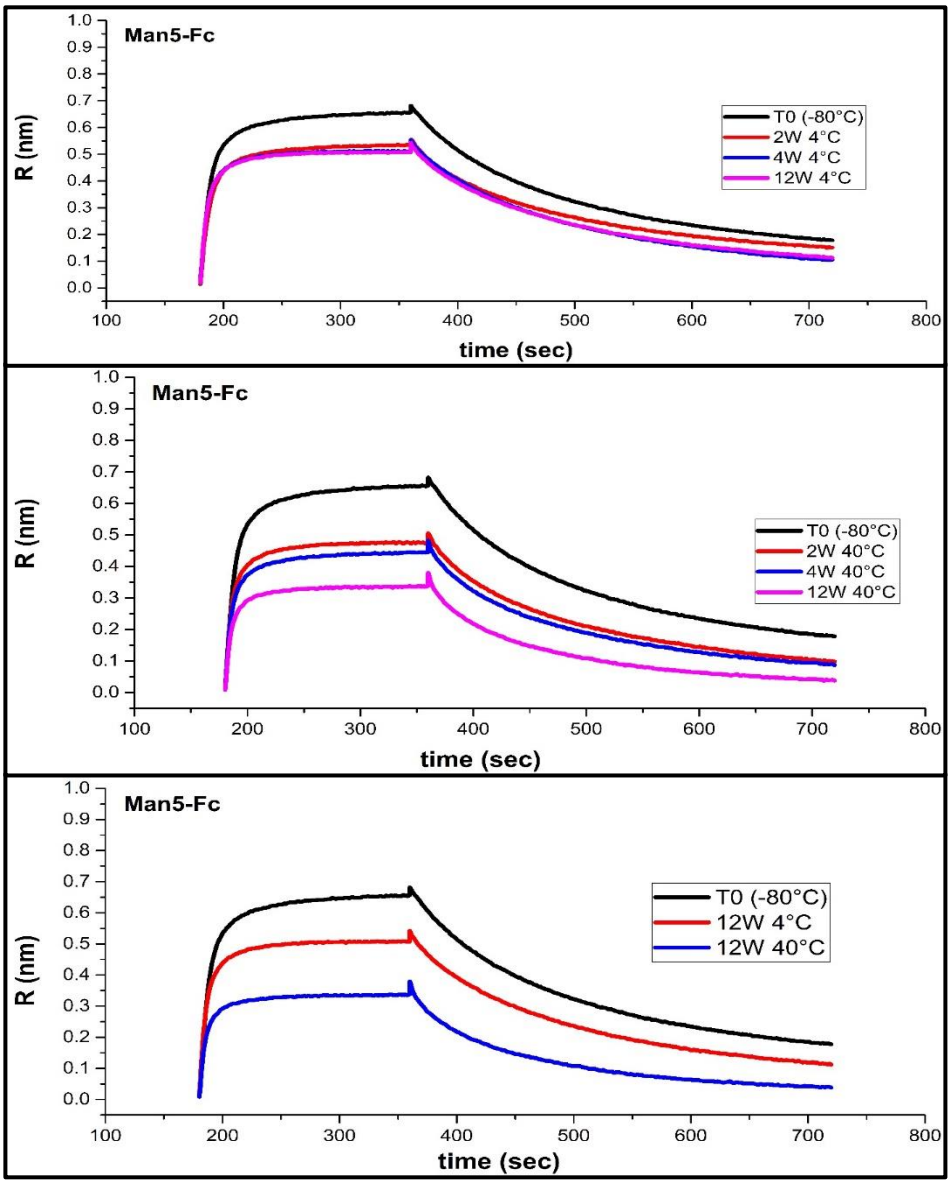
Man5-Fc
R (nm)
time (sec)
T0 (-80°C)
2W 4°C
4W 4°C
12W 4°C
Man5-Fc
R (nm)
time (sec)
T0 (-80°C)
2W 40°C
4W 40°C
12W 40°C
Man5-Fc
R (nm)
time (sec)
T0 (-80°C)
12W 4°C
12W 40°C

Figure 8B

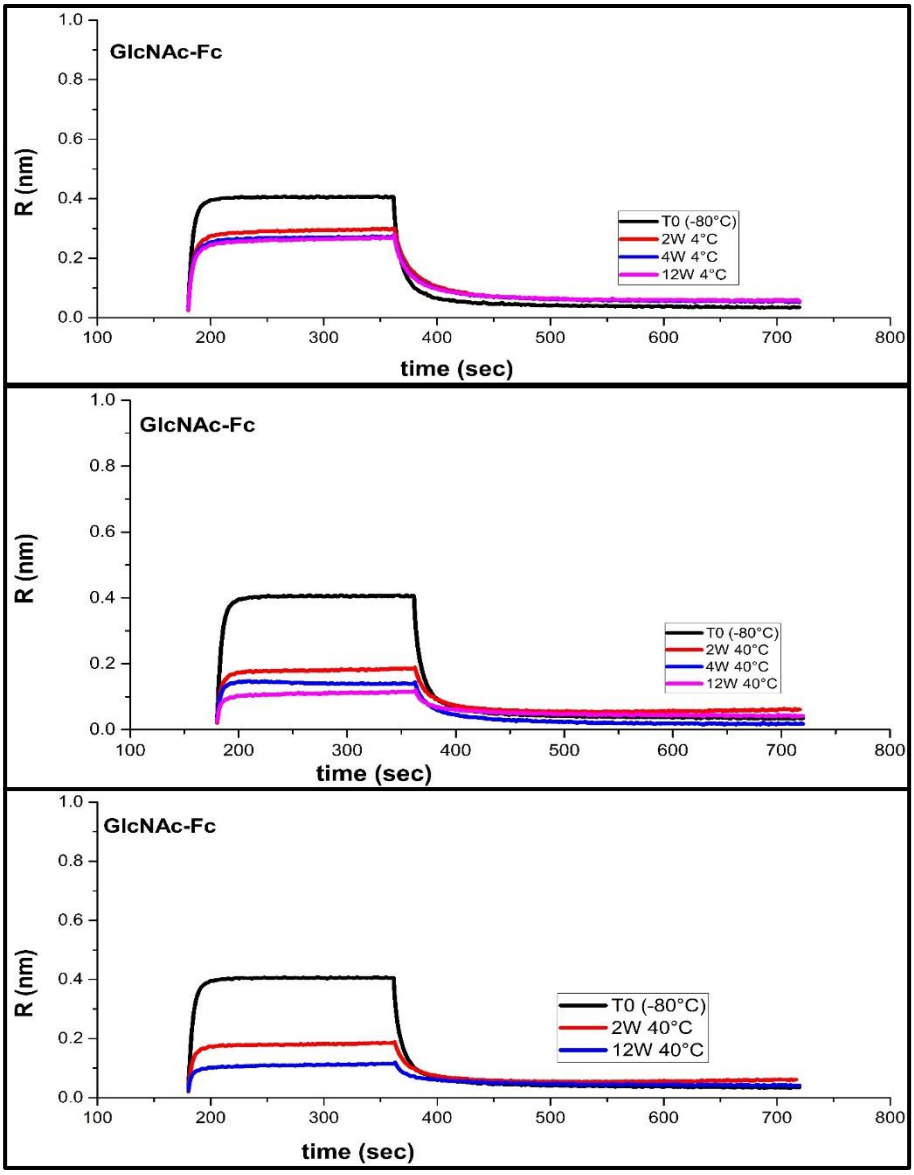
GlcNAc-Fc
R (nm)
time (sec)
T0 (-80°C)
2W 4°C
4W 4°C
12W 4°C
GlcNAc-Fc
R (nm)
time (sec)
T0 (-80°C)
2W 40°C
4W 40°C
12W 40°C
GlcNAc-Fc
R (nm)
time (sec)
T0 (-80°C)
2W 40°C
12W 40°C

Figure 8C

Figure 9. Representative fitting binding curves for the interaction of IgG1 Fc with FcγRIIIa measured using the Fc-immobilized format. Figure 9A, 9B, and 9C represent for HM-Fc, Man5-Fc, and GlcNAc-Fc, respectively.

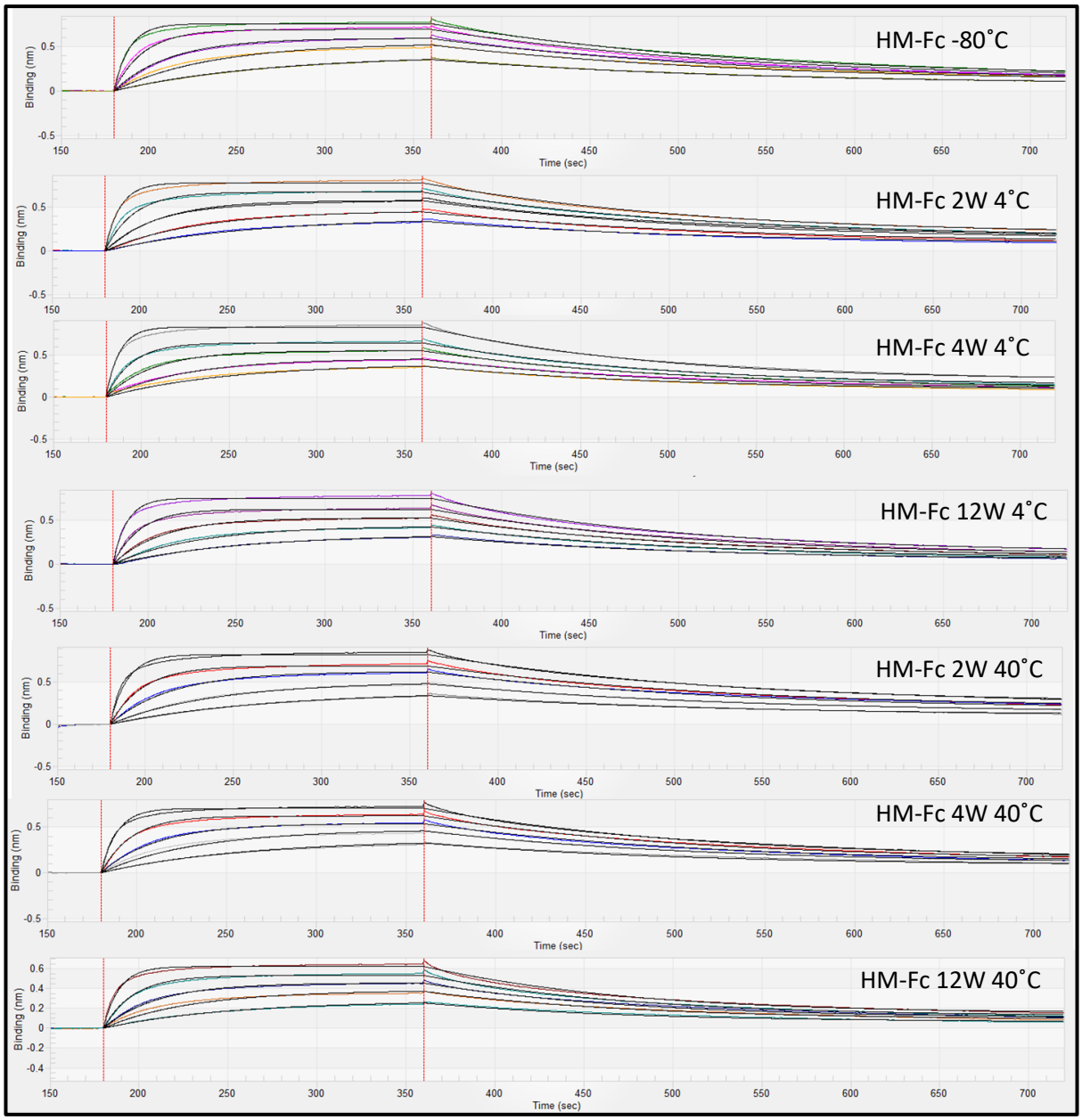

Figure 9A

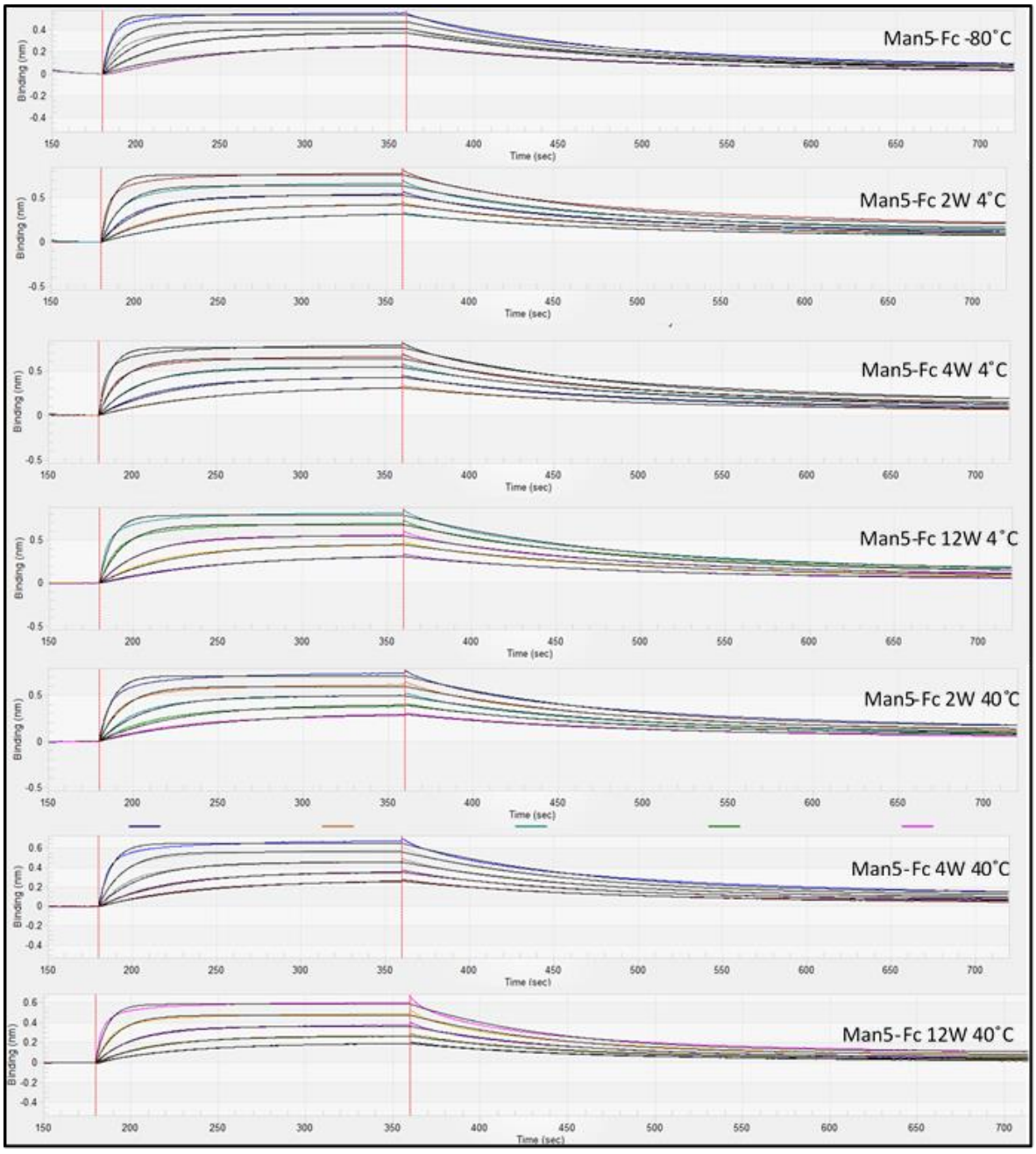
Man5-Fc -80˚C
Man5-Fc 2W 4˚C
Man5-Fc 4W 4˚C
Man5-Fc 12W 4˚C
Man5-Fc 2W 40˚C
Man5-Fc 4W 40˚C
Man5-Fc 12W 40˚C
Binding (nm)
Time (sec)

Figure 9B

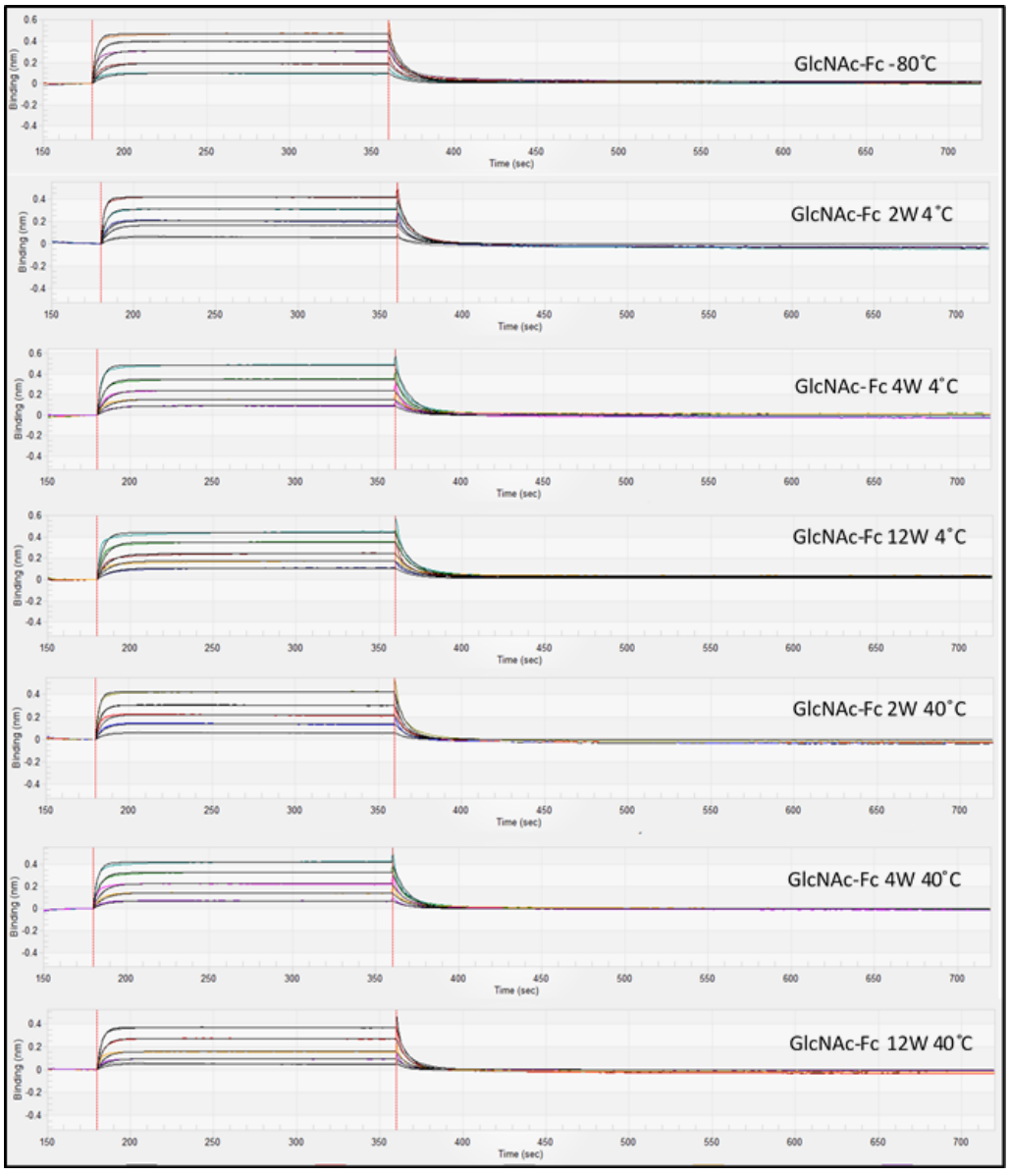
GlcNAc-Fc -80˚C
GlcNAc-Fc 2W 4˚C
GlcNAc-Fc 4W 4˚C
GlcNAc-Fc 12W 4˚C
GlcNAc-Fc 2W 40˚C
GlcNAc-Fc 4W 40˚C
GlcNAc-Fc 12W 40˚C
Binding (nm)
Time (sec)

Figure 9C

Figure 10. Representative fitted binding curves for the interaction of IgG1 Fc with FcγRIIIa. Samples were incubated for twelve weeks at -80˚C, 4˚C, and 40˚C. The binding interactions were measured using the receptor-immobilized format.

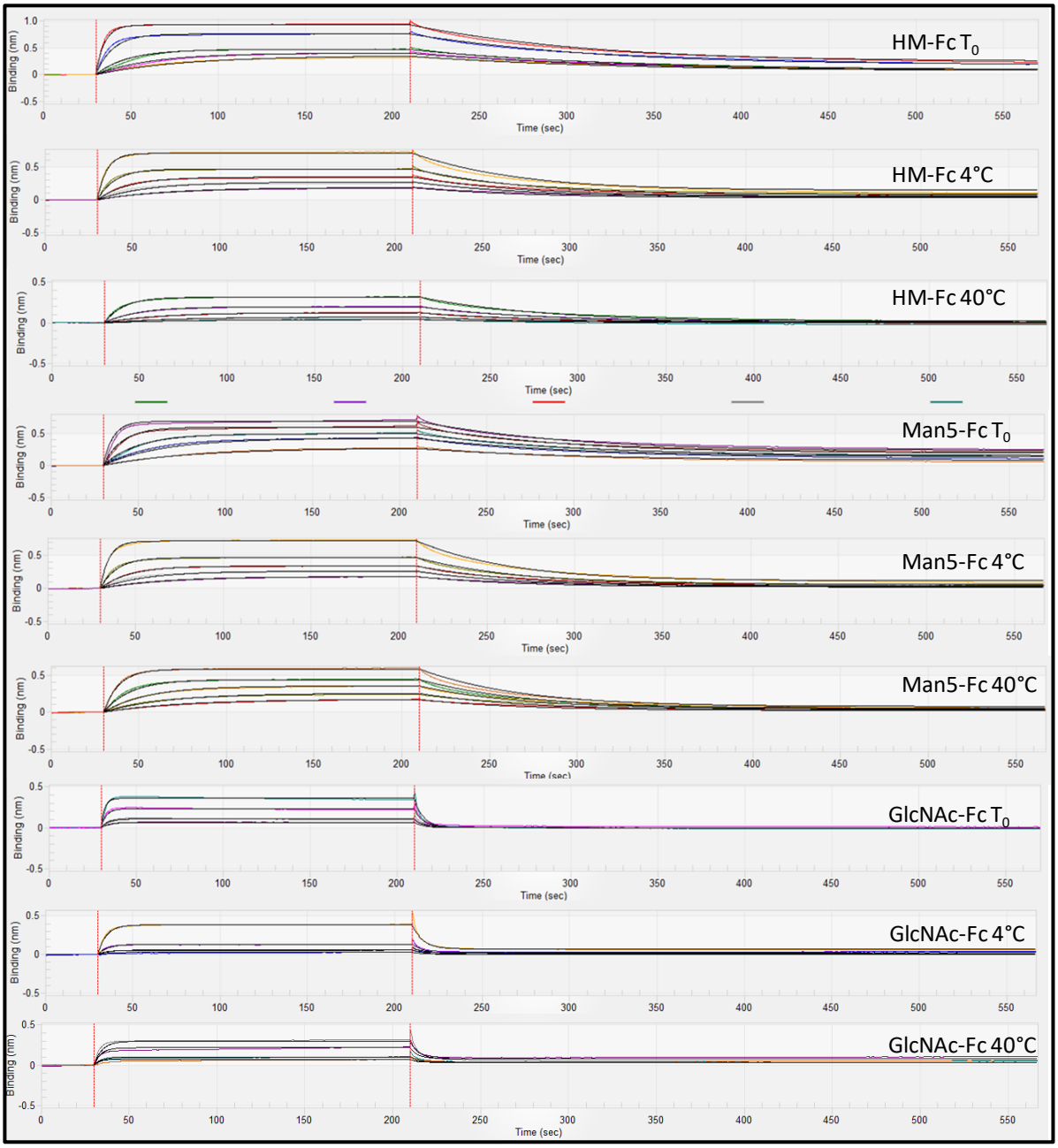

4.7 Tables

Table 1. Samples of IgG1 Fc incubated at low and elevated temperatures and the buffer condition utilized in this study.

IgG1 Fc glycoforms	Buffer condition	Time in weeks	Sample 1	Sample 2
HM-Fc	Citrate-phosphate pH 6.0 buffer with, 150 mM NaCl	0	- 80°C	- 80°C
		2	4°C	40°C
		4	4°C	40°C
		12	4°C	40°C
Man5-Fc	Citrate-phosphate pH 6.0 buffer with, 150 mM NaCl	0	- 80°C	- 80°C
		2	4°C	40°C
		4	4°C	40°C
		12	4°C	40°C
GlcNAc-Fc	Citrate-phosphate pH 6.0 buffer with, 150 mM NaCl	0	- 80°C	- 80°C
		2	4°C	40°C
		4	4°C	40°C
		12	4°C	40°C
N297Q-Fc	Citrate-phosphate pH 6.0 buffer with, 150 mM NaCl	0	- 80°C	- 80°C
		2	4°C	40°C
		4	4°C	40°C
		12	4°C	40°C

Table 2. Percentages of oxidation estimated from the peak intensity of the intact protein.

Incubation time and temperature	Percentages of oxidation			
	HM-Fc	Man5-Fc	GlcNAc-Fc	N297Q-Fc
T_0 -80˚C	8.7	9.5	8.0	7.1
2 WK / 4˚C	8.7	12.1	8.1	10.2
4 WK / 4˚C	9.8	12.9	8.1	10.7
12 WK/ 4˚C	11.6	13.7	8.8	11.1
2 WK / 40˚C	13.4	13.5	10.4	12.5
4 WK / 40˚C	14.1	13.7	14.4	15.4
12 WK/ 40˚C	28.6	26.1	27.2	30.1

Table 3. The concentration of IgG1 Fc glycoforms measured using biolayer interferometry**.**

Incubation time and temperature	Concentration in µg/mL			
	HM-Fc	Man5-Fc	GlcNAc-Fc	N297Q-Fc
T_0 -80˚C	167±6	167±3	167±2	133±1
2 WK / 4˚C	163±3	175±2	163±1	134±2
4 WK / 4˚C	152±2	166±2	149±4	134±2
12 WK/ 4˚C	148±4	168±6	132±4	123 ±1
2 WK / 40˚C	147±2	158±1	166±4	115±3
4 WK / 40˚C	146±4	152±1	151±1	118±1
12 WK/ 40˚C	139±5	143±2	146±6	115±2

Table 4. The k_{on} , k_{off}, and K_D values for samples of IgG1 Fc incubated at -80˚C, 4˚C, and 40˚C for two, four and twelve weeks. The measurement was performed using the Fc-immobilized format. Table 4A, 4B, and 4C represent HM-Fc, Man5-Fc, and GlcNAc-Fc, respectively.

HM-Fc storage time/temperature	k_{on} (1/Ms)	Avg. k_{on} (1/Ms)x10^5	k_{off} (1/s)	Avg. k_{off} (1/s)X10-3	K_D (nM)	Avg. K_D (nM)
T_0 -80 ˚C	1.891e5	1.8±0.0	4.379e-3	5.4±0.3	30.4	29.8±1.8
	1.807e5		5.384e-3		29.80	
	1.786e5		5.143e-3		28.79	
2 WK / 4 ˚C	1.437e5	1.5±0.1	4.695e-3	4.7±0.1	31.95	31.0±1.7
	1.601e5		4.848e-3		30.28	
	1.557e5		4.725e-3		30.34	
4WK / 4 ˚C	1.606e5	1.5±0.1	5.501e-3	5.2±0.3	34.25	35.0±4.2
	1.551e5		5.344e-3		34.46	
	1.329e5		4.821e-3		36.28	
12WK/ 4 ˚C	1.513e5	1.5±0.0	5.646e-3	5.6±0.1	37.29	37.7 ±1.1
	1.487e5		5.501e-3		36.99	
	1.436e5		5.608e-3		39.05	
2 WK / 40 ˚C	1.266e5	1.3±0.1	4.035e-3	4.2±0.1	31.88	31.7±1.5
	1.35e5		4.25e-3		31.49	
	1.348e5		4.25e-3		31.53	
4WK / 40˚C	1.359e5	1.3±0.1	4.968e-3	4.9±0.1	36.57	37.1±1.8
	1.33e5		4.925e-3		37.02	
	1.254e5		4.686e-3		37.37	
12 WK/ 40˚C	1.395e5	1.4±0.0	6.589e-3	6.6±0.3	47.23	47.3±0.2
	1.349e5		6.277e-3		46.52	
	1.418e5		6.854e-3		48.34	

Table 4A

Man5-Fc storage time/temperature	k_{on} (1/Ms)	Avg. k_{on} (1/Ms)x10^5	k_{off} (1/s)	Avg. k_{off} (1/s)X10^{-3}	K_D (nM)	Avg. K_D (nM)
T_0 -80 ˚C	2.15e^5	2.1±0.1	6.94e^{-3}	6.9±0.4	32.76	31.9±2.8
	2.32e^5		7.207e^{-3}		31.07	
	2.015e^5		6.46e^{-3}		32.05	
2 WK / 4 ˚C	1.794e^5	1.9±0.1	6.149e^{-3}	6.4±0.2	34.27	34.3±1.5
	1.905e^5		6.530e^{-3}		34.28	
	1.873e^5		6.472e^{-3}		34.56	
4WK / 4 ˚C	1.732e^5	1.7±0.0	6.068e^{-3}	6.1±0.0	35.04	34.9±2.3
	1.756e^5		6.099e^{-3}		34.74	
	1.732e^5		6.042e^{-3}		34.89	
12 WK/ 4 ˚C	1.627e^5	1.7±0.0	6.232e^{-3}	6.3±0.1	38.31	38.0±1.3
	1.659e^5		6.333e^{-3}		38.18	
	1.734e^5		6.467e^{-3}		37.3	
2 WK / 40 ˚C	1.546e^5	1.6±0.0	6.442e^{-3}	6.4±0.0	41.66	40.9±0.8
	1.6e^5		6.441e^{-3}		40.27	
	1.573e^5		6.397e^{-3}		40.66	
4WK / 40˚C	1.547e^5	1.6±0.0	6.973e^{-3}	7.1±0.2	45.07	43.8±1.9
	1.63e^5		7.384e^{-3}		45.31	
	1.526e^5		7.006e^{-3}		45.90	
12 WK/ 40˚C	1.821e^5	1.8±0.1	9.478e^{-3}	9.7±0.3	52.05	52.8±2.5
	1.788e^5		9.465e^{-3}		52.94	
	1.901e^5		1.004e^{-2}		52.79	

Table 4B

GlcNAc-Fc storage time/temperature	k_{on} (1/Ms)	Avg. k_{on} (1/Ms)x10^5	k_{off} (1/s)	Avg. k_{off} (1/s)X10^{-3}	K_D (nM)	Avg. K_D (nM)
T_0 -80 ˚C	9.471e4	1.1±0.1	1.028e-1	114.0± 10.0	1086	1046±147
	1.153e5		1.222e-2		1060	
	1.168e5		1.166e-1		997.9	
2 WK / 4 ˚C	1.106e5	0.9±0.1	1.223e-2	110.23±11.0	1105	1111±166
	9.842e4		1.082e-1		1099	
	8.82e4		1.002e-1		1131	
4WK / 4 ˚C	7.813e4	0.8±0.1	1.049e-1	112.1±12.1	1342	1333±181
	8.194e4		1.059e-1		1292	
	9.191e4		1.256e-1		1367	
12WK/ 4 ˚C	5.807e4	0.6±0.0	0.9559e-1	97.9±2.0	1646	1675±45
	5.949e4		0.9986e-1		1679	
	5.787e4		0.9825e-1		1698	
2 WK / 40 ˚C	1.365e5	1.1±0.2	1.658e-1	150.7±15.0	1215	1218±162
	1.216e5		1.511e-1		1243	
	1.147e5		1.352e-1		1178	
4WK / 40˚C	0.7926e5	0.8±0.3	1.148e-1	122.0±6.0	1449	1479±89
	0.8444e5		1.25e-1		1480	
	0.8394e5		1.255e-1		1495	
12WK/ 40˚C	0.7098e5	0.7±0.1	1.554e-1	155.2±27.0	2189	2236±596
	0.8281e5		1.815e-1		2192	
	0.5412e5		1.283e-1		2370	

Table 4C

Table 5. The k_{on} , k_{off}, and K_D values for samples of IgG1 Fc incubated at -80˚C, 4˚C, and 40˚C for twelve weeks. The measurement was performed using the receptor immobilization format.

Glycoform storage time/temperature	k_{on} (1/Ms)	Avg. k_{on} (1/Ms)X10^5	k_{off} (1/s)	Avg. k_{off} (1/s)X10^{-3}	K_D (nM)	Avg. K_D (nM)
HM-Fc 4°C 12 WK	2.31E+05	2.4±0.1	1.57E-02	15.4±0.2	65.65	65.2 ± 2.0
	2.43E+05		1.55E-02		63.62	
	2.36E+05		1.52E-02		64.27	
HM-Fc 40 °C 12 WK	9.24E+04	1.0±0.0	1.27E-02	14.0 ± 0.7	137.8	136.3 ± 9.2
	1.00E+05		1.28E-02		126.6	
	9.71E+04		1.40E-02		144	
HM-Fc -80°C T_0	2.44E+05	2.6±0.2	6.85E-03	7.3± 0.5	28.13	27.8 ± 2.8
	2.85E+05		7.80E-03		27.37	
	2.63E+05		7.33E-03		27.91	
Man5-Fc 4°C 12 WK	2.31E+05	2.4±0.1	1.57E-02	15.6 ± 0.1	65.65	65.2± 1.9
	2.43E+05		1.55E-02		63.62	
	2.42E+05		1.56E-02		64.34	
Man5-Fc 40°C 12 WK	1.13E+05	1.2 ±0.1	1.44E-02	14.6±0.2	127.4	121.9± 7.1
	1.25E+05		1.49E-02		118.8	
	1.23E+05		1.47E-02		119.5	
Man5-Fc -80°C T_0	2.16E+05	2.1±0.0	7.26E-03	7.3±0.1	33.61	34.3 ± 0.6
	2.14E+05		7.38E-03		34.37	
	2.10E+05		7.30E-03		34.71	
GlcNAc-Fc 4°C 12 WK	2.60E+04	0.3±0.0	2.29E-01	228.9±0.4	883.6	8770.3 ± 143.4
	2.66E+04		2.29E-01		859.6	
	2.58E+04		2.29E-01		888.1	
GlcNAc-Fc 40°C 12 WK	1.38E+04	0.1 ±0.0	2.51E-01	251.1±0.9	18170	18746.0± 931.8
	1.26E+04		2.52E-01		19970	
	1.38E+04		2.51E-01		18200	
GlcNAc-Fc -80°C T_0	1.87E+05	1.9±0.0	1.86E-01	185.8± 2.7	1007	988.8 ± 21.8
	1.91E+05		1.83E-01		9577	
	1.85E+05		1.89E-01		1018	

Table 6. The binding responses of IgG1 Fc glycoforms to FcγRIIIa measured using the Fc immobilized format.

Incubation time and temperature	Binding Responses		
	HM- Fc	Man5-Fc	GlcNAc-Fc
T_0 -80˚C	0.729± 0.01	0.710± 0.018	0.417± 0.010
2 WK / 4˚C	0.523±0.009	0.529±0.006	0.286±0.011
4 WK/ 4˚C	0.509±0.002	0.512±0.004	0.268±0.004
12 WK/ 4˚C	0.522±0.005	0.508±0.007	0.266±0.001
2 WK / 40˚C	0.495±0.002	0.472±0.004	0.177±0.007
4 WK / 40˚C	0.459±0.001	0.444±0.003	0.134±0.005
12 WK/ 40˚C	0.347±0.003	0.338±0.001	0.112±0.002

4.8 References

1. W. Jiskoot, E. C. B., A.A. de Koning, J.N. Herron, D.J., Analytical approaches to the study of monoclonal antibody stability. *Pharm Res* **1990,** *7* (12).

2. Kroon DJ, B.-F. A., Lalan P, Identification of sites of degradation in a therapeutic monoclonal antibody by peptide mapping. *Pharm Res* **1992,** *9* (11), 1386-93.

3. Rao PE, K. D., Orthoclone OKT3. Chemical mechanisms and functional effects of degradation of a therapeutic monoclonal antibody. *Pharm Biotechnol* **1993,** *5*, 135-58.

4. Manning, M. C.; Chou, D. K.; Murphy, B. M.; Payne, R. W.; Katayama, D. S., Stability of Protein Pharmaceuticals: An Update. *Pharm Res* **2010,** *27* (4), 544-575.

5. Robinson, N. E.; Robinson, A. B., Deamidation of human proteins. *Proceedings of the National Academy of Sciences* **2001,** *98* (22), 12409-12413.

6. Brennan, T. V.; Clarke, S., Spontaneous degradation of polypeptides at aspartyl and asparaginyl residues: effects of the solvent dielectric. *Protein Science : A Publication of the Protein Society* **1993,** *2* (3), 331-338.

7. Geiger, T.; Clarke, S., Deamidation, isomerization, and racemization at asparaginyl and aspartyl residues in peptides. Succinimide-linked reactions that contribute to protein degradation. *Journal of Biological Chemistry* **1987,** *262* (2), 785-794.

8. Brennan TV, C. S., Spontaneous degradation of polypeptides at aspartyl and asparaginyl residues: effects of the solvent dielectric. *Protein Sci.* **1993,** *2*

(3), 331-8.

9. Aswad DW, P. M., Schurter BT, Isoaspartate in peptides and proteins: formation, significance, and analysis. *J Pharm Biomed Anal.* **2000** *21* (6), 1129-36.

10. B A Johnson; and, N. E. F.; Aswad, D. W., Protein carboxyl methyltransferase selectively modifies an atypical form of calmodulin. Evidence for methylation at deamidated asparagine residues. *J. Biol. Chem.* **1985,** *260* (20), 10913-6.

11. D. A. Lewis, A. W. G., W. S. Hancock and M. Costello, Characterization of Humanized Anti-TAC, an Antibody Directed against the Interleukin 2 Receptor, Using Electrospray Ionization Mass Spectrometry by Direct Infusion, LC/MS, and MS/MS. *Analytical Chemistry* **1994,** *66* (5), 585-595.

12. Werner WE, W. S., Mulkerrin M., The removal of pyroglutamic acid from monoclonal antibodies without denaturation of the protein chains. *Anal Biochem* **Anal Biochem. 2005 Jul 1;342(1):120-5,** *342* (1), 120-5.

13. Wang L, A. G., Lambert JM, Blättler W, Zhang W, Structural characterization of a recombinant monoclonal antibody by electrospray time-of-flight mass spectrometry. *Pharm Res.* **2005** *22* (8), 1338-49.

14. Liu, H.; Gaza-Bulseco, G.; Sun, J., Characterization of the stability of a fully human monoclonal IgG after prolonged incubation at elevated temperature. *Journal of Chromatography B* **2006,** *837* (1–2), 35-43.

15. Falconer, R. J.; Jackson-Matthews, D.; Mahler, S. M., Analytical strategies for assessing comparability of biosimilars. *Journal of Chemical Technology & Biotechnology* **2011,** *86* (7), 915-922.

16. Waterman, K. C.; Adami, R. C., Accelerated aging: Prediction of chemical stability of pharmaceuticals. *International Journal of Pharmaceutics* **2005,** *293* (1–2), 101-125.

17. Roberts, C. J., Kinetics of Irreversible Protein Aggregation: Analysis of Extended Lumry−Eyring Models and Implications for Predicting Protein Shelf Life. *The Journal of Physical Chemistry B* **2003,** *107* (5), 1194-1207.

18. Stamper, G. F.; Lambert, W. J., Accelerated Stability Testing of Proteins and Peptides: pH-Stability Profile of Insulinotropin Using Traditional Arrhenius and Non-Linear Fitting Analysis. *Drug Development and Industrial Pharmacy* **1995,** *21* (13), 1503-1511.

19. Hawe, A.; Wiggenhorn, M.; van de Weert, M.; Garbe, J. H. O.; Mahler, H.-c.; Jiskoot, W., Forced degradation of therapeutic proteins. *Journal of Pharmaceutical Sciences* **2012,** *101* (3), 895-913.

20. Wang, W.; Nema, S.; Teagarden, D., Protein aggregation—Pathways and influencing factors. *International Journal of Pharmaceutics* **2010,** *390* (2), 89-99.

21. Q5C Quality of biotechnological products: Stability testing of biotechnological/biological products. *Fed Regis* **1996,** *61* 36466–36474.

22. Barandun, S.; Kistler, P.; Jeunet, F.; Isliker, H., Intravenous Administration of Human γ-Globulin*. *Vox Sanguinis* **1962,** *7* (2), 157-174.

23. Ellis, E. F.; Henney, C. S., Adverse reactions following administration of human gamma globulin. *Journal of Allergy* **1969,** *43* (1), 45-54.

24. Luo, Q.; Joubert, M. K.; Stevenson, R.; Ketchem, R. R.; Narhi, L. O.; Wypych, J., Chemical Modifications in Therapeutic Protein Aggregates Generated under Different Stress Conditions. *Journal of Biological Chemistry* **2011,** *286* (28), 25134-25144.

25. Joubert, M. K.; Luo, Q.; Nashed-Samuel, Y.; Wypych, J.; Narhi, L. O., Classification and Characterization of Therapeutic Antibody Aggregates. *Journal of Biological Chemistry* **2011,** *286* (28), 25118-25133.

26. Carpenter, J. F.; Randolph, T. W.; Jiskoot, W.; Crommelin, D. J. A.; Russell Middaugh, C.; Winter, G.; Fan, Y.-X.; Kirshner, S.; Verthelyi, D.; Kozlowski, S.; Clouse, K. A.; Swann, P. G.; Rosenberg, A.; Cherney, B., Overlooking Subvisible Particles in Therapeutic Protein Products: Gaps That May Compromise Product Quality. *Journal of Pharmaceutical Sciences* **2009,** *98* (4), 1201-1205.

27. Mahler, H.-C.; Friess, W.; Grauschopf, U.; Kiese, S., Protein aggregation: Pathways, induction factors and analysis. *Journal of Pharmaceutical Sciences* **2009,** *98* (9), 2909-2934.

28. Philo, J. S., Is any measurement method optimal for all aggregate sizes and types? *AAPS J* **2006,** *8* (3), E564-E571.

29. JS, P., A critical review of methods for size characterization of non-particulate protein aggregates. *Curr Pharm Biotechnol* **2009** *10* (4), 359-72.

30. Silke Klick, P. G. M., Joop Waterval,* Thomas Eichinger, Christian Korn, Thijs K. Gerding, Alexander J.; Debets, C. S.-v. d. G., Cas van den Beld, Govert W. Somsen, and Gerhardus J. De Jong, Toward a Generic Approach for Stress Testing of Drug Substances and Drug Products. *Pharm Technol* **2005,** *29* 48–64.

31. Jaenicke, R., Stability and stabilization of globular proteins in solution. *Journal of Biotechnology* **2000,** *79* (3), 193-203.

32. Jaenicke, R., Protein stability and molecular adaptation to extreme conditons. *European Journal of Biochemistry* **1991,** *202* (3), 715-728.

33. Burton, L.; Gandhi, R.; Duke, G.; Paborji, M., Use of Microcalorimetry and Its Correlation with Size Exclusion Chromatography for Rapid Screening of the Physical Stability of Large Pharmaceutical Proteins in Solution. *Pharmaceutical Development and Technology* **2007,** *12* (3), 265-273.

34. R.L. Remmele, W. R. G., Differential scanning calorimetry—A practical tool for elucidating stability of liquid biopharmaceuticals. *Pharm Tech Eur 2000* (12), 56–s65.

35. Remmele, R. L.; Nightlinger, N. S.; Srinivasan, S.; Gombotz, W. R., Interleukin-1 Receptor (IL-1R) Liquid Formulation Development Using Differential Scanning Calorimetry. *Pharm Res* **1998,** *15* (2), 200-208.

36. Goldberg, D. S.; Bishop, S. M.; Shah, A. U.; Sathish, H. A., Formulation Development of Therapeutic Monoclonal Antibodies Using High-Throughput Fluorescence and Static Light Scattering Techniques: Role of Conformational and Colloidal Stability. *Journal of Pharmaceutical Sciences* **2011,** *100* (4), 1306-1315.

37. Huus, K.; Havelund, S.; Olsen, H. B.; van de Weert, M.; Frokjaer, S., Chemical and Thermal Stability of Insulin: Effects of Zinc and Ligand Binding to the Insulin Zinc-Hexamer. *Pharm Res* **2006,** *23* (11), 2611-2620.

38. Singh, S.; Singh, J., Effect of polyols on the conformational stability and biological activity of a model protein lysozyme. *AAPS PharmSciTech* **2003,** *4* (3), 101-109.

39. Stability testing of new drug substances and products (second revision). *Fed Regis* **2003,** *68* (225), 65717–65718.

40. Weiss Iv, W. F.; Young, T. M.; Roberts, C. J., Principles, approaches, and challenges for predicting protein aggregation rates and shelf life. *Journal of Pharmaceutical Sciences* **2009,** *98* (4), 1246-1277.

41. Chang, B. S.; Kendrick, B. S.; Carpenter, J. F., Surface-Induced Denaturation of Proteins during Freezing and its Inhibition by Surfactants. *Journal of Pharmaceutical Sciences* **1996,** *85* (12), 1325-1330.

42. Strambini, G. B.; Gabellieri, E., Proteins in frozen solutions: evidence of ice-induced partial unfolding. *Biophysical Journal* **1996,** *70* (2), 971-976.

43. Pikal-Cleland, K. A.; Rodríguez-Hornedo, N.; Amidon, G. L.; Carpenter, J. F., Protein Denaturation during Freezing and Thawing in Phosphate Buffer Systems: Monomeric and Tetrameric β-Galactosidase. *Archives of Biochemistry and Biophysics* **2000,** *384* (2), 398-406.

44. Hawe, A.; Kasper, J. C.; Friess, W.; Jiskoot, W., Structural properties of monoclonal antibody aggregates induced by freeze–thawing and thermal stress. *European Journal of Pharmaceutical Sciences* **2009,** *38* (2), 79-87.

45. Loo, T.; Patchett, M. L.; Norris, G. E.; Lott, J. S., Using Secretion to Solve a Solubility Problem: High-Yield Expression in Escherichia coli and Purification of the Bacterial Glycoamidase PNGase F. *Protein Expression and Purification* **2002,** *24* (1), 90-98.

46. Mao, H.; Hart, S. A.; Schink, A.; Pollok, B. A., Sortase-Mediated Protein Ligation: A New Method for Protein Engineering. *Journal of the American Chemical Society* **2004,** *126* (9), 2670-2671.

47. Cuskin, F.; Lowe, E. C.; Temple, M. J.; Zhu, Y.; Cameron, E. A.; Pudlo, N. A.; Porter, N. T.; Urs, K.; Thompson, A. J.; Cartmell, A.; Rogowski, A.; Hamilton, B. S.; Chen, R.; Tolbert, T. J.; Piens, K.; Bracke, D.; Vervecken, W.; Hakki, Z.; Speciale, G.; Munoz-Munoz, J. L.; Day, A.; Pena, M. J.; McLean, R.; Suits, M. D.; Boraston, A. B.; Atherly, T.; Ziemer, C. J.; Williams, S. J.; Davies, G. J.; Abbott, D. W.; Martens, E. C.; Gilbert, H. J., Human gut Bacteroidetes can utilize yeast mannan through a selfish mechanism. *Nature* **2015,** *517* (7533), 165-169.

48. Zhu, Y.; Suits, M. D. L.; Thompson, A. J.; Chavan, S.; Dinev, Z.; Dumon, C.; Smith, N.; Moremen, K. W.; Xiang, Y.; Siriwardena, A.; Williams, S. J.; Gilbert, H. J.; Davies, G. J., Mechanistic insights into a Ca2+-dependent family of α-mannosidases in a human gut symbiont. *Nat Chem Biol* **2010,** *6* (2), 125-132.

49. Xiao, J.; Tolbert, T. J., Synthesis of Polymerizable Protein Monomers for Protein-Acrylamide Hydrogel Formation. *Biomacromolecules* **2009,** *10* (7), 1939-1946.

50. Porath, J., General methods and coupling procedures. . *Methods in Enzymology* **1974,** *34*, 13-30.

51. Okbazghi, S. Z.; More, A. S.; White, D. R.; Duan, S.; Shah, I. S.; Joshi, S. B.; Middaugh, C. R.; Volkin, D. B.; Tolbert, T. J., Production, Characterization, and Biological Evaluation of Well-Defined IgG1 Fc Glycoforms as a Model System for Biosimilarity Analysis. *Journal of Pharmaceutical Sciences* **2016,** *105* (2), 559-574.

52. Mozziconacci, O.; Okbazghi, S.; More, A. S.; Volkin, D. B.; Tolbert, T.; Schöneich, C., Comparative evaluation of the chemical stability of four well-defined IgG1 Fc glycoforms. *Journal of pharmaceutical sciences* **2016,** *105* (2), 575-587.

Chapter 5

Summary, Conclusion, and Future work

5.1 Summary

The exact chemical structure of small-molecule drugs and their purities can be well-defined. This provides an opportunity for generic manufacturers to avoid costly clinical trials if they can demonstrate that their generic product is "bioequivalent" in pharmacokinetics compared with the brand product. However, unlike small-molecule drugs, protein molecules are complex, containing a mixture of different species generated by posttranslational modifications. For instance, glycosylation is a posttranslational modification, which significantly contributes to the heterogeneity of the protein molecule produced. The majority of protein heterogeneity is attributed to the variably complete glycosylation as well as chemical modifications and differences in physical conformations. In addition, the complexities of bioprocess make the exact replication of the originator molecule a daunting task. Moreover, glycosylation, charge variants, and even the three-dimensional structure can be significantly altered and ultimately can affect the safety and efficacy profiles of these products. Thus, biosimilar molecules are not simple generic molecules and cannot be identical to the originator. Although there are differences in posttranslational modifications, biosimilar products are anticipated to have the same quality, safety, purity, potency, and efficacy.[1]

The complex and heterogeneous nature of glycosylation that ultimately produces a mixture of variably complete glycoforms makes it difficult to precisely account for the contribution of individual glycans to the overall functional activity and stability of therapeutic mAbs. Hence, it is necessary to utilize *in-vitro* enzymatic reactions to produce well-defined homogeneous glycoforms to be used as a model for biosimilar comparability analysis. One way to produce homogenous glycosylated IgG1 Fc glycoforms is to utilize glycoengineered *P.pastoris*

followed by enzymatic reactions.[2] Well-defined homogeneous IgG1 Fc glycoforms, which include HM-Fc, Man5-Fc, GlcNAc-Fc, and N297Q-Fc, were prepared to be used as a model for a biosimilarity study. These glycoforms were produced by utilizing several techniques, such as site-directed mutagenesis, expression in glycoengineered *P. pastoris*, *in-vitro* enzymatic reaction, and purification techniques.[2-3]

The ability of therapeutic monoclonal antibodies to induce ADCC greatly depends on their binding affinity to activating receptors, such as FcγRIIIa and FcγRI.[4] As a result, efforts to analyze and enhance Fc interactions with FcγRs have become an integral part of the biotherapeutic development process. FcγRIIIa is the only activating receptor expressed on natural killer cells related to ADCC. This receptor is implicated in inducing ADCC and patients with high-affinity polymorphic variants to show a higher response to treatment.[5] Binding kinetics of therapeutic mAbs with FcγRIIIa can be used as a surrogate measure for biological activity if the correlation with another bioassay is established.[6]

Two parallel assay methods were developed to precisely evaluate the binding kinetics of IgG1 Fc glycoforms to FcγRIIIa using a bio-layer interferometry (BLI) technique. In addition, these glycoforms were incubated at low and elevated temperatures to evaluate the change in binding affinities after prolonged storage time. Furthermore, these homogeneous glycoforms were mixed to model change in glycosylation typically encountered during biosimilar development.

In the second chapter, four homogenous IgG1 Fc glycoforms were produced using expression in *P. pastoris*, site-directed mutagenesis, and *in-vitro* enzymatic reaction. The four glycoforms were then utilized as a model for biosimilar comparability analysis. Initial characterization was performed using mass spectrometry, SEC, SDS-PAGE, and cIEF. Then, these

glycoforms were used to develop binding assays using BLI. The data demonstrated that the two assays have similar sensitivity to the change in glycoform. In the first method, the Fc was immobilized, and the receptor was kept in solution, while in the second format, the receptor was immobilized and the Fc was maintained in solution. The two formats were complementary to each other and showed similar K_D values for these well-defined Fc-glycoforms. The receptor (FcγRIIIa) was selectively biotinylated and immobilized onto the streptavidin biosensors. In the Fc-immobilized format, the Fc was immobilized, and no modification was required.

In general, the results demonstrated that the two methods provide similar k_{on}, k_{off}, and K_D values and can be used as parallel binding assay methods during comparability and biosimilarity studies. Moreover, the same sensitivity to the change in glycosylation was observed using both immobilization techniques. Overall, high binding affinities were obtained for HM-Fc and Man5-Fc, and relatively lower binding affinity for GlcNAc-Fc. No binding affinity was observed for N297Q-Fc at the highest concentration tested, indicating the loss of potency upon the removal of the glycans.

One advantage of using Protein G biosensor tips (Fc-immobilized) is that the loading of the Fc can be conducted with a variety of formulation conditions without adjusting the buffer as well as the pH. However, this format is not sensitive to the concentration of IgG1 Fc glycoforms in the samples. Because of this, it may be difficult to detect a change in potency during chemical and physical modifications. An advantage of using an immobilized FcγRIIIa binding format is that a binding affinity test can be performed directly in solutions of IgG1 Fc glycoforms. Therefore, this format is potentially sensitive to changes in potency caused by chemical and physical degradations. A disadvantage of this format is that buffer conditions used in the formulation

must be compatible with receptor binding measurements. In addition, high concentrations of sugars and polysorbates can have a detrimental effect on the kinetics and thermodynamics of binding measurements.

In the third chapter, four homogeneous IgG1 Fc glycoforms were produced, which include HM-Fc, Man5-Fc, GlcNAc-Fc, and N297Q-Fc. These glycoforms were mixed to make well-defined mixtures with evident as well as subtle differences in functional and physical characterizations. The mixtures of glycoforms were prepared by mixing HM-Fc with defined proportions of GlcNAc-Fc, Man5-Fc, and N297Q-Fc. The mixtures with subtle differences contained 90%HM:10X in which X represents N297Q-Fc, Man5-Fc, or GlcNAc-Fc. These samples were prepared to model minor shifts in glycoform composition encountered during process and cell-line changes in a biosimilar development process. The second set of mixtures contained 50%HM mixed with 50% of each of the three glycoforms. Again, these mixtures were designed to model major changes in glycoform composition encountered during biosimilar and comparability assessments. The third set of the mixtures contained a 25% mixture of each glycoform aimed at modeling a complex mixture of glycoforms. These four control glycoforms have a broad range of physicochemical and functional quality attributes. This makes them suitable candidates to make the mixture of glycoforms and to be utilized as a model for biosimilar comparability analysis. The mixture of glycoforms was tested using the Fc-immobilized and receptor-immobilized formats to evaluate their binding affinities.

In general, differences in sensitivity between the two assays platforms were observed. These differences in k_{on}, k_{off}, and K_D values depend on the type of mixture, percentage of composition of the mixture, and the assay method used. Binding response measurements using

the Fc-immobilized technique were found to be very sensitive in detecting a change in the type of mixtures as well as compositions of the mixtures of glycoforms. Overall, the data highlighted the need to carefully examine binding assay results since the selected immobilization technique could have a substantial effect on the binding assay results. This is important in biosimilarity assessments because the glycoform composition can change with the expression condition, cell-line, and manufacturing sites.

The main advantage of the Fc-immobilized format was the capacity to measure accurately the sample containing a mixture of high and low binding components typically observed in monoclonal antibodies, such as a mixture of fucosylated and non-fucosylated glycoforms. However, if the sample contains a mixture of inactive and active proteins, then this format will not be able to detect it. On the other hand, the receptor-immobilized format is not sensitive if the sample contains a mixture of the high and low-affinity components. This is because the high-affinity glycoform will displace the low-affinity glycoform, and the resulting K_D values will be greater than anticipated. However, an advantage of this format will be if the sample contains a mixture of active and inactive protein, then this method will provide accurate K_D value that represents the mixture. Overall the concept developed in this study can provide valuable information for the development of glycosylated biosimilar products.

In the fourth chapter, the main goal of the study was to examine the binding kinetics of incubated IgG1 Fc glycoforms at the low and elevated temperatures for twelve weeks. First, the project was designed to assess differences between Fc-immobilized and receptor-immobilized formats in detecting a change in binding affinities of the stressed samples. This study was also designed to understand the correlation between the physicochemical stability and functional

activity using these glycoforms as a model for biosimilar comparability analysis. Finally, the study was designed to understand the behavior of the glycoforms incubated at low and elevated temperatures with regard to the change in binding affinities to the Fc receptors.

In this project, four IgG1 Fc glycoforms were incubated at 4^{o}C, 40^{o}C, and -80^{o}C for two, four, and twelve weeks. This study performed at low and elevated temperatures can be used in comparability assessments to compare pre-change and post-change. Likewise, the differences in functional and physical characteristics, which were not obvious at low-temperature, can be differentiated at an elevated temperature. The differences in functional activity between the glycoforms could be due to the differences in impurity profiles and glycosylation at Asn297. Additionally, the samples were characterized using the Fc-immobilized and receptor-immobilized formats to examine any differences between the two assay methods. First, the samples were examined using the Fc-immobilized format, and lower binding affinities were observed for the glycoforms incubated at the elevated temperature compared to the same samples incubated at a lower temperature. A trend of decreasing binding affinities was also noted with increasing incubation period. For samples incubated at -80^{o}C, no change in binding affinities was observed throughout the incubation period. Furthermore, the decrease in binding affinities was larger at 40^{o}C compared to 4^{o}C when the measurement was performed using the Fc-immobilized format.

In addition to the Fc-immobilized format, the samples of HM-Fc, Man5-Fc, and GlcNAc-Fc were examined using the receptor-immobilized format to examine the differences between the two assay formats. A substantial decrease in binding affinities was observed for the samples incubated at the low and elevated temperatures compared to the same samples measured using the Fc-immobilized format. In addition, a trend of decreasing binding affinities with incubation

time for the samples incubated at low and elevated temperatures was observed. A change in binding affinities was observed for samples incubated at -80^{o}C. Overall, the data highlighted differences between the two immobilization techniques in detecting a change in binding affinities after prolonged incubation at the low and elevated temperatures. These glycoforms proved to be useful models for biosimilar comparability analysis. The data indicated the samples incubated at the elevated temperature showed a substantial decrease in binding affinities to FcγRIIIa compared to the same samples incubated at the low temperature. In general, the receptor-immobilized format was a better method of choice for analysis of stressed samples and in detecting a change in potency during incubation for a prolonged time. One advantage of the Fc-immobilized format was that the sample binding affinity could be determined without measuring the concentration of the samples after incubation at low and elevated temperatures. Therefore, this method provides ease of measurement from a technical point of view. However, during loading the protein G may selectively bind the native protein, leaving the partially unfolded and aggregated forms. Consequently, this selectivity leads to a greater binding affinity than expected. In other words, this method may provide a good estimation of reduction in potency during accelerated stability study. Overall, the sensitivity of this approach for the stressed samples is relatively lower compared to the receptor-immobilized format. Nevertheless, both methods provide valuable information about the change in potency and are found to be useful in evaluating the biological activity of samples incubated at low and elevated temperatures.

5.2 Conclusion and Future Work

The patents of the top-selling originator biologics are expiring soon, and the next-generation of biosimilar candidates will be monoclonal antibody therapeutics. These biologics are structurally complex and heterogeneous attributed to the Fc glycans. In addition, a biosimilar sponsor can never exactly replicate the originator manufacturing processes, and it is well known that the process defines the structural and functional aspects of the product. Therefore, the need to have sensitive and robust analytical methods to demonstrate the similarity of a biosimilar candidate with the originator is urgently needed.

The methods and concepts developed in this work can be applied to other complex glycoforms, such as galactosylated, fucosylated, sialylated, and complex biantennary glycans, to explore the differences in binding affinities. In addition, a correlation between the binding assays and *in-vivo* biological activity tests should be established. This correlation will help to evaluate the biological significance of the differences in K_D values observed between the control glycoforms as well as the mixture of glycoforms. Similarly, to examine the significance of the difference in binding affinities observed between the samples incubated at low and elevated temperatures, a correlation with *in-vitro* cell-based assays and *in-viv*o biological activity should be established

Finally, the functional characterization methods, as well as the binding responses measurement developed in this work, can be used in comparability and biosimilar assessments of glycosylated mAb therapeutics. The application of these methods should be further explored by comparing different batches of a mAb therapeutic and correlate the binding assay with a

change in glycosylation profile. Likewise, the application of the methods should be further explored by comparing a biosimilar with a reference product, then correlate the binding assay results with the glycosylation profile (e.g., fucosylation). In conclusion, the concepts and methods developed in this work are useful in biosimilar comparability analysis and process development of glycosylated mAb therapeutics.

5.3 References

1. Al-Sabbagh, A.; Olech, E.; McClellan, J. E.; Kirchhoff, C. F., Development of biosimilars. *Seminars in Arthritis and Rheumatism* **2016,** *45* (5, Supplement), S11-S18.

2. Okbazghi, S. Z.; More, A. S.; White, D. R.; Duan, S.; Shah, I. S.; Joshi, S. B.; Middaugh, C. R.; Volkin, D. B.; Tolbert, T. J., Production, Characterization, and Biological Evaluation of Well-Defined IgG1 Fc Glycoforms as a Model System for Biosimilarity Analysis. *Journal of Pharmaceutical Sciences* **2016,** *105* (2), 559-574.

3. Alsenaidy, M. A.; Okbazghi, S. Z.; Kim, J. H.; Joshi, S. B.; Middaugh, C. R.; Tolbert, T. J.; Volkin, D. B., Physical Stability Comparisons of IgG1-Fc Variants: Effects of N-Glycosylation Site Occupancy and Asp/Gln Residues at Site Asn 297. *Journal of Pharmaceutical Sciences* **2014,** *103* (6), 1613-1627.

4. Guilliams, M.; Bruhns, P.; Saeys, Y.; Hammad, H.; Lambrecht, B. N., The function of Fc[gamma] receptors in dendritic cells and macrophages. *Nat Rev Immunol* **2014,** *14* (2), 94-108.

5. Mellor, J. D.; Brown, M. P.; Irving, H. R.; Zalcberg, J. R.; Dobrovic, A., A critical review of the role of Fc gamma receptor polymorphisms in the response to monoclonal antibodies in cancer. *Journal of Hematology & Oncology* **2013,** *6* (1), 1.

6. Berkowitz, S. A.; Engen, J. R.; Mazzeo, J. R.; Jones, G. B., Analytical tools for characterizing biopharmaceuticals and the implications for biosimilars. *Nat Rev Drug Discov* **2012,** *11* (7), 527-540.